Reliability assessment of flexible dolphins

Reducing uncertainty in the design approach of flexible dolphins

Rushil Bechan

Delft University of Technology

TU Delft

Reliability assessment of flexible dolphins

Reducing uncertainty in the design approach of flexible dolphins

by

Rushil Bechan

Student Name	Student Number
Rushil Bechan	4778103

Committee:

Dr. ing. M.Z. Voorendt (Chair)	TU Delft
Dr. ir. O.M. Heeres (Supervisor)	Arcadis
Dr. ir. J.G. de Gijt	TU Delft
Prof. dr. ir. P.A.H.J.M. van Gelder	TU Delft
Dr. ir. A.A. Roubos	TU Delft/Port of Rotterdam
Faculty:	Faculty of Civil Engineering, Delft

Cover: Quick release mooring hooks with solar power systems for Port of Rotterdam by Straatman (2018)

An electronic version of this thesis is available at http://repository.tudelft.nl/.

TU Delft

Preface

The thesis that lies before you serves as the final step of my master's degree. I am fortunate to have been able to study at the Delft University of Technology and complete my thesis at Arcadis as a graduate. The journey from the first day till the last was filled with valuable lessons and appreciation for the discipline that is civil engineering.

I feel very grateful for my supervisors at Arcadis, Otto Heeres and Robbin Wesstein. Their guidance was sublime and we had many fruitful discussions every week. They helped me tackle every problem and made the experience of writing this thesis very enjoyable. I would also like to thank other colleagues at the office for their help and insights during the research. Simina Rebegea and Kamal Laghmouchi were particularly helpful with the coding. Without the help of the people and resources at Arcadis, this research would not have been possible.

I am also grateful for the brilliant members of my committee. Every meeting with them was a joy and an incredible transfer of knowledge. My chair dr. ing. Mark Voorendt was incredibly helpful with the guidance and writing of the thesis. My supervisor dr. ir. Otto Heeres was very helpful week in and week out by transferring his knowledge and past experiences. Dr. it. Jarit de Gijt had excellent expertise and vast knowledge of marine structures in the harbour. Prof. dr. ir. Pieter van Gelder had astonishing knowledge of probability theory and was helpful with my understanding of the theory. Dr. ir. Alfred Roubos brought with him an amazing understanding and experience on the topic thus delivering many valuable insights to the study.

In addition, I would also like to thank dr. ir. Timo Schweckendieck, dr ir. Mark van der Krogt and Rob Brinkman for their advice on the software and theory used during the research. Their help alleviated the intimidation the workload initially imposed.

Furthermore, I would like to thank the other graduates at Arcadis for their sympathy towards one another. Their presence made coming to the office an enjoyable experience. Particularly Gerwin van de Wakker, Maurits van Herwijnen and Kevin van Donselaar with whom I played many fun table tennis matches. Amazingly I won every match. (Completely factual statement)

Lastly, I would like to thank my family and friends for their continued support. Especially my parents whose hard work and sacrifices gave me this opportunity to graduate from an esteemed university. They continue to inspire me every day and I hope I will make them and my country Suriname proud.

This thesis was a product of many blessings sent my way. I wish the reader many blessings as well and I hope you enjoy reading!

Rushil Bechan
Delft, February 2024

Summary

A flexible dolphin is a marine structure used for berthing and mooring vessels. It is a single pile extending from above the water surface to far below the bed level. The main function of the dolphin is to provide support and stability to ship berthing. Currently, dolphins are designed according to the CROW C1005 handbook (2018). However, the partial factors in this handbook have not been sufficiently calibrated and the design approach may be conservative. These factors can be calibrated using reliability-based assessments. These assessments consider the uncertainties when designing a dolphin and determine the probability of failure during the design life. However, present-day reliability assessments are incomplete, time-consuming and require large computational power. Moreover, it is still uncertain how the uncertainties can be reduced when incorporating information from test loading and the observational history of berthing. The aim of the report therefore is to improve the design approach of the flexible dolphins. The aim was achieved by answering the following research question.

What benefits can be attained by performing reliability-based approaches for flexible dolphins?

First, the critical failure modes were identified as these determine the main pile dimensions. For the design of the dolphin, the main failure mechanisms are yielding of the steel, local buckling, geotechnical failure and fixity of the pile after the first large berth. The yield limit state defines what diameter and thickness the pile must be to have sufficient bending moment capacity. The buckling limit state determines the ratio between the diameter and the thickness as too slender of a pile will reduce the bending moment capacity. Lastly, the geotechnical and fixity criteria determine the pile toe level. The pile should be embedded so that it is durable enough to not become skewed during berthing procedures. The calculation model used for the design of the dolphins is the API PY-curves since it is internationally acceptable and has a rapid computation speed.

After defining the failure modes, the technique for the probabilistic assessments was determined to calculate the influence factors and reliability index. Directional Sampling is selected due to its ability to provide accurate results for limit states consisting of discontinuities and non-linearities, while still maintaining a relatively low calculation time. The reliability assessments were performed using the automated Dolphin Tool from Arcadis and the Probabilistic toolkit from Deltares. For the reliability-based assessments, the distribution of the input variables had to be determined. To define the statistical properties of these distributions literature was reviewed and simulations were conducted. The stochastic design variables considered in this study were the berthing load, wall thickness, yield stress of steel, internal friction angle, the saturated soil weight, model uncertainties of the occurring moment and buckling capacity. The distributions for the berthing load were determined from Monte Carlo simulations, while the distributions for the other parameters were derived from the literature.

With the failure modes, input variables and probabilistic technique in place, the probabilistic assessments could be performed. The assessments for the failure modes buckling and yield showed that the load-based approach was sufficient and the berthing load was the most important factor for structural safety. This outcome was verified by testing 3 fictional soil compositions that represented soil that can be found throughout the Netherlands. However, this was different for the fixity failure mode as the soil parameters were the most dominant variables. Admittedly, the software used seemed to be unsuitable to properly determine the reliability index and partial factors of the geotechnical and fixity failure mode due to the unrealistic output at 100% soil mobilisation.

Other aspects in the probabilistic assessments that influence the partial factors are the navigation conditions, the arrival rate of the ships and the variation in ship sizes. To analyse the influence of the navigation condition, cases were studied in monitored, favourable, moderate and unfavourable conditions as well as three additional cases with a low variation in ship size, and frequent and infrequent berths. Rougher navigation conditions, frequent arrival rates and low variation in water displacement

led to higher factors. Recommendations for partial factors for monitored, favourable, moderate and unfavourable conditions were made from Monte Carlo simulations and are respectively 1.19, 1.29, 1.31, and 1.39. These factors can then be corrected for the number of arrivals and variation in water displacement.

Lastly, load testing can help reduce uncertainties thereby increasing the reliability index in the probabilistic assessment. This is useful in cases where the lifespan of the dolphin could be extended. As a means to gauge the increase in reliability, data from the Calandkanaal full-scale load tests were used and a Bayesian update was performed. The reliability index increased from 2.43 to 2.95. The load was estimated to be at 60% pile capacity and to have a more significant impact on the reliability index this should be increased to around 100%. The exact load should be determined by a study which weighs the probability of failure during the load against the benefits of a successful load.

In conclusion, the reliability-based assessment gave a better understanding of how to manage the uncertainties when designing a dolphin. These assessments caused up to 20% less material use in designs while still meeting the safety requirements and when combined with test loading the probability of failure can be reduced further by tenfold.

Contents

1 Introduction

1.1. Motivation and societal relevance

A flexible dolphin is a marine structure used for berthing and mooring vessels. It is a single pile that extends from above the water surface down to far below the seabed. The main function of the dolphin is to provide support and stability to ship berthing. In modern engineering, the rise of digital technology and improved computational power can help optimize the design of these dolphins. Engineers can use powerful computer programs to study the effects of the load and soil-structure interaction to design safe and more optimal dolphins. In addition, by utilizing probabilistic calculations engineers can account for uncertainties to further enhance the design of this marine structure.

A recent study has shown that these developments have the potential to significantly enhance the design approach and calculation (Heeres et al., 2023). In 2020, Arcadis developed their own in-house Dolphin Tool that can automatically calculate the dimensions of berthing and mooring dolphins (Figure 1.1) after careful engineering considerations. The tool designs the dolphin to conform to the CRW C1005 'Flexible dolphins' guideline (2018). In addition, Arcadis has coupled the Dolphin Tool with the Deltares Probabilistic Toolkit to make a complete probabilistic assessment. For this reason, the Port of Rotterdam asked Arcadis to make a probabilistic design of a dolphin and compare the results with the regular design. Port of Rotterdam Authority is continuously thriving for innovation to help achieve their sustainability goals (Port of Rotterdam, 2022) and probabilistic assessment may help gain more insight on how to approach uncertainties. It is still uncertain whether or not these assessments may yield trustworthy results. This research delves into the feasibility of reliability-based assessments of dolphins. This thesis will assess whether the current design approach for flexible dolphins is suitable or not.

(a) Mooring dolphin with a bollard

(b) Berthing dolphin with a fender

Figure 1.1: Types of dolphins

1.2. Problem analysis

For the probabilistic design of flexible dolphins, it is crucial to understand and address the complex challenges that come with such an assessment. Starting with the current issue of the design approach which motivates a reliability-based assessment of the dolphin. Then the current knowledge gaps in the reliability-based assessment and where potential improvements can be made are discussed.

1.2.1. Demand for probabilistic assessments

Steel production involves substantial energy consumption and contributes to greenhouse gas emissions (World Steel Assocaition, 2023). By adopting a design approach that minimizes steel usage and potentially extends the lifespan of current structures, the Port of Rotterdam can decrease its carbon footprint, conserve resources and contribute to a cleaner and greener environment. Steel is thus a valuable and costly resource. By optimizing dolphin designs to reduce steel requirements, the Port of Rotterdam can achieve cost savings in construction and maintenance. They want to achieve these savings through smarter calculations, smarter designs and smarter constructions (Port of Rotterdam, 2023). This thesis will contribute to a smarter design and calculation approach. Nevertheless, the improved design approach for dolphins still needs to be safe and durable.

By adopting a complete probabilistic design approach, the potential risks associated with dolphin failure or structural issues can be comprehensively assessed and managed. This includes considering uncertainties in various factors such as environmental loads, material properties, and operational conditions. Such a design approach helps ensure the safety of maritime operations. Moreover, increasing ship sizes, and changing load characteristics pose challenges to traditional deterministic design approaches.

A complete probabilistic approach of dolphins enables engineers to account for uncertainties and potential variations in these conditions. This promotes the development of resilient structures that can adapt to changing circumstances, ensuring the port its long-term viability and maintaining efficient maritime operations. Lastly, a complete probabilistic design approach fosters knowledge advancement and innovation in the field of structural engineering. By conducting probabilistic analyses and gathering data on uncertainties and risk factors, engineers can expand their understanding of structural behaviour and failure mechanisms.

1.2.2. Conservative design approach dolphins

For the design of dolphins, different methods are used that do not always comply with the design philosophy of the Eurocode. The CRW C1005 Flexible Dolphins guideline (2018) provides a uniform design approach. One of the first steps in the design is to select a consequence class and each consequence class has partial safety factors in accordance with NEN-EN 1997. Consequence classes are classification system that categorizes structures based on the potential consequences of their failure. There are three classes in order of increasing consequences of failure; CC1, CC2 and CC3. Schrijver (2016) presented via a probabilistic assessment that the factors for dolphins in CC2 may be conservative and Heeres et al. (2023) concluded the same for CC1. Table 1.1 shows the differences. Admittedly, the study by Schrijver (2016) has limitations. The study only looked at mooring dolphins and did not fully assess the statistical properties of the mooring load, while Heeres et al. (2023) show that precisely the load has a significant impact on the reliability. The study further assumed that the dolphin had a constant thickness, but in reality, the dolphin has a varying thickness throughout its length. Another issue is the non-linear relation in the geotechnical limit state. The probabilistic evaluation by Schrijver (2016) is done with FORM and to do this, modifications were made to the limit state to make it more linear, which in turn introduces inaccuracies. Lastly, the study was conducted assuming that the dolphins are in consequence class II, but it is more common for dolphins to be designed in consequence class I.

The research by Jasper Focks et al. (2015) also supports the statement that the current partial factors may be a bit conservative. Full-scale load tests were conducted on the dolphins, the piles were loaded until buckling occurred. They found that there was a discrepancy with the Eurocode design approach. It seems that dolphins could withstand higher forces than prescribed in the guidelines. So more optimal

Table 1.1: Differences between Eurocode and other research

Parameter	Eurocode γ_{RC2}	Eurocode γ_{RC1}	Schrijver (2016) γ_{RC2}	Heeres et al (2023) γ_{RC1}
Cohesion	1.25	1.15	1.00	1.00
Tangent angle of internal friction	1.175	1.15	1.15	1.00
Soil weight	1.00	1.00	1.00	1.00
Soil Stiffness	1.30	1.30	1.30	1.00
Yield strength	1.00	1.00	1.00	1.00
Wall thickness	1.00	1.00	1.0	1.00
Pile dimeter	1.00	1.00	1.05	1.00
Young's modulus	1.00	1.00	1.00	1.00
Mooring load	1.00	-	1.30	1.00
Berthing load	-	1.45	-	1.39

designs of dolphins can be made which in turn would lead to cheaper and more sustainable dolphins. In addition, by reducing the thickness of the dolphin the structure becomes more flexible and will be able to absorb more energy so larger vessels could berth. But the dolphin should still be elastic enough to bounce back into place after a berthing process or else the pile will remain tilted.

1.2.3. Shortcomings in present reliability assessments of dolphins

Most dolphins located in the Rotterdam area were designed using the method developed by Blum (Blum, 1932). More recent designs are made using software employing the subgrade reaction method, one such example is the Dolphin Tool by Arcadis. The issue with these methods is that designs are quite conservative as mentioned earlier. This is due to the semi-probabilistic nature of the approach that is not yet fully validated by probabilistic assessments based on sufficient data. A full probabilistic approach could lead to more optimal designs (Phoon and Retief, 2016). Experience has already shown that probability-based design codes lead to a notable reduction in steel weight, ranging from 5% to 30% with 10% being typical (Bai and Jin, 2016).

Therefore, Schrijver (2016) did a reliability assessment of the dolphins and did indeed find that lower partial factors could be used. However, the analysis was executed using a level II reliability method. A level III reliability method would provide more accurate reliability and in addition, sharper distributions of the variables should be used in the evaluation. Heeres et al. (2023) made these adjustments to the assessment as well as calculations in consequence class I and indeed found a reduction of 17% in material use. They found that the berthing energy is the most dominant variable as it has a 97% influence on the probability of failure. This study shows that an even better evaluation of berthing energy could lead to a more optimal design. The study found that the partial factor for berthing energy could be different than what is prescribed in the current guidelines. The limit state of yield and buckling were checked based on the unity check for each pile segment. The geotechnical failure mechanisms were checked by making sure that the displacements of the dolphins were sufficiently small. The fixity criterion was also looked at, but not reported. This is due to the fact this criterion was at the time still in development, and led to conservative designs.

In spite of the finding that reliability-based assessments of dolphins can significantly reduce material use, it is still unknown if it is applicable to all dolphin designs. The research conducted by Heeres et al. (2023) was site-specific to the Calandkanaal, but there are other interesting locations where large numbers of dolphins are situated such as the Maasvlakte, more inland in the direction of the city of Rotterdam and other port areas in the Netherlands. Other soils also include clay, where additional factors need to be taken into account such as the undrained condition and shear strength. This can potentially lead to different results from the full probabilistic calculation compared with soil consisting of only sand. Besides the different soil compositions, the different navigation conditions need to be assessed. Ships berth at dolphins under varying conditions caused by different waves, wind speeds and the proficiency of the captain.

Another assumption that was made in past research, was that corrosion was not an issue. The research assumed that the dolphins were fully protected against corrosion. However, research has shown that it does have a significant impact when taking corrosion into account (A. A. Roubos et al., 2020). The

research shows that the inclusion of corrosion in quay walls causes the reliability to drop below the reliability target after 2/3 of its lifetime. Laghmouchi (2021) found similar results as well. In certain designs, an over-thickness is added which is based on the corrosion rate. This extra thickness makes the dolphin more rigid in the early years of its lifespan causing higher bending moments in the dolphin and that can negatively impact the probability of failure at the start of the lifespan. Besides, when taking corrosion into account for probabilistic assessment measurements are necessary to gauge the corrosion rate and consequently update the reliability. An alternative measure recommended by the CRW C1005 is to employ cathodic protection. With this measure, no corrosion can take place so the uncertainty in corrosion does not have to be used in the reliability-based assessment.

1.2.4. Potential improvements in probabilistic analysis

Numerous factors, such as environmental conditions and the intensity of severe loads, can pose a significant threat to the safety of structures. Unfortunately, accurately predicting the exact impacts of these factors in a deterministic manner is often challenging. Therefore, it is necessary to assess these impacts using a probability-based approach that takes into consideration the uncertainties associated with both the performance of the structure itself and the external forces acting upon it. This probabilistic method provides a more comprehensive understanding of potential risks and helps in making informed decisions to ensure structural integrity and safety (Wang, 2021). The structural reliability can be quantitatively measured by the probability that the load effect does not exceed the structural resistance, see Equation 1.1.

$$P_f = 1 - P(R > S) \tag{1.1}$$

Where,

P_f = Probability that structure fails
R = Structural resistance
S = Load effects

However, structures can suffer deterioration of resistance due to severe operating or environmental conditions. In addition, load effects can also increase in intensity and frequency. Therefore, a structural reliability assessment needs to take into account the time-variant characteristics of resistance and load process, especially for long reference periods. Thereby, Equation 1.1 turns into Equation 1.2.

$$P_f(t) = 1 - P((R(\tau) > S(\tau)) \text{ for all } \tau \in (0, t)) \tag{1.2}$$

During the lifespan of a structure, it can be subjected to different loads and the combinations of these different loads need to be taken into careful consideration when performing a reliability assessment such that the chance that the extreme and frequency of each load combination is closely approximated. For an accurate analysis, a lot of information is necessary on the correlation and dependencies between these loads, which is not always available and no clear method exists to handle this interdependence.

Another problem is the computational intensity of the evaluation when employing a level III method. There are ways to reduce the computation time, which were employed for a quay wall (Post et al., 2021). Here the different reliability-based assessments of quay walls were calculated using traditional probabilistic techniques and a more lean alternative technique. Both methods gave more or less the same reliability index, but the leaner method was much faster in computation time. The traditional technique took 10 days and the alternative one needed 1.5 hours. This probabilistic technique could also be employed in this study.

Moreover, the uncertainty can be reduced when also incorporating data from test loading or past performance. Den Adel (2019) as well as Schweckendiek (2010) have shown that the reliability can be significantly improved by such an approach. When incorporating the result of fictitious load testing data, Den Adel found that an additional surcharge of 20 kN/m^2 could be applied behind the quay wall in his case study. Van der Krogt (2022) also found that using settlement information for dikes increases the reliability of dikes. He also determined that proof loading and monitoring are a cost-effective method to reduce reinforcement costs. The Bayesian update could lead to 5 million euros per km saved in dikes.

Such an update could also be attempted for dolphins as there have been full-scale test loading done in the past (Griffioen, 2023).

1.2.5. Problem statement

In summary, current dolphins are designed mostly semi-probabilistically with approximated partial factors, which can lead to conservative designs. These factors may not be optimal and need to be calibrated with a reliability assessment. However, present-day reliability assessments are often still incomplete and are time-consuming and require large computational power. Moreover, it is still uncertain what the impact is of incorporating load testing data into the reliability-based assessment of a dolphin.

1.3. Research objective with scope and limitations

1.3.1. Objective

The objective of this research is to improve the design approach of a flexible dolphin.

1.3.2. Scope and limitations

Since the objective of this report is to improve the probabilistic design approach of dolphins, certain limitations and assumptions are imposed.

- In this study, the methods used were applied to berthing dolphins since mooring dolphins require more information on the occurring mooring forces, which is not extensive enough at the time of this study.
- The dolphin is assumed to be partly filled with sand as this already leads to more optimal designs
- Additionally failure modes related to extreme events such as earthquakes are not taken into account, because this study focuses on the Netherlands where earthquakes are uncommon.
- Effects from pile grouping and repetitive loading are neglected. This is due to the extra calculation time and complexity these effects come with, even though they might be of little influence.
- The Bayesian update will only be applied based on the test loading data from the full-scale tests in the Calandkanaal as this is the most extensive reported test as of this time.
- The research is limited to the dolphins with a lifespan of 50 years and in consequence class I because most dolphins are designed for such a lifespan in that consequence class.
- The study is only limited to sea ships because no berthing records are available for inland vessels as of yet.

1.4. Research questions

This thesis strives to meet the objective by answering the main question:

What benefits can be attained by performing reliability-based approaches for flexible dolphins?

The following sub-questions will aid in answering of the main research question;

i) What are the critical limit states when assessing flexible dolphins?
ii) Which design variables influence the uncertainty or probability of failure of the dolphin?
iii) What is the influence of different soil compositions on the reliability and partial factors of safety?
iv) What is the influence of different navigation conditions on the reliability and partial factors of safety?
v) What set of partial safety factors is recommended to be implemented in the design of dolphins?
vi) How can the full-scale field test data and historical records of observations benefit the probabilistic assessments?

1.5. Approach and outline

The structure of this thesis is shown in Table 1.2 with the approach step and chapter outline explained respectively in Subsection 1.5.1 and Subsection 1.5.2.

Table 1.2: Structure of thesis

Sub-question	Approach step	Chapter
I	1	2
II	2,3	3
	4	4
III	5, 6	5
IV	7	5
V	8	5
VI	9, 10	6

1.5.1. Approach

The approach steps to answer the research questions are:

1. A literature study is conducted to discover what the failure mechanisms of the flexible dolphins are and what the necessary design steps look like to prevent failure of the structure.
2. The literature study is conducted further to find the probabilistic techniques that can be used to determine the reliability of the flexible dolphin.
3. Next the input variables and their corresponding statistical properties are found and summarised using literature study and simulations.
4. Then the case descriptions are given of the different cases for which reliability-based assessments are conducted.
5. The reliability-based assessments are performed and the results are presented.
6. The results of the different soil compositions are compared.
7. The results of the different navigation conditions are compared.
8. From the results, recommended partial factors are derived that can be implemented to ensure sufficient reliability for flexible dolphins.
9. Then the method to update the reliability index by adding information from test loading and historical records of observations is developed and validated.
10. Lastly, the results of the reliability update are presented and compared.

1.5.2. Outline

The approach can be broken then into steps with each step allocated in a different chapter:

1. Chapter 2 gives a literature study on the current method of designing dolphins. This is necessary to understand in order to make reliability-assessments and answer sub-question i.
2. Chapter 3 continues the literature review on how to perform a reliability-based assessment, determine statistical properties of the input variables and execute a Bayesian update according to literature. Thereby, this chapter gives an answer to sub-question ii.
3. Chapter 4 develops the method and inputs for the probabilistic assessments of the dolphins following the previous literature study.
4. Chapter 5 shows the results of this assessment for different cases. The assessment will be done utilizing the Dolphin Tool of Arcadis and the Probabilistic Toolkit of Deltares. Herein, sub-questions iii to v are answered.
5. Chapter 6 elaborates on the effect of incorporating data from a test loading on the reliability of the dolphin and answers sub-question vi.
6. Chapter 7 discusses the study its accuracies and limitations.
7. Finally, in chapter 8 the conclusion and recommendations are given.

2

Design considerations for dolphins

This chapter gives a quick view of how dolphins are currently designed and is needed to understand the calculation steps used in the assessments of the limit states, which is the first step in the approach. This step is necessary for approach step number 5. The design approach used is derived from the 'Flexible Dolphins' handbook (2018). The chapter first describes the main functions of dolphins in Section 2.1 and then moves to Section 2.2 goes more into depth on the loads enacting on the dolphin. Then Section 2.3 discusses different design models. Finally, Section 2.4 summarises how the main dimensions of the dolphin are determined with respect to the critical limit states. For more details, the reader is referred to the CRW C1005 (2018).

2.1. Dolphin functionality and safety

2.1.1. Common functions of dolphins

A dolphin is part of the marine structure family and is often located at ports, waterways and other navigational waterways. The structure has three main functions, namely:

- Allow for safe berthing and mooring
- Protection of waterfront structures
- Directing and guiding marine traffic

The dolphins most frequently found in the Rotterdam harbour area are the breasting and mooring dolphins. The breasting dolphins are used to absorb the kinetic energy of ship berthing and spring lines can also be attached. Mooring dolphins on the other hand are attached with with bow and breast line, see Figure 2.1. The complexity of the structure is due to its necessary ability to be flexible enough to absorb energy, while at the same time having minimum deflection. Usually, the dolphin has different cross-sections throughout its length, because this leads to a more economical design. Next to the function, the design life needs to be considered. Most of the time the dolphins are designed for 50 years, but in certain cases a design life of 25 years is used. The lifespan is the reference period used for the design values of the load and materials.

2.1.2. Safety categories

In the Eurocode, target reliability levels are used and these levels are associated with the consequences of failure considering the fatalities, economic losses and environmental effects. These indices are available for a large number of structures, but not for maritime structures such as dolphins. The NEN-EN 1990 has annual and lifespan reliability targets developed for bridges and buildings, but aleatory and epistemic uncertainty can be different for dolphins. In the CRW C1005 (2018) it is recommended to use the lifespan reliability, because the annual reliability may be overestimated. A summary of the consequence classes with their respective reliability target and examples is shown in Figure 2.2.
The reliability indices are based on structural and geotechnical failure modes. These modes should be considered in the serviceability or ultimate limit state. The serviceability limit states are;

- Residual deformation around sea bed level

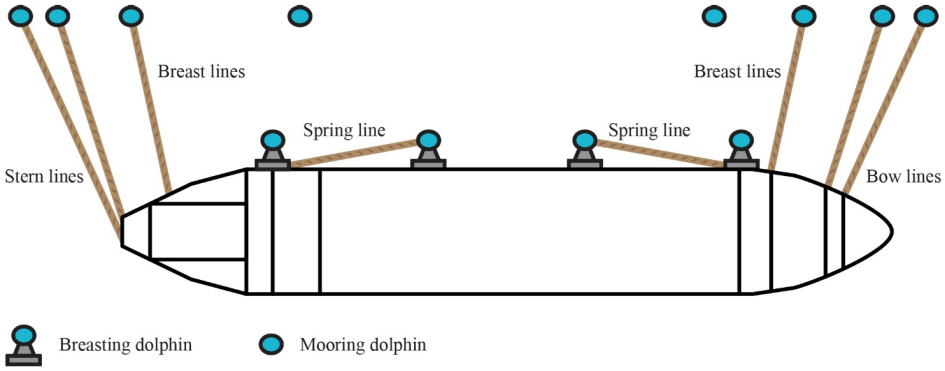

Figure 2.1: Typical configuration of dolphin according to CRW C1005 (2018)

- Excessive deformation in the soil near pile tip
- Exceeding elastic limit steel pile under operation
- Insufficient deformation for berthing energy absorption
- Too much deformation of the top of the pile

The ultimate limit states are:

- Exceeding internal force limits of the pile of bending movement and shear force.
- Reduction of pile capacity due to corrosion
- Bed level change causing a different fixity level in the ground and potential increase of internal forces
- Local buckling leading to insufficient capacity
- Instability of pile
- Accidental limit state due to incorrect use of pile
- Instability of pile due to vessel collision

2.1.3. Partial factors used for design

The use of partial factors follows from the NEN9997-1. For geotechnical structures, it is recommended to use partial factors on the soil and steel parameters (M2) and factors on the berthing, mooring and environmental loads (A1). And lastly, a partial factor of 1.0 should be used for resistance (R3). The magnitude of the factors depends on the consequence class.

Materials

For soil, there are lower and upper-bound strength and stiffness parameters. The lower bounds are important for geotechnical failure, while the upper bounds are more relevant for structural failure. The soil model to be used determines the soil input parameters. Typically effective stress parameters are used. For cohesive soils, the undrained conditions can be dominant and need to be evaluated as well. From laboratory tests or in-situ measurements, the characteristic soil parameters can be determined. The partial factors in accordance with the NEN9997-1 are shown in Figure 2.3. The safety partial factors should be used when the lower bounds are governing. On the other hand, when the upper bounds are governing a factor of 1.0 is sufficient, remarked in the CRW C1005 (2018).

For the mechanical properties of steel, a safety factor of 1.0 should be used according to the EN 1993-1-1. A phenomenon that comes into play when designing ductile structures such as flexible dolphins is local buckling. The recommendation for how to assess this stems from research conducted in the CUR211. The approach differs from empty tubes and sand-filled tubes. For this research, the scope is limited to partly filled tubes.

Loads

The load considered in this study is the berthing load and Figure 2.4 gives the partial factors used in the calculations.

Consequence/ Reliability Class	Description	Examples of dolphins	Reliability index β_{t50}
CC3/ RC3	**High** consequences for loss of human life or economic, social or environmental consequences **very great**.	Dolphins with a primary navigational function, such as entrances of ports, bridges or locks[2)]. Dolphins that protect a structure categorized as CC3 [2)]; Dolphins for which failure will lead to failure of other hazardous structures, such as hazardous installations of chemical or power plants .	4.3
CC2/ RC2	**Medium** consequence for loss of human life, economic, social or environmental consequences **considerable**.	Dolphins that are of a passenger or cruise terminal [1)]; Dolphins that are a part of another system, such as chemical or power plants, but for which failure does not lead to failure of other structures, such hazardous installations [3)]; Dolphins that protect a structure categorized as CC2 [2)].	3.8
CC11 RC1	**Low** consequence for loss of human life, *and* economic, social or environmental consequences **small or negligible**.	Regular flexible dolphins e.g. part of waiting facilities, or single dolphins for ship-to-ship transhipment [1)]; Dolphins that protect a structure categorized as CC1; Flexible dolphins with a secondary nautical or navigational function.	3.3

[1)] In case of a structural component is part of a series system or in the case that progression of failure is not mitigated, a higher consequence class should be considered.
[2)] If failure of the dolphin, such a sacrificial dolphin or crash barrier, will not lead to damage to the structure being protected by the dolphin, a lower reliability index could be considered.
[3)] It should be noted that the follow-up conditional probability that a hazardous installation will fail due to the failure of the dolphin should be taken into consideration. If this conditional probability of failure is quite high, a higher reliability index should be considered.

Figure 2.2: Different reliability classes (CRW C1005, 2018)

Soil parameters, M2	Symbol	Reliability class		
		RC1	RC2	RC3
Tangent angle of internal friction	$\gamma_{\varphi'}$	1.15	1.175	1.20
Effective cohesion	$\gamma_{c'}$	1.15	1.25	1.40
Undrained shear strength	γ_{cu}	1.50	1.60	1.65
Unit soil weight	γ_{γ}	1.00	1.00	1.00
Stiffness	E'	1.30	1.30	1.30

Figure 2.3: Partial safety factors for the material (CRW C1005, 2018)

Load or load effects as result of berthing, A1			Reliability class EN 1990		
Navigation conditions	Pilot assistance	Symbol	RC1	RC2	RC3
Sheltered or exposed	No	γ_v	1.45	1.50	1.55
		C_{ab}	2.10	2.25	2.40
Sheltered and monitored [1)]	Yes	γ_v	1.15	1.20	1.25
		C_{ab}	1.35	1.45	1.55
Sheltered	Yes	γ_v	1.20	1.25	1.30
		C_{ab}	1.45	1.55	1.70
Exposed [2)]	Yes	γ_v	1.30	1.35	1.40
		C_{ab}	1.70	1.80	2.00

[1)] Pilots are aware of the allowable berthing velocity and use berthing aid systems, such as portable pilot units.
[2)] Strong tidal currents and/or waves.

Figure 2.4: Partial factors for berthing velocity (γ_v) and abnormal berthing factor for berthing energy (C_{ab}) (CRW C1005, 2018)

2.2. Loads enacting on the dolphin

When the vessel berths at a flexible dolphin, the vessel contains kinetic energy that needs to be absorbed by the dolphin. This berthing energy is calculated with Equation 2.1 (CRW C1005, 2018).

$$E_k = \frac{1}{2} \cdot M \cdot v^2 \cdot C_E \cdot C_M \cdot C_S \cdot C_c. \tag{2.1}$$

Where,

E_k = Berthing energy
M = Water displacement$[kN/m^2]$
v = Berthing velocity$[m/s]$
C_E = Eccentricity factor$[-]$
C_M = Virtual mass factor$[-]$
C_S = Ship flexibility factor$[-]$
C_C = Configuration factor$[-]$

The water displacement is determined with Equation 2.2. Next to this equation, there exist guidelines which prescribe the displacement based on the vessel class. For instance, the PIANC 121 (2014). Port authorities can also have their own guidelines they employ. These water displacements are more accurate for their specific port because they are based on experience and measurements within the port. On the contrary, the PIANC guidelines tend to be more conservative as those have to apply to multiple ports.

$$M = L \cdot B \cdot D \cdot C_B \tag{2.2}$$

Where,

L = Length of ship$[m]$
M = Width of ship$[m]$
D = Draught of ship$[m]$
C_B = 0.85, Block coefficient for tanker with enough under keel clearance CRW C1005$[-]$

Because the velocity vector of the ship does not pass through exactly the point of contact with the dolphin, this will introduce some dissipation of the kinetic energy. This is corrected by using the eccentricity coefficient. The eccentricity factor can be calculated as follows, with a diagram for calculations in Figure 2.5.

$$C_E = \begin{cases} \frac{k^2+r^2\cos^2\phi}{k^2+r^2} + \frac{\omega r}{v} \cdot \frac{2k^2\sin\phi}{k^2+r^2} + \frac{\omega^2 r^2}{v^2} \cdot \frac{k^2}{k^2+r^2}, \text{translation and rotation} \\ \frac{k^2+r^2\cos^2\phi}{k^2+r^2}, \text{translation only} \\ \frac{k^2}{k^2+r^2}, \text{rotation only} \end{cases} \tag{2.3}$$

$$k = \begin{cases} 0.29L, B < \frac{1}{6}L \\ \frac{k^2}{k^2+r^2}, C_B < 1 \end{cases}$$

Where,

k = Radius of gyration of ship$[m]$
r = Distance of centre of gravity of the ship to point of contact with marine structure$[m]$
v = Total translation velocity at time of first contact$[m/s]$
v_r = Perpendicular velocity due to vessel rotation considered at a distance equal to the radius of gyration from the ship's centre of gravity$[m/s]$
ω = Angular velocity of ship at first contact [rad/s]
ϕ = Angle between velocity factor and distance r [$\circ$]
α = Berthing angle

When the ship is berthing, it causes the surrounding water to move as well. This adds inertia to the system. In order to compensate for the extra mass, a virtual mass factor can be added to the berthing

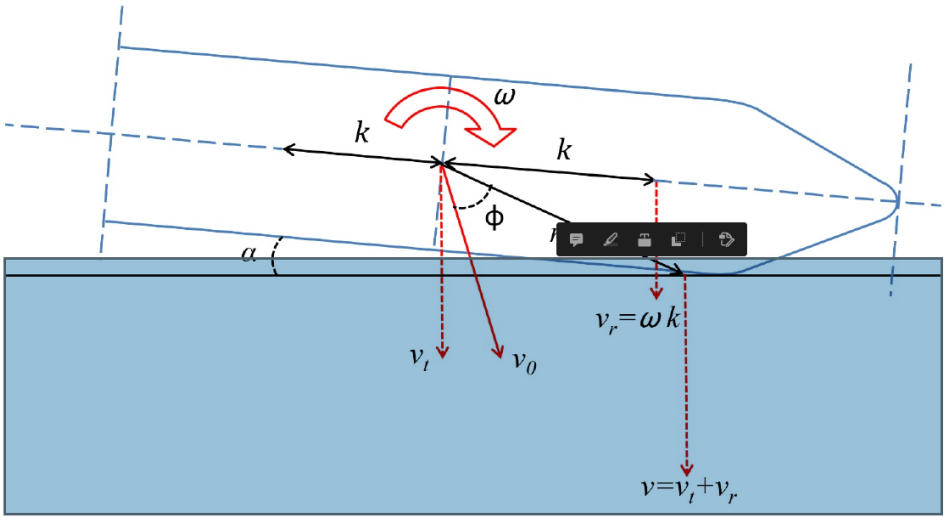

Figure 2.5: Diagram for berthing energy (Roubos et al., 2017)

energy. There are different methods to determine this factor, however, the CRW C1005 (2018) recommends the method described by the PIANC WG33 (2002). The formula for this method is shown in Equation 2.4.

$$C_M = \begin{cases} 1.5, & \frac{K_c}{D} \geq 0.5 \\ 1.8, & \frac{K_c}{D} \leq 0.1 \\ C_m = 1.875 - 0.75\frac{K_c}{D}, & 0.1 \leq \frac{K_c}{D} \leq 0.5 \end{cases} \tag{2.4}$$

With,

$$\begin{aligned} K_c &= \text{Under keel clearance [m]} \\ D &= \text{Draught of the ship) [m]} \end{aligned}$$

Furthermore, the ship flexibility and configuration factor is equal to 1 because the dolphin is seen as an open structure. With the normal berthing energy now determined the abnormal berthing energy is calculated with Equation 2.5.

$$E_{abnormal} = C_{ab} \cdot E_k \tag{2.5}$$

With,

$$\begin{aligned} E_{abnormal} &= \text{Abnormal berthing energy [kNm]} \\ C_{ab} &= \text{Abnormal berthing factor (Figure 2.4) [-]} \end{aligned}$$

When implementing a bucking fender, the energy absorption capacity of the dolphin can be much higher. The fender reduces the berthing energy to be used in the design of the dolphin. While being compressed, the fenders produce a reaction force during a berthing procedure. This reaction force depends on the fender type and deflection. For instance, a cone fender reaches peak reaction force two times, see Figure 2.6. A cylindrical fender on the other hand, the maximum reaction force is only achieved at maximum deflection (Figure 2.7).

Alternatively, no rubber fender could be installed, just the fender plate. In such a case, the pile absorbs all the berthing energy. The berthing energy can be translated into a berthing force following Equation 2.6. This is an approximation of the berthing energy as shown in Figure 2.8.

$$E_k = 0.5 \cdot F_{berthing} \cdot deflection \tag{2.6}$$

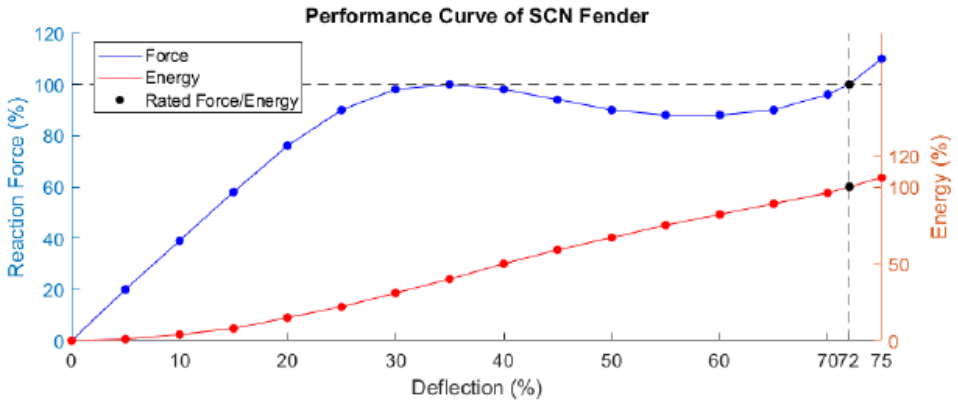

Figure 2.6: Reaction force of a cone fender (Trelleborg, 2018)

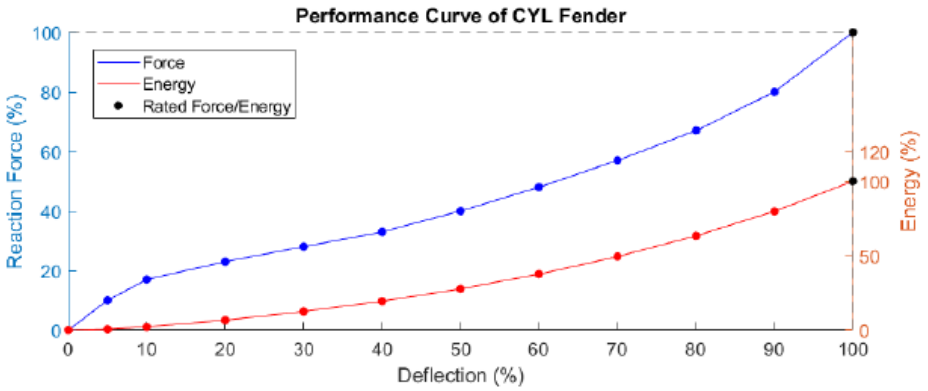

Figure 2.7: Reaction force of a cylindrical fender (Trelleborg, 2018)

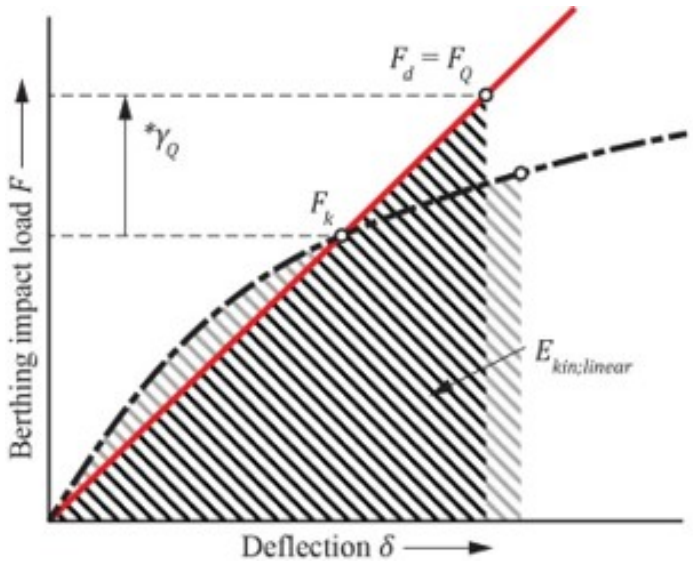

Figure 2.8: Berthing force (CRW C1005, 2018)

2.3. Common calculation models

There exist many methods and software packages to model soil-structure interaction. For this research, a method should be selected and used for the reliability-based assessment. The most commonly used are summarised here and a comparison between the models is shown in Table 2.1.

2.3.1. Blum Method

One of the most used methods for laterally loaded piles is the method of Blum 1932. This old model remains popular due to its relatively simple and quick way of designing. Blum assumes that the soil resistance is completely passive and does not regard elastic deformation. Thus, Blum considers the pile toe to be fixed at the toe and the entire pile is rotating on said point. He assumes the soil wedge as shown in Figure 2.9.

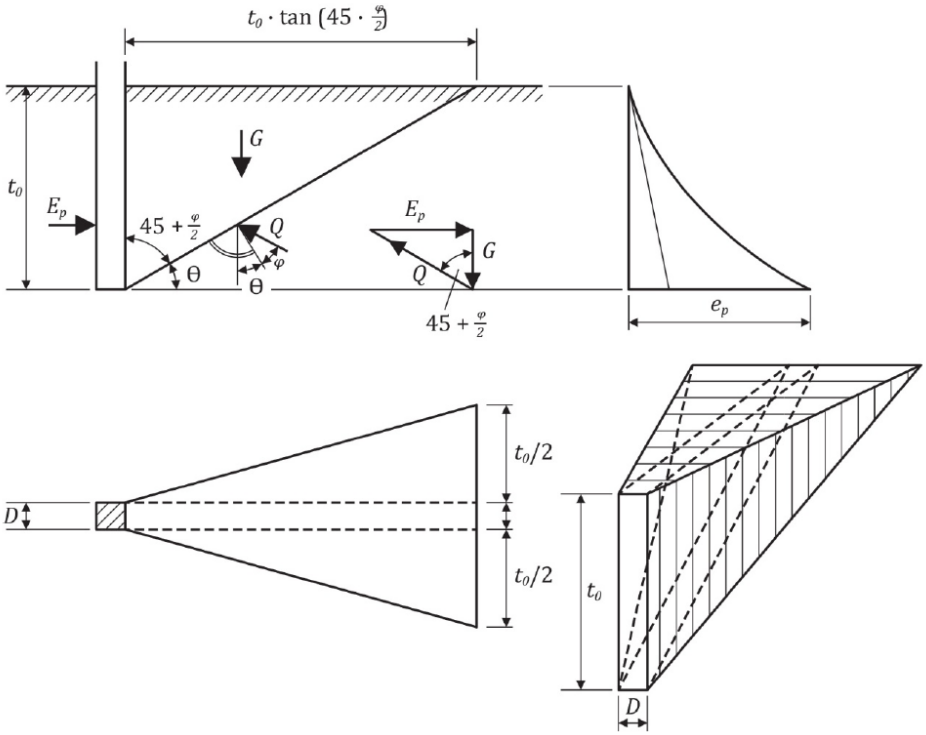

Figure 2.9: Blum soil wedges (CRW C1005, 2018)

Furthermore, the required penetration depth can be calculated utilizing n Equation 2.7, which states an equilibrium between the berthing force and force delivered by the soil.

$$\frac{24P}{f_w} = t_0^3 \frac{t_0 + 4b}{h + t_0} \tag{2.7}$$

In which:

P = Horizontal force at static loading [kN]
f_w = Soil resistance $\left[\text{kNm}^3\right] = \gamma\lambda_p$
λ_p = Passive pressure coefficient $= \frac{1+sin\phi}{1-sin\phi}[-]$
Φ = angle of internal friction [deg]
γ = Dry volumetric weight $\left[\text{kNm}^3\right]$
t_o = Theoretically necessary penetration depth [m]
b = Width of pile [m]
h = Height of load P [m]

Because Blum made some crude estimations, there are limitations with this method:

- Only homogeneous and non-cohesive soils are applicable
- The assumption that a full passive resistance is achieved makes this an ultimate strength model
- Solely the failure loads can be considered
- Different cross-sections of the pile cannot be taken into account

Brinch-Hansen did improve this model to make it applicable for layered and cohesive soil (Ruigrok, 2010).

2.3.2. P-y curves

P-Y curves are a fundamental tool used in geotechnical engineering and structural analysis to model the lateral response of a pile (or a sheet pile wall) embedded in soil subjected to lateral loads. The name ”P-Y” comes from the variables involved in the curve: P represents lateral soil force acting on the pile, and Y represents the lateral deflection of the pile, see Figure 2.10. The behaviour of a pile under lateral load is complex, as it involves the interaction between the pile and the surrounding soil. The P-Y curves are empirical curves developed to represent the lateral soil resistance along the depth of the pile. They help engineers understand how the soil's lateral resistance changes at different depths as the pile deflects laterally due to applied loads.

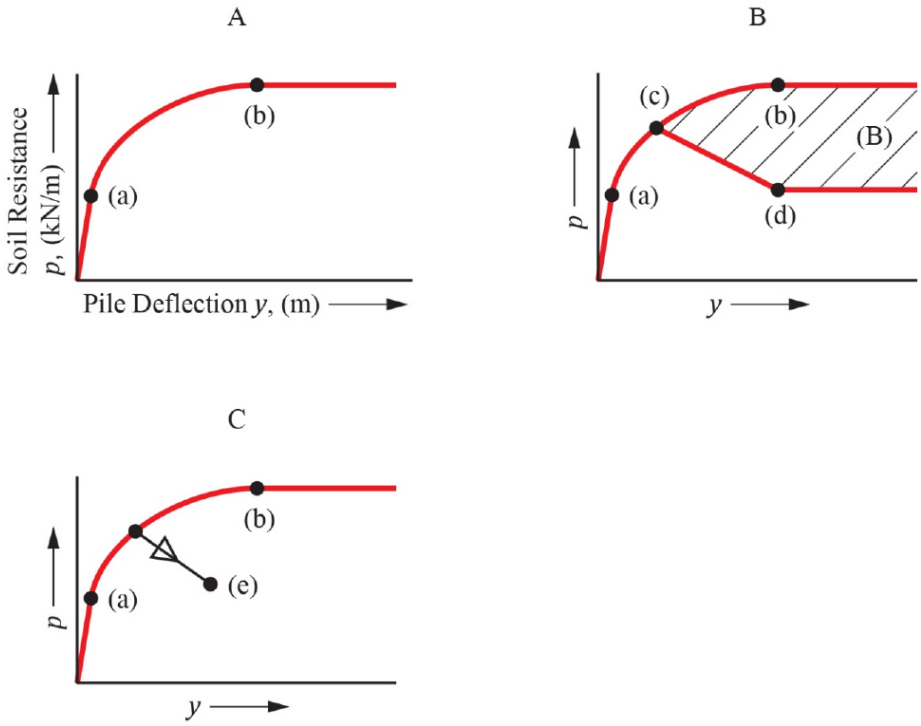

Figure 2.10: Usual shapes of p-y curves. A = static, B = cyclic, C = sustained loading (Ruigrok, 2010)

These curves are developed based on extensive research and testing in the field and laboratory (American Petroleum Institute, 1993). The curves account for the linear and non-linear behaviour of soil. For small defections, the soil responds linearly, while for larger displacements the soil responds non-linearly due to yielding. As the pile deflects laterally, it mobilizes the soil which is illustrated in the P-Y curves. The shape is determined by the properties of the soil, namely the shear strength, unit weight and soil stiffness. Thus, different soils have different P-Y curves. The shape is usually determined iteratively. In an initial analysis, the soil displacement is estimated and then the corresponding forces are calculated. These forces are then again used to determine the deflection. This process is repeated until convergence is reached. The exact details of the curves and how to use them in the design of dolphins are prescribed in the CRW C1005 (2018).

2.3.3. Finite Element Method

The finite element method (FEM) is a powerful tool for analysing the behaviour and design of geotechnical structures (Potts and Zdravkovic, 1999). One such program is PLAXIS. Herein, the dolphin and its surrounding soil are modelled and divided into a finite elements mesh, which can either be 2D or 3D. The soil properties are assigned to each element in the model. Within each element, the displacement and stress distribution are approximated. The governing equations for the dolphin structure, such as the equations of equilibrium and compatibility, are transformed into weak or variational forms. These

forms involve multiplying the equations by appropriate test functions and integrating over the element. The element equations are assembled to form a global system of equations. This system represents the entire dolphin structure and its interaction with the surrounding soil. Numerical techniques, such as direct matrix inversion or iterative solvers, are used to solve the system and obtain the displacements, stresses, and strains within the structure. Boundary conditions are applied to the model to represent the real-world constraints and loading conditions. For example, fixed supports can be applied to the dolphins' foundations to simulate their interaction with the soil. Loadings, such as wave loads or forces from connected structures, can also be applied to the dolphins. Once the system is solved, the FEM provides detailed information about the response of the dolphins under various loading conditions. This includes displacements, stresses, strains, and safety factors. The results can be used to assess the structural integrity of the dolphins, optimize their design, and ensure they can withstand the expected loads and environmental conditions.

PLAXIS 3D gives the most accurate representation of the forces within the dolphin and soil behaviour (Jasper Focks et al., 2015). Yet this design model has its cons. PLAXIS 3D requires many input parameters which can only be acquired by extensive laboratory testing. Besides that, this advanced model also requires long computation times, making the program time-consuming and expensive to use.

Table 2.1: Comparison of different design models

Calculation model	Pros	Cons
Blum Method	- Simple calculation - Fast	- Only applicable for one soil - Only in the ULS
P-Y curves	- Relatively fast - Easy to automate calculation process	- Still simplification of real-world process - Overestimates displacement
FEM	- Most accurate	- Slow - Computationally intensive - Requires many inputs

2.4. Main dimensions of the dolphin determined by the governing failure modes

The dolphin has many failure modes, a number of which are already mentioned in Subsection 2.1.2. For the main dimensions, four are the most important, namely yielding of steel, local buckling, geotechnical failure and fixity (Figure 2.12). The design steps to determine the dimensions of the dolphin are summarised in Figure 2.13. However, these steps will be updated in the new version of the handbook.

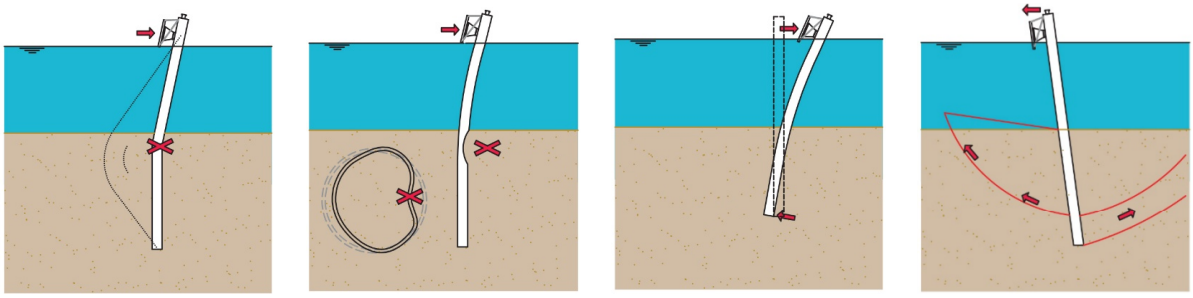

(a) Limit state yield **(b)** Limit state local buckling **(c)** Limit state fixity **(d)** Limit state geo

Figure 2.12: Failure modes considered (CRW C1005, 2018)

For the design of the dolphin, different calculation combinations are necessary to pass the limit state checks. These combinations are shown in Figure 2.11.

Limit State	Calculation objective	Soil parameters		Bed level		Impact level		Berthing energy		Berthing load	Acting load
		Low	High	DD_{low}	DD_{high}	Low	High	E_{SLS}	E_{ULS}	Output	Input
Breasting dolphin without fender											
B1) ULS-STR	Bending moments for dolphin and forces on elements		design		x	x			x	$F_{s;STR1;d}$	γ_{Sd} x $F_{s;STR1;d}$
B2) ULS-STR	Bending moments for higher section transitions		design		x		x		x	$F_{s;STR2;d}$	γ_{Sd} x $F_{s;STR2;d}$
B3) ULS-GEO	Minimum pile length and bending moment for lower section transitions	design		x		x			x	$F_{s;GEO;d}$	γ_{Sd} x $F_{s;GEO;d}$
B4) SLS	Maximum deformation	char.		x			x	x		$F_{s;SLS;k}$	-
Mooring dolphin											
M1) ULS-STR/ GEO	Bending moments and pile length for dolphin and forces on elements	design		x			x	n/a	n/a	n/a	$F_{s;max;d}$
M2) SLS	Deformation	char.		x			x	n/a	n/a	n/a	$F_{s;max;k}$
M3) ALS	Bending moments dolphin	char.		x			x	n/a	n/a	n/a	$F_{s;ALS}$

Figure 2.11: Calculation steps for the limit states CRW C1005

2.4.1. Yield

Upon impact with the ship, a bending moment occurs in the dolphin. This bending moment leads to stress in the pile and when this stress exceeds the elastic limit of steel, the structure deforms permanently. This deformation can cause the dolphin to be unsuitable for use, Therefore, the pile should have sufficient bending moment capacity to prevent the deformation. The capacity is determined by the cross-sectional area of the pile and the yield stress. The stress used to determine the capacity depends on the class of the cross-section as defined in NEN-EN 1993-1-1. The guidelines classify 4 classes which are based on the ratio of the thickness and diameter of tubular piles. These classes determine the limits of resistance, rotation capacity and analysis method. These classes are:

- Class 1 Plastic: These sections can offer full plastic hinge without reduction in resistance due to local buckling. These sections have full plastic moment capacity.
- Class 2 Compact: These sections can develop their full plastic moment resistance, similar to Class 1. However, they have limited rotation capacity because local buckling in specific parts might occur before reaching full plastic deformation.
- Class 3 Semi-compact: Here full elastic moment capacity is allowed to be used for calculations.
- Class 4 Slender: these sections have limited effectiveness because they experience local buckling before yield strength is reached.

Besides the classes, an important factor to take into consideration when designing the dolphin is the allowance of corrosion. Over the lifespan of a dolphin, the cross-sectional area will become smaller due to the loss of thickness in the pile. Thereby lowering the capacity of the bending moment. The NEN 6766 provides a guideline on how to design for corrosion. Possible strategies could be employing coatings, cathodic protection or designing an over-thickness for corrosion allowance.

- Coatings only protect the dolphin for a limited duration of 5 to 15 years and have a risk of local corrosion if the coating is imperfect. It is recommended to coat a dolphin from the top to just below the waterline and the remaining part with cathodic protection.
- Cathodic protection reduces the electric potential of a dolphin by placing sacrificial anodes. These anodes last 25 years so replacement is also necessary.

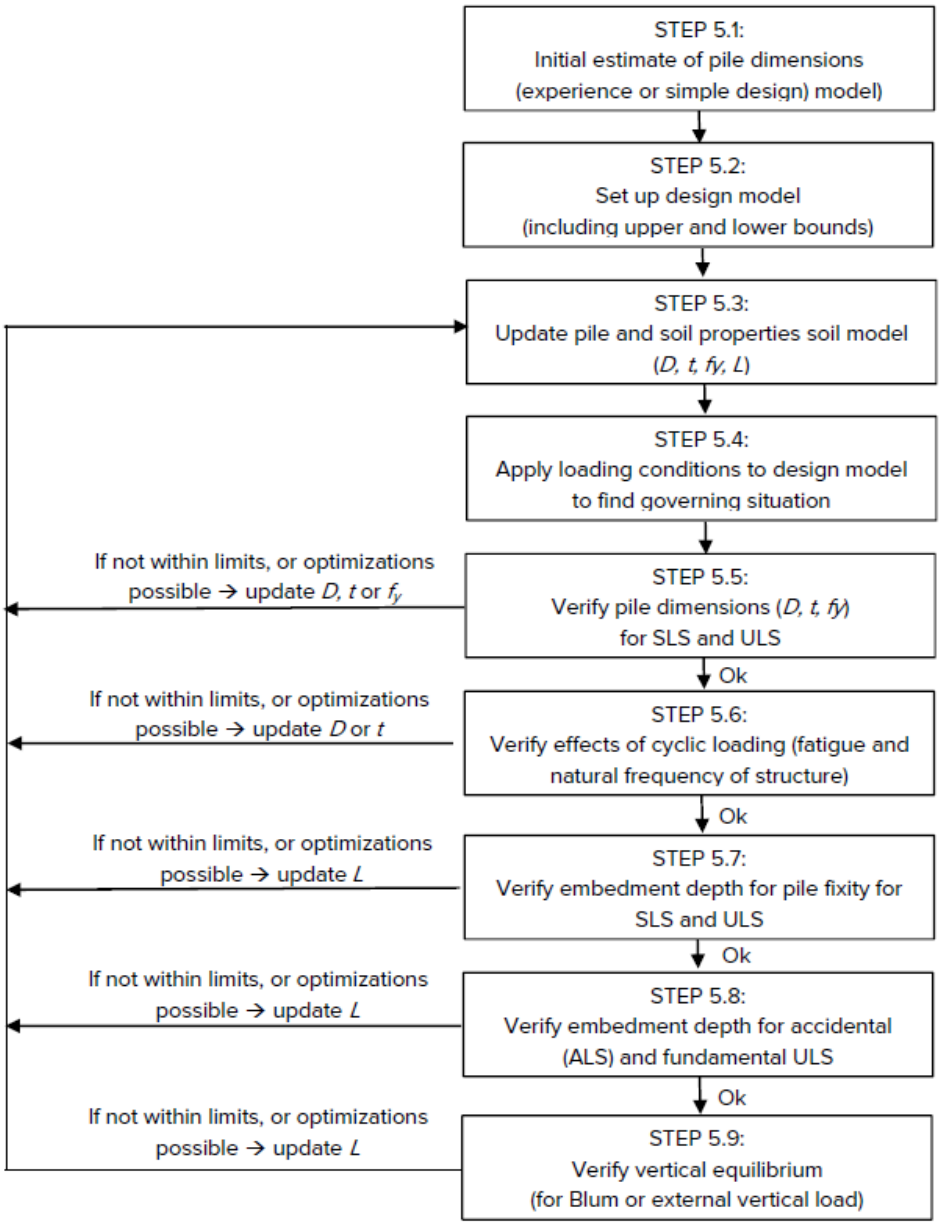

Figure 2.13: Design steps of dolphin CRW C1005 (2018)

- Over-thickness in the pile will account for the decrease in moment of resistance and inertia, but in turn causes the dolphin to be able to absorb less energy. To determine the reserve, an estimate of the corrosion rate must be made. These are found in the NEN 6766 as well.

2.4.2. Local buckling

Local buckling is a phenomenon that occurs in slender structural elements, such as beams, columns, or plates, when they experience compressive loads. It refers to the sudden and localized deformation or failure of a portion of the element due to the compressing stresses exceeding its capacity to resist buckling. When a slender structural member is subjected to compressive loads, it may buckle or bend out of its original straight shape. Local buckling specifically refers to the buckling of a short segment or section within the member, rather than the overall buckling of the entire member. This localized buckling is typically observed in thin-walled or thin-flanged members, where a portion of the cross-section becomes unstable under compression. The chosen method is Gresingt's mehtod.

To avoid local buckling, engineers can take several design measures, such as decreasing the section's slenderness ratio (the ratio of length to width or thickness), using thicker materials, introducing stiffeners or bracing, and choosing appropriate cross-sectional shapes. These design techniques help to improve the member's resistance against buckling and enhance its load-carrying capacity under compressive loads. The zones that need to be checked for a dolphin together with the assessment are illustrated in Figure 2.14.

	Clay	Sand loose	Sand moderately/dense
		q_c < 7 MPa, at reference soil stress of 100 kPa	q_c > 7 MPa, at reference soil stress of 100 kPa
Zone 1	EN 1993-1-1 or EN 1993-1-6		
Zone 2	EN 1993-1-1 or EN 1993-1-6, including one-sided soil pressure	CUR 211[E]-2013 para. 6.6.6.2 Ovalization induced by one-sided soil pressure and bending moment Empty tube	CUR 211[E]-2013 para. 6.6.6.4 Ovalization induced by one-sided soil pressure and bending moment Sand fill: E_{sand} = 5 MPa
Zone 3	EN 1993-1-1 or EN 1993-1-6	CUR 211[E]-2013 para. 6.6.6.4 Ovalization induced by bending moment E_{sand} = 5 MPa	CUR 211[E]-2013 para. 6.6.6.4 No ovalization induced by one-sided soil pressure E_{sand} = 10 MPa

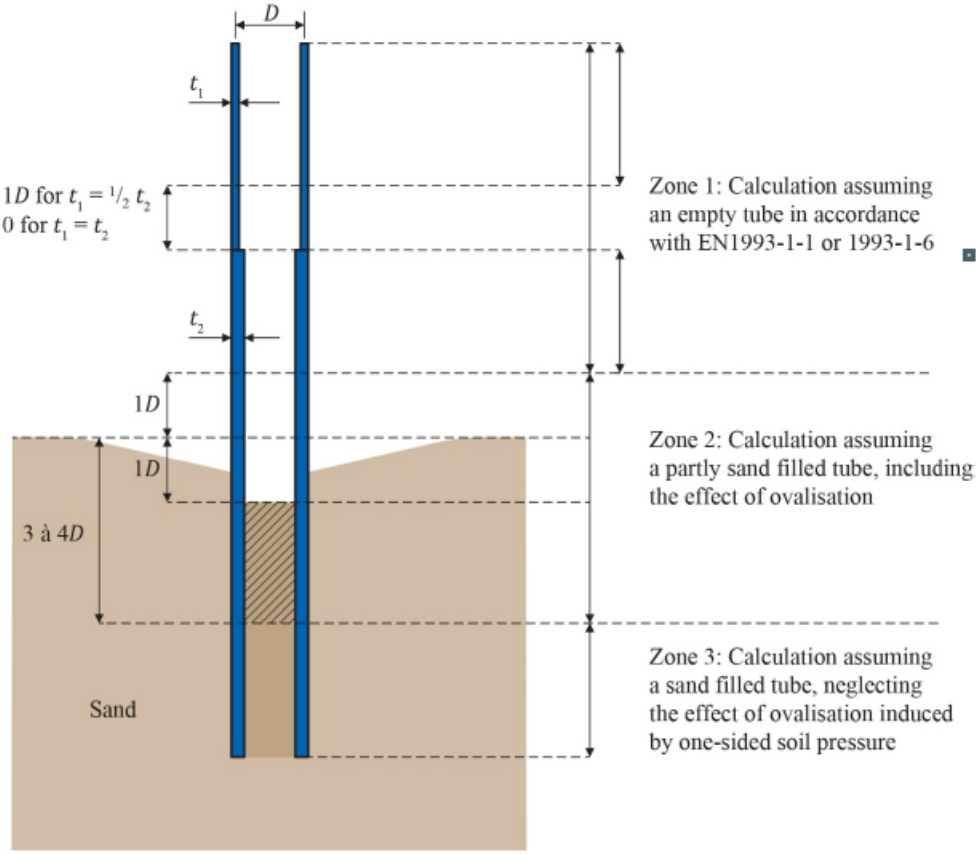

Figure 2.14: Cross section checks for buckling (CRW C1005, 2018)

2.4.3. Fixity

To ensure that dolphins do not end up tilted, it has to suffice the fixity criterion. The criterion as described in the CRW C1005 (2018) will be updated in the newer version. The old version prescribed that the pile which is 5 times the diameter deeper than the toe level, should have a deflection that is less than 2% of the designed pile. This test came with some challenges, for instance, in certain cases the

pile designs would need to have quite conservative toe levels in order to meet the criterion. Another challenge was the difference in pile lengths when using different calculation models to model the soil-structure interaction.

This updated criterion is different per design model and used to optimise the pile toe level. For PY-curves, the fixity is defined as follows. Firstly, a check must be conducted that the lowest spring in the does not reach 100% mobilisation in ULS conditions. Then the berthing energy in SLS conditions and lower soil characteristics should lead to not more than 50% mobilisation of the deepest spring. This calculation should be based on the second impact load. Studies and load testing have shown that after the first impact, the pile does not retreat to its original position. Thus, the second impact has a stiffer behaviour. A practical approach to applying this principle to the PY-curve is shown in Figure 2.15.

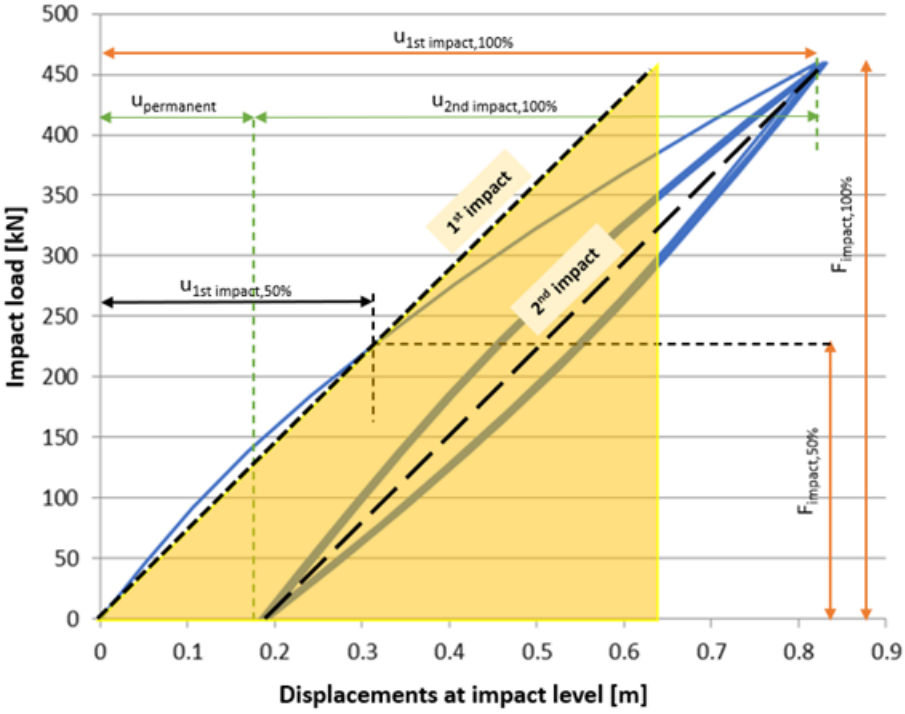

Figure 2.15: Reloading curve for second impact load CRW C1005

2.4.4. Geotechnical failure

Lastly, the geotechnical failure mode is an important failure mode to consider. Specifically, the failure due to the lateral soil pressure. During the berthing procedure soil pressure can rise and this can lead to instability of the soil. This has dire consequences because the dolphin can then collapse potentially damaging ships or injuring workers. Even a tilt in the dolphin can disrupt port operations. That is why this failure mode is averted through conservative values and designs. The dolphins should also be designed in such a way that they first fail structurally before they can fail geotechnically. The geotechnical check when using PY-curves is that there should not be 100 % mobilisation of the soil springs.

2.5. Conclusion

In this chapter multiple aspects of the design approach of the dolphin are mentioned. For the soil structure interaction, the PY-curves are used, because of their combination of fast calculation time and accurate results. Corrosion is not considered in the research as the dolphins have cathodic protection. So to conclude this chapter by answering the first research question, the critical limit states when designing a dolphin are yield, buckling, fixity and geotechnical, because these failure modes determine the main dimension of the pile and have severe consequences.

3

Principles for probabilistic analysis

In this chapter, the probabilistic analysis and statistical properties of variables used in this study are explained, which corresponds to approach step number 2 and 3. These steps are necessary to perform for the assessments of dolphins, Section 3.1 reviews how probabilistic analyses are done and then Section 3.1 goes more in-depth on how statistical values of the relevant variables are defined. Then Section 3.3 shows an existing framework on a Bayesian update. At last, Section 3.4 answers the second sub-question.

3.1. General probabilistic methods

3.1.1. Probability of failure

A structure is defined reliable when during its lifetime the Resistance R is larger than the load S. This is simply defined as the limit state Z, Equation 3.1.

$$Z = R - S > 0 \tag{3.1}$$

If the resistance is greater than the load then the structure is safe. However, many uncertainties come with the load and resistance. Therefore, a probability of failure is determined to take these uncertainties into account as Equation 3.2 shows.

$$P_f = P(Z < 0) = P(S > R) \tag{3.2}$$

For the design, a consequence class is defined which determines the accepted probability of failure. It is common to define the probability of failure in terms of reliability index β., which is related to the probability of failure following Equation 3.3.

$$P(Z < 0) = \Phi\left(\frac{0 - \mu_z}{\sigma_z}\right) = \Phi\left(-\frac{\mu_z}{\sigma_z}\right) = \Phi(-\beta) \tag{3.3}$$

Where,

Φ = Probability distribution function of normal distribution
β = Reliability index

Recall Equation 3.4, where during the lifespan of a structure the probability of failure is below the defined threshold. Herein, the resistance (R) and load (S) are seen as stochastic variables dependent on time. subsection 3.2.4 shows the different time variations of the processes. During the lifespan of a structure, usually, the resistance deteriorates and the load increases. For the classical reliability analysis, the literature does not look at the variation of time, but simply assumes the minimum resistance and the maximum load during the time frame, as shown in Equation 3.5.

$$P_f(t) = 1 - P((R(\tau) > S(\tau)) \text{ for all } \tau \in (0, t)) \tag{3.4}$$

$$P_f' = 1 - P(R_{max} > S_{min}) \tag{3.5}$$

The problem with such an analysis is that the probability of failure is overestimated. See the following example by Wang (2021).

Suppose that the resistance and load change in time according to Equation 3.6.

$$\begin{aligned} R(t) &= X_R \cdot (4 - \frac{t}{50}) \\ S(t) &= X_S \cdot (2 - \frac{t}{50}) \end{aligned} \tag{3.6}$$

Whereby X_R and X_s are two statistically independent variables both following a lognormal distribution with a mean value of 1 and standard deviation of 0.2. Following Equation 3.4, the probability of failure becomes:

$$P_f(0,50) = 1 - P\left(4X_R > 2X_S \cap 3X_R > X_S\right) = 1 - P\left(\frac{X_R}{X_S} > \frac{1}{2}\right) = 0.0067$$

While approximating the failure as Equation 3.5, the probability of failure is:

$$P_f(0,50) = 1 - P\left(3X_R > 2X_S\right) = 1 - P\left(\frac{X_R}{X_S} > \frac{2}{3}\right) = 0.0738$$

Thus, when using the minimum and maximum values the failure probability is extremely overestimated. A correct estimate would be looking at the probability of the failure over time. Until now the reliability-based assessment of dolphins has been done time-independent. A time-dependent assessment may offer a much better indication of the probability of failure. Wang (2021) mentions that in a unique case whereby the resistance remains constant in time but the load is time-variant, then the probability of failure can be defined as Equation 3.7.

$$P_f = 1 - (R > S_{max}) \tag{3.7}$$

This transforms Equation 3.4 into a classic reliability analysis, which can be solved using the common probabilistic techniques. This method is also suggested by Li et al. (2023) to deal with the time dependency by eliminating the parameter time by introducing the lifetime as one unit. So, using the lifetime maximum the probability of failure can be determined. The difficulty lies in determining the probability distribution of the maximum load effect. This problem can only be overcome with extensive data mining, experiments and surveys over time.

3.1.2. Probabilistic techniques

For solving the probability of failure, different levels of analysis can be applied which can use different techniques to solve the limit state functions.

Level I

The first method aims to be a relatively simple method of estimating the probability of failure without employing complicated calculation methods. For the load the characteristic value is chosen, which is usually a value with a 5% chance of exceeding. On the other hand, the value for resistance is a low characteristic value which has a 95% chance of exceeding. Hereafter, partial factors are placed on the characteristic values to ensure the probability of failure is low enough. Equation 3.8 summarises this process.

$$\frac{R_k}{\gamma_R} - \gamma_S S_k > 0 \tag{3.8}$$

The partial factors are derived from guidelines and literature. Here the partial factors are calculated with the higher levels of reliability analysis as in Equation 3.9.

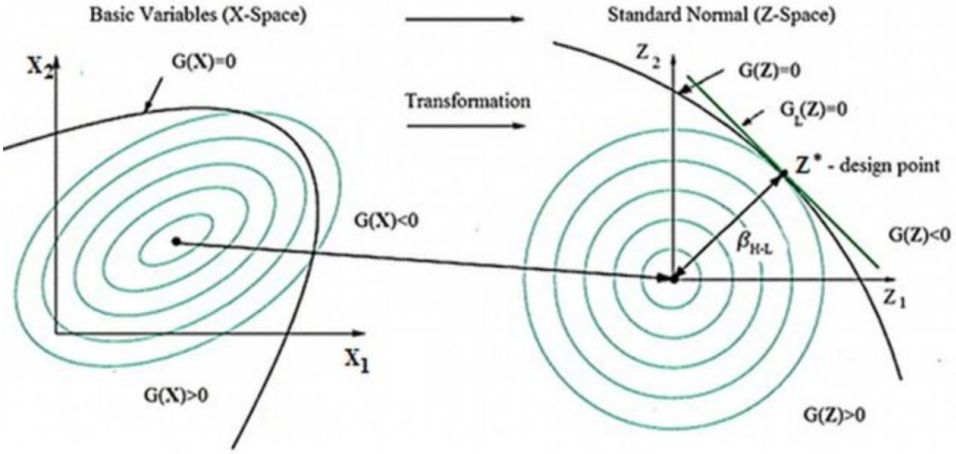

Figure 3.1: Example illustration of FORM (Dudzik, 2017)

$$\gamma_r = \frac{R_k}{\mu_r - \alpha\beta\sigma_r}$$
$$\gamma_s = \frac{\mu_s - \alpha\beta\sigma_s}{S_k} \tag{3.9}$$

Where,

$\gamma_{r,s}$ = partial factor for resistance and load variable
R_k = Characteristic value of resistance parameter
S_k = Characteristic value for load parameter
α = Influence factor
β = Reliability index
$\mu_{r,s}$ = Mean of variable
$\sigma_{r,s}$ = Standard deviation of variables

Level II

For Level II methods, typically, only the mean values of fundamental variables and the first and second-order moments (covariance matrix) are employed. In many instances, the joint probability density function is streamlined, and computational complexity is diminished through the linearization of the limit state function. This linearization is commonly achieved using a technique known as the First Order Reliability Method. Within this method, the limit state function is linearized at the designated design point, which corresponds to the point on the function g(X) = 0 possessing the highest probability density. Essentially, this point represents the juncture where failure is deemed most likely. Hasofer and Lind (1974) developed the widely used technique FORM (First Order Reliability Method). The method approximates the solution by linearising the limit state surface around a specific design point and then applying probabilistic principles to estimate the reliability.

First, the design point is selected which lies on the limit state surface at the point with the highest probability density function. Then a Taylor series expansion is performed around the design point utilizing partial derivatives of the limit state function concerning the input variables. The next step is standardizing the variables by dividing the difference between the actual values and design point values by the standard deviation of those values. Hereafter, based on the standardized values and Taylor expansion the reliability index is determined. Its accuracy is limited by how well the limit state can be approximated as linear around the chosen design point.

In summary, the FORM method by Hasofer and Lind is a valuable tool for estimating the probability of failure for systems with nonlinear limit state functions. It provides a balance between accuracy and computational efficiency, making it a popular choice for practical engineering applications.

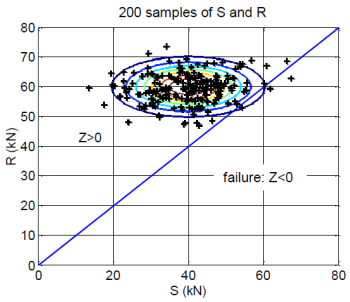

Figure 3.2: Example illustration of Monte Carlo (Jonkman et al., 2017)

Level III

When utilizing a Level III reliability analysis approach, the precise calculation of the probability of failure (Pf) involves employing exact probabilistic formulations. These formulations are determined through methods such as analytical expressions, numerical integration, or Monte Carlo simulations. The utilization of analytical expressions for problem resolution is feasible only within a restricted set of uncomplicated scenarios. Numerical integration is practicable solely when the count of fundamental variables is relatively small. The most popular method is Monte Carlo.

The Monte Carlo process starts with identifying the relevant input variables together with their probability distribution functions. From these variables and their pdf random samples are generated. For low probabilities of failure, many samples need to be generated to achieve accurate results. Using these samples in the mathematical model that describes how the structural system works, outputs are generated. Based on the failure criterion the output is placed in either failed or not failed. The ratio of failed runs to the total number of runs provides an estimate of the probability of failure.

Directional Sampling

The downside of Monte Carlo is the large amount of realisations required for an accurate result. A more effective kind of Monte Carlo simulation is Directional Sampling. Instead of realisations, this method uses directions in the parameter space. Along these directions, the failure point is searched and its corresponding distance to the origin is determined. The remaining probability of failure is determined and added to the total probability of failure. The process is illustrated in Figure 3.3.

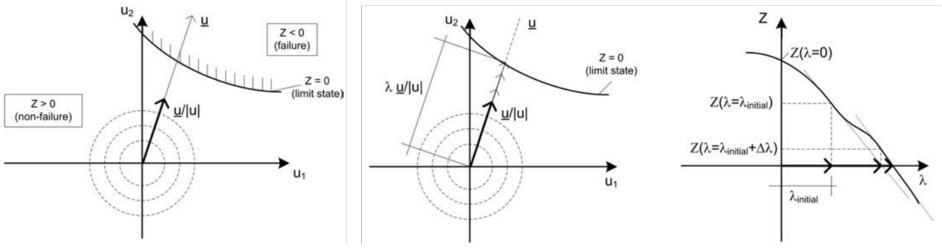

Figure 3.3: Example illustration of Directional Sampling (Schweckendiek, 2006)

For sampling techniques, the influence factors are calculated with Equation 3.10 (Deltares, 2022).

$$\alpha_j = f_{\text{normal}} \cdot \frac{\sum_{\text{failing realizations i}} u_{i,j} \cdot W_i}{\sum_{\text{failing realizations i}} W_i} \tag{3.10}$$

Where,

i = indicates a realisation in the applied technique
j = indicates a variable
u = is a realisation in the applied technique
w = is the weight of the realization (for Crude Monte Carlo: 1)
f = is a normalizing factor so that $\sum \alpha_j^2 = 1$

Response surface

Even still the vast amount of realisations needed for efficient sampling methods can remain troublesome. Therefore, Echard et al. (2011) introduced a novel approach named the Active learning method combining Kriging and Monte Carlo Simulation (AK-MCS) for structural reliability analysis. The strategy proves to be cost-effective by minimizing the number of evaluations required for the expensive performance function while maintaining highly accurate results for the probability of failure. By integrating the strengths of Kriging metamodeling and Monte Carlo simulation, the method conducts simulations by predicting the population using a Kriging metamodel based on a limited subset of evaluated population points. This focus on high-density probability configurations ensures accurate approximations primarily where Monte Carlo points are situated, instead of across the entire design space, Figure 3.4 visualises this interpolation method.

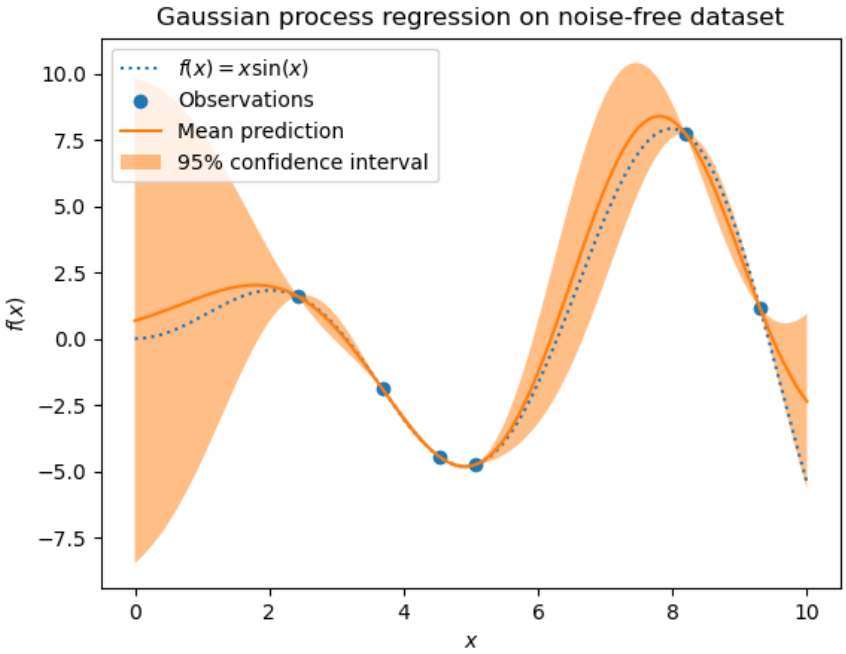

Figure 3.4: Visualisation of a Kriging, otherwise known as Gaussian Process Regression (Rasmussen and Williams, 2006)

The AK-MCS approach showcased adaptability, efficiency, and robustness across various structural reliability analysis scenarios. Its ability to reduce computational demands while maintaining accuracy presents promising prospects for various engineering applications.

3.1.3. Derivation of partial factors

Partial factors can be derived with the influence coefficients provided by the probabilistic technique. Together with the influence coefficients and the reliability index, the design point can determined by Equation 3.11.

$$X_d = F_X^{-1}\left(\Phi\left(-\alpha_X \beta\right)\right) \tag{3.11}$$

Where,

X_d = Design value of variable
F_X^{-1} = Inverse cumulative distribution function of variable
Φ = Cumulative distribution function of a normal distribution
α = Influence coefficient
β = Target reliability index

In civil engineering, the properties of the materials and loads are represented by their characteristic values. The characteristic value in the p-quantile is determined by Equation 3.12.

$$X_k = F_X^{-1}(p) \tag{3.12}$$

The quantiles are defined in EN 1992 to EN 1990. For materials and product properties the low and high characteristic values correspond to the 5- and 95-quantile (Jonkman et al., 2017). For variable loads, the EN 1990 prescribes a value corresponding to a 2% exceedance probability per year or a 50 year return period (T_r). The exceedance probability can be determined with Equation 3.13. This probability is capped off at 63.8% as shown by Jonkman et al. (2017).

$$p = 1 - \left(1 - \frac{1}{T_r}\right)^{t_{\text{ref}}} \tag{3.13}$$

With the characteristic values now defined, the partial factors can be calculated with Equation 3.14.

$$\begin{aligned} \gamma_r &= \frac{X_k}{X_d}, \text{partial factors for resistance} \\ \gamma_s &= \frac{X_d}{X_k}, \text{partial factors for loads} \end{aligned} \tag{3.14}$$

3.2. Variables used in the analysis

For the semi-probabilistic design, characteristic values are used. However, for a full probabilistic design, the expected values and their distributions are needed. Again, the variables can be categorised into structural parameters, soil parameters, load and model parameters.

3.2.1. Structural parameters

The structural parameters to be considered are the strength of the steel and the geometric properties of the pile.

Strength of steel

According to JCSS (2001) the mean value of the yield strength is given by Equation 3.15

$$f_y = f_{ysp} \cdot \alpha \cdot exp(-u \cdot CoV) - C \tag{3.15}$$

Whereby,

f_y	=	Mean steel strength
f_{ysp}	=	Nominal value of steel strength
α	=	Spatial position factor equal to 1.05 for webs of hot rolled sections and 1 otherwise
u	=	is a factor related to the fractile of the distribution used in describing the distance between the code specified or nominal value and the mean value; u is found to be in the range of -1.5 to -2.0 for steel produced in accordance with the relevant EN standards
C	=	20 MPa, a constant reducing the yield strength as obtained from usual mill tests to the
	=	static yield strength
CoV	=	Coefficient of variation

This outdated formula leads to conservative estimations of the yield strength of steel. In other studies such as Alfred Roubos (2019) and Allaix et al. (2022) a more favourable distribution is used, which are based on tests carried out by the Port of Rotterdam.

Thickness

In terms of dimensions, the normal distribution is also a suitable fit. The dimensional deviation derived from the evaluation of the data from the cross-sectional rolled products shows that the standard deviation is less than 1 mm irrespective of its geometrical property (JCSS, 2001). There exists another Eurocode, namely the NEN-EN 10219-2, which prescribes the tolerance for cold welded steel pipes.

For thickness, a maximum of 10% or 2 mm tolerance is prescribed, which is still quite large. In consultation with one of the largest suppliers of steel pipes in the Netherlands, the deviations are more akin to NEN-EN 10051 for which a tolerance of 0.63 mm to 0.7 mm is used. The distribution is assumed to a uniform because in the factory a batch of pipes is made with the same equipment. There are two ways the dolphins can be produced, both processes are shown in Figure 3.5. Spirally welded piles are cheaper and can be produced in the Netherlands, though it is limited to the diameter-to-thickness ratio. For lower ratios, the pile needs to be longitudinally welded, which is a more expensive process.

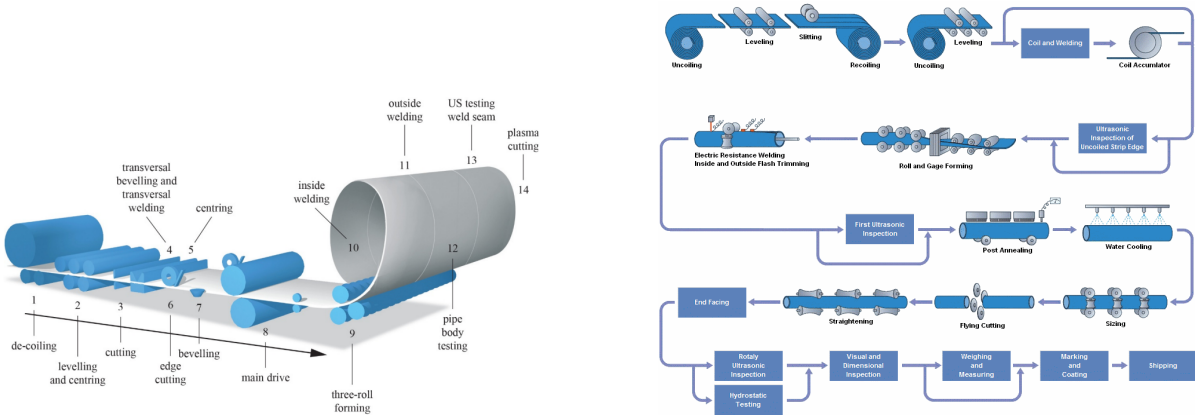

(a) Production process of a spirally welded pile (CRW C1005, 2018)

(b) Production process of a longitudinally welded pile (wermac.org, nd)

Figure 3.5: Different production processes for dolphins

Geometrical properties

Furthermore, in the design of the dolphin, different levels are of importance. First is the impact level of the vessel. In the presence of a buckling fender, the impact level remains constant. Whereas, a rigid fender plate can have multiple impact levels. This depends on how loaded the ship is and the water level, see Figure 3.6. For berthing dolphins, the stiffer circumstance will most likely be governing. This is the lower impact level of a fully loaded ship because a lower impact level leads to less deflection of the pile which in turn means that there is a higher berthing force. Because this study assumes no correlation between mass and berthing velocity (Roubos, 2017), a fully loaded ship will also lead to higher berthing energy as there is much more water displacement. So, for this study rigid fender is chosen which has the same impact level at every berth. A rigid fender has multiple connection points to the pile ranging from around water level to almost at the top of the pile. Because the sea ships have a very large freeboard, the resultant force of these two connection points is set at 1.70m + NAP. Admittedly, the fixed impact level for a rigid fender is not conventional and may be conservative, but this assumption helps this study stay within the scope. In order to properly incorporate the effect of the different water levels, a time-dependent analysis needs to be conducted which falls outside the scope of this thesis.

Secondly, the topsoil level varies throughout time as well. The level can change due to erosion and siltation. In the case of siltation, the top level increases, which is not beneficial for the absorbable berthing energy. Despite this, the effects are negligible due to the properties of the sludge, which behaves more akin to water than soil. At last, the pile toe level is seen as constant for the calculations as the tolerance during construction is very low, so the variance is inconsequential. Throughout the lifespan of a dolphin, the bed level will vary. However, the exact progression of this level can differ per location. Even more so, a combination of the time-dependent bed level, impact level and berthing load would most likely require a time-dependent analysis. For these reasons, this study uses the conservative value of the NGD, see Figure 3.7. Assuming that this level remains constant introduces conservatism in the reliability, but ensures that the probability of failure is not underestimated.

3.2.2. Soil parameters

The characteristic values of the soil parameter and their coefficient of variation are derived from Table 2b of the Eurocode 7. The weight of the soil and the angle of internal friction have been assumed

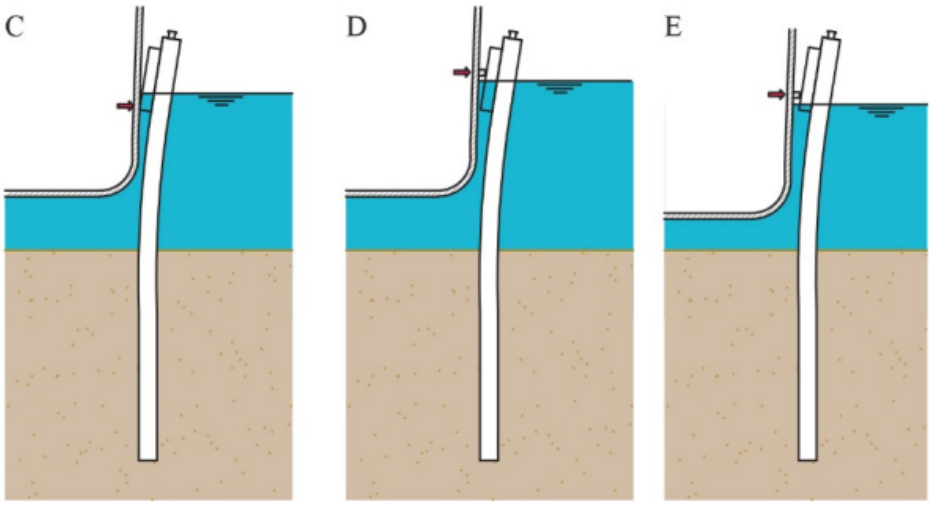

Figure 3.6: Impact level under different circumstances with C = unloaded ship, D=high water level, E=low water level (CRW C1005, 2018)

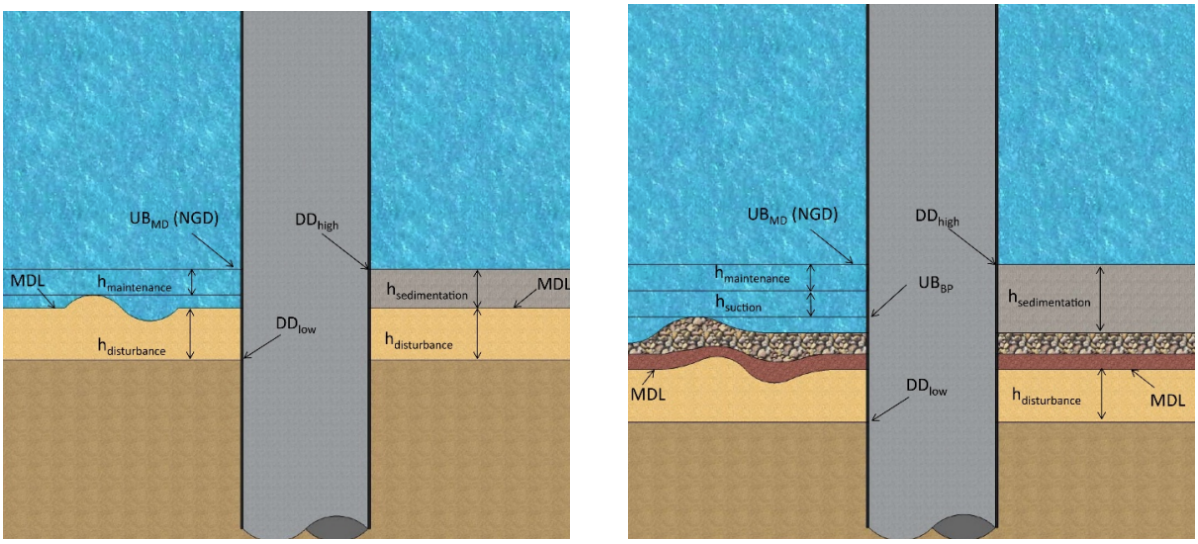

(a) Depth levels in case of no scour protection

(b) Depth levels in case of scour protection

Figure 3.7: Determination design depth level (CRW C1005, 2018)

to have a normal distribution in the literature (Heeres et al., 2023; Roubos, 2019; Wolters, 2012). In order to determine the mean values of the soil, the upper and lower values obtained from Table 2b in NEN9997-1 can be averaged.

For the mean values and standard deviation of the internal friction angle, the same method as Heeres et al. (2023) is utilised. Equation 3.16 provides the equations of the said method. Essentially, a CoV of 0.10 from Table 2b in Eurocode 7 is applied on the tangent of the friction angle. So firstly the tangent is determined. Then the mean value is determined by the mean of the high and low characteristic values used in Figure 4.1 to Figure 4.3. The distribution is a student's t-distribution. With this knowledge, the CoV of the internal friction angle is determined. Figure 3.8 gives a visualisation of the steps of deriving the distribution function from table 2b in the NEN9997-1.

$$
\begin{aligned}
\mu_{\tan\varphi} &= \tan\left(\frac{\varphi_{k;low}+\varphi_{k;high}}{2}\right) && \text{Average of } tan(\varphi)\\
\sigma_{\tan\varphi} &= \text{CoV}^{*}\mu\tan\varphi && \text{Standard deviation of } tan(\varphi)\\
\mu_{\varphi} &= \frac{\varphi_{k;low}+\varphi_{k;high}}{2} && \text{Average of } \varphi\\
\sigma_{\varphi} &= \frac{1}{\cos^2(\varphi)}\sigma_{\tan(\varphi)} && \text{Standard deviation of } \varphi\\
\varphi_{d;low} &= \mu_{\varphi}-\alpha^{*}\beta^{*}\sigma_{\varphi} && \text{Low design value of } \varphi \text{ whereby } \beta = 3.3 \text{ RC1.}\\
& && \text{The influence factor is calibrated such that } \gamma_{\varphi}=\frac{\tan(\varphi_{k:laag})}{\tan(\varphi_{d;low})} \text{ is 1,15}\\
\varphi_{\text{d;hoog}} &= \mu_{\varphi}+\alpha^{*}\beta^{*}\sigma_{\varphi} && \text{High design value of } \varphi\\
\varphi_{1,645;\text{ Low}} &= \mu_{\varphi}-1,645^{*}\sigma_{\varphi} && \text{Low characteristic value of } \varphi\\
\varphi_{1,645;\text{ High}} &= \mu_{\varphi}+1,645^{\star}\sigma_{\varphi} && \text{High characteristic value of } \varphi\\
n &= \left(\frac{1,64\sigma_{\varphi}}{\mu_{\varphi}-\varphi_{k;\text{laag}}}\right)^{2} && \text{Number of tests assuming that } \sigma_{\varphi} \text{ is known}
\end{aligned}
\tag{3.16}
$$

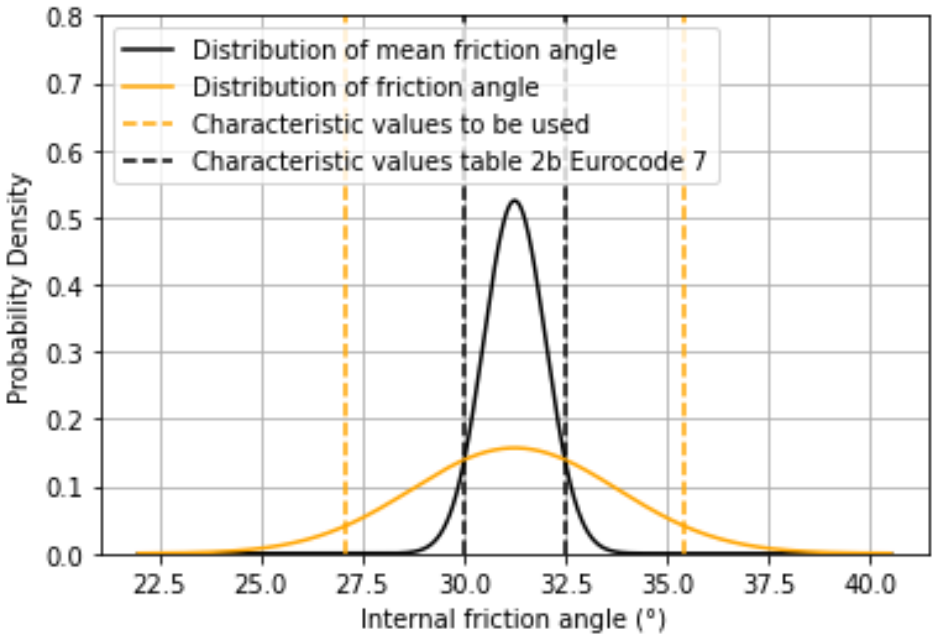

Figure 3.8: The visualisation of the steps used in Equation 3.16 to derive the distributions for the internal friction angle

The mean value of the shear stress is determined similarly, but the shear stress has a lognormal distribution (Rijkswaterstaat, 2021).

3.2.3. Berthing load

As mentioned before, the sole enacting load on the breasting dolphin is from the berthing energy. To make the berthing energy suitable for a time-independent analysis, a Monte Carlo analysis was conducted for the extreme value distribution according to recommendations for the Eurocode handbooks (Leonardo Da Vinci pilot project, 2004). The berthing energy is determined by Equation 2.1. For the water displacement, a uniform distribution derived from AIS data was used and for the velocity distributions found by 2017 (2017). These distributions are only applicable to tankers. The extreme value distribution was found by the following steps:

1. Simulating the berthing energy of 50 years and extracting the maximum value

2. That process is repeated 200 times, therefore leading to 200 extreme values
3. Fitting this data set with different distributions
4. Repeat for other navigation conditions

Multiple analyses were conducted and fitted. The results can be found in Appendix A. From the analysis, the best fit is the Gumbel distribution. Therefore, the mean and characteristic value can be easily determined with Equation 3.17 (Roubos, 2019).

$$x_p = x_{\text{ mod }} - \frac{1}{c}\ln(-\ln(p)) \cong \mu - (0,45 + 0,78\ln(-\ln(p)))\sigma \tag{3.17}$$

Assuming a characteristic fractile of 98%, the characteristic value is given as Equation 3.18 and the design value Equation 3.19.

$$Q_k = \mu(1 - (V_Q(0,45 + 0,78\ln(-\ln(p))) \tag{3.18}$$

$$Q_{\text{d}} = \mu_Q\left(1 - V_Q\left(0,45 + 0,78\ln\left(-\ln\left(\Phi^{-1}\left(-\alpha_E\beta\right)\right)\right)\right)\right) \tag{3.19}$$

With,

Q_k = Characteristic value of annual extreme
Q_d = Design value of annual extreme
μ_d = mean value
V_q = Coefficient of variation of annual mean
α = Sensitivity factor of variable

To determine the mean value for the lifetime maxima, the mean of the Gumbel distribution is moved following Equation 3.20.

$$\mu_{lifetime} = \mu_{annual} + \frac{ln(t_{ref})}{\alpha} \tag{3.20}$$

Where,

$\mu_{lifetime}$ = Mean value of lifetime extreme
μ_{annual} = Mean value of annual extreme
t_{ref} = Reference period
V_q = Coefficient of variation of annual mean
α = Scale factor of Gumbel distribution

3.2.4. Model parameters

Model parameters account for the uncertainty that arises from simplification, approximations and assumptions made when creating a mathematical model to represent the behaviour of a structure. Because no mathematical model can capture the complexities and intricacies of real-world structures completely, the parameter is added to the limit state functions to help account for this uncertainty. This has a significant impact by reducing the reliability, as shown by Roubos (2019). The model uncertainty is seen as a random variable, which statistical properties can be derived from either experiments or observations. Preferably, the parameter should obtained from experiments. However, in most cases, the experiments are lacking or introduce measurement errors as well. Thus, the uncertainties are determined by engineering judgment. JCSS (2001) recommends a lognormal distribution for the bending moment capacity with a mean of 1 and CoV of 0.1. For the buckling reduction factor, a normal distribution with a mean of 1 and CoV of 0.1 was found for quay walls (Peters et al., 2017).

However, both Griffioen (2023 and Peerden (2023) have shown that FEM models and PY-curves tend to be more conservative calculation models. When comparing measurements from the test loads done by Griffioen (2023) and modelling with the PY-curves the models typically overestimate the maximum moment. Each load applied to the dolphin in the Calandkanaal was modelled with the PY-curves using the expected values for the soil properties, same as the values used by Griffioen (2023). For each step, the maximum course of the bending moment looked like Figure 3.9. When assessing all the load steps with corresponding calculated maximum moments, the mean for the model uncertainty is 0.94 with a standard deviation of 0.05.

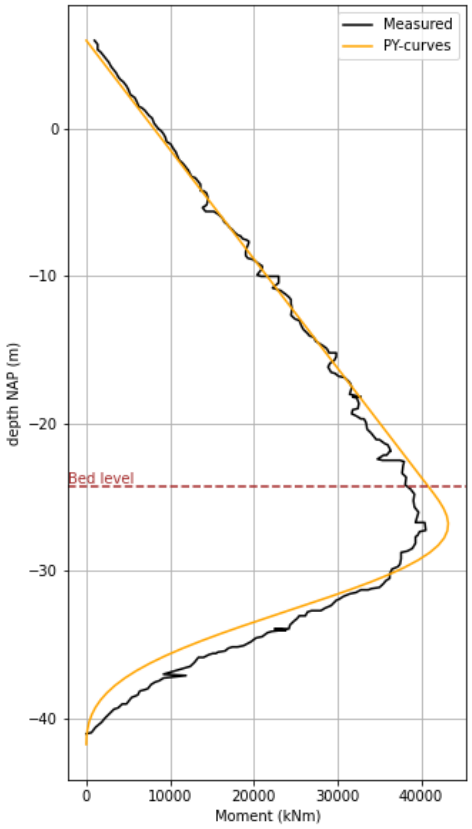

Figure 3.9: Typical comparison between measured and calculated moment

3.3. Improving the reliability with a Bayesian update

3.3.1. Framework Bayesian update

When analysing the probability of failure, the assessment is often based on expert judgement and historical or preliminary analysis. This initial assessment is referred to as the prior reliability assessment. Here, no new data or observations are taken into account. However, when new data or observations become available the prior reliability can be updated. This newly updated reliability is called posterior reliability. This is a refined estimate of the probability of failure. The update is constructed based on the Bayes' rule (Bayes, 1763) in Equation 3.21.

$$P(A \mid B) = \frac{P(B \mid A)P(A)}{P(B)} \tag{3.21}$$

Schweckendiek (2014), as well as van der Krogt (2022), describe the observation based on the type of information, namely:

- Inequality information: This pertains to cases where observations contain details indicating whether a limit state has been surpassed. For instance, when survival information is available. This is denoted as $h(x) > 0$
- Equality information: This type of information comes into play when observations provide insights into the measured performance value. An example is displacement measured at a certain force. This is symbolised as $h(x) = 0$

Inequality information can be added to Equation 3.21 transforming it into Equation 3.22.

$$P(\mathsf{F} \mid \varepsilon) = \frac{P(\mathsf{F} \cap \varepsilon)}{P(\varepsilon)} = \frac{P(g(\mathbf{X}) < 0 \cap h(\mathbf{X}) < 0)}{P(h(\mathbf{X}) < 0)} \tag{3.22}$$

The problem with equality information is that the denominator in Equation 3.22 is 0, because the probability of $h(x) = 0$ is 0. Straub (2011) proposes a solution to turn the equality information into inequality. The observation function is rewritten as Equation 3.23.

$$h(\mathbf{x}, u) = u - \Phi^{-1}(c \cdot L(\mathbf{x})) \tag{3.23}$$

With,

u = Outcome of standard normally distributed variable
$L(\mathbf{x})$ = Likelihood of observation $P(\varepsilon \mid \mathbf{x})$
Φ^{-1} = Inverse cumulative distribution function of the standard normal distribution
c = Normalising constant to keep the likelihood between 0 and 1

The likelihood function can be written as follows in Equation 3.24.

$$L(\mathbf{x}) = f_{e_m}[s_m - s(\mathbf{x})] \tag{3.24}$$

Where,

f_{e_m} = PDF of the measurement error
s_m = Measured value
$s_{(x)}$ = Calculated value

Most measurement errors follow a normal distribution, whereby the likelihood function can be written as Equation 3.25.

$$L(x) = \frac{1}{\sqrt{2\pi\sigma^2}} e^{-\frac{(x-\mu)^2}{2*\sigma^2}} \tag{3.25}$$

With,

μ = Mean of measurement value
σ = Standard deviation of measurement
x = Calculated value according to mathematical model

With the PDF of the likelihood function known, the normalising constant can also be determined. The normalising constant is equal to the maximum of the likelihood function (Equation 3.26).

$$c = \sqrt{2\pi\sigma^2} \tag{3.26}$$

3.3.2. Incorporating data from test loading

Zhang (2004) shows how data from load tests can be used to update the reliability of foundation pile capacity. It is recommended to use a larger load than the design loads in the test because this will give more information about the capacity statistics. It is further mentioned that it is not particularly necessary to reach failure as all results can help update the probability of failure. The load to be carried out for an update is recommended as 1.5 times the design load. Albeit, the failure of the tested foundation pile is accepted.

Even though there are many stop-criteria defined for test loading (Lantsoght et al., 2017), there is still little attention paid to the relation between the magnitude of the test load and the structural reliability (de Vries et al., 2022). Preliminary analysis shows that high-proof loads should be applied to demonstrate the reliability index (Lantsoght et al., 2017).

3.3.3. Incorporating AIS-data

Port authorities have also started collecting data transmitted by vessels. This is called Automatic Identification System (AIS). This information typically includes:

- Position data
- Speed over ground
- Navigational Status

- Vessel dimension
- Type of vessel

This data can be used when determining the berthing energy. Heeres et al. (2023) showed that the reliability increases significantly when adding site-specific knowledge on vessel calls to the extreme value analysis. The reliability increases from 3.59 to 4.87. An updated distribution for berthing energy can thus be of prolific use when assessing the reliability of a dolphin.

An alternative method of proof loading could also be measured during the user phase of a structure. Updating based on maxima events can prove a viable solution in planning maintenance and monitoring programs (de Koker at al., 2020).

In addition, using the information on the survival of construction can aid in the reliability update (Allaix et al., 2022). This proven strength method could also be applied to the dolphin as every berthing could be seen as a proof load. This progression of the probability of failure over the structure its lifespan is described with the bathtub curve (Jonkman et al., 2017).

An example of how data from proof load measurement, increase in load trend and deterioration could help extend the lifespan of a bridge was demonstrated by de Vries et al. (2022) in Figure 3.10. Due to the increasing traffic and deterioration, the bridge drops down below the annual reliability. Then a proof load is executed to assess its structural reliability. This leads to an extension of its lifespan. The magnitude of the load is chosen such that the lifespan is extended by 10 years. Such a strategy could also be used for dolphins but has yet to be seen what increase there may be.

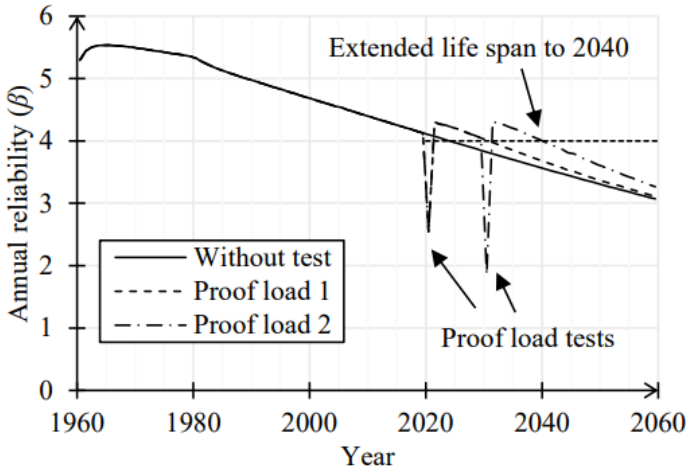

Figure 3.10: Effect of proof load testing on annual reliability (de Vries et al., 2022)

3.4. Conclusion

To summarise, there are multiple techniques to determine the probability of failure and require stochastic input variables. The design variables which influence the probability of failure of the dolphin can be categorised. The first category is the structural parameters, which consist of the yield strength of steel and the thickness of the pile. Their statistical properties can be derived from the literature. Then there are the geometrical properties, however, they are seen as deterministic to keep the research within the time-independent scope. Next are the soil parameters, like the volumetric soil weight, internal friction angle and shear stress. The characteristics of the values are also derived from literature. Furthermore, the model uncertainty influences the probability of failure. The distributions are determined by comparison of measurements with calculated values. Lastly, the berthing load is of importance and its statistical properties were determined with the help of Monte Carlo simulations. The specific values of all these input variables depend on the case study. These are presented in the next chapter.

4

Introduction to the case studies

In this chapter, the case studies and their corresponding variables are presented, which is approach step number 4. The case studies are fictitious but are based on real examples in the Netherlands. The difference lies in the soil stratification and the navigation conditions. Section 4.1 shows the different variations. In Section 4.2 the limit states are repeated and their functions are presented. The variables and their distribution are summarised in Section 4.3.

4.1. Introduction to cases

The different cases to be assessed are shown in Figure 4.1 till Figure 4.6. The different soil compositions were chosen to assess whether the results are generically applicable to all soil investigations. The first 3 cases cover the spectrum of soils found in Dutch harbours. Case ”Clay” (Figure 4.1) represents very loose soil which can be found in the Botlek area. Case ”Sand” (Figure 4.2) on the other hand models a much more dense soil composition that is usually found in the Maasvlakte. Finally, case ”Mix” (Figure 4.3) is a soil composition in between those two, with multiple clay layers throughout. Such soil compositions can be located in the Port of Amsterdam. While the soil investigations are fictional, the soil parameters are heavily inspired by projects in those locations. The properties of those soils were derived from Table 2b in Eurocode 7. Their respective semi-probabilistic designs are in Appendix B.

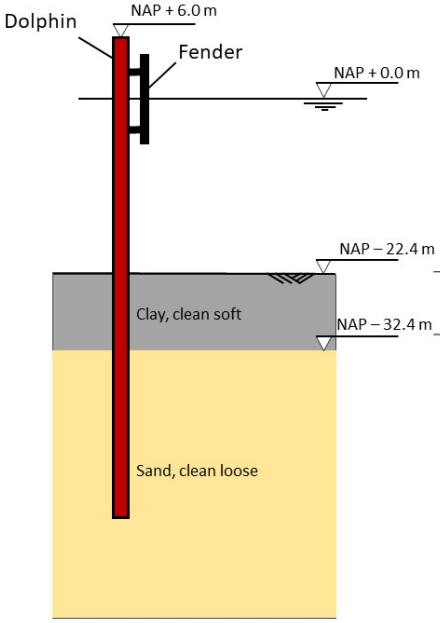

Soil type	Top layer	Bottom layer	Υ_{sat} [kN/m³]	C_u [kPa]	φ [°]
Clay, clean soft	NAP-22.4m	NAP-32.4m	14	25-50	
Sand, clean loose	NAP-32.4m		19	-	30-32.5

Figure 4.1: Case ”Clay” with characteristic soil properties from table 2b in Eurocode 7

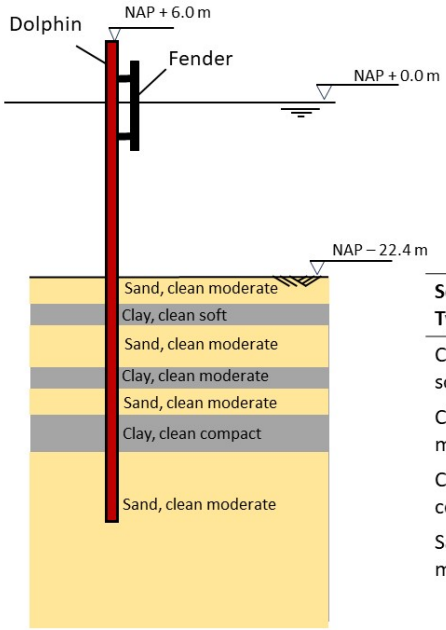

Soil Type	Top layer	Bottom layer	Υ_{sat} [kN/m³]	C_u [kPa]	φ [°]
Clay, clean soft	NAP-24.4m	NAP-27.4m	14	25-50	
Clay, clean moderate	NAP-32.4m	NAP-37.4m	17	50-100	
Clay, clean compact	NAP-40.4m	NAP-43.4m	20	100-200	
Sand, clean moderate			20	-	32.5-35

Figure 4.2: Case ”Mix” with characteristic soil properties from table 2b in Eurocode 7

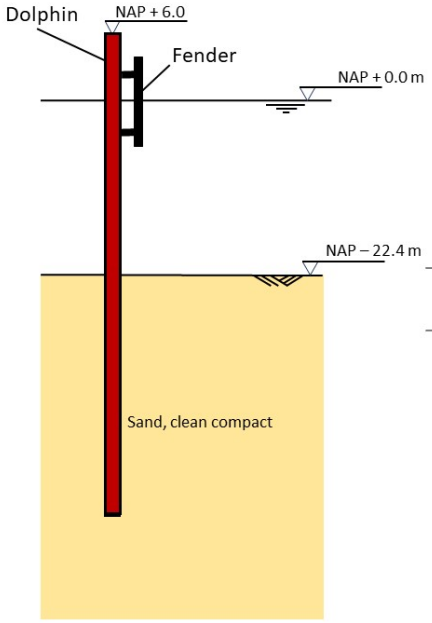

Soil type	Top layer	Bottom layer	Υ_{sat} [kN/m³]	C_u [kPa]	φ [°]
Sand, clean compact	NAP-22.4m		22	-	35-40

Figure 4.3: Case ”Sand” with characteristic soil properties from table 2b in Eurocode 7

In addition to the normal case ”Clay”, there will also be a case of a dolphin designed according to the standards of Port of Rotterdam. The wall thickness of the supplied dolphins to the Port of Rotterdam is measured and it should be exactly the designed measurements. In addition, the yield strength is tested until the minimum stress is achieved in the dolphin without failing. For this case, the stochastic variable of the wall thickness will be set as deterministic and the yield strength will be truncated at the minimum allowable yield tress of X70 steel, 483 MPA. This case is called case ”Clay Port of Rotterdam”.

For the case ”Sand”, two designs are made. One design in cross-sectional class 4 and another in

cross-sectional class 2 (Figure 4.4). The former is much more susceptible to buckling and comparing the two will give more insight. Plus, the larger thinner pile can be produced in the Netherlands as they can be spirally welded, while the thicker pile needs to be rolled in the longitudinal seam abroad. So although the latter design uses less steel, engineers might still opt for the locally produced pipe. This case is called case ”Sand Alternative”.

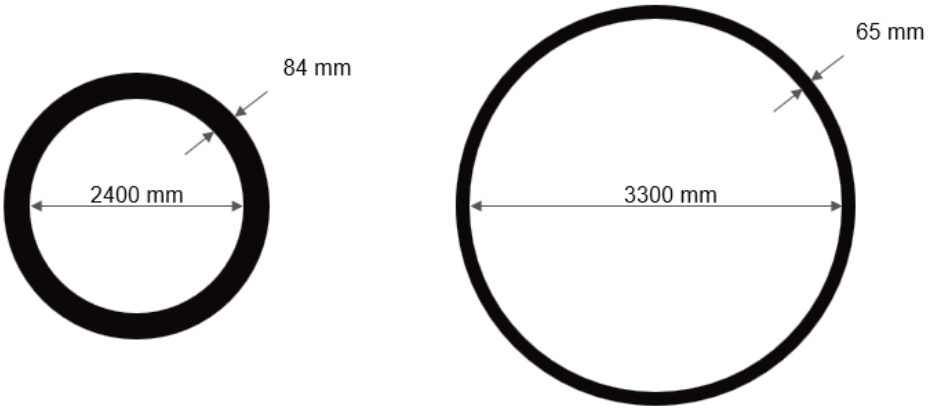

Figure 4.4: case ”Sand” and case ”Sand Alternative”

In order to study the influence of different navigation conditions, different distributions of the berthing velocities derived from measurements in the Netherlands and Germany were used (Iversen et al., 2022). The soil composition of the bed remains the same, see Figure 4.6. These consist of 4 categories and together with their berthing velocity distributions found by Roubos et al. (2017), they are:

- Monitored, Weibull (scale= 0.052, shape= 2.69, CoV=0.41)
- Favourable, Weibull (scale= 0.049, shape= 2.29, CoV=0.47)
- Moderate, Weibull (scale= 0.052, shape= 2.05, CoV=0.52)
- Unfavourable, Weibull (scale= 0.074, shape=1.61, CoV=0.64)

A more detailed description of the navigation condition is presented in Figure 4.5. The monitored condition is the same as the favourable case, but the captains can monitor their speed as they are mooring. This leads to on average higher velocities, but less extreme ones. Next to the different velocities, multiple arrival rates and variations in water displacement were studied. Table 4.1 gives an overview of the run simulations and in orange the combinations for which reliability-based assessments were performed. These 7 simulations already give a range of coefficient of variation in the Gumbel distribution in which the remaining combinations also are. Since the coefficient of variation is the most important factor for the influence factor, these 7 combinations cover enough CoV’s. Performing reliability assessments for all combinations would not fit within the time scope of this thesis.

Table 4.1: Combination of the simulations performed and combinations used for for reliability-based assessments

	Monitored Weibull (λ=5.2, k=2.69)	Favourable Weibull (λ=4.9, k=2.29)	Unfaourable Weibull (λ=5.2, k=2.05)	Unfavourable Weibull (λ=7.4, k=1.61)
CoVm 0% Uniform 122850-122850 kdwt	100 arrivals	100 arrivals	100 arrivals	100 arrivals
CoVm 10% Uniform 85000-122850 kdwt	100 arrivals	100 arrivals	100 arrivals	100 arrivals
CoVm 25% Uniform 49000-122850 kdwt	100 arrivals	100 arrivals	100 arrivals	100 arrivals
CoVm 50% Uniform 8000-122850 kdwt	1 arrival 10 arrivals 50 arrivals 100 arrivals 500 arrivals 1000 arrivals 2000 arrivals	1 arrival 10 arrivals 50 arrivals 100 arrivals 500 arrivals 1000 arrivals 2000 arrivals	1 arrival 10 arrivals 50 arrivals 100 arrivals 500 arrivals 1000 arrivals 2000 arrivals	1 arrival 10 arrivals 50 arrivals 100 arrivals 500 arrivals 1000 arrivals 2000 arrivals

	Navigation Conditions		
	Favourable	**Moderate**	**Unfavourable**
Vessel approach strategy	The vessel can be brought to a controlled stop during the final berthing manoeuvre; AND	Vessels cannot be brought to a controlled stop during the final berthing manoeuvre, e.g. manoeuvring onto the berth by making use of the vessel momentum; OR	The capability to control the vessels approach, even with tug assistance, is significantly affected by the environmental conditions; OR
Propulsion	Vessels and tugs have good propulsion characteristics and are hence able to fully control their movements, e.g. using bow / stern thrusters or adequate tug assistance; AND	Vessels and tugs have good propulsion characteristics, however, are responding to moderate environmental conditions which require active use of the propulsion to maintain control of the vessel; OR	Environmental forces are significant compared to the propulsion characteristics of the vessel and/or tugs. Minimal propulsion resources in reserve to respond to changing conditions or the pilot/ship's master is reliant on the use of vessel anchors to control the approach to the berth; OR
Currents	During the berthing process currents at oblique angles or parallel to the berth having minimal effect on the manoeuvring vessel. Current forces are small and marginally effect the efficiency of the available tug power and/or vessel propulsion; AND	During the berthing process currents are generally parallel to the berth, however, may require continuous use of elevated vessel propulsion and/or tug power to stabilise control of the vessel in its final approach. Oblique current forces are controllable by available tug power and/or vessel propulsion; OR	During the berthing process, strong currents e.g. turbulent currents, at an oblique angle or parallel that require substantial use of propulsion to control the vessel; OR
Waves	During the berthing process wave effects on both the berthing vessel and the assisting tugs are negligible; AND	During the berthing process wave effects on the berthing vessel are small, however, the effectiveness of the tug assistance may be reduced; OR	During the berthing process waves substantially influence both the berthing vessel and the assisting tugs; OR
Wind	During the berthing process wind speeds and/or windage area result in small wind forces that marginally reduce the effectiveness of the available tug power and/or vessel propulsion.	During the berthing process wind speeds and/or windage area result in moderate wind forces that reduce the effectiveness of the available tug power and/or vessel propulsion.	During the berthing process wind speeds and/or windage area result in high wind forces that substantially reduce the effectiveness of the available tug power and/or vessel propulsion.

Figure 4.5: Description of different navigation conditions (PIANC WG211, 2024)

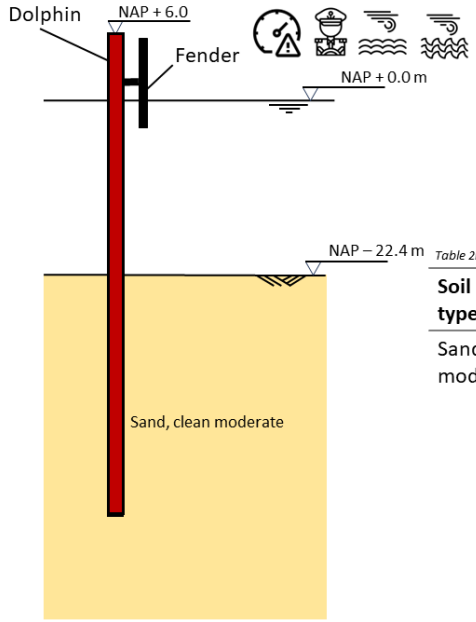

Table 2b Eurocode 7

Soil type	Top layer	Bottom layer	Υ_{sat} [kN/m³]	C_u [kPa]	φ [°]
Sand, clean moderate	NAP-22.4m		20	-	32.5-35

Figure 4.6: Case used for navigation conditions assessment

4.2. Limit state functions used for the assessments

For this research, the limit states considered are yield/buckling combined (Equation 4.1) and fixity (Equation 4.2) as these are the most important failure mechanisms determining the pile dimensions The failure mechanisms regarding geotechnical failure such as passive soil wedge and exceeding of vertical equilibrium are disregarded, because of the design philosophy that a dolphin must fail structurally first before geo-failure can occur. Therefore, structural failure is very important. Moreover, Post et al. (2021) found that quay wall geo reliability is very high and needs unrealistic adjustments to be made to fail. In addition, if the dolphin suffices for the fixity check then it will not likely fail on geotechnical issues. Thus, it is assumed in this study that structural failure and fixity are governing.

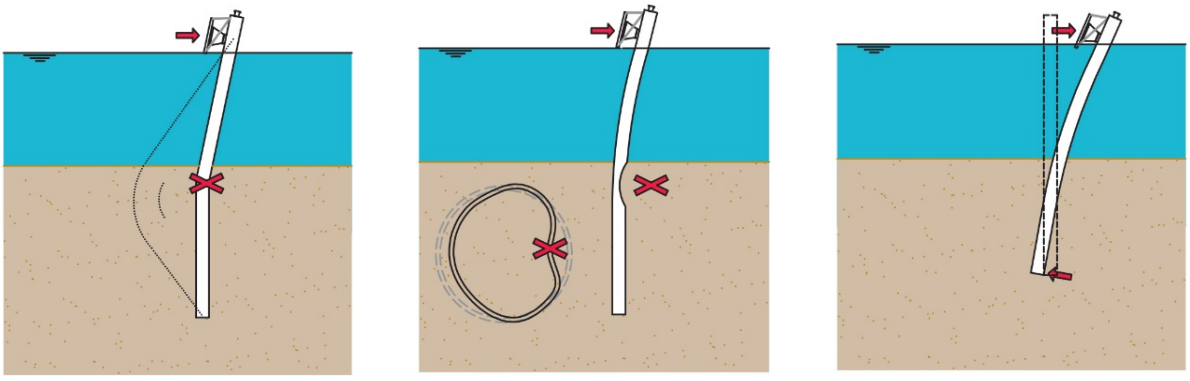

(a) Limit state yield **(b)** Limit state local buckling **(c)** Limit state fixity

Figure 4.7: Failure modes considered (CRW C1005, 2018)

$$Z_{structural} = \frac{M_{Ed}}{M_{Rd}} = max(\frac{\theta_m M_{Ed}}{W_{el} f_y}, \frac{\theta_m M_{Ed}}{W_{pl} f_y}, \frac{\theta_m M_{Ed}}{\theta_b W_{eff} f_y}) - 1 \tag{4.1}$$

$$Z_{fixity} = 0.5 - \frac{\text{mobilisation of lowest spring}}{\text{mobilisation capacity of lowest spring}} \tag{4.2}$$

Where,

$Z_{structural}$ = Limit state function of maximum stress in the dolphin
Z_{fixity} = Limit state function of fixity
f_y = Yield Strength of steel$[kN/m^2]$
M_{Ed} = Bending moment in dolphin$[kNm]$
W_{el} = Elastic section modulus dolphin$[m^3/m]$
W_{pl} = Plastic section modulus dolphin$[m^3/m]$
W_{eff} = Effective section modulus dolphin$[m^3/m]$
θ_m = Model uncertainty for bending moments$[-]$
θ_b = Model uncertainty for buckling experiments$[-]$

4.3. Distribution functions for the input variables of the assessments

Table 4.2 provides an overview of all the parameters relevant to the reliability-based assessments. The determination of the values is elaborated in Section 3.2. The soil parameters are based on the Eurocode 7 (2012), while the structural and model parameters are predominantly based on other Eurocode guidelines.

The distribution of the berthing energy was determined using Monte Carlo simulations. Recall Equation 2.1, which can be used to determine the berthing energy.

$$E_k = \frac{1}{2} \cdot M \cdot v^2 \cdot C_E \cdot C_M \cdot C_S \cdot C_c.$$

The extreme value analysis followed from Monte Carlo simulation as explained in Subsection 3.2.3 and Appendix A. The simulation samples values for each parameter in this equation. The distribution for each parameter is explained below:

- The berthing velocity was sampled from the distributions found by Roubos et al. (2017).
- For the water displacement it was decided to sample from a uniform distribution because each of the exact distribution of water displacement differs per location and a uniform distribution gives each ship an equal chance to be sampled. The range goes from the minimum water displacement of Handymax ships to the maximum water displacement of the Aframax ships. Larger ship classes led to extreme berthing energy in the disadvantageous navigation classes, causing unrealistic dolphin designs. The exact value of the water displacements was derived from a standard from an undisclosed port authority. The exact values may not be presented, but the range of the distribution was around 10.000 - 120.000 tons.
- The eccentricity factor is always equal to 1 for open structures such as dolphins.
- The mass coefficient is assumed fixed at 1.5 because the keel clearance is always more than 0.5 times the draught of the ship.
- The softness coefficient is set as 1.
- The ship flexibility factor is also set to 1 again because the dolphin is an open structure.
- The eccentricity factor depends on the berthing angle. This study had no information available on this parameter, therefore the assumption was made that the berthing angle was always equal to 3 degrees.

The monitored, favourable, moderate and unfavourable cases were sampled with 100 arrivals per year. The favourable case was also sampled for 10 and 1000 arrivals per year. Also less variation in the water displacement, this can be achieved by sampling from the minimum and maximum water displacement of the Aframax ship class. The resulting sets of berthing energies from the extreme value analysis were fitted, with the best fit being the Gumbel distribution, presented in Table 4.2.

Table 4.2: Variables and distributions used for probabilistic assessment

Description	Random variable	SI	Characteristic value	Mean	Type of distribution	Standard deviation	Coefficient of Variation
Soil Parameters							
Saturated weight clay, clean soft	γ_{sat}	kN/m^3	14	12.94	Normal	0.65	0.05
Saturated weight clay, clean moderate	γ_{sat}	kN/m^3	17	15.71	Normal	0.79	0.05
Saturated weight clay, clean compact	γ_{sat}	kN/m^3	20	18.48	Normal	0.92	0.05
Saturated weight sand, clean loose	γ_{sat}	kN/m^3	19	17.56	Normal	0.88	0.05
Saturated weight sand, clean moderate	γ_{sat}	kN/m^3	20	18.48	Normal	0.92	0.05
Saturated weight sand, clean compact	γ_{sat}	kN/m^3	22	20.33	Normal	1.03	0.05
Shear stress clay, clean soft	c_u	kPa	25 - 50[1]	37.50	Lognormal	7.50	0.2
Shear stress clay, clean moderate	c_u	kPa	50 - 100[1]	75	Lognormal	15	0.2
Shear stress clay, clean compact	c_u	kPa	100 - 200[1]	150	Lognormal	30	0.2
Internal friction angle sand, clean loose	φ	°	30 - 32.5[1]	31.25	Normal	2.54	0.0813
Internal friction angle sand, clean moderate	φ	°	32.5 - 35[1]	33.75	Normal	2.65	0,0784
Internal friction angle sand, clean compact	φ	°	35 - 40[1]	37.50	Normal	2.76	0,0737
Structural parameters							
Thickness steel	t	mm	See semi-prob designs		Uniform		-
Yield strength for t <40 mm	f_y	N/mm^2	483	517	Lognormal	20,68	0.04
Impact level			NAP + 1.7m		Deterministic	-	-
Bottom level			See semi-prob designs		Deterministic	-	-
Pile toe level			See semi-prob designs		Deterministic	-	-
Extreme value analysis of berthing load t_{ref}= 50 years							
Berthing energy soil	E	kNm	2095[2]	2213.8	Gumbel	264.5	0,120
Berthing energy monitored	E	kNm	661[2]	554.44	Gumbel	65.41	0.118
Berthing energy favourable	E	kNm	776[2]	658.71	Gumbel	94.91	0,144
Berthing energy moderate	E	kNm	1087[2]	893.8	Gumbel	146.21	0,164
Berthing energy unfavourable	E	kNm	3898[2]	2389.4	Gumbel	439	0,184
Berthing energy favourable 10 arrivals/year	E	kNm	776[2]	478.13	Gumbel	95.27	0,199
Berthing energy favourable 1000 arrivals/year	E	kNm	776[2]	821.24	Gumbel	73.21	0,089
Berthing energy CoV ships 10%	E	kNm	776[2]	762.91	Gumbel	102.57	0,134
Model parameters							
Model uncertainty buckling	θ_b	-	-	1	Normal	-	0.1
Model uncertainty bending moment capacity	θ_m	-	-	0.94	Lognormal	-	0.05

[1] The 95%- and 5%-characteristic value respectively

[2] Characteractistic value when using the 99.8% characteristic velocity and water ship displacement in Equation 2.1

5

Results and interpretation of the reliability-based assessment

In this chapter the results of reliability assessments are discussed, these are approach steps 5 to 8. In Section 5.2 sub-question iii is answered. In Section 5.3 answers are given to sub-question iv and finally Section 5.4 answers to sub-question v. Section 5.5 summarises the findings.

5.1. Validation of calculation model

For the purpose of having certainty in the results of the reliability-based assessments, the calculation needs to be validated. The calculations are performed with different probabilistic techniques to assess the differences. The most recognised and accepted techniques are Form and Monte Carlo. These are compared with the other techniques mentioned in Chapter 3. If those methods show comparable results then these can be used as well. The chosen case is the case "Sand Alternative" and the structural limit state will be assessed. The resulting reliability index and influence coefficients are shown in Table 5.1.

Table 5.1: Comparison between different probabilistic techniques

Variables	FORM	Monte Carlo	Directional Sampling	Kriging
β	**3.17**	**3.31**	**3.27**	**3.26**
E	-0.755	-0.728	-0.713	-0.775
f_y	0.362	0.268	0.293	0.43
t_1	-0.000512	-0.12	-0.148	-0.142
t_2	-0.00423	-0.263	-0.257	0.007
t_3	-0.00748	0.0892	0.105	0.095
$t_{4,\text{ maximum moment}}$	0.091	0.151	0.143	0.173
t_5	-0.0111	-0.07	-0.0836	-0.05
$\varphi_{\text{layer 1}}$	-0.13	-0.274	-0.261	-0.253
$\gamma_{\text{sat. layer 1}}$	-0.0205	-0.0278	-0.0278	-0.0456
θ_m	-0.436	-0.31	-0.286	-0.274
θ_b	0.29	0.34	0.36	0.12

The results are quite comparable but do differ. FORM had trouble converging and the convergence eventually started oscillating. This led to untrustworthy results. The most likely cause would be the discontinuities introduced by the definition of the limit state. The Monte Carlo and Directional Sampling give the same results, while the Kriging method gives quite different influence coefficients. Since the influence coefficients play a crucial role in the definition of the partial factors, this method is not suitable for this chapter. Monte Carlo is a more accurate method than Directional Sampling, but takes significantly longer to calculate. Since the results are more or less the same and can be achieved in a shorter period, the Directional Sampling method is used for the calculations in this chapter.

5.2. Influence of different soil compositions

5.2.1. Structural limit state

The resulting partial factors of the reliability assessments are shown in Table 5.2 and the intermediate steps of the derivation of these factors are found in Appendix C. The influence factors and reliability indices of these cases are summarised in Figure 5.1. The dimensions of the dolphins were adjusted until the reliability target of 3.3 was achieved. Case ”Sand Alternative” was not altered as it achieved the reliability target. Case ”Clay Port of Rotterdam” was kept in the same dimensions as case ”Clay” to illustrate the effect of the stricter demands. The negative signs of the influence coefficient show that the variable acts as a load variable and positive as a resistance variable. The partial factors were calculated following Equation 3.9.

Table 5.2: Resulting partial factors with load and material factors

Variables	Current	Case ”Sand”	Case ”Clay”		Case ”Mix”	Case ”Sand Alternative”	
β	**3.3**	3.2	3.49	3.48	3.23	3.27	3.3
E	**1.45**	1.373	1.495	1.617	1.436	1.445	1.506
f_y	**1**	0.970	0.962	0.985	0.961	0.968	0.954
t_1	**1**	1.003	1.015	1.001	1.007	1.007	1.008
t_2	**1**	1.001	1.000	1.002	1.008	1.010	1.007
t_3	**1**	1.016	1.005	1.011	1.001	1.008	0.994
$t_{4,\text{ maximum moment}}$	**1**	1.012	1.019	1.006	1.004	1.011	1.011
t_5	**1**	1.018	1.003	1.004	1.002	1.008	1.011
$\varphi_{\text{layer 1}}$	**1**	1.166	-	-	0.984	0.994	1.018
$\varphi_{\text{layer 2}}$	**1**	-	1.012	0.984	-	-	-
$\varphi_{\text{layer 3}}$	**1**	-	-	-	0.967	-	-
$\varphi_{\text{layer 5}}$	**1**	-	-	-	-	-	-
$\varphi_{\text{layer 7}}$	**1**	-	-	-	0.997	-	-
$c_{\text{u, layer 1}}$	**1**	-	0.742	0.834	-	-	-
$c_{\text{u, layer 2}}$	**1**	-	-	-	0.784	-	-
$c_{\text{u, layer 4}}$	**1**	-	-	-	0.686	-	-
$c_{\text{u, layer 6}}$	**1**	-	-	-	1.012	-	-
$\gamma_{\text{sat, layer 1}}$	**1**	1.102	1.000	1.048	1.004	1.004	1.016
$\gamma_{\text{sat, layer 2}}$	**1**	-	1.012	1.029	1.000	-	-
$\gamma_{\text{sat, layer 3}}$	**1**	-	-	-	1.000	-	-
$\gamma_{\text{sat, layer 4}}$	**1**	-	-	-	1.015	-	-
$\gamma_{\text{sat, layer 5}}$	**1**	-	-	-	1.005	-	-
$\gamma_{\text{sat, layer 6}}$	**1**	-	-	-	1.003	-	-
$\gamma_{\text{sat, layer7}}$	**1**	-	-	-	0.997	-	-
θ_m	**1.05**	0.972	1.000	-	1.040	0.986	-
θ_b	**1/1.1**	1.012	1.000	-	1.006	1.061	-

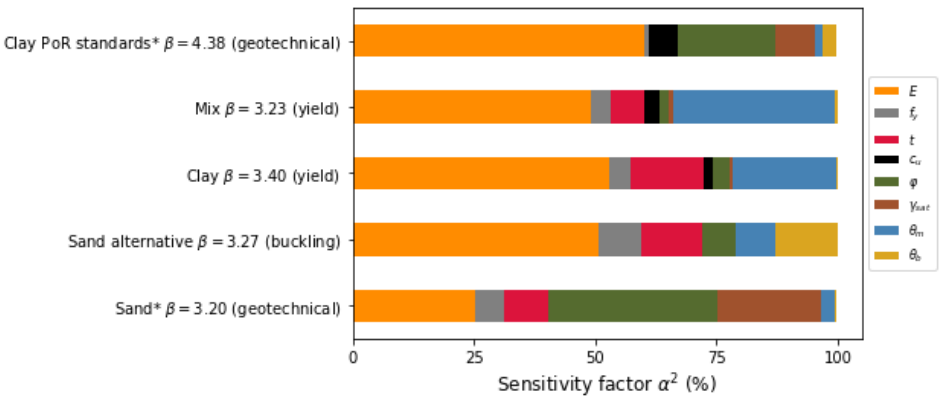

Figure 5.1: Influence of the input variables on the probability of failure of the dolphin per case

Case "Clay"
First, the case ”Clay”. When analysing the results, the berthing energy has the most impact on the reliability, followed by the model uncertainty and structural parameters. What is interesting to note is that the upper pile section has a deleterious effect on the reliability, thus larger thickness may lead to higher bending moments in the lower section. This could be caused by a higher stiffness of the pile when the upper sections are thicker. The soil parameters have little to no influence, but when deriving the partial factor for the shear stress, it seems low. This may be due to the definition of the characteristic value. The current definition of characteristic value is the 95% value, but the low partial factor suggests that this value may already be too conservative.

Case "Mix"
In the following case ”Mix”, the berthing energy is again the most important parameter. The results are similar to the previous case except for the influence coefficient of the shear stress. This parameter acts as a load variable. It is known that soil can behave as either a load or resistance variable.

Case "Sand"
Case ”Sand” on the other hand seems to be more dominated by the soil parameters than the berthing energy. Upon further inspection, the failed realizations occurred for lower values of the soil parameters. A plausible explanation would thus be that geotechnical failure is the dominant mechanism in this scenario. Because of the larger wall thickness the springs modelled with the PY-curves the collapse quicker than the yield stress being achieved. It is worth noting that this particular failure mechanism leads to unrealistic displacements and bending moments in the realisations where the PY-curves are in the collapsing branch. Consequently, the results of the failure probability may be untrustworthy, hence the asterisk in Figure 5.1.

The calculation model uses the displacement to determine the force on the dolphin. However, when the curves show 100% mobilisation off the springs, the Dolphin tool returns unrealistic forces and displacements which then are used in the Deltares Probabilistic Toolkit. Additionally, PY-curves typically represent simplified relationships between input parameters and failure probabilities, neglecting the spatial variability and correlations among these parameters. Moreover, geotechnical failure mechanisms can exhibit non-linear behaviour and complex interactions, making it challenging to accurately model and predict failure probabilities solely based on PY-curves. Therefore, while PY-curves can provide valuable insights into geotechnical behaviour, they may not always be suitable for assessing geotechnical failure.

Case "Sand Alternative"
Next in the alternative case ”Sand” in cross-sectional class 4, the buckling model uncertainty has much more influence compared with other cases. This suggests that the main failure mechanism here is buckling. This in turn leads to larger values of the material partial factors. This is in line with the current design philosophy of dolphins, which also recommends adding extra safety to the materials.

Case "Clay Port of Rotterdam Standards"
At last, the case ”Clay” but designed according to the Port of Rotterdam requirements. The same dimensions as the pile in the case ”Clay”, but more certainty on the yield stress capacity and wall thickness causes the reliability index to go from 3.40 to 4.3. This massive jump would lead to even less material use in the dolphin. This illustrates that the margin currently prescribed in the NEN-EN 10219-2 and NEN-EN 10051 is a lot and a smaller margin can lead to significant steel reduction in dolphins. Further study of the design point shows that the failure also occurs for lower values of the internal friction angle and soil weight. Hence the larger influence of these variables. This would also suggest that when removing the uncertainty in the structural parameters, the design becomes so much safer in the structural safety aspect that the geotechnical failure takes over.

Cases with no model uncertainty
Besides the cases with model uncertainty, the effects of discarding this parameter were assessed as well for case ”Clay” and case ”Sand Alternative”. Remarkably, the reliability stayed more or less the same in contrast with the results found by Roubos (2019). This could be the simple reason that the

dominant model uncertainty of the acting moment has a favourable effect on the probability of failure due to the mean being lower than 1. Therefore the unfavourable effect of the variation on the model uncertainty is counteracted. It was found that the case with no model uncertainty is that the factors for loads are higher, but the factors for materials are lower. Thus, they balance each other out leading to the same reliability index.

5.2.2. Fixity

The fixity criterion is a serviceability limit state. This limit state does not have any minimum formal requirements. The reliability target can be chosen by the client, designer or contractor and usually depends on the consequences of exceeding SLS limit. These can range from repair costs to indirect costs due to loss of functionality. In the case of a dolphin, exceeding the fixity limit state will cause the dolphin to not spring back into its original position. In most cases, this is just an aesthetic issue, but if the dolphin has a structure close by then there can be more severe consequences. Thus, a project-specific reliability target would be best suited in such a case. The EN1990 and ISO 13822:2020 recommend a target value of 1.5. The results of the reliability-based assessments in Figure 5.2 do show that this new criteria meets the recommended target value. Here it is also much more clear that the soil properties are of much more influence than the berthing energy in Figure 5.1. The friction angle in the compact case ”Sand” has notably more influence than the other cases. This could be attributed to the same type of springs throughout the entire soil, which can easily be more mobilised than if there were more different types throughout the soil. A combination of stiff and flexible springs will most likely lead to less mobilisation of the lowest spring during berthing. So, the reliability target achieved in reality will most likely be around 2, which is more than the recommended target values.

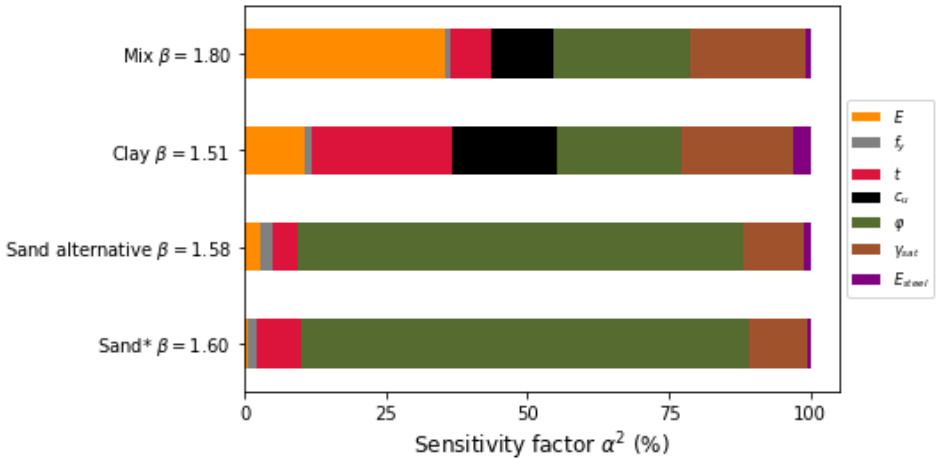

Figure 5.2: Influence of the input variables on the probability of failure for the fixity criterion

Another reason that the berthing is of such little influence in the case ”Sand” may be due to the stability of the calculation model. As previously stated, the sand case has numerical stability problems due to the large thickness of the pile. This may cause the soil parameters to have a larger influence on the results. Figure 5.3 shows that for the case ”Sand” the fixity criterion is exceeded for low values of the berthing energy and close to the mean. Recalling that the influence factor is determined with the weighted standard deviation of failed samples, this seems to be the cause that berthing energy has so little influence in the case ”Sand”. In Figure 5.3 the failed samples do not deviate far from the mean for case ”Sand”, thus leading to little to no influence of the berthing energy in reliability-based assessments.

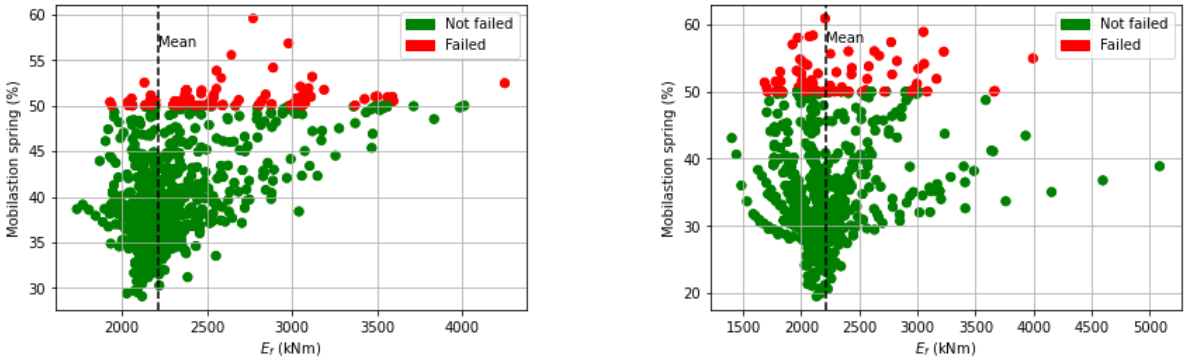

(a) Samples for case "Mix"

(b) Samples for case "Sand"

Figure 5.3: Comparison illustrating the difference in influence factors caused by the standard deviation of the failed samples

5.3. Influence of different navigation conditions

As a result of the high dominance of the berthing energy on the reliability, it is necessary to further study the effects of this variable. In the design of the dolphin, different navigation conditions are classified. The effects of each of these conditions on the variables are shown in Figure 5.4. The large influence of the berthing energy remains more or less the same. In the case "Monitored" it seems to have a bit more influence. The ratios are comparable to that of the different soil cases. Therefore, the berthing energy remains the most important parameter to consider. The resulting partial factors are shown in Table 5.3.

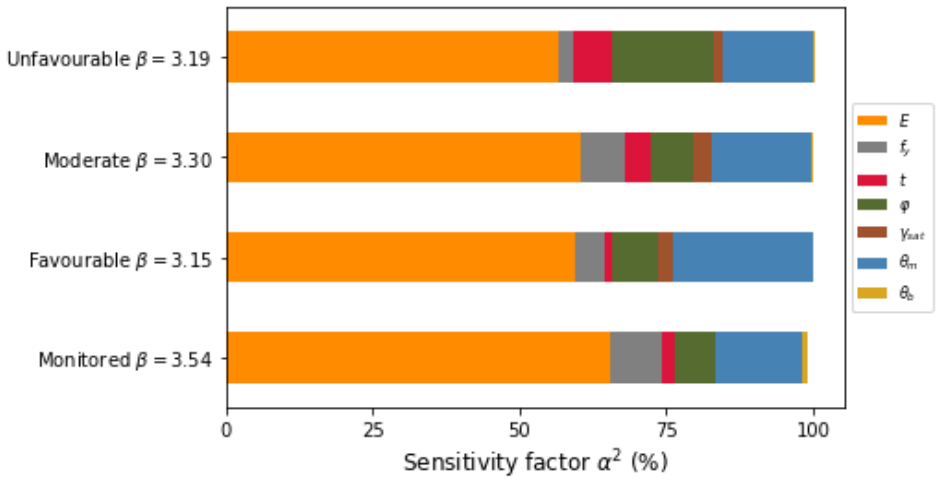

Figure 5.4: Influence of the input variables on the probability of failure of the structural limit state

When assessing the resulting partial factors of the berthing energy, it seems odd that the partial factors do not increase with more adverse navigation conditions. When in fact, the current guidelines suggest that they should be higher. This can attributed to the method used to determine the design point of the berthing energy. The design point is now determined for different reliability indices and influence factors. The design point can be easily determined with Equation 3.19. The reliability index is set to 3.3 because this is the reliability target in CC1. The influence factor impacts the partial factor as well, as can be seen in Figure 5.5. According to the ISO 2394 (2015), for dominant loads the influence factor can have a value of -0.7. However, the berthing energy in the reliability-based assessments had a range of influence factors varying from -0.60 to -0.77 (Appendix C). To ensure that the partial factors are not too low in certain cases, the maximum influence factor 0f -0.77 was used to determine the design points. It is worth mentioning that this value could be too conservative because the bed level and impact level are seen as constant. The inclusion of these levels as a stochastic variable will most likely mean a lower influence coefficient for the berthing energy.

Table 5.3: Resulting partial factors for navigation conditions with load and material factors

Variables	Current	Case "Monitored"	Case "Favourable"	Case "Moderate"	Case "Unfavourable"
β	**3.3**	3.54	3.15	3.3	3.19
E	**1.35/1.45/1.7**	1.672	1.598	1.728	1.353
f_y	**1**	0.976	0.960	0.969	0.953
t_1	**1**	1.005	1.005	1.008	1.004
t_2	**1**	1.007	0.997	1.004	1.004
t_3	**1**	1.003	1.003	1.005	1.013
$t_{4,\text{ maximum moment}}$	**1**	1.006	1.002	1.007	1.007
t_5	**1**	1.003	1.002	1.003	1.000
$\varphi_{\text{layer 1}}$	**1**	0.945	0.938	0.938	0.974
$\gamma_{\text{sat, layer 1}}$	**1**	1.006	1.025	1.030	1.021
θ_m	**1,05**	1.015	1.015	1.012	1.003
θ_b	**1.1**	1.027	1.027	1.010	1.009

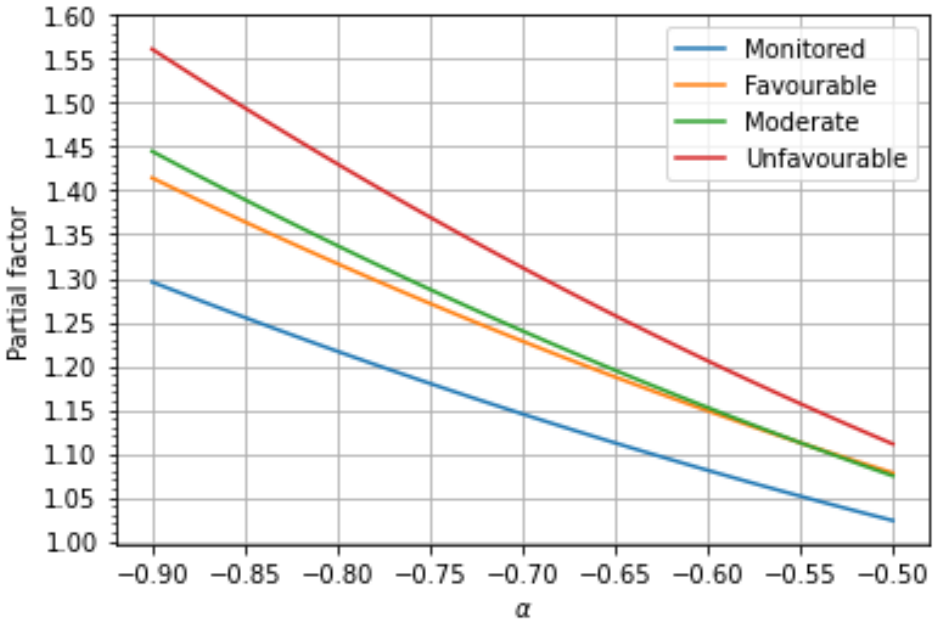

Figure 5.5: Sensitivity analysis of the influence factor on the partial factor per navigation condition

With the design points now sorted, the characteristic energy may be determined. As mentioned in Subsection 3.1.3, for variable loads the characteristic value should have a 2% exceedance value per year. For 50 years this translates to the 36.5%-value of the extreme value distribution of 50 years. However, this would require performing a simulation to conduct the extreme value analysis and this is not the preferred method used by design engineers. The preferred method is using Equation 2.1 and using the 2% exceedance per year value for the velocity and the water displacement of the maximum ship. In certain cases, the exceedance value is not known and then the velocities are recommended in guidelines such as the PIANC WG211 (2024). Each of the three methods leads to different characteristic berthing energies, which in turn lead to different partial factors showcased in Table 5.4.

Table 5.4: Comparison of the partial factors using different characteristic berthing energies

	Monitored	Favourable	Moderate	Unfavourable
Mean berthing energy	554.44	658.71	893.8	3134
Std berthing energy	65.41	94.91	146.21	638
CoV	0.1180	0.1441	0.1636	0.2036
Influence coefficient	-0.77	-0.77	-0.77	-0.77
Reliability index	3.3	3.3	3.3	3.3
Design point	790.07	1000.61	1420.51	5432.33
Characteristic berthing velocity 99.98%	0.115	0.125	0.148	0.280
Characteristic berthing velocity Pianc 211	0.100	0.100	0.175	0.275
Characteristic value 99.98%	661.44	776.17	1086.87	3897.95
Characteristic value Pianc wg211	497.54	497.54	1523.72	3762.67
Characteristic berthing energy 36.5% EVD	524.48	615.24	826.83	2841.76
Partial factor using 99.98% velocity	1.19	1.29	1.31	1.39
Partial factor using PIANC wg211 velocities	1.59	2.01	0.93	1.44
Partial factor characteristic berthing energy	1.51	1.63	1.72	1.91

When assessing the characteristic berthing energies of the preferred method of engineers (orange) and the simulation method (black), it can be noted that the preferred method leads to conservative values of the characteristic berthing energy consequently leading to lower partial factors. It seems that the variation in water displacement does have an impact on the partial factor. To confirm this, simulations were performed where there were no variations in the water displacement. The maximum water displacement was used. Following this method, the simulation would lead to the same characteristic value as the preferred method. As can be seen in Table 5.5, the resulting partial factors are indeed the same. Furthermore, the velocities of the PIANC WG211 (2024) differ from the 2% exceedance value (blue). This also leads to different partial factors. The different ways the characteristic values are defined are determined all lead to different outcomes of the partial factors. Keeping in mind that the design engineers use the maximum water displacement and the characteristic berthing velocity, the resulting partial factors for this method are used (orange) in Table 5.4.

Table 5.5: Comparison of the partial factors using no variation in water displacement for the simulations

	Monitored	Favourable	Moderate	Unfavourable
Mean berthing energy	696	819	1155	4206
Std berthing energy	71	94	157	745
CoV	0.1020	0.1148	0.1359	0.1771
Influence coefficient	-0.77	-0.77	-0.77	-0.77
Reliability index	3.3	3.3	3.3	3.3
Design point	951.77	1157.63	1720.58	6889.78
Characteristic berthing velocity 99.98%	0.115	0.125	0.148	0.280
Characteristic value 99.98%	661.44	777.41	1089.82	3897.95
Characteristic berthing energy 36.5% EVD	663.48	775.94	1083.09	3864.75
Partial factor using 99.98% velocity	1.44	1.49	1.58	1.77
Partial factor characteristic berthing energy	1.43	1.49	1.59	1.78

Next to the navigation conditions, other factors also impact the berthing energy, particularly the arrival rate and variation of types of ships that berth at a specific location. To study the effects of these two principles, extreme value analysis was conducted with 10 arrivals over a year, 1000 arrivals per year, and water displacements with 10% and 50%. As mentioned in the previous paragraph, the variation already seemed to influence the resulting partial factors. Regarding the number of arrivals, The usual arrival rate from which the previous partial factors for berthing are derived is based on 100 arrivals per year. However, different arrival rates can influence the extreme value distribution and in turn, the resulting partial factor as noted by Roubos (2019). Therefore, the influence of very low arrivals and high arrivals is assessed in order to cover the range of possible arrivals. By performing the simulations for 10

and 1000 arrivals, the coefficient of variation of the berthing energy becomes quite larger and smaller than the CoV of the 100 arrivals per year simulation. To investigate the effect of different coefficients of variations on the resulting influence factors, these calculations are conducted. The results are shown in Figure 5.6. The dimensions of the dolphin were adjusted until a reliability index of around 3.3 was met.

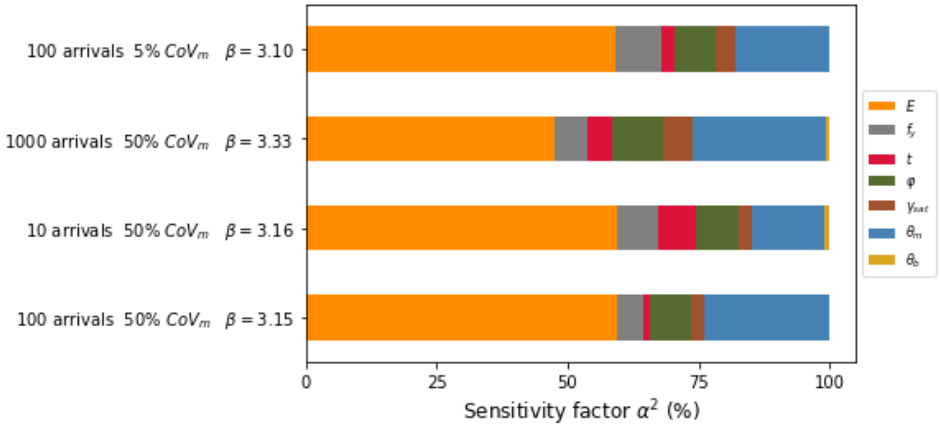

Figure 5.6: Effects of arrivals and variation in water displacement

Intuitively it was thought that different coefficients of variation would lead to different influence factors for the berthing energy, however, they remain more or less the same (Appendix C). This can be explained by the different sizes of the dolphin of each corresponding berthing energy distribution. For larger berthing energies, the size of the pile increases which in turn increases the influence of the uncertainty of the structural parameters such as the yield strength. This increase causes the influence factor of the berthing energy to remain relatively the same at -0.77. When analysing the partial factors in Table 5.6 they differ, signalling that perhaps correction factors could be applied.

Table 5.6: Resulting partial factors for navigation conditions with load and material factors

Variables	**Current**	**case "Favourable" 100 arrivals CoV_m 50%**	**case "Favourable" 10 arrivals CoV_m 50%**	**case "Favourable" 1000 arrivals CoV_m 50%**	**case "Favourable" 100 arrivals CoV_m 5%**
β	**3.3**	3.16	3.16	3.33	3.10
E	**1.45**	0.983	0.818	1.062	1.118
f_y	**1**	0.960	0.966	1.006	1.004
t_1	**1**	1.005	1.013	1.004	1.001
t_2	**1**	0.997	1.009	1.005	1.005
t_3	**1**	1.003	1.009	1.012	1.010
$t_{4,\text{ maximum moment}}$	**1**	1.002	1.002	1.012	1.010
t_5	**1**	1.003	1.003	1.006	1.001
$\varphi_{\text{layer 1}}$	**1**	0.934	0.939	0.953	0.933
$\gamma_{\text{sat, layer 1}}$	**1**	0.947	0.947	0.962	0.951
θ_m	**1.05**	1.020	1.002	1.031	1.007
θ_b	**1.1**	1.001	1.018	1.014	1.000

Again, the partial factors in Table 5.6 were determined with the characteristic 63.5% exceedance probability value of berthing energy, different reliability indices and influence factors. The partial factors need to be corrected for this with the same influence factor of -0.77 and a reliability index of 3.3. Multiple extreme value analyses can be used to estimate the design points and partial factors. The characteristic value of the berthing energy using the characteristic berthing velocity and largest water displacement remains the same regardless of the number of arrivals or variation in water displacement. The resulting correction factors were then fitted leading to Figure 5.8 and Figure 5.7. If the information on the arrival rate and ships exists then these factors can used and could lead to a reduction in material use.

Take for instance a dolphin in the Calandkanaal. A design was made according to the CROW C1005 (2018) and another one using the partial factors using the partial Section 5.4. The AIS data for this location shows that there are approximately 10 berths per year and a large variation in ship size, thus large CoVs in water displacement. The navigation conditions are assumed to be in moderate conditions. Much material can be saved, as shown in Figure 5.9, almost 15%. Even more material use can be reduced when performing a probabilistic assessment, an additional 3%. Removing the uncertainty in the wall thickness and testing the yield strength further saves 3%. This design approach leads to a severe reduction in costs as well as CO_2 emissions.

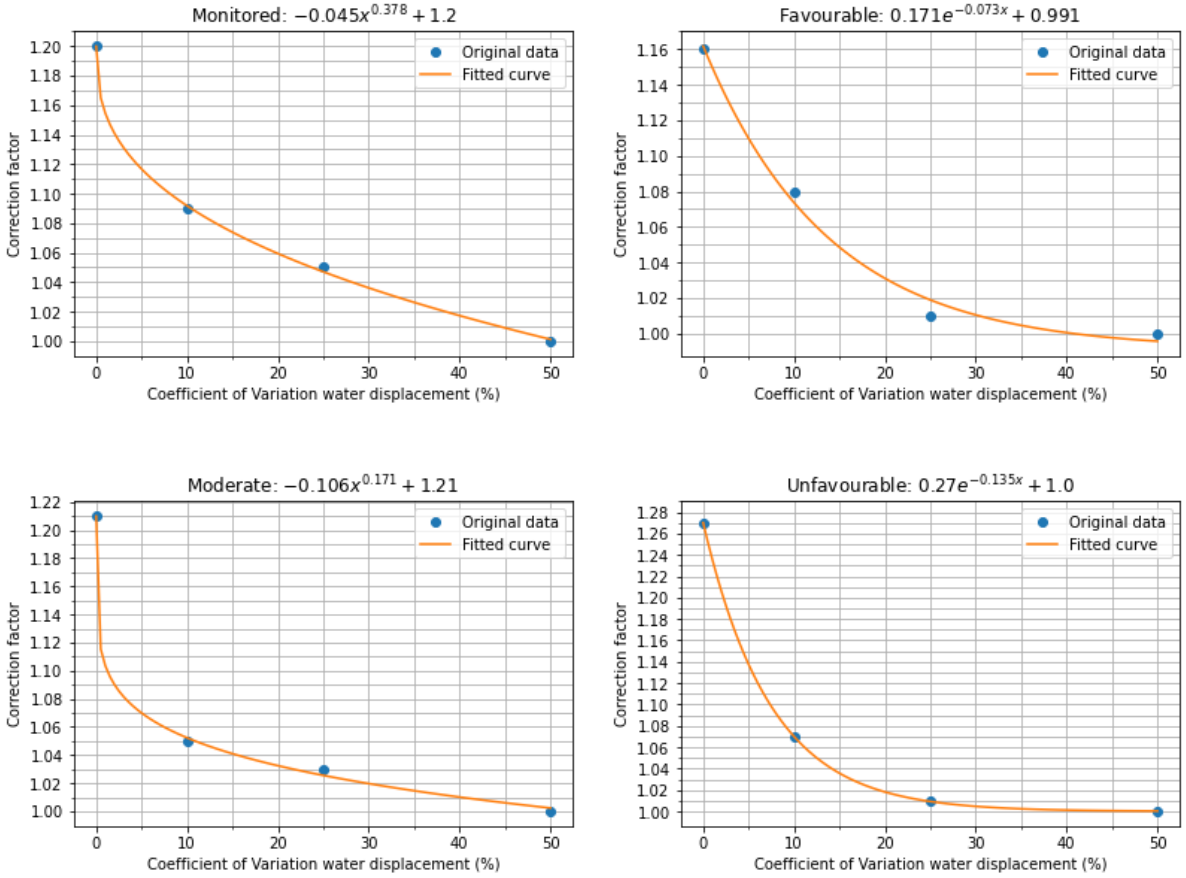

Figure 5.7: Resulting correction factors for the variation in water displacement

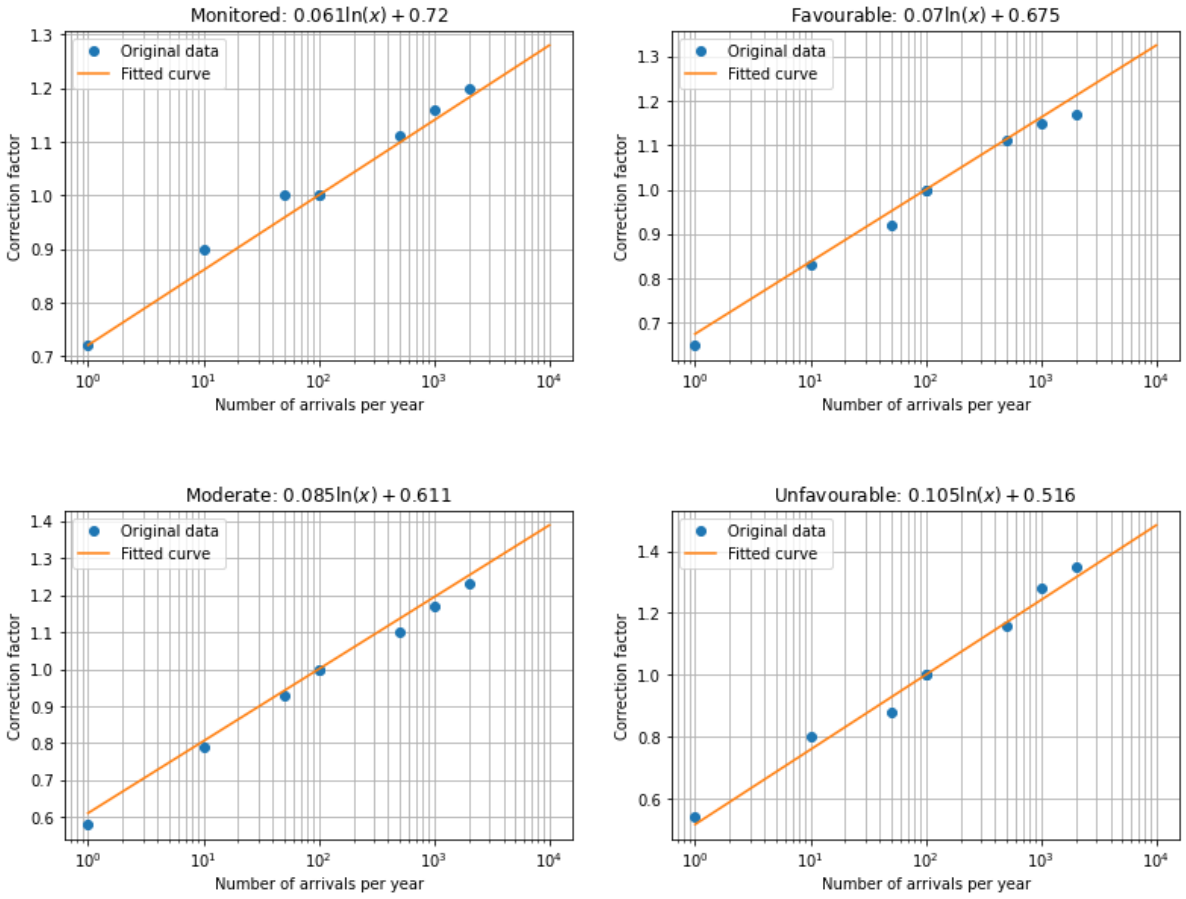

Figure 5.8: Resulting correction factors for the arrival rate

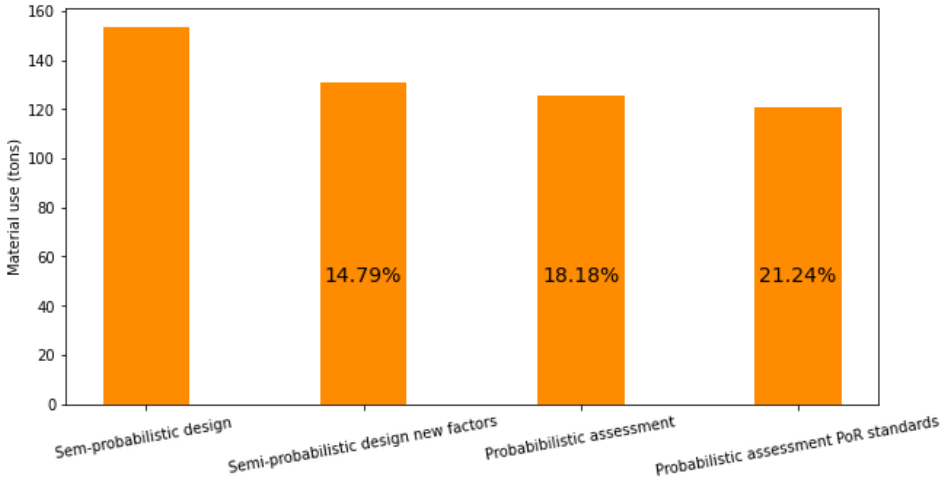

Figure 5.9: Reduction in steel use compared with the current CROW C1005 factors

5.4. Recommended set of partial factors

Taking all the results into account, a set of partial factors can be recommended. As has been noted in Section 5.2, the soil parameters have barely any influence on the structural reliability of the dolphin and even the high characteristic values can be conservative. Therefore, the soil partial factors can be

set to 1. The berthing energy is the most important factor and is heavily influenced by the navigation conditions as shown in Section 5.3. Hence, it is recommended that the partial factors be related to the information available. If information on the characteristic berthing velocity and largest ship are available then the partial factors in Table 5.7 are to be used. Furthermore, if there is information available on the arrival rate of ships and their properties then correction factors from Figure 5.10b and Figure 5.10a can be applied. Consequently, the design berthing energy for berthing dolphins can be calculated with Equation 5.1, similar to that of fenders (Iversen et al., 2022).

Table 5.7: Recommendations $\gamma_{E,ref}$ in CC1

Variable	Monitored	Favourable	Moderate	Unfavourable
$\gamma_{E,ref}$	1.19	1.29	1.31	1.39

$$E_{design} = \gamma_{E,ref} \cdot \gamma_n \cdot \gamma_m \cdot E_k \tag{5.1}$$

With,

$\gamma_{E,ref}$ = Reference berthing energy for 100 intervals, see Table 5.7
γ_n = Correction factors for number of arrivals per year, see Figure 5.10b
γ_m = Correction factors for variation in water displacement, see Figure 5.10a
E_k = Characteristic berthing energy using 2% exceedance value for characteristic berthing velocity and largest water displacement

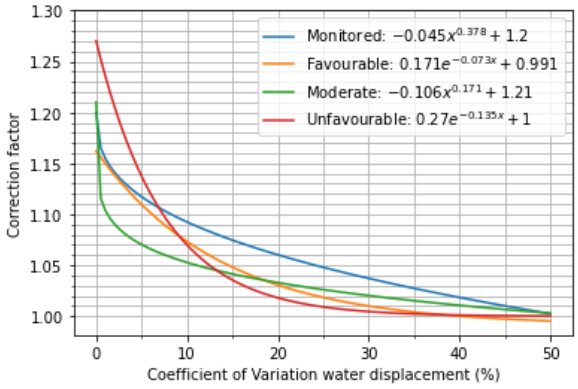

(a) Correction factors for the variation of water displacement in all navigation conditions

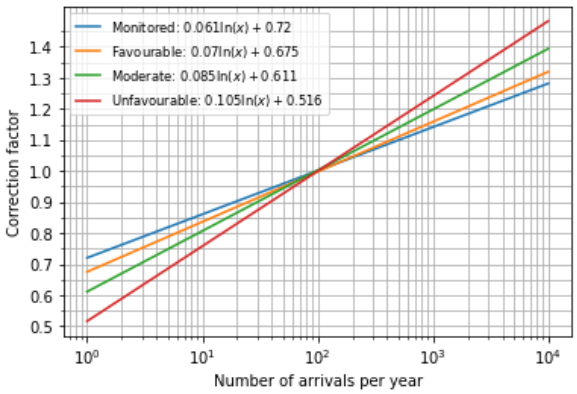

(b) Correction factors for the arrival rate in all navigation conditions

Figure 5.10: Correction factors to applied in Equation 5.1

5.5. Summary of the findings

This chapter started by first validating the probabilistic calculation model by comparing different probabilistic techniques. The calculation model was valid because all techniques showed similar results. For the calculation, one technique needs to be selected. The chosen technique was Directional Sampling due to its robustness and efficiency. Three different soil compositions were analysed and the results showed that there was little influence of the soil composition on the partial factors of safety for the failure modes yield and buckling ($\pm$ 2% difference in the sensitivity factor). For the analysis of the fixity and geotechnical failure modes, the software used in this study was deemed unsuitable. What did seem to influence the partial factors were the navigation conditions, the arrival rate of ships and variation in the water displacement. Rougher navigation conditions, frequent arrival rates and low variation in water displacement led to higher factors for the structural failure modes. Recommendations for partial factors were made from Monte Carlo simulations. This recommended set of factors led to a reduction in material use. Next to the new set, it was found that probabilistic assessments and reduction in uncertainty of the input variables also help to improve the reliability index and reduce material use. The reduction of uncertainty will be explored further in the next chapter.

6

Effects of the Bayesian update on the reliability assessment

Up until now in the research, reliability assessments were conducted based on preliminary analysis before additional information becomes available. When new information is available, the reliability of the dolphin can be updated. That is why in this chapter the effects of the Bayesian update are showcased, thereby answering the final sub-question. Section 6.1 recalls the Bayesian update framework and specifies it for the Calandkanaal case used in this chapter (approach step 9). Updates on the structural reliability were performed, one adding extra information received during the full-scale load tests and the other from observing an extreme load. Both are presented correspondingly in Section 6.2 and Section 6.3 (approach step 10). Finally, Section 6.4 provides the insight gained from the Bayesian updates.

6.1. Method used for reliability updating

6.1.1. Chosen framework

As mentioned before, adding information can be beneficial to the probability of failure of a dolphin. The algorithm used to update this probability is straightforward and based on a Monte Carlo simulation (Betz, Papaioannou, and Straub, 2022). The steps of the algorithm are shown in Figure 6.1. Straub (2015) presented two types of observation functions, namely equality and inequality. The equality definition requires considerably more samples than the inequality method and due to software memory constraints, the samples from the equality method could not be properly saved. Therefore, solely the inequality definition was checked.

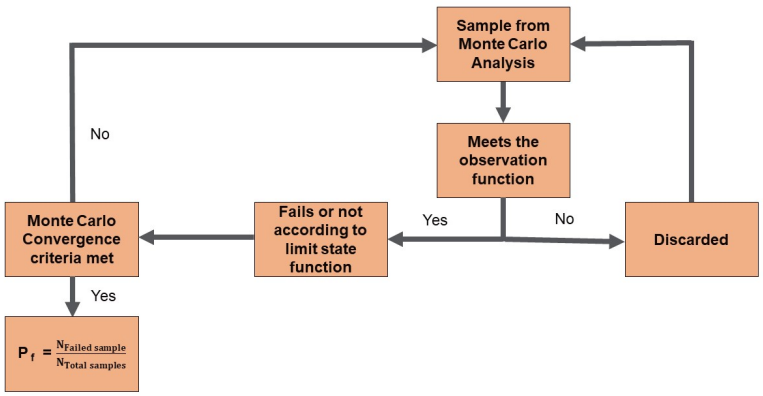

Figure 6.1: Algorithm used to perform Bayesian update

6.1.2. Building the response surface

The challenge with this algorithm is the large quantity of samples necessary to achieve an outcome, thus leading to a long calculation time. Faster methods such as the aforementioned Kringing method exist in order to reduce the number of samples necessary (van der Krogt, 2022), however, setting these methods up would not be possible due to time constraints. Moreover, the response surface models such as the Ak-MCS are criticised for their suitability in a Bayesian update. The model is constructed in the prior space and can thus lead to inaccurate results in the posterior space (Tian et al., 2023). Because of these reasons, for this study it was chosen to reduce the calculation time of a single sample by using a Gaussian Process Regression from the Python package sklearn (Pedregosa, 2011). The constructed response surface mimics the Dolphin Tool but calculates a result in a fraction of the time necessary by the Dolphin Tool. The shorter calculation time and suitability in both the prior and posterior space, make this the chosen method to perform the Bayesian update. More detail on the building of the response surface can be found in Appendix D.

6.1.3. Validation response surface

The dolphin in the Calandkanaal was used to perform the update, Figure 6.2. To further reduce the calculation time, the number of variables can also be reduced. In the previous assessments the upper soil layer, where the maximum bending moment is located, tends to be the dominant soil layer. Seeing that the other soil layers have little to no influence, as well as the soil weight of the dominant soil layer, these variables are made deterministic in the reliability assessments. Next to the soil parameters, the thickness is also considered to be deterministic, because they can be measured and the values are chosen as the as-built shows. The distribution used for the berthing energy is retrieved from Heeres et al. (2023). This is the Gumbel distribution based on AIS data.

In order to validate the response surface, the results of the prior assessments of the dolphin are compared with that of the response surface in Table 6.1 using the same probabilistic technique, namely Directional Sampling. The results are quite comparable, although the reliability index is lower and the influence coefficients differ slightly. This was also uncovered during the analysis by Post et al. (2021). Nonetheless, for the Bayesian Update, the reliability index is the most important outcome and how it compares a posteriori. To this end, the response surface suffices.

Note also that the prior reliability index is lower than the minimum requirement of 3.3. After further investigation, it seems that the original design used a lower characteristic berthing velocity than what is currently recommended by the PIANC (2022). The recommended velocity is 10 m/s, while the original design used 8 m/s (van Splunter, 2015). At the time of the design, information on berthing velocities was not yet available (Roubos et al., 2017).

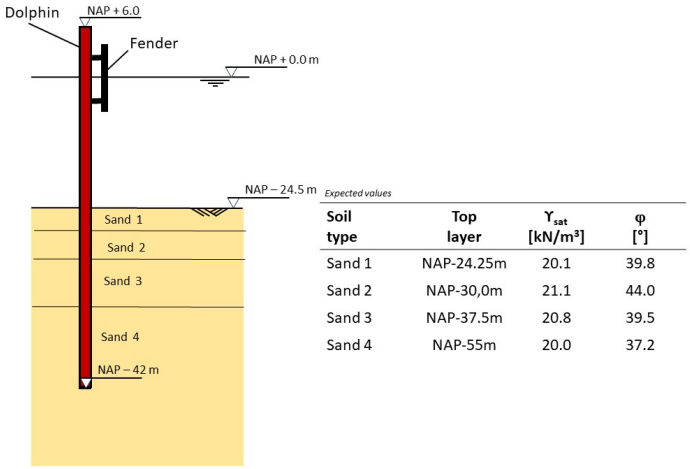

Expected values

Soil type	Top layer	γ_{sat} [kN/m³]	φ [°]
Sand 1	NAP-24.25m	20.1	39.8
Sand 2	NAP-30,0m	21.1	44.0
Sand 3	NAP-37.5m	20.8	39.5
Sand 4	NAP-55m	20.0	37.2

Figure 6.2: Case Calandkanaal used for Bayesian update

Table 6.1: Comparison influence coefficients between the Dolphin tool and created response surface

Variables	Dolphin Tool	Response Surface
β	**2.51**	**2.42**
E	-0,884	-0,802
f_y	0,142	0,398
$\varphi_{\text{layer 1}}$	-0,136	-0,215
θ_m	-0,271	-0,283
θ_b	0,327	0,271

6.2. Update based on test load

The first type of information that can be added is the results from the full-scale load tests. During these tests, bending moments were measured when the dolphin was subjected to different loads (Griffioen, 2023). The measurements from the highest load are used, which was at 60% capacity of the pile. These measurements can be used to update the variables that influence the occurring moment. These are the model uncertainty and internal friction angle of the upper layer. The other variables are not updated as they have little influence and were discarded for this study. The observation function in this study can be defined as Equation 6.1.

$$M_{calculated} < M_{measured} \tag{6.1}$$

With,

$M_{measured}$ = 40494 kNm, maximum moment measured at the load of 1350 kN applied on the top of the dolphin

$M_{calculated}$ = Calculated moment at the same load for the measured moment

The resulting reliability index after the Bayesian update was 2.91. The posterior distributions are presented in Figure 6.3. The mean of the effective friction angle becomes larger and the CoV drops a bit. The larger mean could lead to an improvement of the PY curves used for the upper soil layer, but the effects are negligible. The most reduction of the uncertainty is in model uncertainty of the occurrent moment. The mean of this variable becomes lower as well as the standard deviation. The posterior distribution resembles a truncated normal distribution, which is slimmer than the prior distribution.

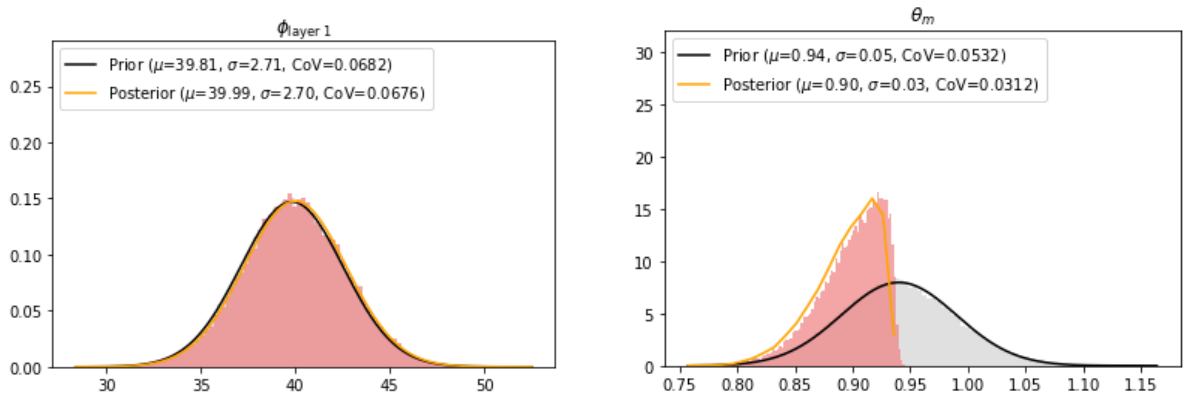

Figure 6.3: Resulting distributions of the updated variables when incorporating load testing data

6.3. Update based on an observed load

Another type of information that can be added to update the reliability, is the observation that the dolphin survived an extreme load, much like de Koker et al. (2020). The benefit of this update compared with the previous one would be that all variables can be updated. At the end of the lifetime of the dolphin, it could be re-assessed as there is potential its lifespan can be prolonged if the reliability can be updated

by an observed load. Such a load could be derived from AIS records. The maximum load can then be used to perform a Bayesian update. In the original design of the dolphin, the design load was equal to 2704 kNm. Let us assume that at the end of the lifespan, the dolphin has survived a load of 2250 kNm, around 80% of the design load. Thereby, the observation function can be defined as Equation 6.2.

$$Z(E_{obs}) < 0 \tag{6.2}$$

With,

$Z(x)$ = Structural limit state as defined in Equation 4.1
E_{obs} = 2250 kNm, assumed maximum survived load during the dolphin lifespan

After the Bayesian update is performed, the updated reliability index is equal to 2.75. This is a slight increase from the prior reliability. The resulting posterior distributions of the updated variables are shown in Figure 6.4. The mean and standard deviations of the variables are barely updated, there are negligible shifts in the mean reduction of the standard deviations. These slight changes in these variables are what lead to the slightly higher reliability index.

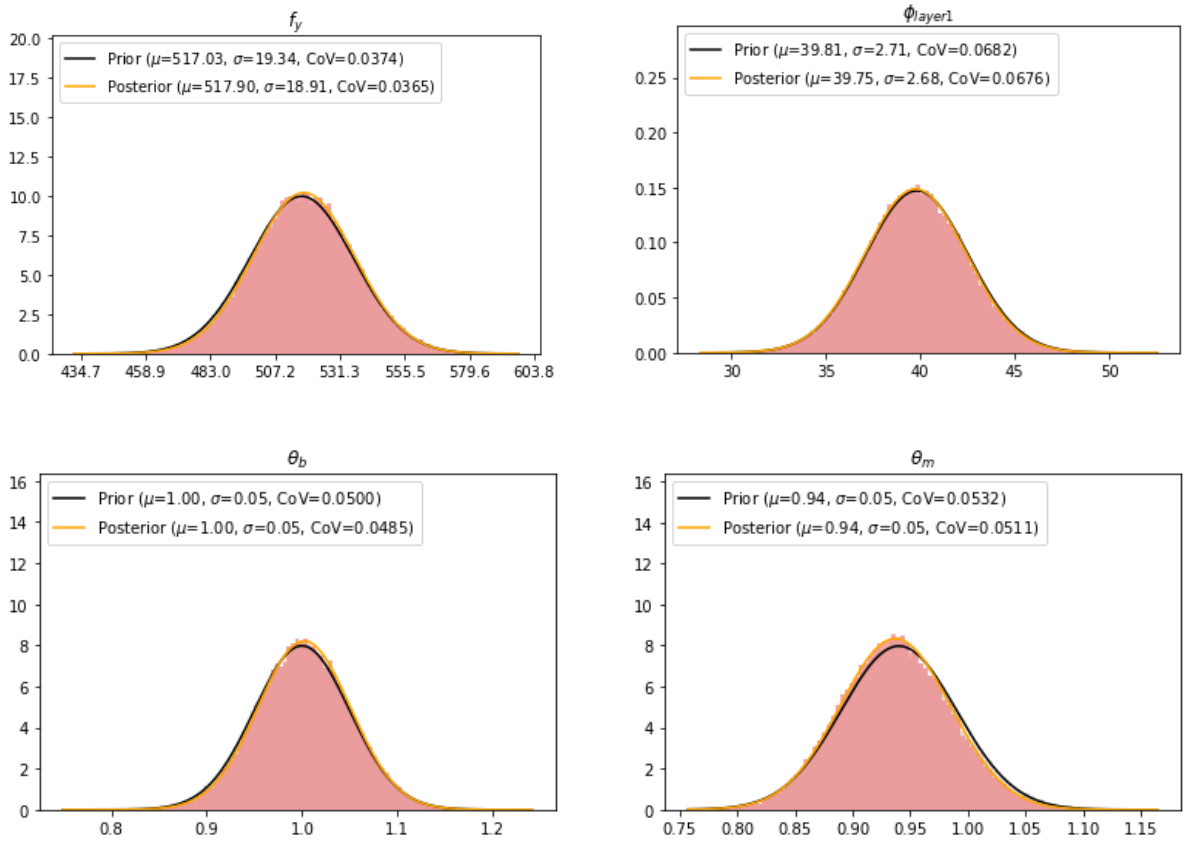

Figure 6.4: Resulting distributions of the updated variables when observing an extreme load

Now let us say that the dolphins survived a load slightly higher than the design load of 2620275 kN, for example, 2700 kN. This has significantly more impact on the reliability index of the dolphin because the posterior reliability is then 3.28. The posterior distributions are also much more favourable, see Figure 6.5.

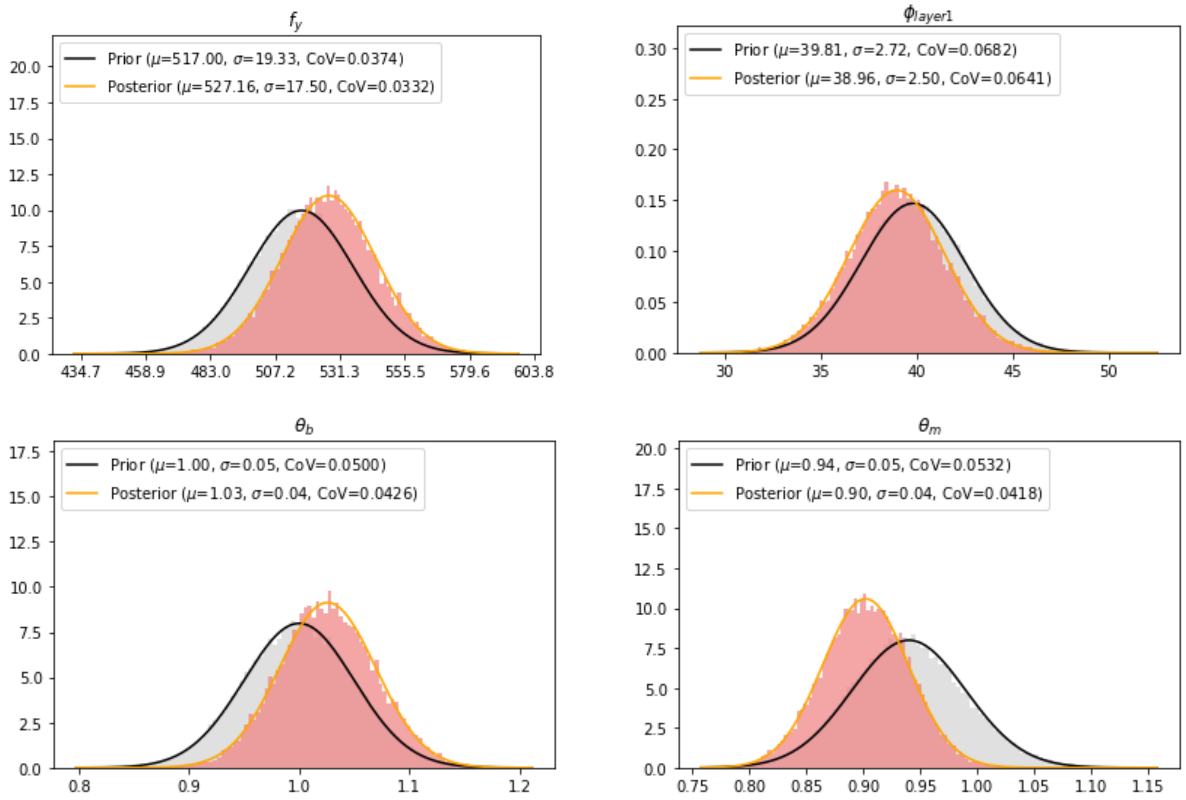

Figure 6.5: Resulting distributions of the updated variables when observing an extreme load

6.4. Insights provided through Bayesian updates

The chosen observations do increase the reliability index, but its effects are not great. In order to receive more information and have a higher reliability index, the loads need to be increased so that they are near or surpass the design load of the pile, just as Zhang (2004) suggested. The challenge with this is that there is a significant increase in the probability of failure. Because of this increase in failure, it is recommended to do a cost-benefit analysis to assess if the high-load tests have any merit. It is interesting to note that the test loading was at a lower capacity than the fictional observed load and updated fewer variables, but still yielded a higher reliability update. This is most likely due to knowing the exact bending moment at that instance. So this is significant information to have for a reliability update. Another piece of information that one could add is testing the yield strength of the pile before installation, which is a less cumbersome operation to undergo. Similar to the case ”Clay” according to the Port of Rotterdam standards, the distribution is truncated at 483 MPa and the reliability analysis is conducted. This leads to a reliability of 2.50, which is still less than the other updates. The reliability indices are shown in Table 6.2. To summarize, the Bayesian update can help increase the reliability index in order for a dolphin to extend its lifespan, however, the loads necessary are very high and lead to an increase in failure probability. Therefore an analysis should be made beforehand if it is worth it and how much the load imposed should be such as Goulet (2015).

Table 6.2: Summary reliability indices resulting from different Bayesian updates

	β	P_f	Less likely to fail
Prior	**2.43**	**2.08%**	
Posterior observed load 102% pile capacity	3.28	0.18%	11.3
Posterior load testing 60% capacity	2.95	0.51%	4.05
Posterior observed load 80% pile capacity	2.75	0.91%	2.29
Posterior truncation yield stress pile	2.50	1.75%	1.19

7 Discussion

During the research discussion points regarding the methods and results were encountered. These points and their implications which they may have on the conclusion are discussed in this chapter. Firstly, Section 7.1 delves deeper into the accuracy of the results. Then Section 7.2 discusses the limitations of the research. Last, in Section 7.3 the comparison with other studies is made.

7.1. Accuracy of the results

The accuracy of the results is largely dependent on the inputs and calculation method. Each one is correspondingly explained in this section.

7.1.1. Accuracy of inputs

The starting points of the reliability assessments are the input parameters used. Each has a mean and standard deviation, which were found in the literature. These factors influence the reliability of the structure and results of the assessment. The inputs used for the soil parameters were derived from the Eurocode and a distribution was allocated based on those values. However, these values have been scrutinised and were most likely derived with many simplifications based on assumptions (Calle et al., 2021). The actual stochastic parameters for these properties may differ if a soil investigation is performed. For structural reliability, the impact of more precise values of the soil properties will most likely have little impact due to the low influence factors found, but for the fixity reliability, it may have a larger impact. Thus, a shorter pile might be designed.

Another potential inaccuracy is the value for the model parameter. This value is determined by comparing the calculated maximum bending moment with the measured one in the load tests from the Calandkanaal. This value would only be applicable for that soil composition but used for the other calculations for the other soil compositions as well. For a proper value of the model uncertainty, different tests should be conducted in different soil compositions to assess whether the value derived in this study is generic. Furthermore, the model uncertainty varies throughout the depth as shown in Figure 3.9. In this study, the correction of the model parameter was constant throughout the depth leading to an underestimation of the moments at certain locations of the dolphins. Although this underestimation, it will most likely have not a high impact on the reliability, because most failures occurred at the location of the maximum moment.

Moreover, the derivations of the extreme value distributions of the berthing energy also have underlying assumptions. The berthing energy was calculated with Equation 2.1 using distributions for the velocity and water displacement. Conversely, the other constants were based on assumptions about the berthing angle and load which the ship bears. The study conducted by Iversen et al. (2022) also made the berthing angle a stochastic variable, while Heeres et al. (2023) showed that this does not significantly influence the reliability. The other factors also influence the berthing energy, notably the virtual mass factor which depends on the load. No data is available for these values, so conservative estimates were used. For a more accurate estimate, these factors should be measured as well or

even better would be measuring the factors on the other side of Equation 2.6. If the berthing force and deflection can be measured, then the berthing energy can be determined. If these measurements are done for a long enough time duration, extreme value analysis can be conducted as well. This might give a better and more favourable extreme value distribution for the berthing energy.

Furthermore, when conducting the extreme value analysis it was not considered that the ship sizes will increase over time. From 1982 to 2014 the average container ship size increased from 596 TEU to 2256 TEU (Tran and Haasis, 2015). This growth size can have an enormous effect on the temporal evolution of the extreme value analysis, as an extreme value distribution 50 years from now will be fairly larger than the ones determined in this study. On the other hand, ship propulsion systems have also improved considerably in the past 50 years (Carlton, 2012) and this would lead to lower berthing velocity. The increase in ship size and decrease in berthing velocity could perhaps counteract each other, but the exact effect cannot be determined without data. The data available only consisted of the ship size, but no berthing velocity over time. Even more importantly, the time span of the data is not extensive enough to conduct a non-stationary extreme value analysis (Ragno et al., 2019). Thus, much more information is needed to capture the temporal effects of the probability of extreme berthing energies.

7.1.2. Accuracy of calculation method

The probabilistic technique used for the reliability assessments was Directional Sampling. In order to reach significant convergence, the recommended coefficient of variation for this technique is less than 0.1 (Deltares, 2022). However, due to time constraints, this stop criterion was not always reached. This introduces a larger than preferred error to the final reliability. Additionally, this may also impact the influence factors of the variables as these are determined by the weighted mean of the failed realisations. An earlier stop to the realisations may lead to unrealised samples that fail. Therefore, the derived partial factors in this study need to be used cautiously. In addition, the calculated reliability index was not always equal to the prescribed 3.3 in the current Eurocode 0. Though, studies have suggested that this value may not be a minimum requirement, but an average over the entire lifespan of the structure. Thus, a range of 0.2 is deemed acceptable (Meinen et al., 2018).

For the Bayesian update, a response surface was used and was created with a Gaussian Process Regression. Although it is an accurate method for the training samples, it does introduce an error in the values in between the training data. Nonetheless, this is the most accurate method for a regression process (Rasmussen and Williams, 2006). Besides, using a response surface helps reduce the calculation time for the Bayesian update considerably by turning a calculation time which most likely be in the order of weeks into a mere couple of hours. A broad selection of sample points helps reduce the inaccuracies (Vosooghi, Sriramula, and Ivanoviç, 2022). That is why in this study extensive training data was selected to construct the response surface.

Furthermore, the observed occurring moment for the observation function in Section 6.2 was seen as a definitive value, while in reality it was subjected to a measurement error of 10% (Griffioen, 2023). A more accurate assessment would be seeing the observed load as a stochastic variable which is normally distributed with a coefficient of variation of 10%. This would decrease the reliability update and most likely have the same posterior reliability as the prior reliability. In order to still have some form of update, the equality type of observation function could be used.

7.2. Limitations of the research

This study considered many factors that influence the reliability of the dolphin, however, some assumptions were made. The first assumption is that the dolphin is under cathodic protection and therefore it will not corrode. This assumption was made because the method of protection against corrosion is preferred in Dutch ports. After all, it can be more sustainable. Cathodic protection leads to less material loss than adding extra corrosion thickness to the pile. Besides, contrary to quay walls, no extensive studies on corrosion in dolphins exist as of yet. So, no clear guidelines exist on how the corrosion of the pipes develops over time. Thus, in this study, the no corrosion assumption leads to no degradation

of the material over time. This an optimistic assumption, because the cathodic protection is not always 100% effective (Angst, 2019). The corrosion can be very detrimental to the reliability of marine structures (Roubos et al., 2020; Allaix et al., 2022). Given these points, the development of corrosion must carefully be assessed during its lifetime if the results of this study are used for the design of dolphins.

Not only an optimistic assumption was made, but also a conservative one. The study assumed that the bed level is at the nautical guaranteed depth. This is the minimum depth the port authorities must provide for ships to navigate through. For berthing dolphins higher bed levels, mean higher bending moments in the pile which is unfavourable. That the bed level is at this high level throughout the lifespan of the dolphin is unlikely and up till this level, a large part is fluid mud which behaves quite differently than soil (Kirichek et al.,2017). The fluid mud would make the dolphin react more flexibly and would lead to smaller bending moments. Thus, the occurring bending moment varies throughout time thanks to the varying bed level. In order to effectively capture this effect a time-dependent reliability analysis should be conducted, while also taking into account the combination of bed level and berths. Such studies have already been conducted for other structures, for example, bridges (Das et al., 2022). It is expected that this type of analysis would lead to a higher reliability index.

This study was limited to sea-going vessels because berthing records of only these vessels exist as of now. There are also a lot of inland vessels in the Netherlands that berth at dolphins. They have a smaller water displacement than the larger sea-going vessels and their behaviour during a berthing process could potentially be different. This could lead to different distributions for the berthing velocity and in turn different distributions for the extreme value analysis of the berthing energy. And since the berthing energy has the most influence, this could potentially lead to different results.

At last, the study did not consider the effects of a fender. The dolphin was considered to fully absorb the energy from the berthing ship. Many dolphins are installed with a fender which also absorbs a part of the berthing energy and transfers said energy as a constant force on the dolphin. In that case, the dolphin has the same bending moment throughout the berthing process, no matter how much the dolphin bends. No fenders means that more bending in the dolphin leads to lower bending moments. Therefore, with a fender the limit state should be defined differently. The dolphin needs to be able to absorb the remaining energy, while simultaneously having enough bending moment capacity to not fail. With a fender, it might be possible that the soil parameters are more of an influence.

7.3. Comparison other studies

This study resulted in partial factors for the berthing load. Past studies also derived partial factors and were already mentioned in the introduction. The study performed by Schrijver (2016) cannot be used as a comparison as that study derived factors in CC2. The study by Heeres et al. (2023) can be compared with this study. Their study conducted a reliability assessment of a pile in moderate navigation conditions with 100 arrivals per year. The resulting partial factor for the berthing load was 1.39. For similar conditions, this thesis found 1.31, which is lower. Some differences might explain this discrepancy. For instance, the study performed by Heeres et al. (2023) did not include model uncertainty, thus leading to a higher influence factor for the berthing load. This causes the partial factor to be higher. The model uncertainty, however, is uncertainty which should be considered in the probabilistic approach (van Gelder, 2000). Another cause for the discrepancy could be the reliability index used by Heeres et al. (2023) was slightly higher than 3.3. For an exact CC1 partial factor, the reliability target should be corrected for 3.3.

A similar approach as this study to derive the partial factors was used for fenders by Orlin (2020). In that study, Monte Carlo simulations were performed and reliability-based assessments were done. The simulations and assessments also included the berthing angle, while this thesis did not. Orlin (2020) showed that for single fender contact, the angle has an insignificant influence. For berthing at flexible dolphins there is also single fender contact, so no consideration for the berthing angle may not be an issue. Orlin (2020) did find higher partial factors for berthing, but this could be due to more design considerations for dolphins such as wall thickness and yield strength.

8

Conclusion and Recommendations

This chapter concludes the research by answering the sub and main research questions. Before this study, the calibration of the partial factors for flexible dolphins was incomplete. A singular case was studied, but it was still unknown if those results apply to different cases. This study calibrated the partial factors for cases with different soil compositions and different navigation conditions. Additionally, this thesis also shows how information from test loading and historical berthing records can be used to update the reliability of the dolphin. In Section 8.1, answers are given to subquestions iii till vi and the main question. Answers to subquestions i and ii were found in literature, therefore they are not repeated here. In the end, recommendations for future studies are provided.

8.1. Conclusion

8.1.1. Answers to the sub-questions

iii. What is the influence of different soil compositions on the reliability and partial factors of safety?

The reliability index and partial factors of safety remained almost the same for different soil compositions in the Netherlands. When adjusting the pile dimensions to meet the reliability target, neither clay, loose soil nor dense soil led to different influence factors for structural reliability. All the soil types assessed showed that the berthing load was by far the most dominant factor and in each case had the same influence coefficient. The cases showed that the sensitivity factor of the berthing load differed $\pm$ 2%. Therefore, the load-based design approach be generically applied to different soil compositions.

For the fixity, on the other hand, the influence factors do differ. Homogeneous soil compositions show more susceptibility to exceed the fixity criterion than heterogeneous ones. Nevertheless, the reliability indices remained more than the literature-recommended 1.5 target value. And since this limit state is a serviceability limit state partial factors do not need to be applied. However, the software used in the study was not completely suitable to assess the fixity and geotechnical limit states fully. This was due to the PY-curves returning unrealistic displacements and bending moments when 100% mobilisation was achieved in the springs.

iv. What is the influence of different navigation conditions on the reliability and partial factors of safety?

The more disadvantageous the navigation conditions, the more likely the probability of failure. Thus, a larger pile is necessary for those disadvantageous conditions. For that purpose, larger partial factors need to be applied. Next to the different conditions, the arrival rate of ships influences the reliability. If a lot of ships are arriving then there is a larger probability of extreme berthing energies leading to a lower reliability index. Vice versa for a lower arrival rate. To incorporate this effect in the design approach of the dolphin, correction factors need to be applied to the partial factors for the navigation conditions. Lastly, the variation of ships which arrive plays a role. If there is a low variation among ships berthing then the larger ships berth more frequently. This leads to larger distributions in the extreme value analysis. Therefore, larger partial factors must be applied to the characteristic berthing energy.

v. What set of partial safety factors are recommended to be implemented in the design of dolphins?
For the design of dolphins, it is recommended to apply safety factors only on the berthing load, because the berthing load was the only input variable that had a significant influence factor (-0.77). The value of the partial factor is dependent on the 3 elements, namely the navigation conditions, arrival rate and variation in water displacement. The main factor is determined by navigation conditions. If the characteristic berthing energy can be determined by using the largest ship and characteristic berthing velocity then the partial factors found for monitored, favourable, moderate and unfavourable conditions are respectively 1.19, 1.29, 1.31 and 1.39.

On this main factor, two correction factors can be applied. Those factors depend on the arrival rate of the ships and the variation of those arrived ships. Figures 5.10b and 5.10a show the exact values of the correction factors. These factors can be applied when designing new dolphins in the Netherlands for the assessment of the failure modes yield and buckling.

vi. How can the full-scale field test data and historical records of observations benefit the probabilistic assessments?
Information on observed load and full-scale field tests can be used to update the reliability index for lifespan extension. However, loads larger than the design load are necessary to reduce the probability of failure tenfold. Loads close to the design load can occur throughout the lifespan of the dolphin, but the probability of occurring is very low. That is why it is better to impose such a large load with a full-scale load test. The value of this load should be close to the design load as this would lead to a larger update. The exact value depends on the probability of failure during such a load and what the quantified benefits of this update would be.

8.1.2. Answer to the main research question
The main research question of this study was formulated as follows:

What benefits can be attained by performing reliability-based approaches for flexible dolphins?

In conclusion, probabilistic assessments help engineers better understand the uncertainties that come with designing a dolphin and design the dolphin in such a manner that 5 to 20% of material can be saved while still meeting the minimum target reliability. The most important uncertainty is the berthing load and this load is largely dependent on the berthing velocity, arrival rate and variation in water displacement. The assessments show that by taking these factors into account as well then a more optimal design can be made. The reliability-based assessments resulted in a calibrated partial factor for the dolphin that can be implemented in a semi-probabilistic manner and still have an improved and safe design.

Reliability-based assessments also help manage uncertainties in the other variables important in the design of the dolphin. By measuring the wall thickness and yield strength of the steel, the dolphin improves its reliability coefficient and taking this reduction of the uncertainties into account then an even more optimal design can be realised. Furthermore, a reliability-based approach combined with test loading can reduce the probability of failure for dolphins four- to tenfold.

8.2. Recommendations
This study focused on improving the design approach of dolphins through reliability-based assessments. The results showed promising outcomes that can lead to more optimal designs. This section gives recommendations to further improve the design approach of the dolphin and for further studies.

- This study derived partial factors for the failure modes yield and buckling, The factors for the geotechnical failure due to software limitations. It is recommended to derive the geotechnical partial factors using a calculation model that can capture the soil complexity such as a FEM-based model.
- The study was limited by the information available for conducting the extreme value analysis. To improve this analysis it is recommended that more data should become available. The data

should include the berthing angle and load on the ship as well. Another option would be to measure the force the ship exerts on the dolphin during the berths and its corresponding deflection. This would lead to a more precise load which the dolphin needs to withstand.

- The study was conducted by transforming the time-dependent problem into a time-independent one. A time-independent analysis would help better approximate the reliability index as through such an analysis the assumption on the constant bed level and temporal evolution of berthing load do not need to be made.
- A time-dependent factor would also help include the effects of corrosion. The results showed that the uncertainty in the wall thickness has a significant influence on the probability of failure of the dolphin. Corrosion would reduce the wall thickness and this is detrimental to the pile. This study assumed that it would have no effect because of cathodic protection, however, not all piles are designed with such a measure. And even such a measure may not work 100% effectively. In addition, the corrosion rate of dolphins also needs to be measured to conduct a time-dependent analysis.
- The study only showed the potential effects a large load may have on a dolphin, but not what load is recommended. Therefore, a pre-posterior analysis is necessary. It is recommended to perform such an analysis on a dolphin which is at the end of its lifespan and could be potentially extended.
- The study only considered sea-going vessels because these had existing berthing records. It is recommended to also measure the berthing velocities of inland vessels.
- The partial factors in this study are applicable for dolphins with a design lifetime of 50 years in CC1. It is recommended to do similar calculations for different design lifetimes and consequence classes.
- The use of a response surface helped reduce the calculation time remarkably. For analysis which requires many calculations, it is recommended to make use of a response surface.
- The knowledge gained from reliability-based assessments shows that such an analysis can be applied not only to dolphins but also to other types of maritime infrastructure, contributing to improved designs, construction techniques, and maintenance practices. Sharing this knowledge with the broader engineering community further enhances safety and efficiency in port operations worldwide.

References

Allaix, Diego et al. (2022). *Richtlijn bewezen sterkte damwanden en kademuren-Eindrapport smartport.nl*. Tech. rep. URL: www.smartport.nl.

American Petroleum Institute (July 1993). *Recommended Practice for Planning, Designing and Constructing Fixed Offshore Platforms – Load and Resistance Factor Design*. Vol. 1. Washington: American Petroleum Institue.

Angst, Ueli M. (Dec. 2019). "A Critical Review of the Science and Engineering of Cathodic Protection of Steel in Soil and Concrete". In: *Corrosion* 75.12, pp. 1420–1433. ISSN: 0010-9312. DOI: 10.5006/3355.

Bai, Yong and Wei-Liang Jin (2016). *Marine Structural Design*. Elsevier. ISBN: 9780080999975. DOI: 10.1016/C2013-0-13664-1.

Bayes, T. (1763). "An essay towards solving a problem in the doctrine of chances". In: *Philosophical Transactions of the Royal Society of London* 53, pp. 370–418.

Betz, Wolfgang, Iason Papaioannou, and Daniel Straub (Nov. 2022). "Bayesian post-processing of Monte Carlo simulation in reliability analysis". In: *Reliability Engineering & System Safety* 227, p. 108731. ISSN: 09518320. DOI: 10.1016/j.ress.2022.108731.

Blum, H (1932). *Wirtschaftliche dalbenformen und deren berechnung*.

Calle, E.O.F., W. Kanning, and T. Schweckendiek (June 2021). *Characteristic values of soil properties in Dutch codes of practice*. Tech. rep. Delft: Deltares.

Carlton, J.S. (2012). "Propulsion Systems". In: *Marine Propellers and Propulsion*. Elsevier, pp. 11–28. DOI: 10.1016/B978-0-08-097123-0.00002-2.

CRW C1005 (Feb. 2018). *Flexible Dolphins*. Ed. by SBRCURnet Committee 1720. Delft.

CUR211 (2013). *Handbook of quay walls*. Tech. rep.

Das, Joydeep and Arjun Sil (Dec. 2022). "Assessment of time-dependent structural resistance of RC bridges in Barak Valley, Assam, India". In: *Proceedings of the Institution of Civil Engineers - Bridge Engineering* 175.4, pp. 263–275. ISSN: 1478-4637. DOI: 10.1680/jbren.21.00031.

De Koker, N. et al. (May 2020). "Updating structural reliability efficiently using load measurement". In: *Structural Safety* 84, p. 101939. ISSN: 01674730. DOI: 10.1016/j.strusafe.2020.101939.

Deltares (2022). *Probabilistic Toolkit User Manual*. Tech. rep. URL: https://www.deltares.nl.

Den Adel, N (2019). *Load testing of a quay wall Evaluating the use of load testing by application of Bayesian updating, MSc thesis*. Delft University of Technology. URL: http://repository.tudelft.nl/..

Dudzik, Agnieszka (Oct. 2017). "Reliability Assessment of Steel-Aluminium Lattice Tower". In: *IOP Conference Series: Materials Science and Engineering* 245, p. 032072. ISSN: 1757-8981. DOI: 10.1088/1757-899X/245/3/032072.

Echard, B., N. Gayton, and M. Lemaire (Mar. 2011). "AK-MCS: An active learning reliability method combining Kriging and Monte Carlo Simulation". In: *Structural Safety* 33.2, pp. 145–154. ISSN: 01674730. DOI: 10.1016/j.strusafe.2011.01.002.

EN 1993-1-1 (2005). *Design of steel structures – Part 1-1: General rules and rules for buildings*. Stichting Koninklijk Nederlands Normalisatie Instituut.

Gelder, P.H.A.J.M. van (2000). "Statistical methods for risk-based design of civil structures". PhD thesis. Delft: Delft University of Technology.

Goulet, James-A., Armen Der Kiureghian, and Binbin Li (Jan. 2015). "Pre-posterior optimization of sequence of measurement and intervention actions under structural reliability constraint". In: *Structural Safety* 52, pp. 1–9. ISSN: 01674730. DOI: 10.1016/j.strusafe.2014.08.001.

Griffioen, P.J. (May 2023). *Paalproef Calandkanaal*. Tech. rep. Deventer: Witteveen+Bos Raadgevende ingenieurs B.V.

Hasofer, Abraham M. and Niels C. Lind (Feb. 1974). "Exact and Invariant Second-Moment Code Format". In: *Journal of the Engineering Mechanics Division* 100.1, pp. 111–121. ISSN: 0044-7951. DOI: 10.1061/JMCEA3.0001848.

Heeres, O et al. (2023). *Probabilistisch ontwerp van afmeerpalen*. Tech. rep.

ISO 2394 (2015). *General principles on reliability for structures*. Geneva: International Organisation for Standardisation.

Iversen, Rune, Alfred Roubos, and Prasanthi Mirihagalla (Sept. 2022). "PIANC Working Group 211: Reliability Based Design of Marine Fenders—No More Abnormal Berthing Factor". In: *Ports 2022*. Reston, VA: American Society of Civil Engineers, pp. 435–443. ISBN: 9780784484395. DOI: 10.1061/9780784484395.044.

James, Gareth et al. (July 2021). *An Introduction to Statistical Learning*. 2nd ed. Springer.

Jasper Focks, D.J, J.M. van der Meer, and A. Roubos (Dec. 2015). "Innovatie Flexible Dolphins - Aangescherpt paalontwerp op basis van grootschalige proeven". In: *Geotechniek*, pp. 57–64.

JCSS (2001). *Probabilistic model code, part 3, Resistance model*.

Jonkman, S N et al. (2017). *Probabilistic Design: Risk and Reliability Analysis in Civil Engineering Lecture notes CIE4130*. Delft University of Technology.

Kirichek, Alex et al. (2017). *Characterization of fluid mud layers for navigational purposes*. Tech. rep. URL: https://www.researchgate.net/publication/330089313.

Krogt, Mark van der (2022). "Reliability updating for slope stability improving dike safety assessments using performance information". PhD thesis. ISBN: 978-94-6366-531-5.

Laghmouchi, K. (2021). *Reliability updating of existing quay walls based on the effects of past performance Introduction of a novel mathematical application in the probabilistic assessment and evaluation of quay walls, Msc thesis*. URL: http://repository.tudelft.nl/..

Lantsoght, Eva O.L., Cor van der Veen, Ane de Boer, et al. (Oct. 2017). "Required proof load magnitude for probabilistic field assessment of viaduct De Beek". In: *Engineering Structures* 148, pp. 767–779. ISSN: 01410296. DOI: 10.1016/j.engstruct.2017.07.010.

Lantsoght, Eva O.L., Cor van der Veen, Dick A. Hordijk, et al. (Dec. 2017). "Development of recommendations for proof load testing of reinforced concrete slab bridges". In: *Engineering Structures* 152, pp. 202–210. ISSN: 01410296. DOI: 10.1016/j.engstruct.2017.09.018.

Leonardo Da Vinci pilot project (2004). *Basis of Structural design*. Garston.

Li, Chun-Qing and Wei Yang (2023). *Time-Dependent Reliability Theory and Its Applications*. Elsevier. ISBN: 9780323858823. DOI: 10.1016/C2020-0-02657-5.

NEN 6766 (Feb. 2023). *Corrosie van stalen elementen in de ondergrond - Eisen voor ontwerp en toepassing*. Stichting Koninklijk Nederlands Normalisatie Instituut.

NEN-EN 10051 (Dec. 2010). *Continuously hot-rolled strip and plate/sheet cut from wide strip of non-alloy and alloy steels - Tolerances on dimensions and shape*. Delft: Nederlands Normalisatie Instituut.

NEN-EN 10219-2 (Dec. 2010). *Cold formed welded steel structural hollow sections - Part 2: Tolerances, dimensions and sectional properties*. Delft: Nederlands Normalisatie Instituut.

NEN-EN 1993-1-1 (2006). *Eurocode 3: Design of steel structures - Part 1- 1: General rules and rules for buildings*. Delft: Stichting Koninklijk Nederlands Normalisatie Instituut.

NEN-EN 1997 (June 2012). *NEN-EN 1997-1 Geotechnisch ontwerp*.

NEN9997-1 (Nov. 2017). *Geotechnical design of structures*. Nederlands Normalisatie-instituut.

Orlin, Felix (Nov. 2020). *Reliability-Based Assessment for Fender Systems, Msc thesis*. Delft: Delft University of Technology.

Pedregosa, F. et al. (2011). "Scikit-learn: Machine Learning in {P}ython". In: *Journal of Machine Learning Research* 12, pp. 2825–2830.

Peerden, Jur (June 2023). *The behaviour of a flexible dolphin in the Port of Rotterdam, Msc thesis*. Delft: TU Delft.

Peters, Dirk Jan et al. (Sept. 2017). "Calibration of Eurocode design models of thin-walled cylinder under bending with full scale tests". In: *ce/papers* 1.2-3, pp. 3729–3740. ISSN: 25097075. DOI: 10.1002/cepa.429.

Phoon, K.K. and J.V. Retief (Nov. 2016). *Reliability of Geotechnical Structures in ISO2394*. Leiden,The Netherlands : CRC Press/Balkema, [2016]: CRC Press. ISBN: 9781315364179. DOI: 10.1201/9781315364179.

PIANC 121 (2014). *Harbour Approach Channels Design Guidelines*. Tech. rep. Brussels: Maritime Navigation Commission.

PIANC WG33 (2002). *Guidelines for the design of Fender Systems*. Tech. rep. Brussels: Maritime Navigation Commission.

Port of Rotterdam (2022). *Jaarverslag 2022*.

Port of Rotterdam (2023). *Port Development*.
Post, M. et al. (2021). *Reliability analysis of quay walls Exploring a metamodeling approach for more robustness and efficiency*. Tech. rep. Deltares.
Potts, D.M. and L Zdravkovic (1999). *Finite Element Analysis in Geotechnical Engineering theory*. Vol. 1. London: Thomas Telford.
Ragno, Elisa et al. (Aug. 2019). "A generalized framework for process-informed nonstationary extreme value analysis". In: *Advances in Water Resources* 130, pp. 270–282. ISSN: 03091708. DOI: 10.1016/j.advwatres.2019.06.007.
Rasmussen, C.E. and K.I. Williams (2006). *Gaussian Processes for Machine Learning*. Massachusetts Institute of Technology.
Rijkswaterstaat (May 2021). *Schematiseringhandleiding macrostabiliteit*. Tech. rep. Ministerie van Infrastructuur en Waterstaat.
Roubos, Alfred (2019). "Enhancing reliability-based assessments of quay walls". PhD thesis. DOI: 10.4233/uuid:40632b7a-970e-433d-9b4e-ff2d2249b156. URL: https://doi.org/10.4233/uuid:40632b7a-970e-433d-9b4e-ff2d2249b156.
Roubos, Alfred, Leon Groenewegen, and Dirk Jan Peters (Jan. 2017). "Berthing velocity of large seagoing vessels in the port of Rotterdam". In: *Marine Structures* 51, pp. 202–219. ISSN: 09518339. DOI: 10.1016/j.marstruc.2016.10.011.
Roubos, Alfred A. et al. (Nov. 2020). "Time-dependent reliability analysis of service-proven quay walls subject to corrosion-induced degradation". In: *Reliability Engineering and System Safety* 203. ISSN: 09518320. DOI: 10.1016/j.ress.2020.107085.
Ruigrok, J (2010). *Laterally Loaded Piles Models and Measurements, Msc thesis*.
Schrijver, I J M (2016). *Reliability of flexible dolphins: determination of the partial safety factors for parameters in the flexible dolphin design, Msc thesis*.
Schweckendiek, T (Dec. 2006). *Structural Reliability Applied to Deep Excavations, Msc thesis*. Delft University of Technology.
Schweckendiek, Timo (2010). "Reassessing reliability based on survived loads". PhD thesis.
— (2014). *On reducing piping uncertainties: A Bayesian decision approach*. Tech. rep.
Splunter, M van (Mar. 2015). *STS palen Calandkanaal Rotterdam*. Tech. rep. B.V. INgenieursbureau M.U.C.
Straatman (2018). *Quick release mooring hooks with solar power systems for Port of Rotterdam*.
Straub, Daniel (Apr. 2011). "Reliability updating with equality information". In: *Probabilistic Engineering Mechanics* 26.2, pp. 254–258. ISSN: 02668920. DOI: 10.1016/j.probengmech.2010.08.003.
Straub, Daniel and Iason Papaioannou (Mar. 2015). "Bayesian Updating with Structural Reliability Methods". In: *Journal of Engineering Mechanics* 141.3. ISSN: 0733-9399. DOI: 10.1061/(ASCE)EM.1943-7889.0000839.
Tian, Huaming et al. (Sept. 2023). "Auxiliary Bayesian updating of embankment settlement based on finite element model and response surface method". In: *Engineering Geology* 323, p. 107244. ISSN: 00137952. DOI: 10.1016/j.enggeo.2023.107244.
Tran, Nguyen Khoi and Hans-Dietrich Haasis (Jan. 2015). "An empirical study of fleet expansion and growth of ship size in container liner shipping". In: *International Journal of Production Economics* 159, pp. 241–253. ISSN: 09255273. DOI: 10.1016/j.ijpe.2014.09.016.
Trelleborg (2018). *Fender application Design Manual*.
Vosooghi, Navid, Srinivas Sriramula, and Ana Ivanoviç (July 2022). "Response surface based reliability analysis of critical lateral buckling force of subsea pipelines". In: *Marine Structures* 84, p. 103246. ISSN: 09518339. DOI: 10.1016/j.marstruc.2022.103246.
Vries, R. de et al. (June 2022). "Reliability assessment of existing reinforced concrete bridges and viaducts through proof load testing". In: *Bridge Safety, Maintenance, Management, Life-Cycle, Resilience and Sustainability*. London: CRC Press, pp. 467–475. DOI: 10.1201/9781003322641-54.
Wang, C (2021). *Structural Reliability and Time-Dependent Reliability*. Cham: Springer International Publishing. ISBN: 978-3-030-62504-7. DOI: 10.1007/978-3-030-62505-4.
wermac.org (n.d.). *Longitudinally Welded Pipes*.
WG145 (2022). *Berthing velocity analysis of seagoing vessels over 30,000 dwt*. PIANC.
WG211 (2024). *The new Fender design Guideline*. Brussels: PIANC.
Wolters, Herm-Jan (2012). *Reliability of Quay Walls, MSc thesis*.
World Steel Assocaition (2023). *Climate change and the production of iron and steel*. Brussels.

Zhang, Limin (Nov. 2004). “Reliability Verification Using Proof Pile Load Tests”. In: *Journal of Geotechnical and Geoenvironmental Engineering* 130.11, pp. 1203–1213. ISSN: 1090-0241. DOI: 10.1061/(ASCE)1090-0241(2004)130:11(1203).

A

Outcome of Monte Carlo simulations

This appendix summarises the results of the Monte Carlo simulations used to determine the design points in Chapter 5. Section A.1 describes how the simulation was conducted. Then in Section A.2 the samples from the simulation are fitted. Finally in Section A.3 the design points and partial factors are derived.

A.1. Performing the simulations

The distribution of the berthing energy was determined using Monte Carlo simulations. Recall Equation 2.1, which can be used to determine the berthing energy.

$$E_k = \frac{1}{2} \cdot M \cdot v^2 \cdot C_E \cdot C_M \cdot C_S \cdot C_c.$$

The extreme value analysis followed from Monte Carlo simulation as explained in Chapter 3. The simulation samples values for each parameter in this equation. The distribution for each parameter is explained below:

- The berthing velocity was sampled from the distributions found by Roubos et al. (2017)
- For the water displacement it was decided to sample from a uniform distribution because each of the exact distribution of water displacement differs per location and a uniform distribution gives each ship an equal chance to be sampled.
- The eccentricity factor is always equal to 1 for open structures as dolphins
- The mass coefficient is assumed fixed at 1.5 because the keel clearance is always more than 0.5 times the draught of the ship
- The softness coefficient is set as 1
- The ship flexibility factor is also set to 1 again because the dolphin is an open structure.
- The eccentricity factor depends on the berthing angle. This study had no information available on this parameter, therefore the assumption was made that the berthing angle was always equal to 3 degrees

The extreme value distribution was found by the following steps:

1. Simulating the berthing energy of 50 years and extracting the maximum value
2. That process is repeated 200 times, therefore leading to 200 extreme values
3. Fitting this data set with different distributions
4. Repeat for other navigation conditions

The combinations of the different simulations that were run are shown in Table A.1

Table A.1: Combination of the simulations performed

	Monitored Weibull (λ=5.2, k=2.69)	**Favourable Weibull (λ=4.9, k=2.29)**	**Unfaourable Weibull (λ=5.2, k=2.05)**	**Unfavourable Weibull (λ=7.4, k=1.61)**
CoVm 0% Uniform 122850-122850 kdwt	100 arrivals	100 arrivals	100 arrivals	100 arrivals
CoVm 10% Uniform 85000-122850 kdwt	100 arrivals	100 arrivals	100 arrivals	100 arrivals
CoVm 25% Uniform 49000-122850 kdwt	100 arrivals	100 arrivals	100 arrivals	100 arrivals
CoVm 50% Uniform 8000-122850 kdwt	1 arrival 10 arrivals 50 arrivals 100 arrivals 500 arrivals 1000 arrivals 2000 arrivals	1 arrival 10 arrivals 50 arrivals 100 arrivals 500 arrivals 1000 arrivals 2000 arrivals	1 arrival 10 arrivals 50 arrivals 100 arrivals 500 arrivals 1000 arrivals 2000 arrivals	1 arrival 10 arrivals 50 arrivals 100 arrivals 500 arrivals 1000 arrivals 2000 arrivals

A.2. Fitting of samples

The resulting samples need to be fitted. The three extreme value distributions considered are the Gumbel, Weibull and General Extreme. The parameters of the distributions were determined with the maximum likelihood estimation (MLE). This method is widely used to estimate the parameters of a statistical model based on a set of observations. The basic idea is to find the values of the parameters that make the observed data most likely under the assumed model. The function is shown in Equation A.1.

$$L(\hat{\theta} \mid \mathbf{X}) = \prod_{i=1}^{n} f\left(x_i \mid \hat{\theta}\right) \tag{A.1}$$

Where,

$L(\hat{\theta} \mid X)$ = Likelihood function
$\hat{\theta}$ = Estimated parameter
X = Observed data
$f\left(X_i \mid \hat{\theta}\right) 7 =$ probability density function of X_i given $\hat{\theta}$

After the parameters for the three distributions are determined, they need to be compared to assess what the best fit is. This is evaluated with the Residual Sum of Squares (RSS), Akaike Information Criterion (AIC) and Bayesian Information Criterion (BIC). These are viable methods to compare distribution fits (James et al., 2021).

The RSS measures the total squared distance between the actual data points and the predicted values, see Equation A.2.

$$RSS = \sum_{i=1}^{n} \left(y^i - f\left(x_i\right)\right)^2 \tag{A.2}$$

With,

y^i = The ith value of the variable to be predicted
$f(x_i)$ = Predicted value of y_i
n = Upper limit of summation

AIC is a mathematical method for evaluating the model fits. It uses the number of independent variables used to build the model and the maximum likelihood estimate of the mode. The AIC assess the trade-off between complexity and fit.

$$AIC = 2K - 2ln(L) \tag{A.3}$$

Where,

K = The number of parameters
L = The maximum log-likelihood estimate of the model

In combination with AIC, the BIC is used to get a broader picture and validate the model selection. The BIC punishes complexity more harshly than the AIC because a too complex model can lead to overfitting. The formula for the BIC is given in Equation A.4.

$$BIC = kln(n) - 2ln(L) \tag{A.4}$$

Where,

K = The number of independent variables
L = The maximum log-likelihood estimate of the model
n = The sample size

For each criterion, lower values indicate better fits. The criterion values for each simulation are shown in Table A.2. The Gumbel distribution has the lowest average value for each criterion. Therefore the Gumbel distribution is the best extreme value distribution for the berthing load.

Table A.2: Fits of the simulation samples

Simulation	RSS Gumbel	RSS Weibull	RSS GEV	AIC Gumbel	AIC Weibull	AIC GEV	BIC Gumbel	BIC Weibull	BIC GEV
1 arrival monitored	2,11E-06	4,03E-06	2,25E-06	2257	2267	3113	2263	2276	3123
10 arrivals monitored	2,97E-06	4,03E-06	3,16E-06	2257	2315	3577	2264	2325	3587
50 arrivals monitored	2,16E-06	1,58E-06	1,21E-04	2272	2282	2273	2278	2291	2283
100 arrivals monitored	9,37E-07	3,59E-06	9,57E-07	2236	2241	2238	2242	2251	2248
500 arrival monitored	4,10E-06	5,02E-06	1,56E-04	2224	2240	2224	2230	2250	2234
1000 arrivals monitored	2,34E-06	2,45E-06	3,61E-06	2210	2257	2245	2217	2229	2239
2000 arrivals monitored	8,09E-07	1,31E-06	5,34E-06	2234	2269	2267	2198	2208	2278
CoVm 0% monitored	2,51E-06	9,24E-06	2,50E-06	2222	2225	2224	2229	2235	2234
CoVm 10% monitored	2,24E-06	4,75E-06	1,49E-04	2207	2209	2209	2213	2219	2218
CoVm 25% monitored	8,54E-06	9,99E-06	7,45E-06	2196	2209	2197	2203	2219	2207
CoVm 50% monitored	4,10E-06	5,02E-06	1,56E-04	2224	2240	2224	2230	2250	2234
1 arrival favourable	1,47E-06	2,30E-06	1,30E-06	2333	2350	2340	2340	2341	2344
10 arrivals favourable	4,83E-07	8,07E-07	3,66E-07	2373	2386	2375	2380	2396	2385
50 arrivals favourable	2,32E-06	3,79E-06	1,64E-06	2345	2387	3133	2346	2350	3168
100 arrivals favourable	1,30E-06	2,24E-06	8,79E-05	2339	2340	3158	2346	2350	3168
500 arrival favourable	1,57E-06	1,38E-06	1,58E-06	2379	2374	2381	2385	2384	2390
1000 arrivals favourable	3,07E-08	4,14E-08	2,89E-08	2315	2364	2391	2354	2383	2396
2000 arrivals favourable	5,30E-08	1,34E-07	1,86E-06	2270	2295	2398	2357	2375	2395
CoVm 0% favourable	1,84E-06	2,90E-06	5,70E-05	2367	2368	2308	2373	2378	2379
CoVm 10% favourable	3,44E-06	3,54E-06	2,45E-06	2330	2338	3261	2336	2347	3271
CoVm 25% favourable	3,68E-06	3,83E-06	3,99E-06	2337	2352	2339	2343	2362	2349
CoVm 50% favourable	1,75E-06	2,75E-06	1,67E-06	2339	2340	3158	2346	2350	3168
1 arrival moderate	1,13E-06	1,22E-06	1,34E-06	2490	2493	2489	2496	2497	2499
10 arrivals moderate	1,52E-06	1,88E-06	7,45E-06	2525	2546	3465	2532	2556	3475
50 arrivals moderate	4,80E-07	1,63E-06	4,77E-07	2548	2565	2549	2554	2574	2559
100 arrivals moderate	3,97E-07	3,82E-07	3,80E-07	2534	2543	3324	2541	2553	3334
500 arrival moderate	6,16E-07	1,18E-06	8,91E-06	2514	2520	3440	2521	2530	3450
1000 arrivals moderate	1,13E-06	1,57E-06	1,45E-05	2507	2521	3241	2522	2534	3408
2000 arrivals moderate	8,07E-09	5,45E-08	1,37E-06	2498	2514	2819	2527	2542	3456
CoVm 0% moderate	9,29E-07	7,75E-07	9,30E-07	2513	2515	3428	2520	2525	3438
CoVm 10% moderate	9,96E-07	1,63E-06	1,10E-06	2519	2524	2521	2525	2534	2531
CoVm 25% moderate	1,78E-06	2,03E-06	1,77E-06	2490	2492	2492	2497	2501	2501
CoVm 50% moderate	3,97E-07	3,82E-07	3,80E-07	2534	2543	3324	2541	2553	3334
1 arrival unfavourable	1,943-7	3,24E-07	2,28E-07	2993	2998	2994	2999	3001	3004
10 arrivals unfavourable	9,37E-08	7,50E-08	9,54E-08	3078	3084	3078	3085	3094	3088
50 arrivals unfavourable	2,87E-08	8,66E-08	6,89E-07	3116	3138	4084	3123	3148	4094
100 arrivals unfavourable	7,35E-08	6,02E-08	3,31E-07	3117	3133	3119	3123	3143	3128
500 arrival unfavourable	2,94E-08	4,28E-08	2,91E-08	3132	3135	3950	3139	3145	3960
1000 arrivals unfavourable	3,07E-08	4,14E-08	2,89E-08	3104	3145	3933	3145	3154	3789
2000 arrivals unfavourable	7,90E-08	1,74E-07	1,81E-06	3102	3132	3987	3127	3138	3845
CoVm 0% unfavourable	3,58E-08	7,56E-08	1,53E-06	3166	3168	4163	3172	3181	4193
CoVm 10% unfavourable	4,65E-08	1,05E-07	2,06E-06	3121	3125	3287	3128	3135	3297
CoVm 25% unfavourable	2,45E-08	4,93E-08	1,74E-06	3106	3106	4015	3113	3116	4015
CoVm 50% unfavourable	7,35E-08	6,02E-08	3,31E-07	3117	3133	3119	3123	3143	3128
Average	**1,41E-06**	**2,01E-06**	**1,85E-05**	**2547,5**	**2561,8**	**2928,5**	**2557,4**	**2569,7**	**2950,5**

A.3. Resulting design point and partial factors

Now proven that the Gumbel distribution is the best fit, the design value can calculated simply with Equation 3.19, recalled below.

$$Q_{\mathsf{d}} = \mu_Q \left(1 - V_Q \left(0,45 + 0,78 \ln\left(-\ln\left(\Phi^{-1}\left(-\alpha_E \beta\right)\right)\right)\right)\right) \tag{A.5}$$

After the design values were determined, the partial factors were calculated by dividing the design value by the characteristic value. Again, the characteristic value was determined with the maximum water

displacement and characteristic berthing velocity.

The base is identified as the navigation condition with 100 rivals and 50% variation in water displacement. The correction factors were determined by dividing the remaining factors by the base case per navigation condition. The correction factors are shown in Table A.3.

Table A.3: Simulation of the berthing energy and resulting partial factors

Simulation	Mean	Standard Deviation	CoV	Design value	Partial factor	Correction factors
1 arrival monitored	290	77	0,27	567,38	0,85	0,72
10 arrivals monitored	431	77	0,18	708,38	1,07	0,90
50 arrivals monitored	530	72	0,14	789,37	1,19	1,00
100 arrivals monitored	554	65	0,12	790,07	1,19	1,00
500 arrival monitored	639	65	0,10	873,16	1,32	1,11
1000 arrivals monitored	681	65	0,10	915,16	1,38	1,16
2000 arrivals monitored	713	65	0,09	947,16	1,43	1,20
CoVm 0% monitored	696	71	0,10	951,77	1,43	1,20
CoVm 10% monitored	615	68	0,11	859,96	1,30	1,09
CoVm 25% monitored	581	69	0,12	829,57	1,25	1,05
CoVm 50% monitored	554	65	0,12	790,07	1,19	1,00
1 arrival favourable	307	94	0,31	645,63	0,83	0,65
10 arrivals favourable	478	99	0,21	834,64	1,08	0,83
50 arrivals favourable	595	91	0,15	922,82	1,19	0,92
100 arrivals favourable	659	95	0,14	1000,61	1,29	1,00
500 arrival favourable	764	95	0,12	1106,23	1,43	1,11
1000 arrivals favourable	811	94	0,12	1149,63	1,48	1,15
2000 arrivals favourable	856	87	0,10	1169,41	1,51	1,17
CoVm 0% favourable	819	94	0,11	1157,63	1,49	1,16
CoVm 10% favourable	728	97	0,13	1077,43	1,39	1,08
CoVm 25% favourable	673	93	0,14	1008,02	1,30	1,01
CoVm 50% favourable	659	95	0,14	1000,61	1,29	1,00
1 arrival moderate	384	122	0,32	823,49	0,76	0,58
10 arrivals moderate	640	134	0,21	1122,72	1,04	0,79
50 arrivals moderate	815	139	0,17	1315,73	1,21	0,93
100 arrivals moderate	894	146	0,16	1420,51	1,31	1,00
500 arrival moderate	1063	137	0,13	1556,53	1,44	1,10
1000 arrivals moderate	1156	139	0,12	1656,73	1,53	1,17
2000 arrivals moderate	1225	146	0,12	1750,95	1,61	1,23
CoVm 0% moderate	1155	157	0,14	1720,58	1,59	1,21
CoVm 10% moderate	1007	136	0,14	1496,93	1,38	1,05
CoVm 25% moderate	936	145	0,15	1458,35	1,34	1,03
CoVm 50% moderate	894	146	0,16	1420,51	1,31	1,00
1 arrival unfavourable	1209	474	0,39	2916,53	0,75	0,54
10 arrivals unfavourable	2169	597	0,28	4319,63	1,11	0,80
50 arrivals unfavourable	2718	576	0,21	4792,98	1,23	0,88
100 arrivals unfavourable	3134	638	0,20	5432,33	1,39	1,00
500 arrival unfavourable	3933	652	0,17	6281,76	1,61	1,16
1000 arrivals unfavourable	4398	714	0,16	6970,11	1,78	1,28
2000 arrivals unfavourable	4760	718	0,15	7346,52	1,88	1,35
CoVm 0% unfavourable	4206	745	0,18	6889,78	1,76	1,27
CoVm 10% unfavourable	3610	612	0,17	5814,67	1,49	1,07
CoVm 25% unfavourable	3336	600	0,18	5497,44	1,41	1,01
CoVm 50% unfavourable	3134	638	0,20	5432,33	1,39	1,00

B

Semi-probabilistic design of the case studies

This appendix shows the results of the Dolphin Tool used to design the dolphins of the different cases used for the probabilistic assessment. The design steps of the output are according to Chapter 2.

B.1. Case "Sand"

PROJECT TITLE:			Pname test				
SUBJECT:			comments test				
PROJECT NO:	Pnumber test	FILE REF:		REV:	0.1		
PREPARED BY:		DATE:	09/11/2023	CHECKED BY:		DATE:	CPT Code: CPTcodetest

Input:

Top of pile at:	6	m NAP
Toe of pile at:	-43,5	m NAP
Amount of sections:	5	
MDL	-24,1	m NAP
Type of pile:	Berthing	

Berthing

Berthing energy:	2093	kNm, SLS
Bottom level, DD high:	-24,1	m NAP
Bottom level, DD low:	-24,9	m NAP
Force level, high:	1,7	m NAP
Force level, low:	1,7	m NAP

Slope

Consider slope:	No	
Slope inclination 1:	2,5	vert : horiz

Sections of pile

	Level of top of section [m NAP]	Diameter [mm]	Thickness [mm]	Steel grade [-]	Length of section [m]
1	6,0	3300	34	X70	10,0
2	-4,0	3300	37	X70	8,0
3	-12,0	3300	58	X70	8,0
4	-20,0	3300	65	X70	20,0
5	-40,0	3300	55	X70	3,5

Division into zones based on Figure 6-6 CROW 1005

Zone	Top [m NAP]	Bottom [m NAP]
1	6,00	-20,80
2a	-20,80	-27,40
2b	-27,40	-34,00
3	-34,00	-43,50

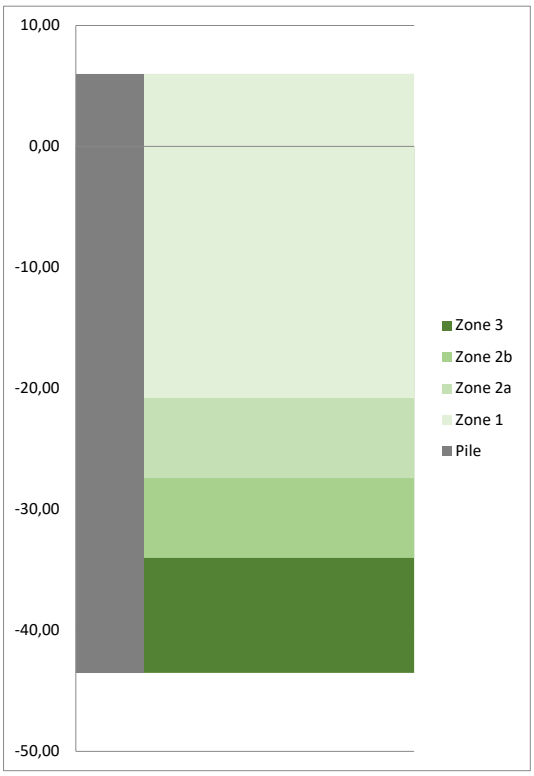

Output:

Berthing

	Berthing energy:	3035	kNm, ULS
B1	Berthing energy:	2984	kNm
	Berthing force:	7636,3	kN
	Disp - berthing force:	781,7	mm
	Displacement:	923,7	mm, top
		-8,3	mm, pile toe
B2	Berthing energy:	2984	kNm
	Berthing force:	7636,3	kN
	Disp - berthing force:	781,7	mm
	Displacement:	923,7	mm, top
		-8,3	mm, pile toe
B3	Berthing energy:	3740	kNm
	Berthing force:	4738,4	kN
	Disp - berthing force:	1578,4	mm
	Displacement:	854,1	mm, top
		-31,8	mm, pile toe
B4	Berthing energy:	2074	kNm
	Berthing force:	5754,0	kN
	Disp - berthing force:	721,0	mm
	Displacement:	842,5	mm, top
		-17,7	mm, pile toe

*Note: Top and toe displacements are based on the design force: 1.05 * Berthing force (only for Sea-going vessels).*

Results for berthing per zone

Case	Ø	t	Level	Ved	Med	Zone	Class	UC	
								elastic	buckling
	[mm]	[mm]	[m NAP]	[kN]	[kNm]	[-]	[-]	[-]	[-]
1	3300	34	-4	7636	43527	z1	Class 4	0,36	0,40
2	3300	37	-12	7636	104618	z1	Class 4	0,72	0,87
3	3300	58	-20	7636	165708	z1	Class 4	0,77	0,86
4	3300	65	-20,8	7636	171817	z1	Class 4	0,72	0,79
5	3300	65	-27,4	3230	218316	z2a	Class 4	0,91	0,91
6	3300	65	-28,6	552	221058	z2b MaxM	Class 4	0,92	0,98
7	3300	65	-34	21366	164451	z2b	Class 4	0,72	0,69
8	3300	65	-34	21366	164451	z3	Class 4	0,72	0,59
9	3300	55	-40	14224	68957	z3	Class 4	0,39	0,30

	Top level [m NAP]	Diameter [mm]	Thickness [mm]	Steel grade [-]	Length of section [m]	Weight [mtons]
1	6	3300	34	X70	10,0	27,4
2	-4	3300	37	X70	8,0	23,8
3	-12	3300	58	X70	8,0	37,1
4	-20	3300	65	X70	20,0	103,7
5	-40	3300	55	X70	3,5	15,4
						207,4

Embedding check

According to CROW 1005 a check should be done for the embedding of the pile. B4 is compared with a pile that is 5 times the diameter longer, the difference of top displacement should be less than 2 %

B4			A 5 times the diameter longer pile					
Displacement:	842,5	mm, top	Displacement:	808,3	mm, top	4,2 %	>	2,0 %

Does not comply

Embedding check (soil pressure)

B1	B2	B3	B4
TRUE	TRUE	FALSE	FALSE
31,70%	31,70%	58,43%	50,46%

For more details, check sheet 'Results berth'

Graphics

Moments

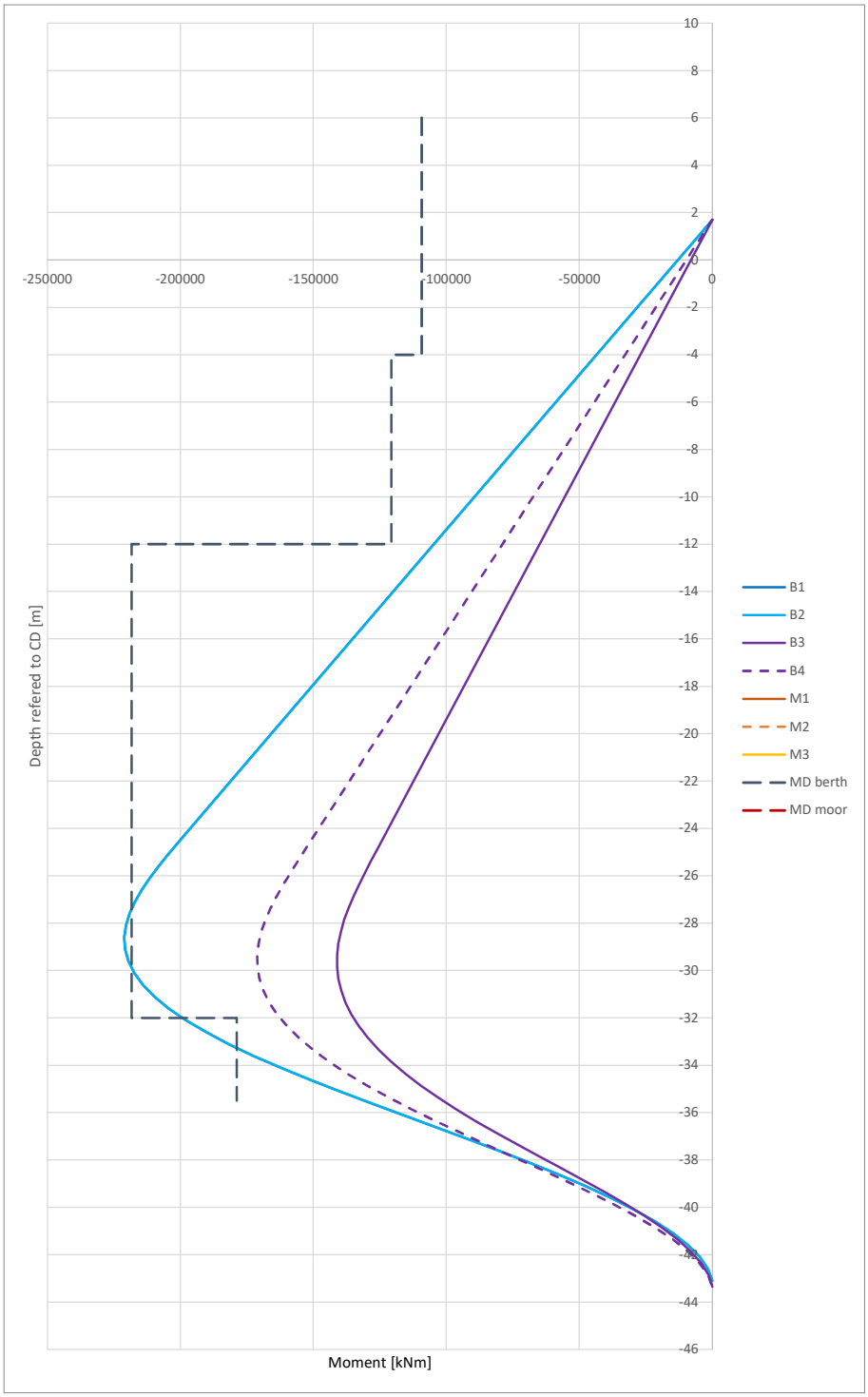

Displacements

Indicated displacements at top is at the level of acting force

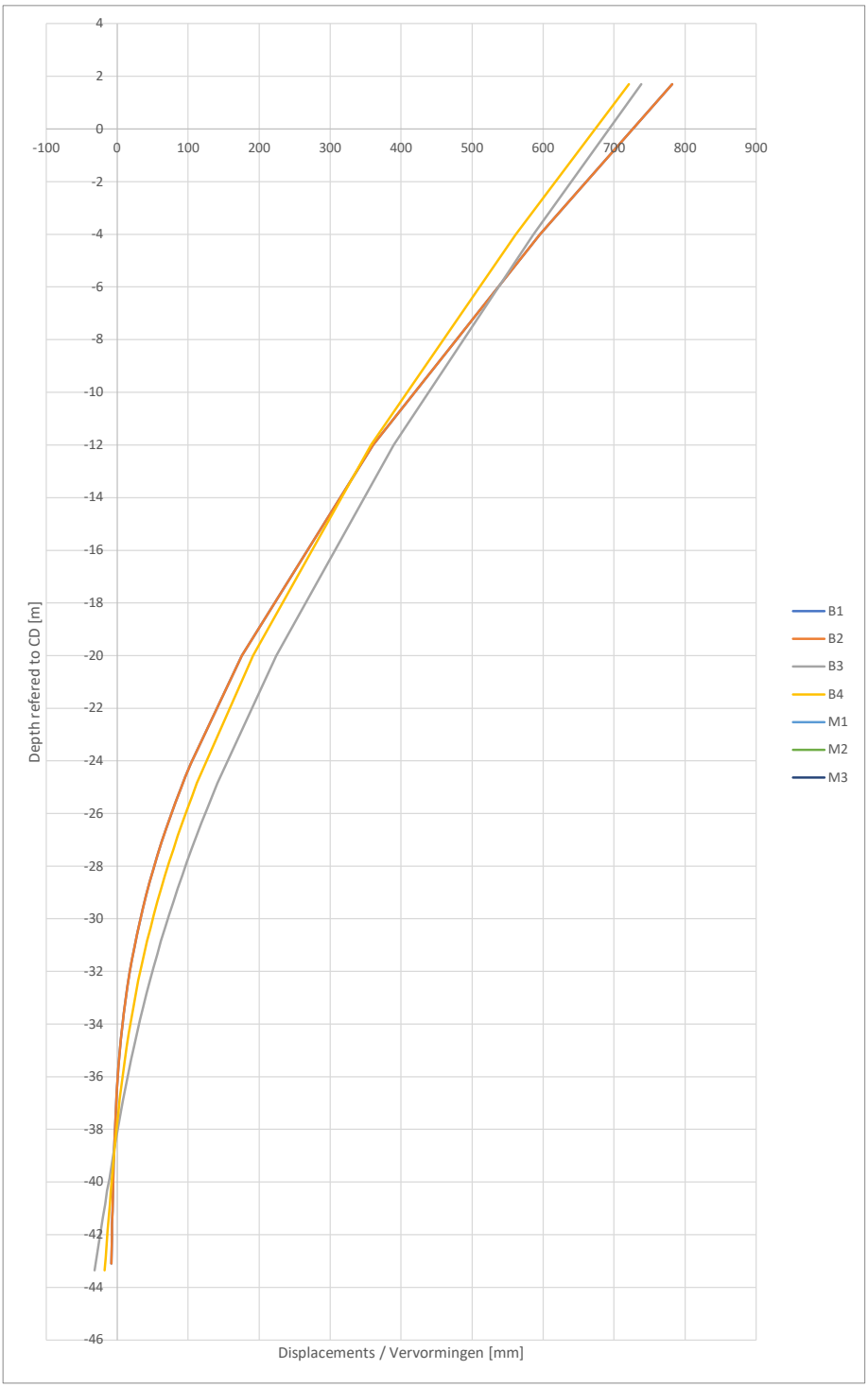

Shear force

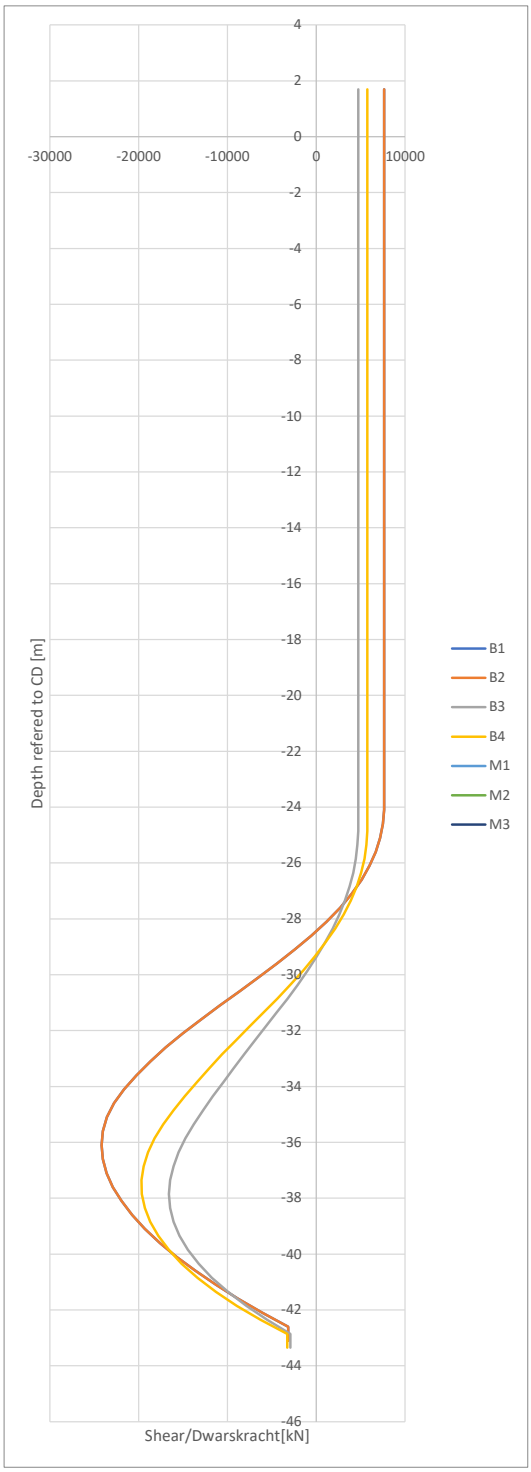

Horizontal soil pressure

Values to be divided by diameter of pile

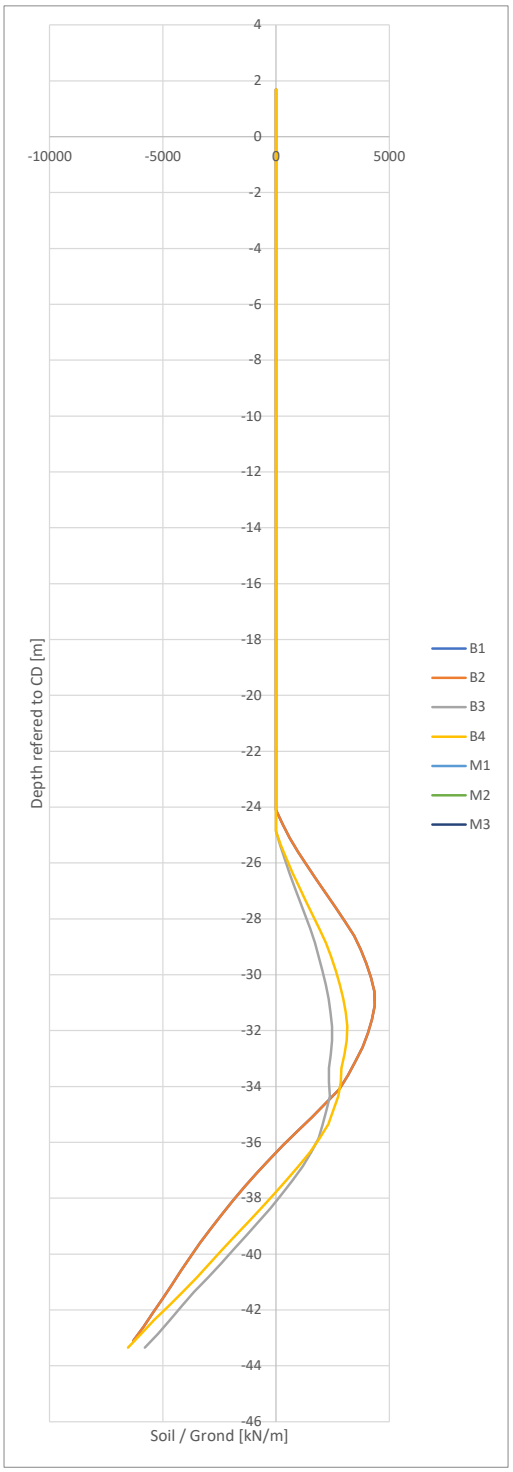

Berthing energy

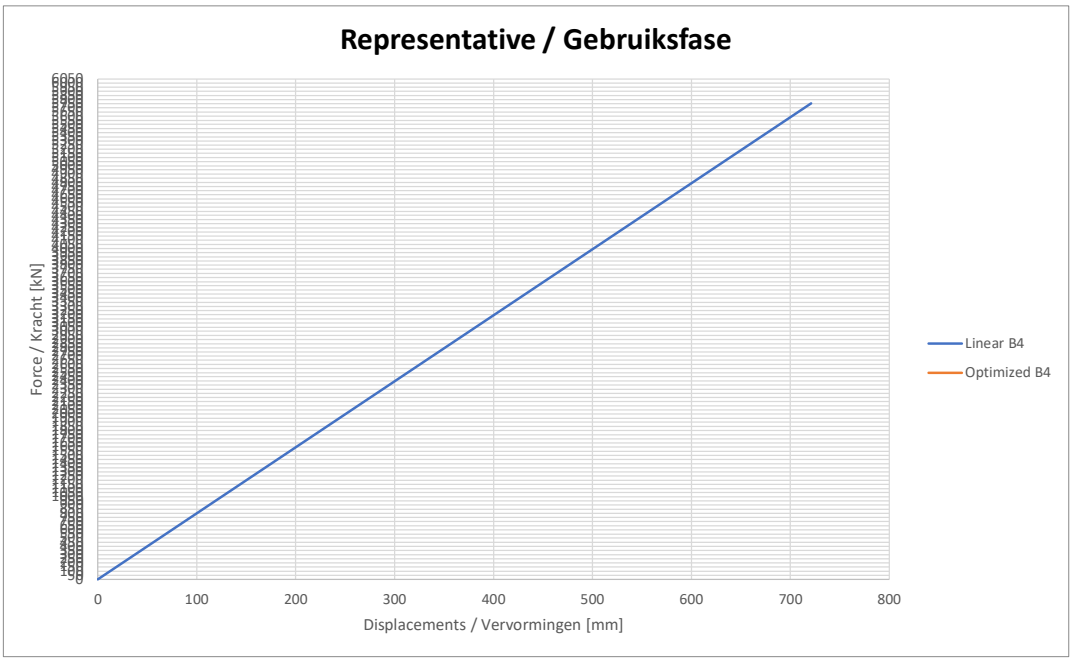

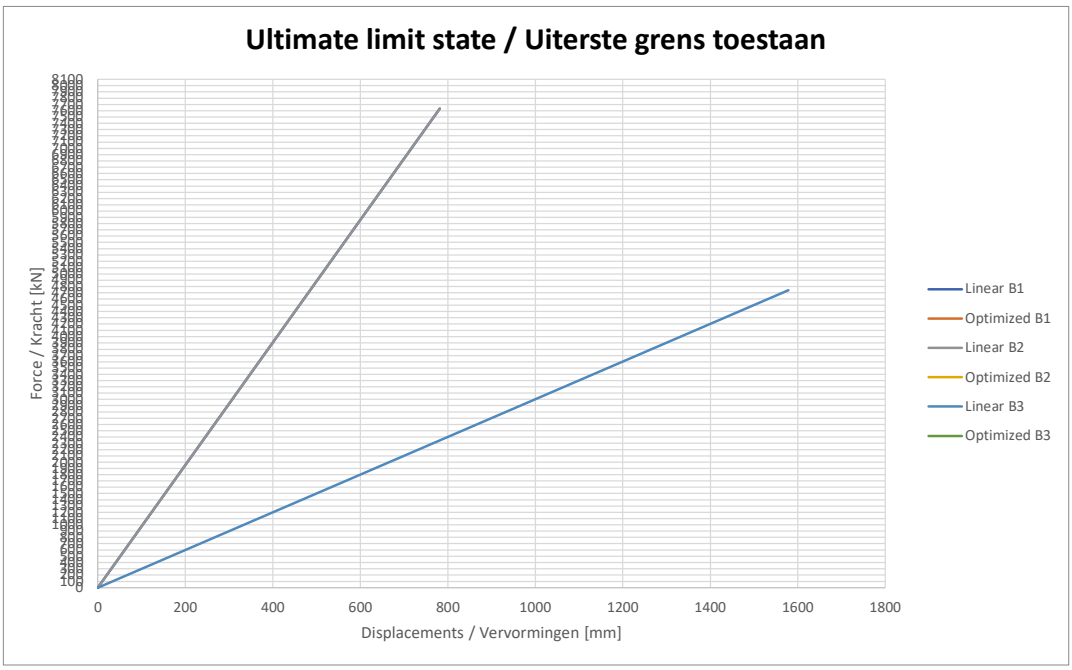

B.2. Case "Sand Alternative"

PROJECT TITLE:			Pname test				
SUBJECT:			comments test				
PROJECT NO:	Pnumber test	FILE REF:		REV:	0.1		
PREPARED BY:		DATE:	05/12/2023	CHECKED BY:		DATE:	CPT Code: CPTcodetest

Input:

Top of pile at:	6	m NAP
Toe of pile at:	-43	m NAP
Amount of sections:	5	
MDL	-24,1	m NAP
Type of pile:	Berthing	

Berthing

Berthing energy:	2093	kNm, SLS
Bottom level, DD high:	-24,1	m NAP
Bottom level, DD low:	-24,9	m NAP
Force level, high:	1,7	m NAP
Force level, low:	1,7	m NAP

Slope

Consider slope:	No	
Slope inclination 1:	2,5	vert : horiz

Sections of pile

	Level of top of section [m NAP]	Diameter [mm]	Thickness [mm]	Steel grade [-]	Length of section [m]
1	6,0	2400	34	X70	10,0
2	-4,0	2400	45	X70	8,0
3	-12,0	2400	63	X70	8,0
4	-20,0	2400	84	X70	14,0
5	-34,0	2400	63	X70	9,0

Division into zones based on Figure 6-6 CROW 1005

Zone	Top [m NAP]	Bottom [m NAP]
1	6,00	-21,70
2a	-21,70	-26,50
2b	-26,50	-31,30
3	-31,30	-43,00

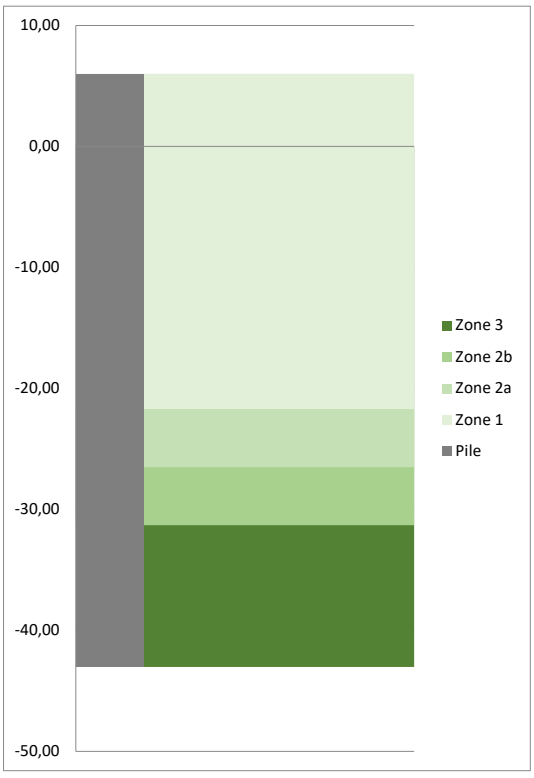

Output:

Berthing

	Berthing energy:	3035	kNm, ULS
B1	Berthing energy:	3000	kNm
	Berthing force:	5272,4	kN
	Disp - berthing force:	1138,2	mm
	Displacement:	1351,6	mm, top
		-4,6	mm, pile toe
B2	Berthing energy:	3000	kNm
	Berthing force:	5272,4	kN
	Disp - berthing force:	1138,2	mm
	Displacement:	1351,6	mm, top
		-4,6	mm, pile toe
B3	Berthing energy:	3051	kNm
	Berthing force:	3172,1	kN
	Disp - berthing force:	1923,5	mm
	Displacement:	2474,3	mm, top
		-148,8	mm, pile toe
B4	Berthing energy:	2118	kNm
	Berthing force:	3637,8	kN
	Disp - berthing force:	1164,5	mm
	Displacement:	1353,2	mm, top
		-33,6	mm, pile toe

*Note: Top and toe displacements are based on the design force: 1.05 * Berthing force (only for Sea-going vessels).*

Results for berthing per zone

Case	Ø	t	Level	Ved	Med	Zone	Class	UC	
								elastic	buckling
	[mm]	[mm]	[m NAP]	[kN]	[kNm]	[-]	[-]	[-]	[-]
1	2400	34	-4	5272	30053	z1	Class 4	0,45	0,49
2	2400	45	-12	5272	72232	z1	Class 4	0,82	0,91
3	2400	63	-20	5272	114412	z1	Class 3	0,94	0,85
4	2400	84	-21,7	5272	123375	z1	Class 2	0,78	0,54
5	2400	84	-26,5	3483	147609	z2a	Class 2	0,94	0,64
6	2400	84	-28,6	779	151919	z2b MaxM	Class 2	0,97	0,66
7	2400	84	-31,3	8239	141947	z2b	Class 2	0,90	0,62
8	2400	84	-31,3	8239	141947	z3	Class 2	0,90	0,62
9	2400	63	-34	17038	109339	z3	Class 3	0,90	0,81

	Top level [m NAP]	Diameter [mm]	Thickness [mm]	Steel grade [-]	Length of section [m]	Weight [mtons]
1	6	2400	34	X70	10,0	19,8
2	-4	2400	45	X70	8,0	20,9
3	-12	2400	63	X70	8,0	29,1
4	-20	2400	84	X70	14,0	67,2
5	-34	2400	63	X70	9,0	32,7
						169,7

Embedding check

According to CROW 1005 a check should be done for the embedding of the pile. B4 is compared with a pile that is 5 times the diameter longer, the difference of top displacement should be less than 2 %

B4			A 5 times the diameter longer pile					
Displacement:	1353,2	mm, top	Displacement:	1241,8	mm, top	9,0 %	>	2,0 %

Does not comply

Embedding check (soil pressure)

B1	B2	B3	B4
TRUE	TRUE	FALSE	FALSE
19,27%	19,27%	78,73%	61,62%

For more details, check sheet 'Results berth'

Graphics

Moments

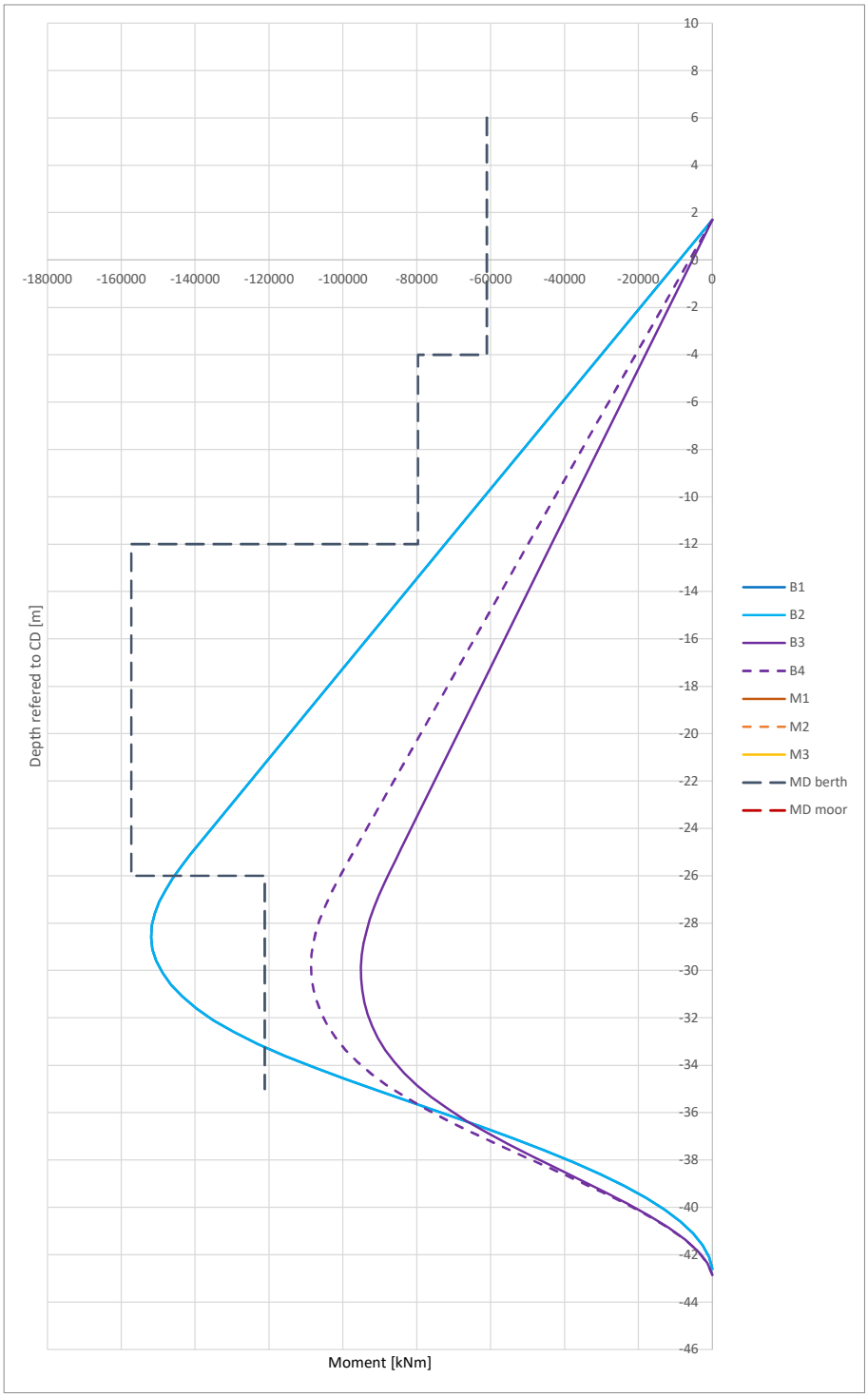

Displacements

Indicated displacements at top is at the level of acting force

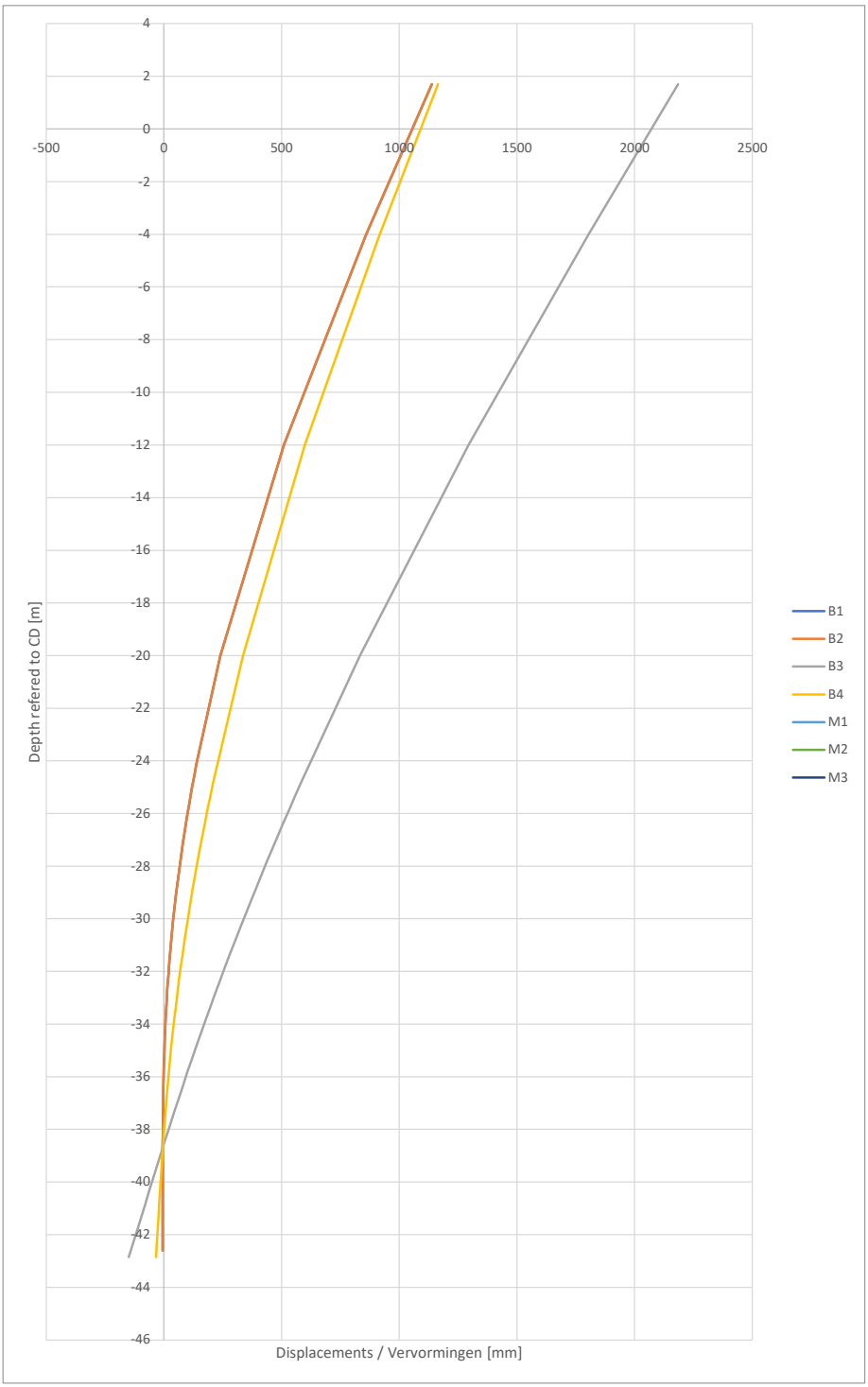

Shear force

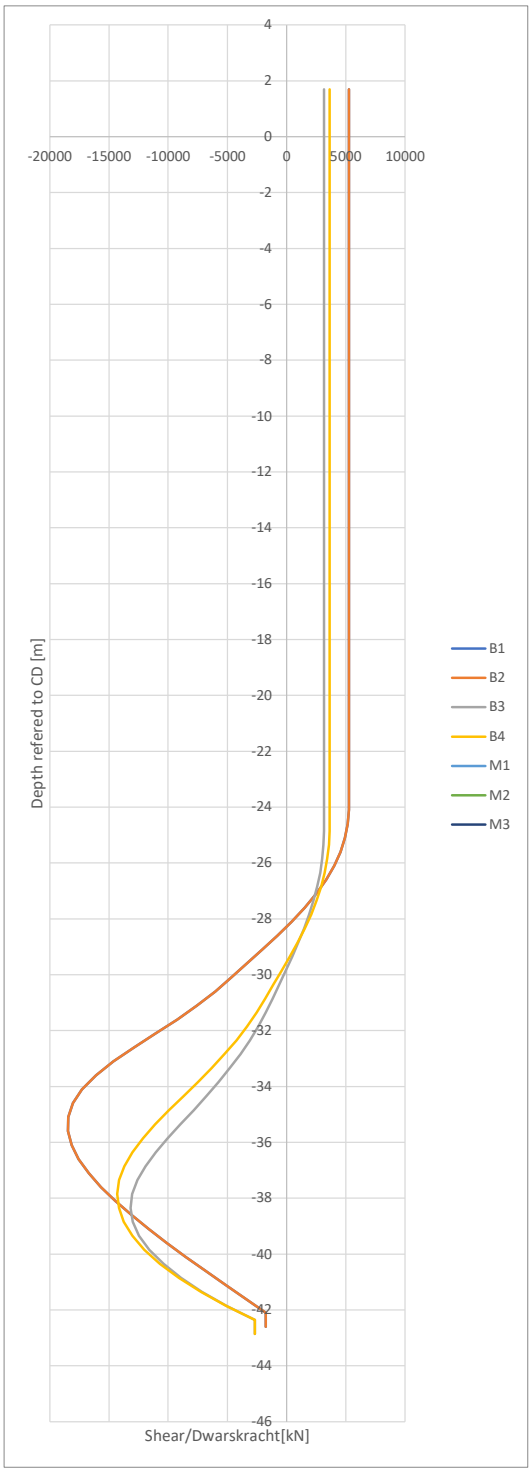

Horizontal soil pressure
Values to be divided by diameter of pile

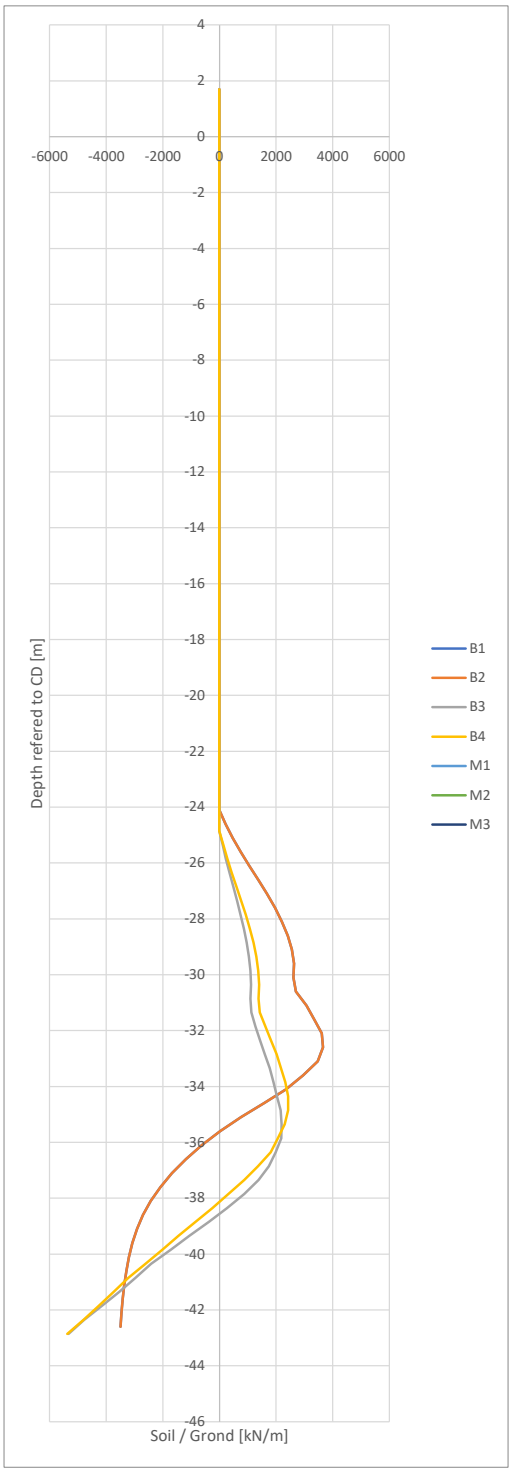

Berthing energy

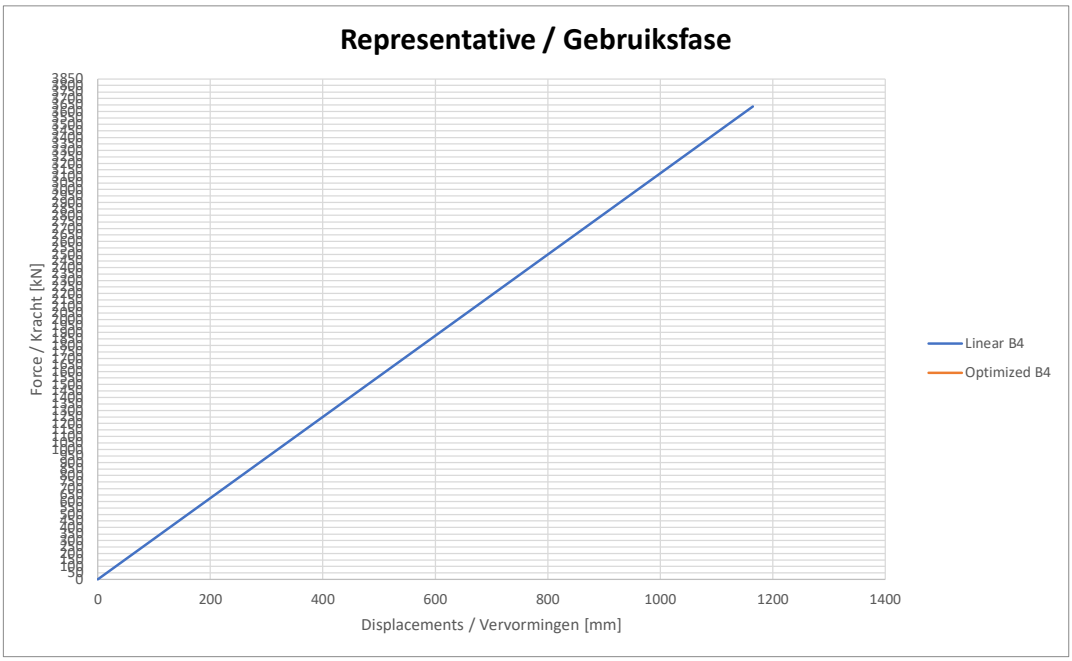

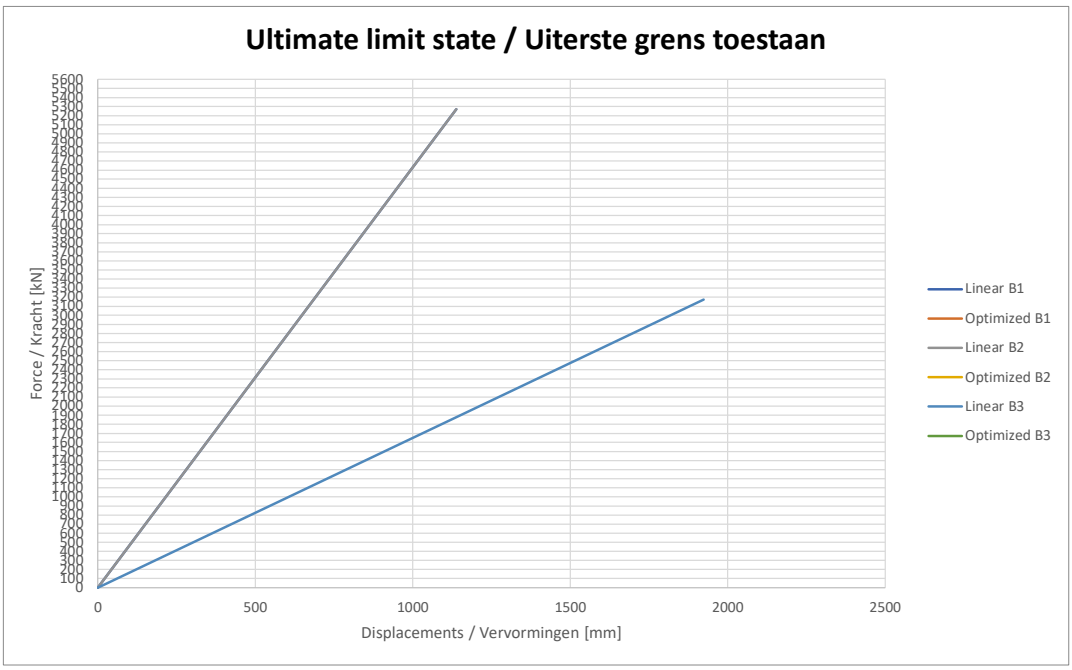

B.3. Case "Clay"

PROJECT TITLE:			Pname test				
SUBJECT:			comments test				
PROJECT NO:	Pnumber test	FILE REF:		REV:	0.1		
PREPARED BY:		DATE:	16/11/2023	CHECKED BY:		DATE:	CPT Code: CPTcodetest

Input:

Top of pile at:	6	m NAP
Toe of pile at:	-47	m NAP
Amount of sections:	5	
MDL	-24,1	m NAP
Type of pile:	Berthing	

Berthing

Berthing energy:	2093	kNm, SLS
Bottom level, DD high:	-24,1	m NAP
Bottom level, DD low:	-24,9	m NAP
Force level, high:	1,7	m NAP
Force level, low:	1,7	m NAP

Slope

Consider slope:	No	
Slope inclination 1:	2,5	vert : horiz

Sections of pile

	Level of top of section [m NAP]	Diameter [mm]	Thickness [mm]	Steel grade [-]	Length of section [m]
1	6,0	2200	26	X70	10,0
2	-4,0	2200	37	X70	8,0
3	-12,0	2200	55	X70	8,0
4	-20,0	2200	71	X70	20,0
5	-40,0	2200	55	X70	7,0

Division into zones based on Figure 6-6 CROW 1005

Zone	Top [m NAP]	Bottom [m NAP]
1	6,00	-21,90
2a	-21,90	-26,30
2b	-26,30	-30,70
3	-30,70	-47,00

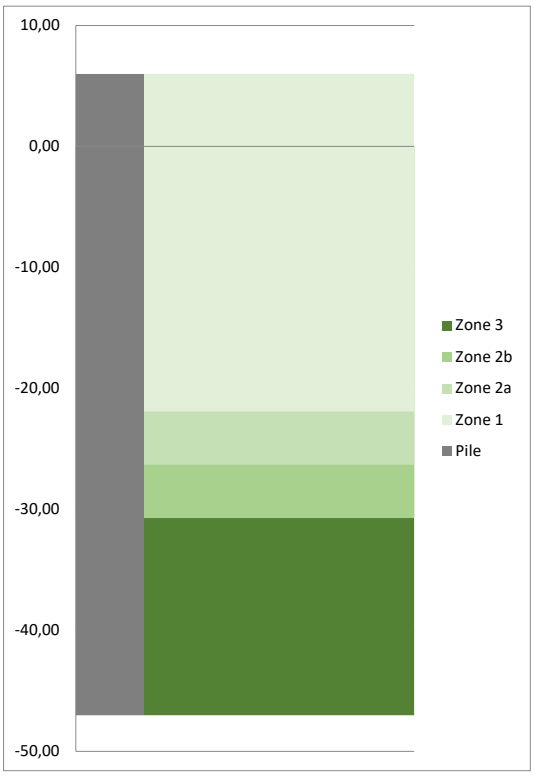

Output:

Berthing

	Berthing energy:	3035	kNm, ULS
B1	Berthing energy:	3061	kNm
	Berthing force:	3628,8	kN
	Disp - berthing force:	1686,9	mm
	Displacement:	1963,6	mm, top
		-14,9	mm, pile toe
B2	Berthing energy:	3061	kNm
	Berthing force:	3628,8	kN
	Disp - berthing force:	1686,9	mm
	Displacement:	1963,6	mm, top
		-14,9	mm, pile toe
B3	Berthing energy:	3186	kNm
	Berthing force:	2739,9	kN
	Disp - berthing force:	2325,9	mm
	Displacement:	4093,6	mm, top
		-200,9	mm, pile toe
B4	Berthing energy:	2064	kNm
	Berthing force:	2699,9	kN
	Disp - berthing force:	1529,3	mm
	Displacement:	1762,7	mm, top
		-29,4	mm, pile toe

*Note: Top and toe displacements are based on the design force: 1.05 * Berthing force (only for Sea-going vessels).*

Results for berthing per zone

Case	Ø	t	Level	Ved	Med	Zone	Class	UC	
								elastic	buckling
	[mm]	[mm]	[m NAP]	[kN]	[kNm]	[-]	[-]	[-]	[-]
1	2200	26	-4	3629	20684	z1	Class 4	0,47	0,54
2	2200	37	-12	3629	49715	z1	Class 4	0,78	0,87
3	2200	55	-20	3629	78745	z1	Class 3	0,88	0,79
4	2200	71	-21,9	3552	85640	z1	Class 2	0,76	0,52
5	2200	71	-26,3	2692	100584	z2a	Class 2	0,89	0,61
6	2200	71	-30,7	1068	109293	z2b	Class 2	0,97	0,66
7	2200	71	-30,7	1068	109293	z3	Class 2	0,97	0,66
8	2200	71	-33,1	342	110898	z3 MaxM	Class 2	0,98	0,67
9	2200	55	-40	9076	72634	z3	Class 3	0,81	0,73

	Top level [m NAP]	Diameter [mm]	Thickness [mm]	Steel grade [-]	Length of section [m]	Weight [mtons]
1	6	2200	26	X70	10,0	13,9
2	-4	2200	37	X70	8,0	15,8
3	-12	2200	55	X70	8,0	23,3
4	-20	2200	71	X70	20,0	74,6
5	-40	2200	55	X70	7,0	20,4
						147,9

Embedding check

According to CROW 1005 a check should be done for the embedding of the pile. B4 is compared with a pile that is 5 times the diameter longer, the difference of top displacement should be less than 2 %

B4			A 5 times the diameter longer pile					
Displacement:	1762,7	mm, top	Displacement:	1686,5	mm, top	4,5 %	>	2,0 %

Does not comply

Embedding check (soil pressure)

B1	B2	B3	B4
FALSE	FALSE	FALSE	FALSE
51,31%	51,31%	97,26%	61,69%

For more details, check sheet 'Results berth'

Graphics

Moments

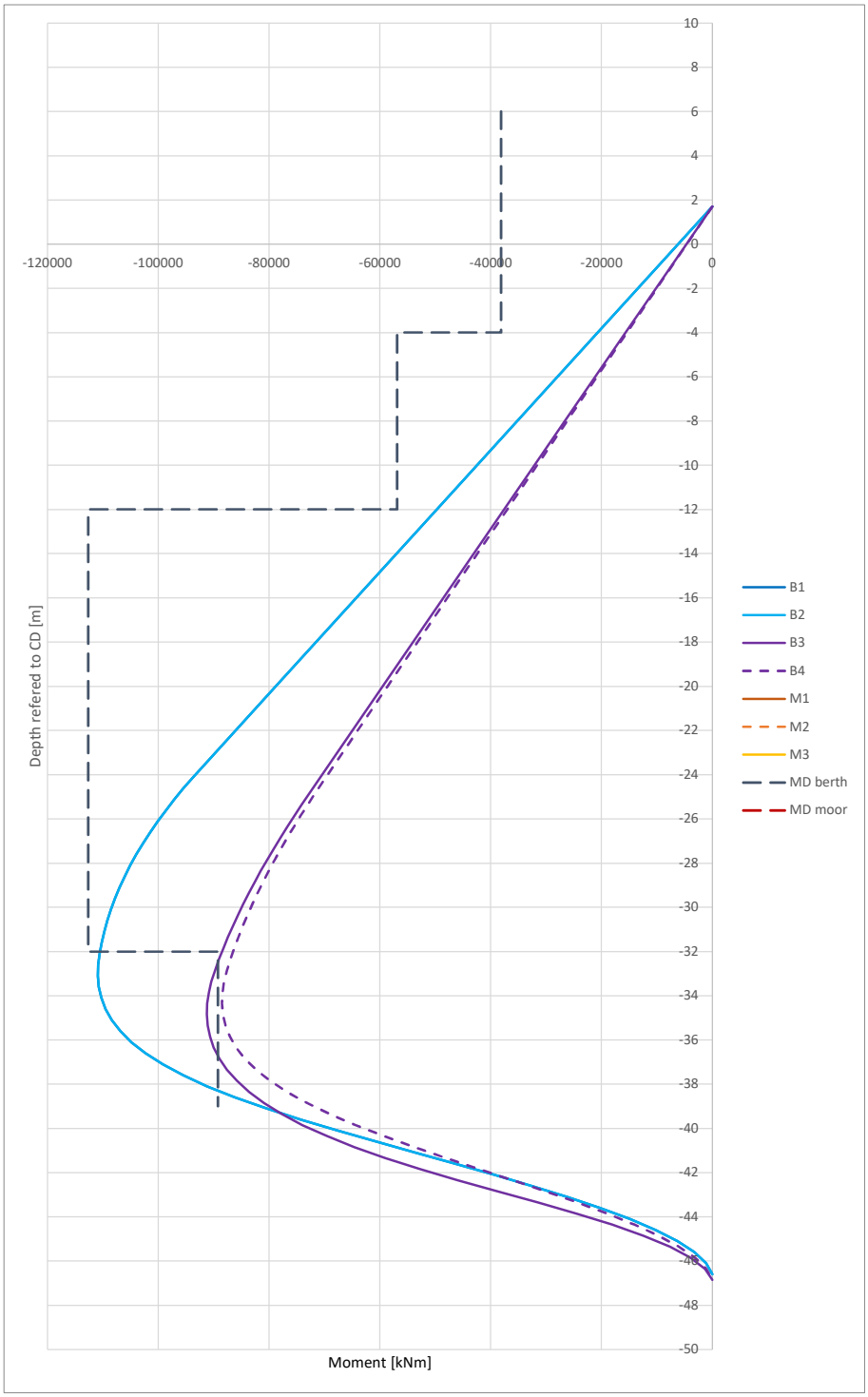

Displacements

Indicated displacements at top is at the level of acting force

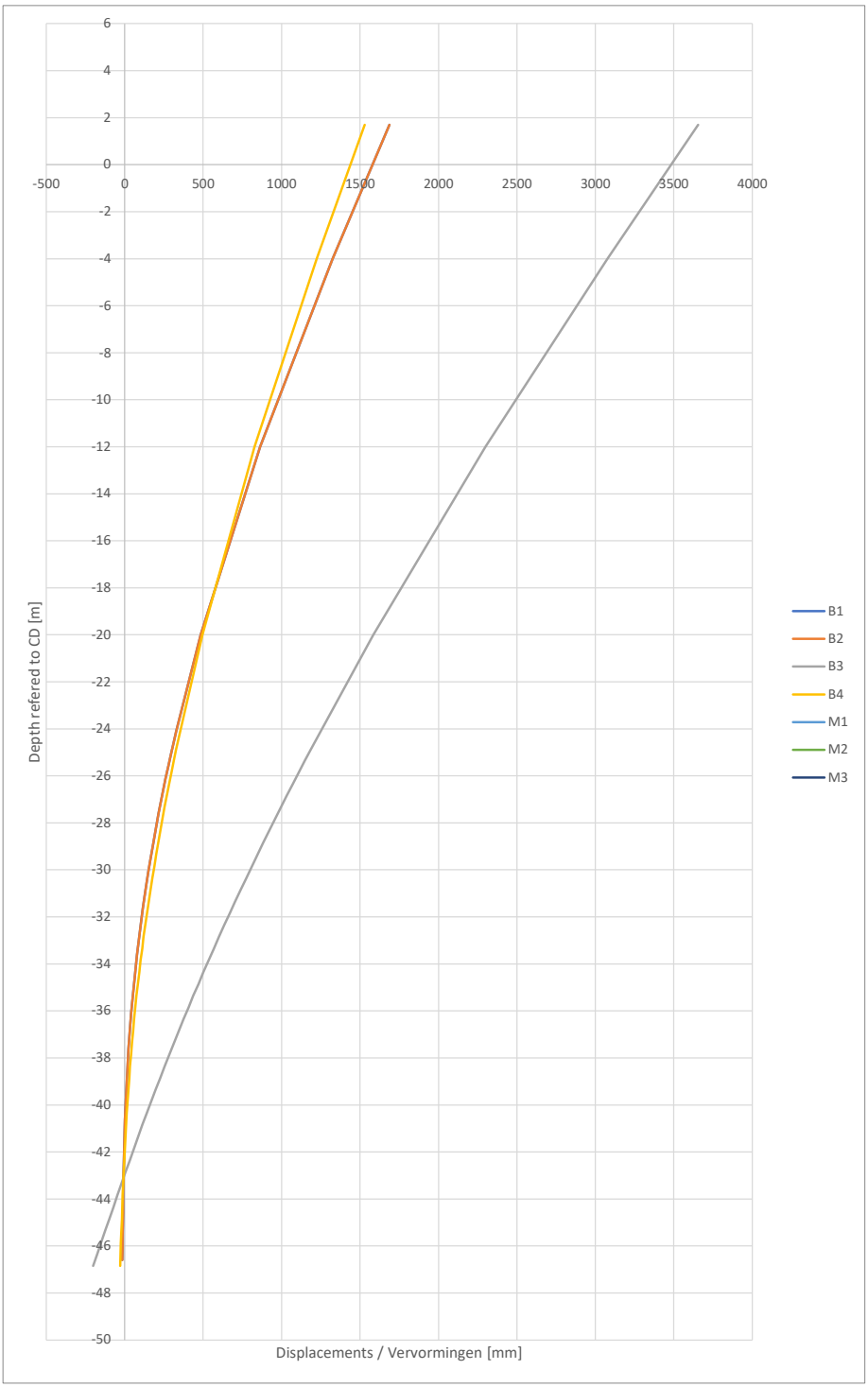

Shear force

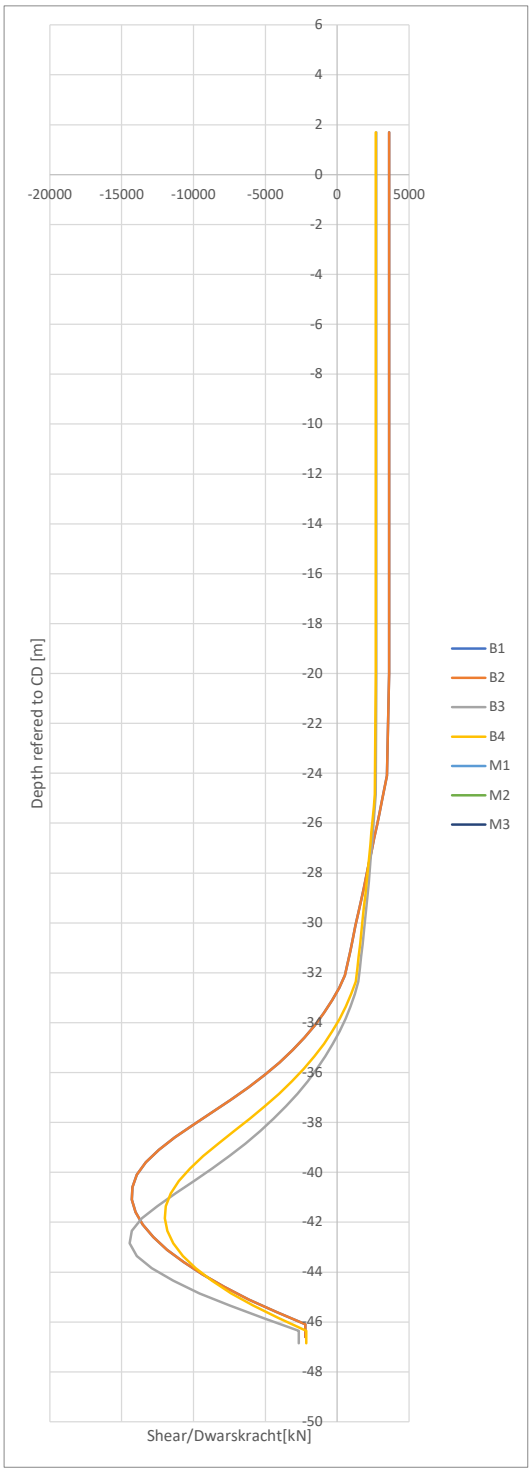

Horizontal soil pressure

Values to be divided by diameter of pile

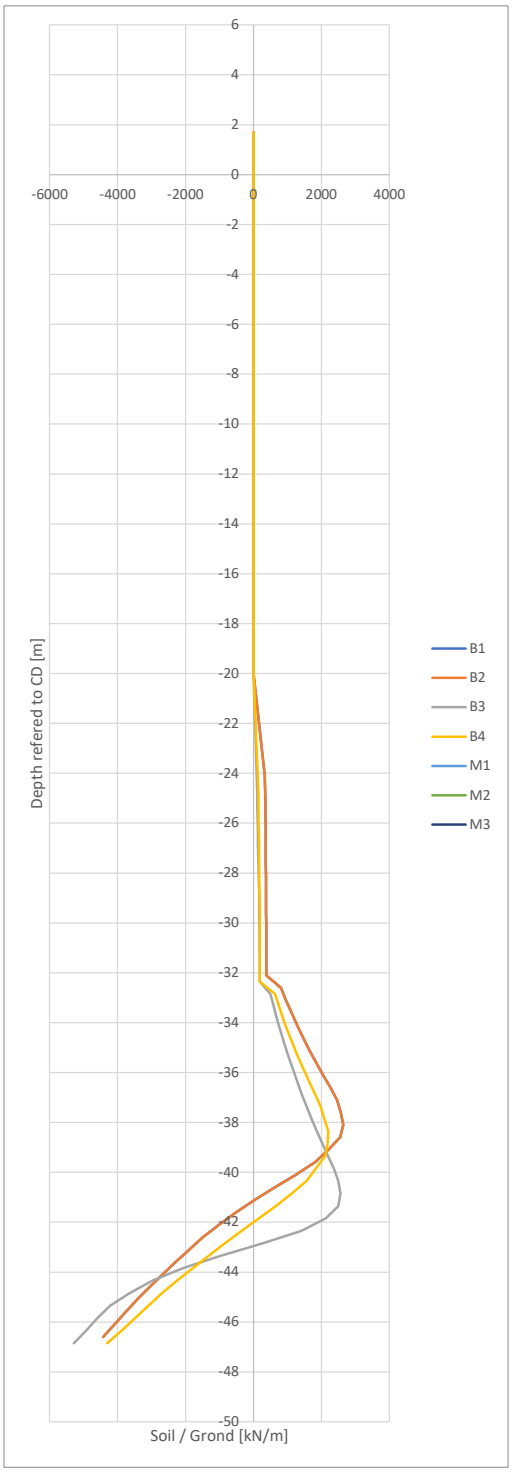

Berthing energy

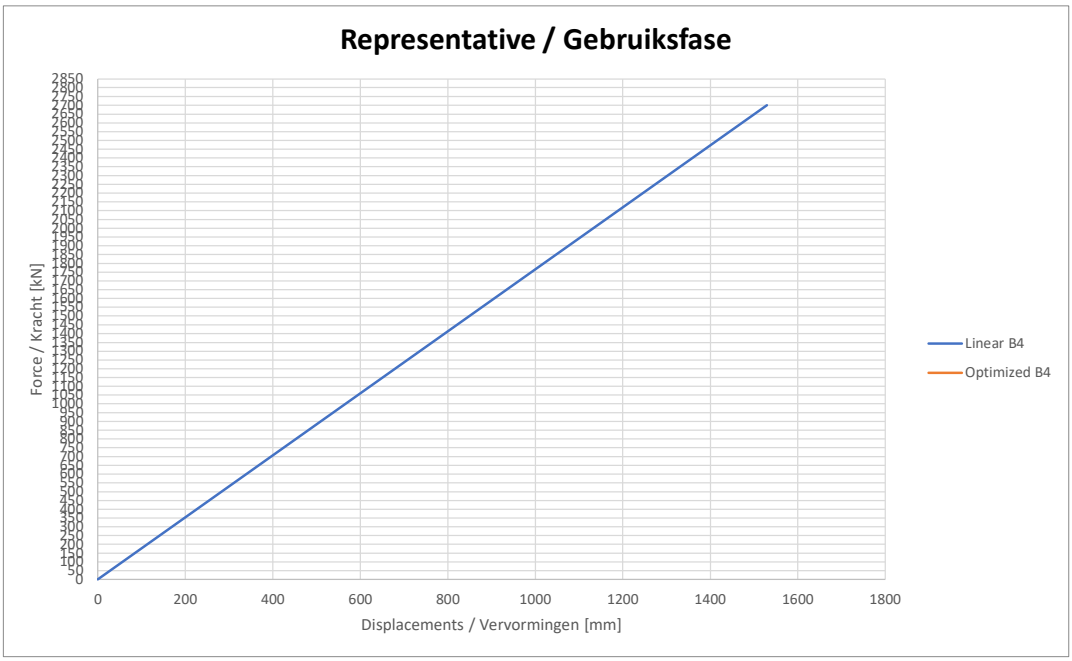

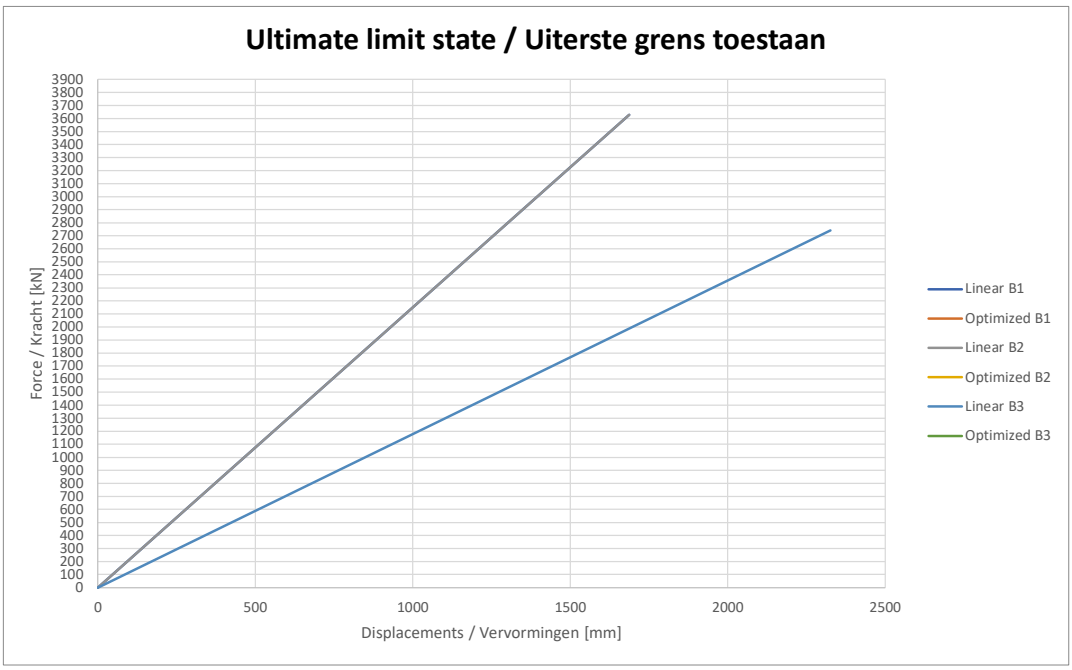

B.4. Case "MIx"

PROJECT TITLE:			Pname test				
SUBJECT:			comments test				
PROJECT NO:	Pnumber test	FILE REF:		REV:	0.1		
PREPARED BY:		DATE:	03/11/2023	CHECKED BY:		DATE:	CPT Code: CPTcodetest

Input:

Top of pile at:	6	m NAP
Toe of pile at:	-46	m NAP
Amount of sections:	5	
MDL	-24,1	m NAP
Type of pile:	Berthing	

Berthing

Berthing energy:	2093	kNm, SLS
Bottom level, DD high:	-24,1	m NAP
Bottom level, DD low:	-24,9	m NAP
Force level, high:	1,7	m NAP
Force level, low:	1,7	m NAP

Slope

Consider slope:	No	
Slope inclination 1:	2,5	vert : horiz

Sections of pile

	Level of top of section [m NAP]	Diameter [mm]	Thickness [mm]	Steel grade [-]	Length of section [m]
1	6,0	2400	26	X70	10,0
2	-4,0	2400	35	X70	8,0
3	-12,0	2400	55	X70	8,0
4	-20,0	2400	66	X70	20,0
5	-40,0	2400	55	X70	6,0

Division into zones based on Figure 6-6 CROW 1005

Zone	Top [m NAP]	Bottom [m NAP]
1	6,00	-21,70
2a	-21,70	-26,50
2b	-26,50	-31,30
3	-31,30	-46,00

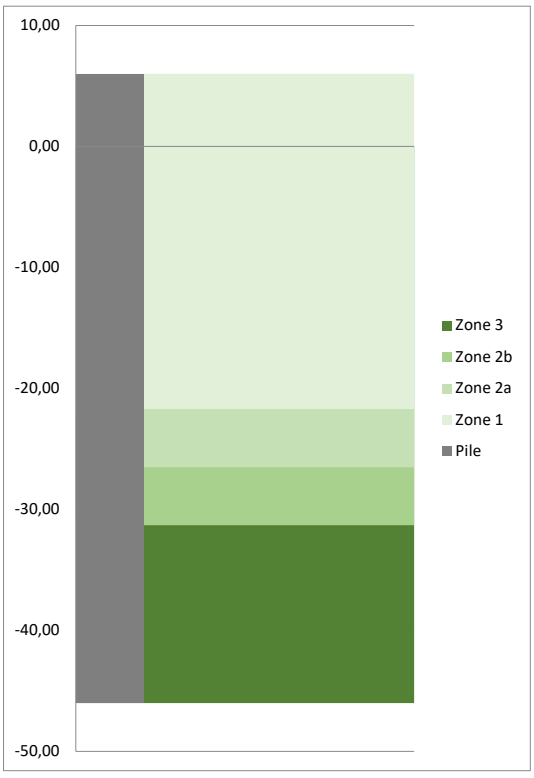

Output:

Berthing

	Berthing energy:	3035	kNm, ULS
B1	Berthing energy:	3045	kNm
	Berthing force:	4056,6	kN
	Disp - berthing force:	1501,4	mm
	Displacement:	1747,3	mm, top
		-17	mm, pile toe
B2	Berthing energy:	3045	kNm
	Berthing force:	4056,6	kN
	Disp - berthing force:	1501,4	mm
	Displacement:	1747,3	mm, top
		-17	mm, pile toe
B3	Berthing energy:	29928074	kNm
	Berthing force:	1013,0	kN
	Disp - berthing force:	59087603,7	mm
	Displacement:	500,7	mm, top
		-17,4	mm, pile toe
B4	Berthing energy:	2065	kNm
	Berthing force:	3085,3	kN
	Disp - berthing force:	1338,3	mm
	Displacement:	1545	mm, top
		-25	mm, pile toe

*Note: Top and toe displacements are based on the design force: 1.05 * Berthing force (only for Sea-going vessels).*

Results for berthing per zone

Case	Ø	t	Level	Ved	Med	Zone	Class	UC	
								elastic	buckling
	[mm]	[mm]	[m NAP]	[kN]	[kNm]	[-]	[-]	[-]	[-]
1	2400	26	-4	4057	23123	z1	Class 4	0,45	0,52
2	2400	35	-12	4057	55576	z1	Class 4	0,77	0,88
3	2400	55	-20	4057	88029	z1	Class 3	0,82	0,74
4	2400	66	-21,7	4057	94925	z1	Class 3	0,75	0,68
5	2400	66	-26,5	3203	113588	z2a	Class 3	0,90	0,81
6	2400	66	-30,6	124	121938	z2b MaxM	Class 3	0,96	0,87
7	2400	66	-31,3	1081	121720	z2b	Class 3	0,96	0,87
8	2400	66	-31,3	1081	121720	z3	Class 3	0,96	0,87
9	2400	55	-40	9121	74351	z3	Class 3	0,70	0,63

	Top level [m NAP]	Diameter [mm]	Thickness [mm]	Steel grade [-]	Length of section [m]	Weight [mtons]
1	6	2400	26	X70	10,0	15,2
2	-4	2400	35	X70	8,0	16,3
3	-12	2400	55	X70	8,0	25,5
4	-20	2400	66	X70	20,0	76,0
5	-40	2400	55	X70	6,0	19,1
						152,1

Embedding check

According to CROW 1005 a check should be done for the embedding of the pile. B4 is compared with a pile that is 5 times the diameter longer, the difference of top displacement should be less than 2 %

B4			A 5 times the diameter longer pile					
Displacement:	1545	mm, top	Displacement:	1467,5	mm, top	5,3 %	>	2,0 %

Does not comply

Embedding check (soil pressure)

B1	B2	B3	B4
FALSE	FALSE	TRUE	FALSE
59,89%	59,89%	13,93%	68,58%

For more details, check sheet 'Results berth'

Graphics

Moments

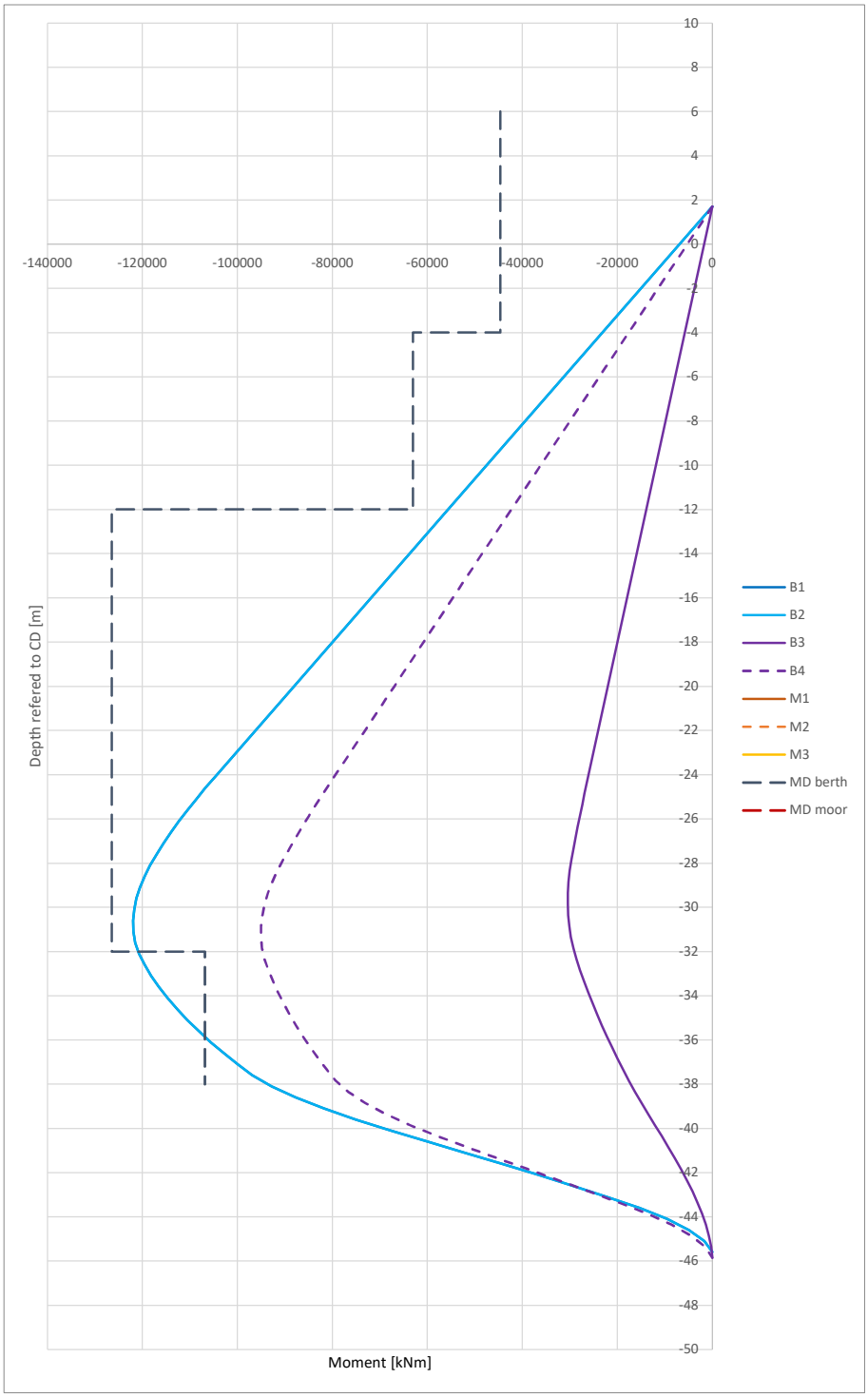

Displacements

Indicated displacements at top is at the level of acting force

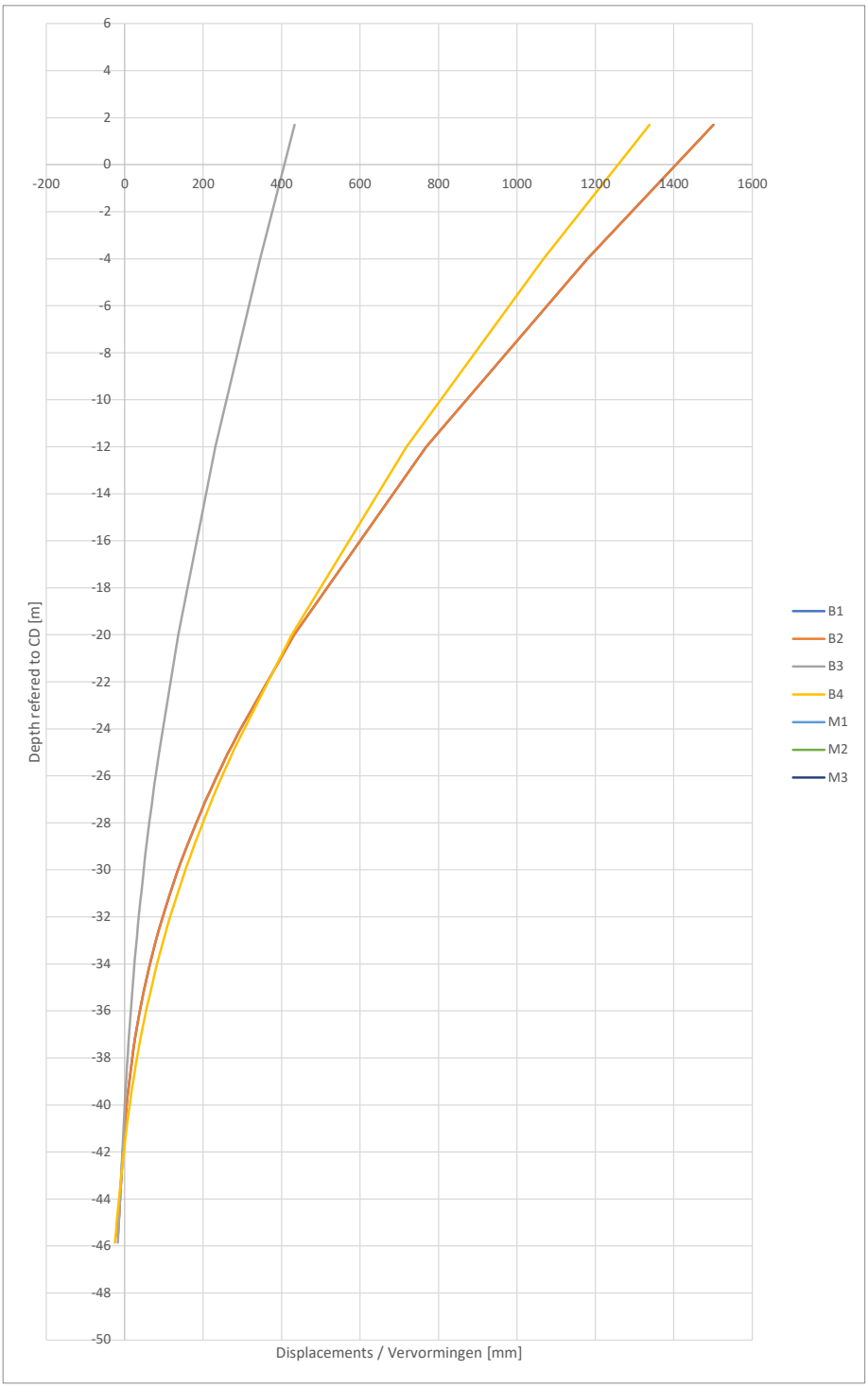

Shear force

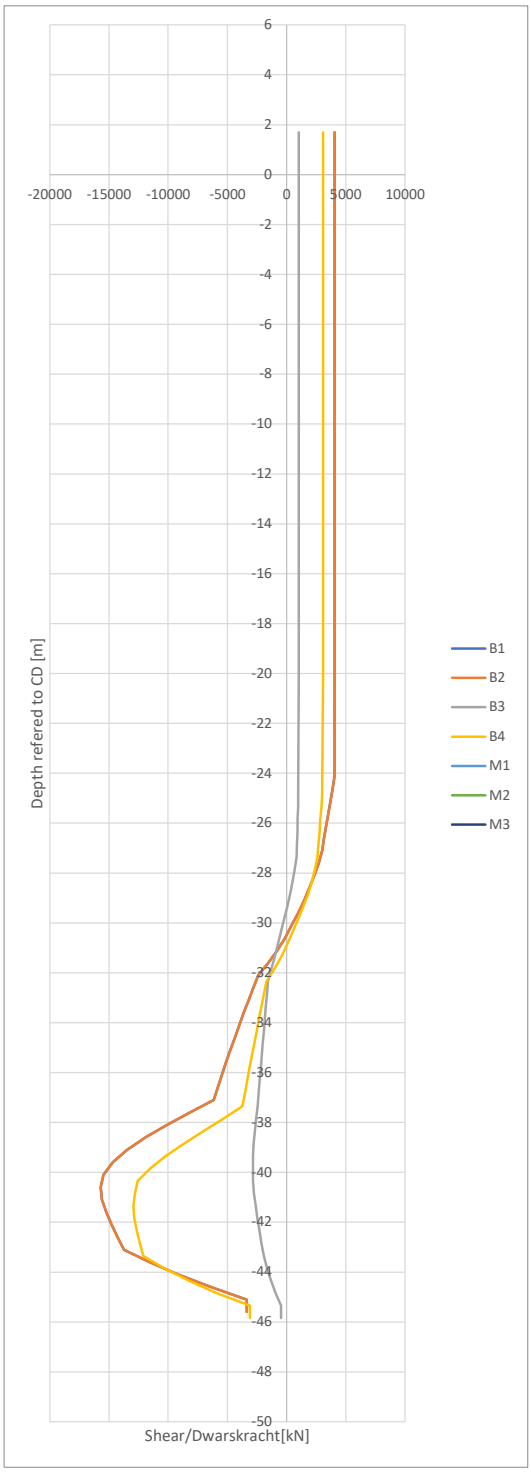

Horizontal soil pressure
Values to be divided by diameter of pile

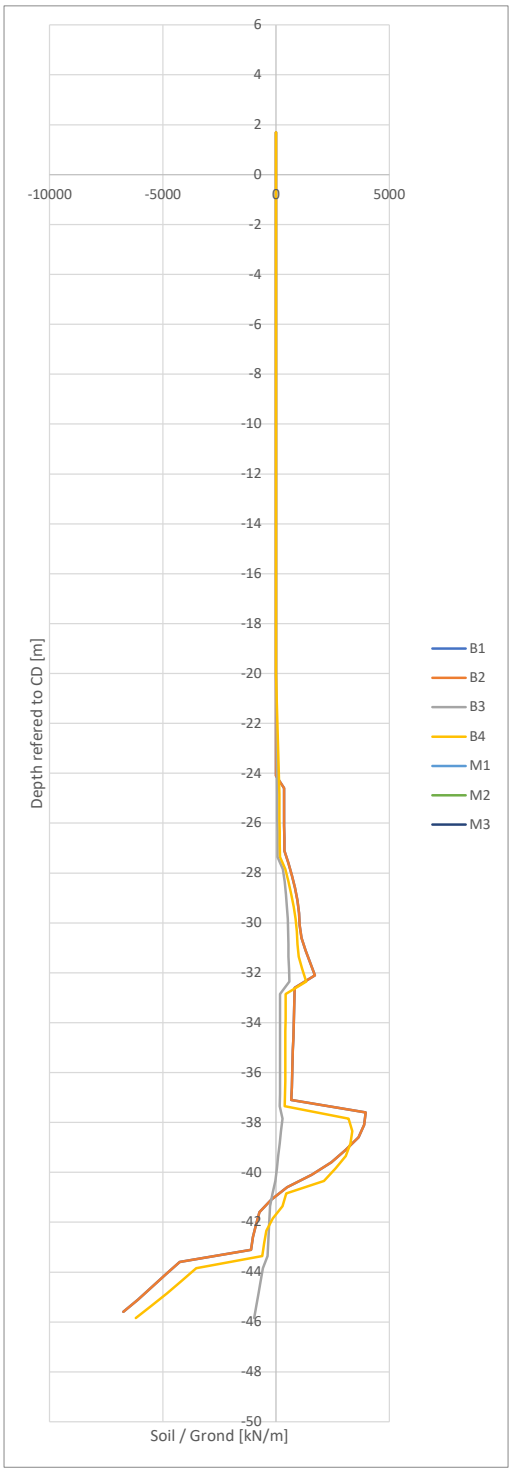

Berthing energy

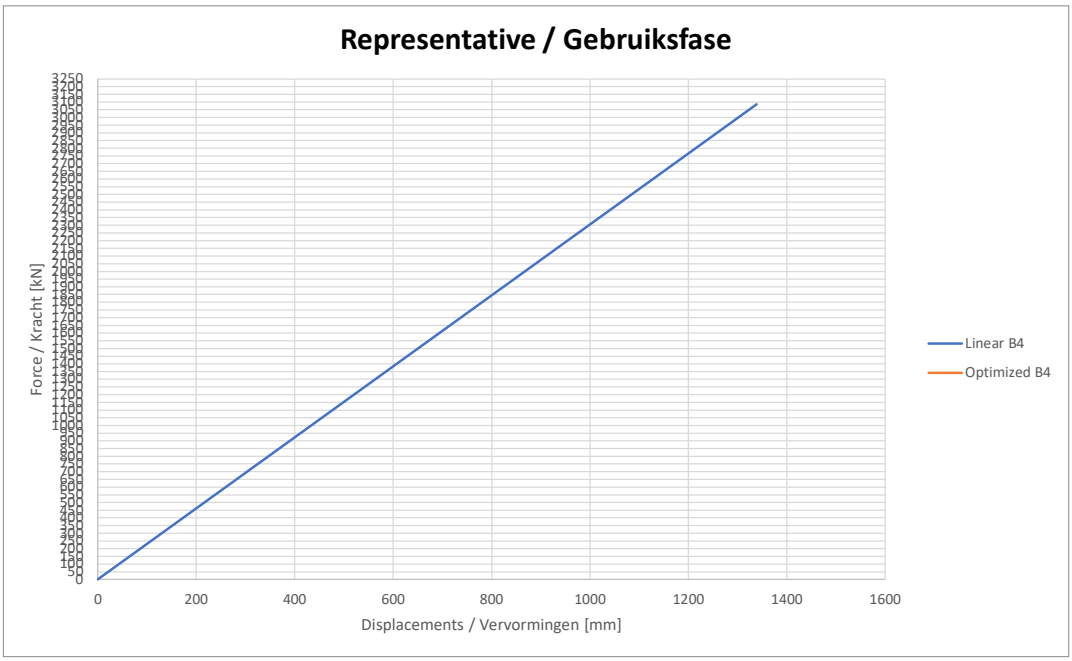

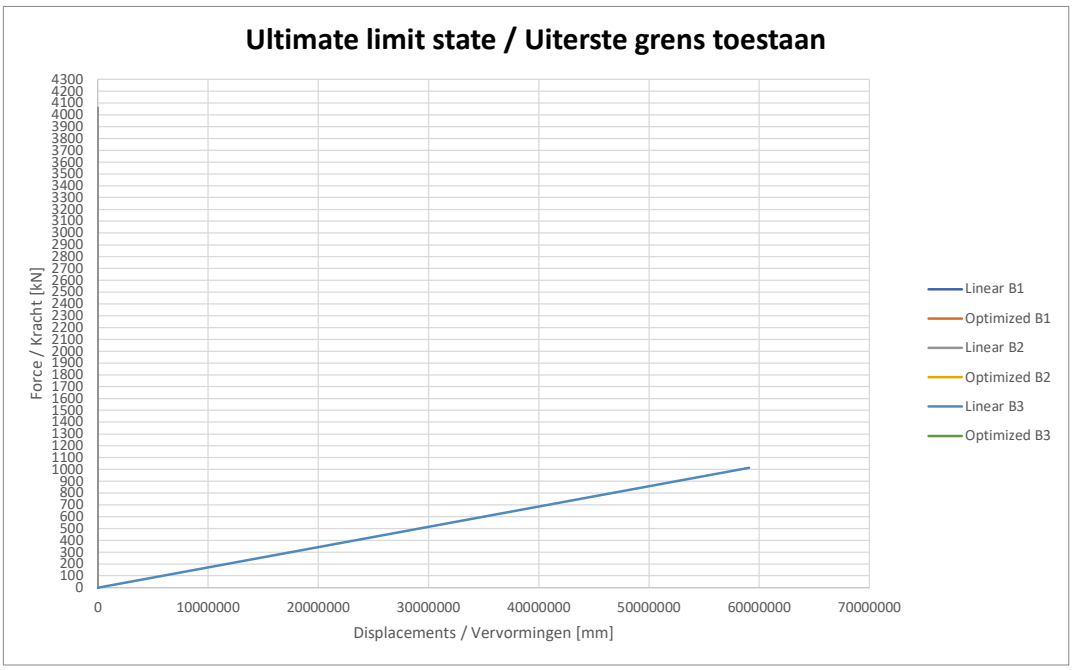

B.5. Case "Monitored"

PROJECT TITLE:			Pname test				
SUBJECT:			comments test				
PROJECT NO:	Pnumber test	FILE REF:		REV:	0.1		
PREPARED BY:		DATE:	12/12/2023	CHECKED BY:		DATE:	CPT Code: CPTcodetest

Input:

Top of pile at:	6	m NAP
Toe of pile at:	-30	m NAP
Amount of sections:	5	
MDL	-15	m NAP
Type of pile:	Berthing	

Berthing

Berthing energy:	594	kNm, SLS
Bottom level, DD high:	-15,0	m NAP
Bottom level, DD low:	-15,9	m NAP
Force level, high:	1,7	m NAP
Force level, low:	1,7	m NAP

Slope

Consider slope:	No	
Slope inclination 1:	2,5	vert : horiz

Sections of pile

	Level of top of section [m NAP]	Diameter [mm]	Thickness [mm]	Steel grade [-]	Length of section [m]
1	6,0	2000	20	X70	8,0
2	-2,0	2000	22	X70	5,0
3	-7,0	2000	29	X70	6,0
4	-13,0	2000	33	X70	10,0
5	-23,0	2000	29	X70	7,0

Division into zones based on Figure 6-6 CROW 1005

Zone	Top [m NAP]	Bottom [m NAP]
1	6,00	-13,00
2a	-13,00	-17,00
2b	-17,00	-21,00
3	-21,00	-30,00

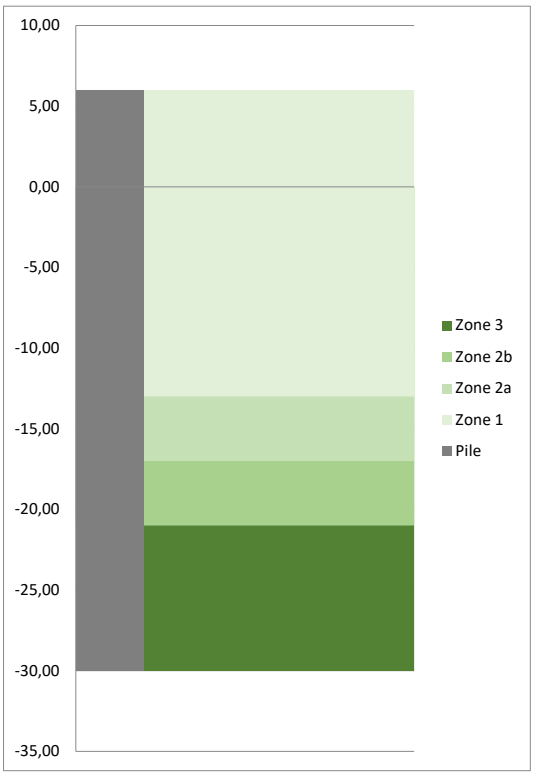

Output:

Berthing

	Berthing energy:	802	kNm, ULS
B1	Berthing energy:	795	kNm
	Berthing force:	2272,9	kN
	Disp - berthing force:	699,3	mm
	Displacement:	875,8	mm, top
		-7,2	mm, pile toe
B2	Berthing energy:	795	kNm
	Berthing force:	2272,9	kN
	Disp - berthing force:	699,3	mm
	Displacement:	875,8	mm, top
		-7,2	mm, pile toe
B3	Berthing energy:	817	kNm
	Berthing force:	1462,8	kN
	Disp - berthing force:	1117,1	mm
	Displacement:	1333,3	mm, top
		-81,6	mm, pile toe
B4	Berthing energy:	601	kNm
	Berthing force:	1788,1	kN
	Disp - berthing force:	671,8	mm
	Displacement:	829,7	mm, top
		-15,4	mm, pile toe

*Note: Top and toe displacements are based on the design force: 1.05 * Berthing force (only for Sea-going vessels).*

Results for berthing per zone

Case	Ø	t	Level	Ved	Med	Zone	Class	UC	
								elastic	buckling
	[mm]	[mm]	[m NAP]	[kN]	[kNm]	[-]	[-]	[-]	[-]
1	2000	20	-2	2273	8410	z1	Class 4	0,31	0,36
2	2000	22	-7	2273	19774	z1	Class 4	0,62	0,75
3	2000	29	-13	2273	33412	z1	Class 4	0,80	0,92
4	2000	33	-17	1624	42197	z2a	Class 4	0,89	0,92
5	2000	33	-19	113	44279	z2b MaxM	Class 4	0,93	0,96
6	2000	33	-21	2377	42451	z2b	Class 4	0,89	0,97
7	2000	33	-21	2377	42451	z3	Class 4	0,89	0,81
8	2000	29	-23	5398	35434	z3	Class 4	0,87	0,80

Errors encountered in calculation: soil pressure might be too high. Consider increasing pile thickness or length. Please check sheet "Unity ckecks", column "m_a" and the corresponding "checks_cases" sheet.

	Top level [m NAP]	Diameter [mm]	Thickness [mm]	Steel grade [-]	Length of section [m]	Weight [mtons]
1	6	2000	20	X70	8,0	7,8
2	-2	2000	22	X70	5,0	5,4
3	-7	2000	29	X70	6,0	8,5
4	-13	2000	33	X70	10,0	16,0
5	-23	2000	29	X70	7,0	9,9
						47,5

Embedding check

According to CROW 1005 a check should be done for the embedding of the pile. B4 is compared with a pile that is 5 times the diameter longer, the difference of top displacement should be less than 2 %

B4			A 5 times the diameter longer pile					
Displacement:	829,7	mm, top	Displacement:	787,4	mm, top	5,4 %	>	2,0 %

Does not comply

Embedding check (soil pressure)

B1	B2	B3	B4
TRUE	TRUE	FALSE	FALSE
34,06%	34,06%	64,88%	55,50%

For more details, check sheet 'Results berth'

Graphics

Moments

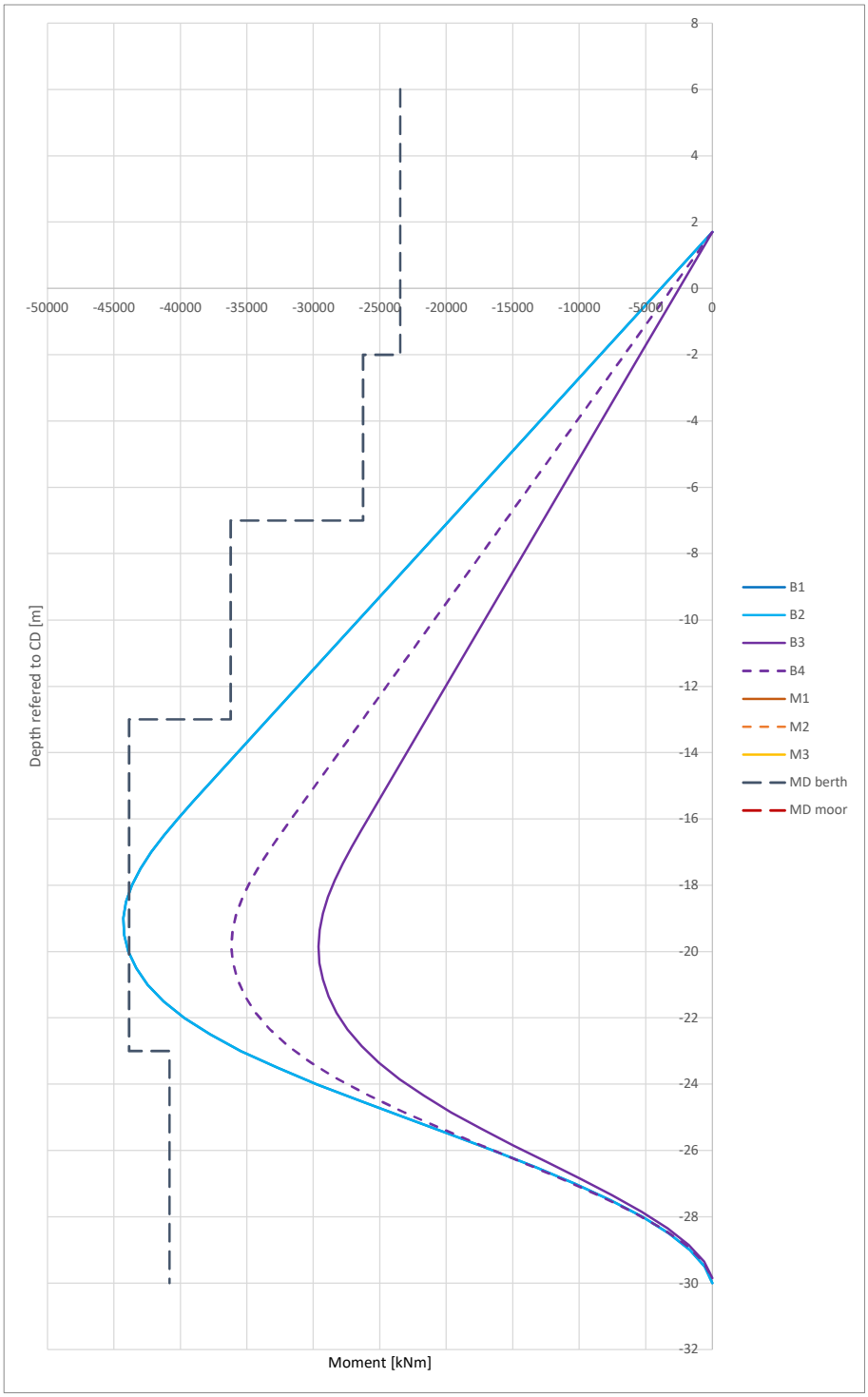

Displacements

Indicated displacements at top is at the level of acting force

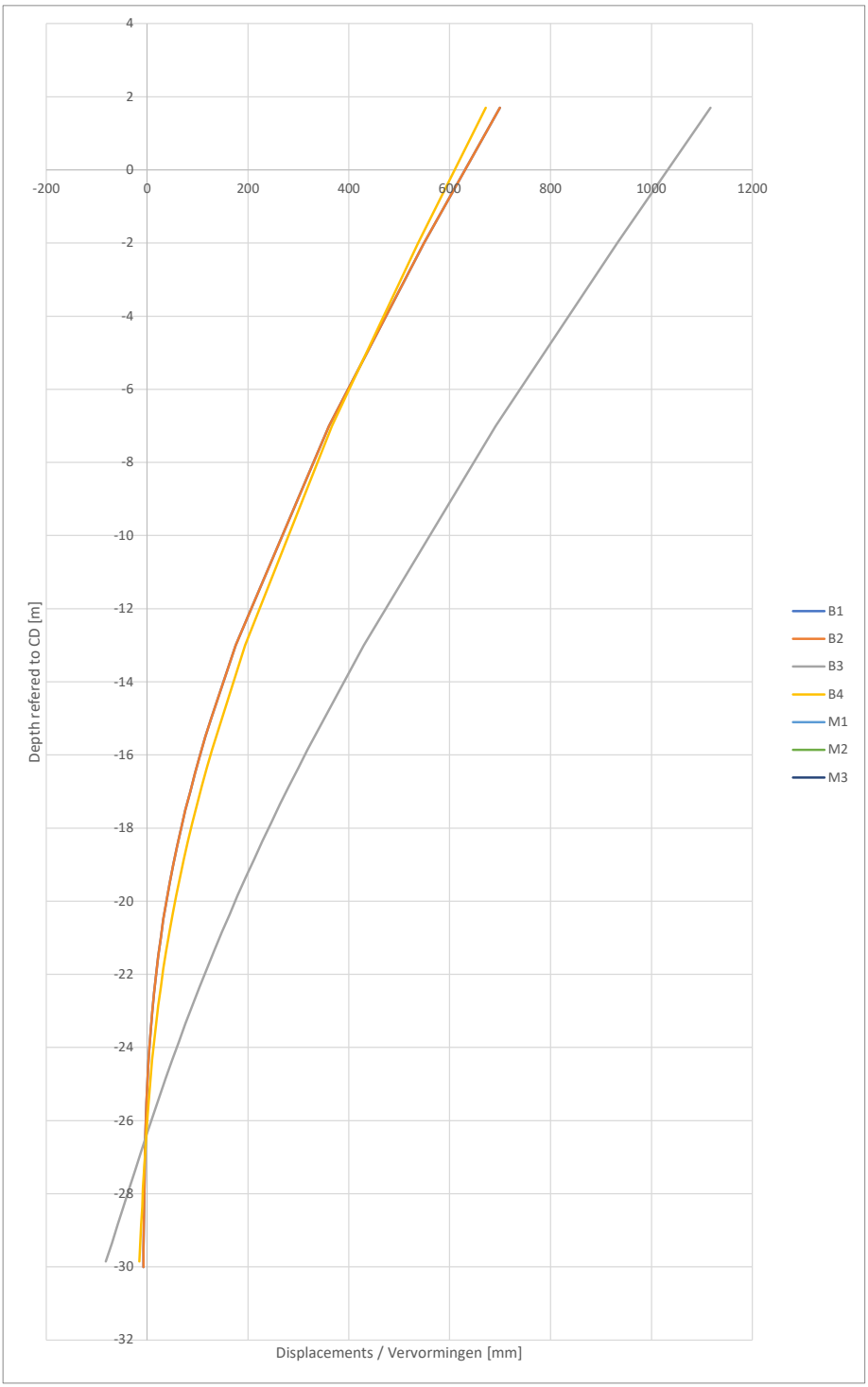

Shear force

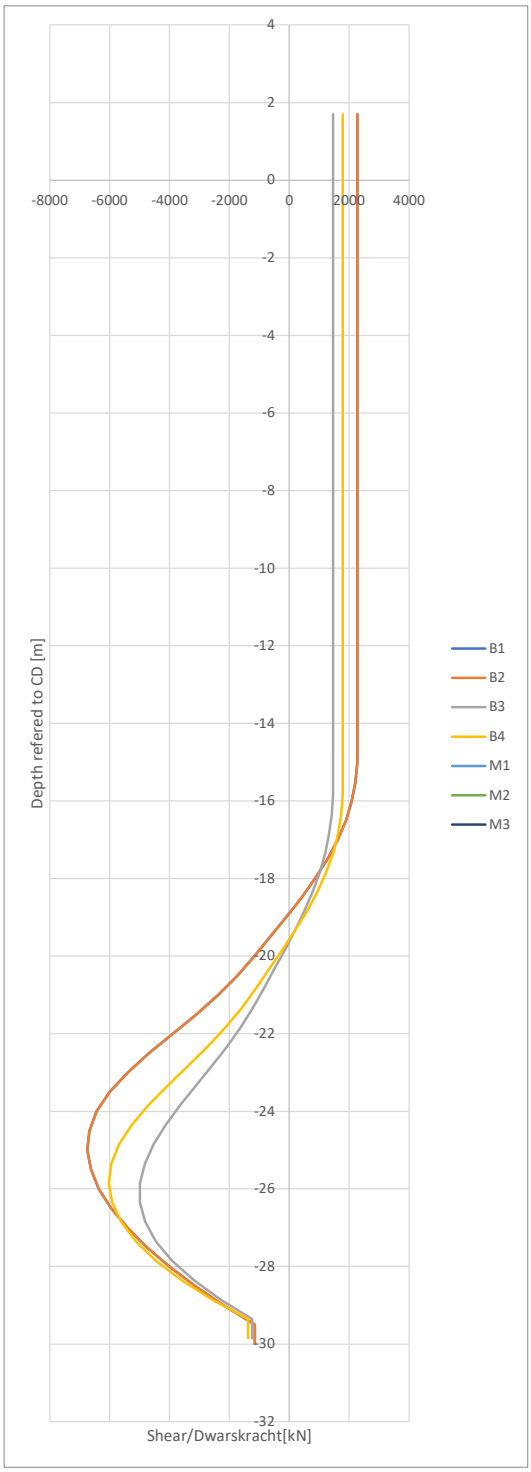

Horizontal soil pressure

Values to be divided by diameter of pile

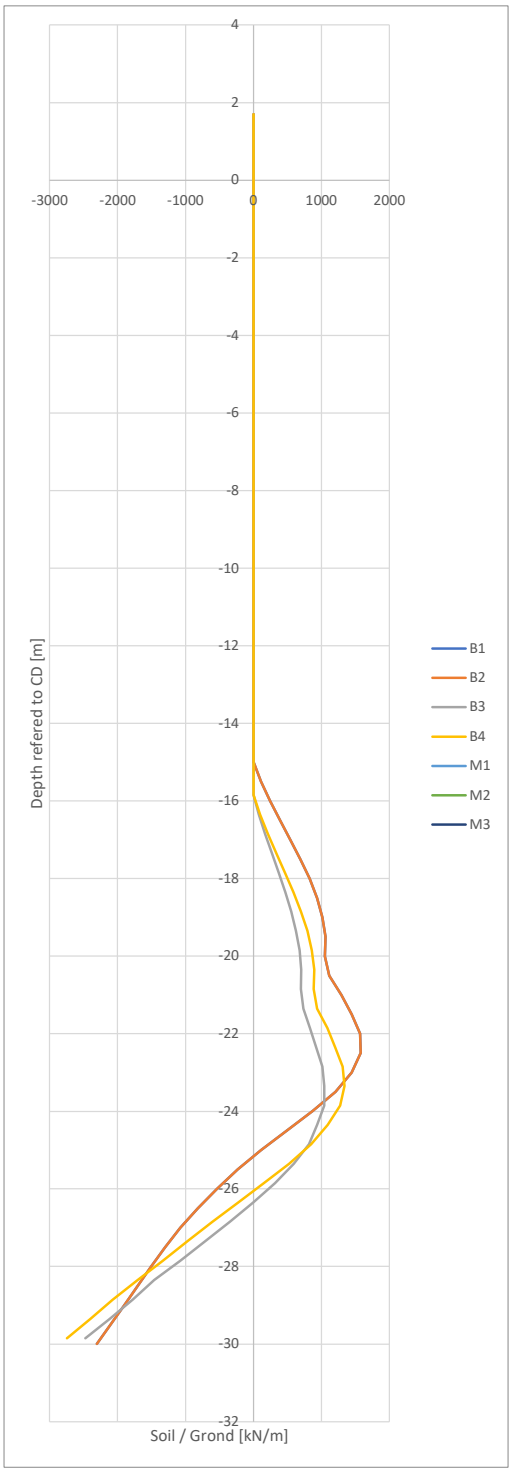

Berthing energy

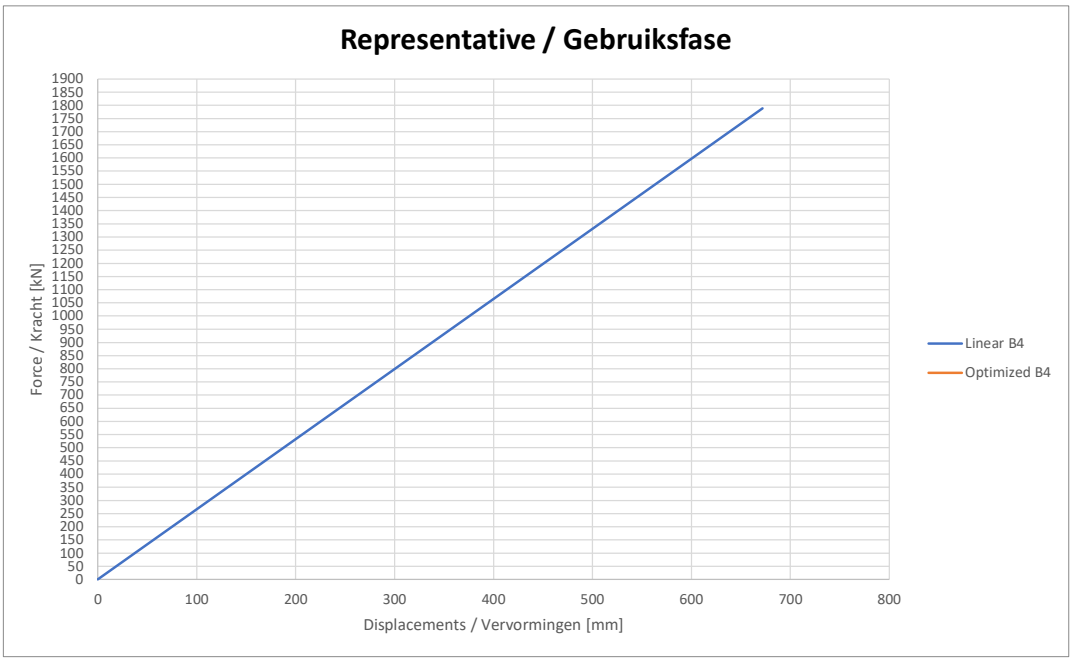

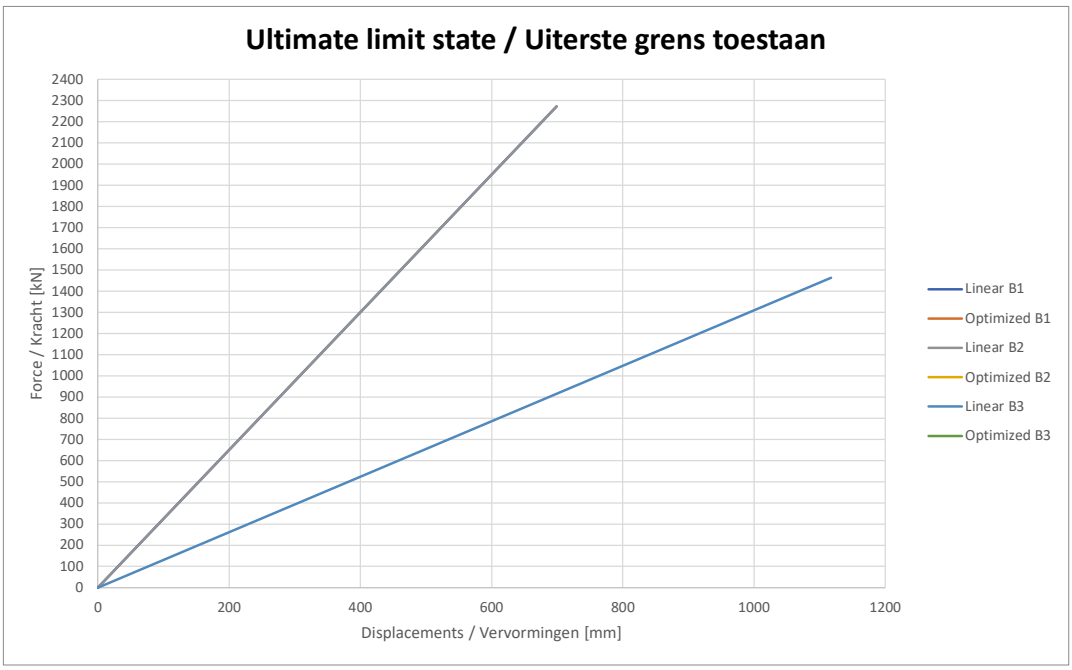

B.6. Case "Favourable"

PROJECT TITLE:			Pname test				
SUBJECT:			comments test				
PROJECT NO:	Pnumber test	FILE REF:		REV:	0.1		
PREPARED BY:		DATE:	12/12/2023	CHECKED BY:		DATE:	CPT Code: CPTcodetest

Input:

Top of pile at:	6	m NAP
Toe of pile at:	-30	m NAP
Amount of sections:	5	
MDL	-15	m NAP
Type of pile:	Berthing	

Berthing

Berthing energy:	594	kNm, SLS
Bottom level, DD high:	-15,0	m NAP
Bottom level, DD low:	-15,9	m NAP
Force level, high:	1,7	m NAP
Force level, low:	1,7	m NAP

Slope

Consider slope:	No	
Slope inclination 1:	2,5	vert : horiz

Sections of pile

	Level of top of section [m NAP]	Diameter [mm]	Thickness [mm]	Steel grade [-]	Length of section [m]
1	6,0	2000	20	X70	8,0
2	-2,0	2000	24	X70	6,0
3	-8,0	2000	30	X70	5,0
4	-13,0	2000	34	X70	10,0
5	-23,0	2000	29	X70	7,0

Division into zones based on Figure 6-6 CROW 1005

Zone	Top [m NAP]	Bottom [m NAP]
1	6,00	-13,00
2a	-13,00	-17,00
2b	-17,00	-21,00
3	-21,00	-30,00

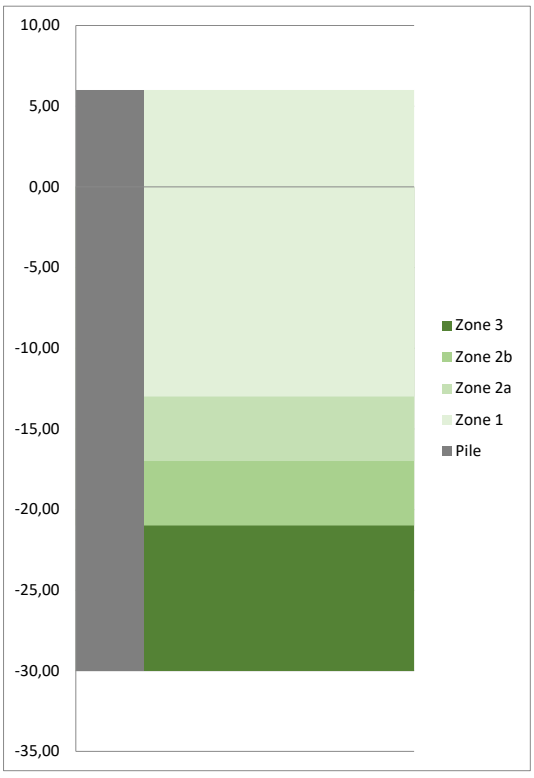

Output:

Berthing

	Berthing energy:	861	kNm, ULS
B1	Berthing energy:	850	kNm
	Berthing force:	2355,1	kN
	Disp - berthing force:	721,6	mm
	Displacement:	901,4	mm, top
		-8	mm, pile toe
B2	Berthing energy:	850	kNm
	Berthing force:	2355,1	kN
	Disp - berthing force:	721,6	mm
	Displacement:	901,4	mm, top
		-8	mm, pile toe
B3	Berthing energy:	862	kNm
	Berthing force:	1474,1	kN
	Disp - berthing force:	1169,1	mm
	Displacement:	1347,6	mm, top
		-83,4	mm, pile toe
B4	Berthing energy:	602	kNm
	Berthing force:	1800,7	kN
	Disp - berthing force:	668,4	mm
	Displacement:	824,7	mm, top
		-15,7	mm, pile toe

*Note: Top and toe displacements are based on the design force: 1.05 * Berthing force (only for Sea-going vessels).*

Results for berthing per zone

Case	Ø	t	Level	Ved	Med	Zone	Class	UC	
								elastic	buckling
	[mm]	[mm]	[m NAP]	[kN]	[kNm]	[-]	[-]	[-]	[-]
1	2000	20	-2	2355	8714	z1	Class 4	0,33	0,37
2	2000	24	-8	2355	22844	z1	Class 4	0,66	0,78
3	2000	30	-13	2355	34620	z1	Class 4	0,80	0,92
4	2000	34	-17	1706	43734	z2a	Class 4	0,89	0,91
5	2000	34	-19	31	45980	z2b MaxM	Class 4	0,94	0,95
6	2000	34	-21	2295	44317	z2b	Class 4	0,91	0,96
7	2000	34	-21	2295	44317	z3	Class 4	0,91	0,81
8	2000	29	-23	5466	37408	z3	Class 4	0,91	0,85

Errors encountered in calculation: soil pressure might be too high. Consider increasing pile thickness or length. Please check sheet "Unity ckecks", column "m_a" and the corresponding "checks_cases" sheet.

	Top level [m NAP]	Diameter [mm]	Thickness [mm]	Steel grade [-]	Length of section [m]	Weight [mtons]
1	6	2000	20	X70	8,0	7,8
2	-2	2000	24	X70	6,0	7,0
3	-8	2000	30	X70	5,0	7,3
4	-13	2000	34	X70	10,0	16,5
5	-23	2000	29	X70	7,0	9,9
						48,5

Embedding check

According to CROW 1005 a check should be done for the embedding of the pile. B4 is compared with a pile that is 5 times the diameter longer, the difference of top displacement should be less than 2 %

B4			A 5 times the diameter longer pile					
Displacement:	824,7	mm, top	Displacement:	780,1	mm, top	5,7 %	>	2,0 %

Does not comply

Embedding check (soil pressure)

B1	B2	B3	B4
TRUE	TRUE	FALSE	FALSE
37,23%	37,23%	65,96%	56,35%

For more details, check sheet 'Results berth'

Graphics

Moments

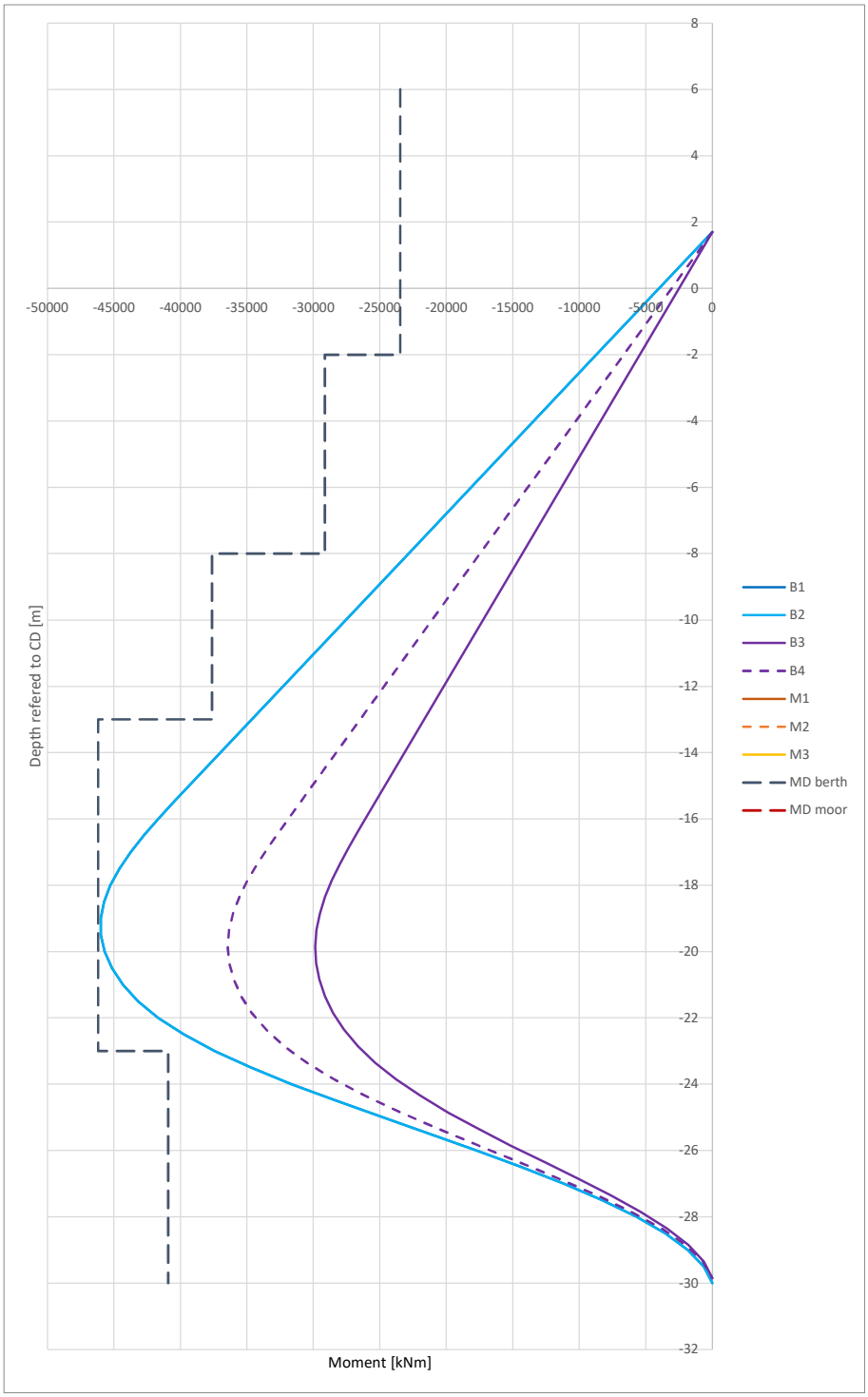

Displacements

Indicated displacements at top is at the level of acting force

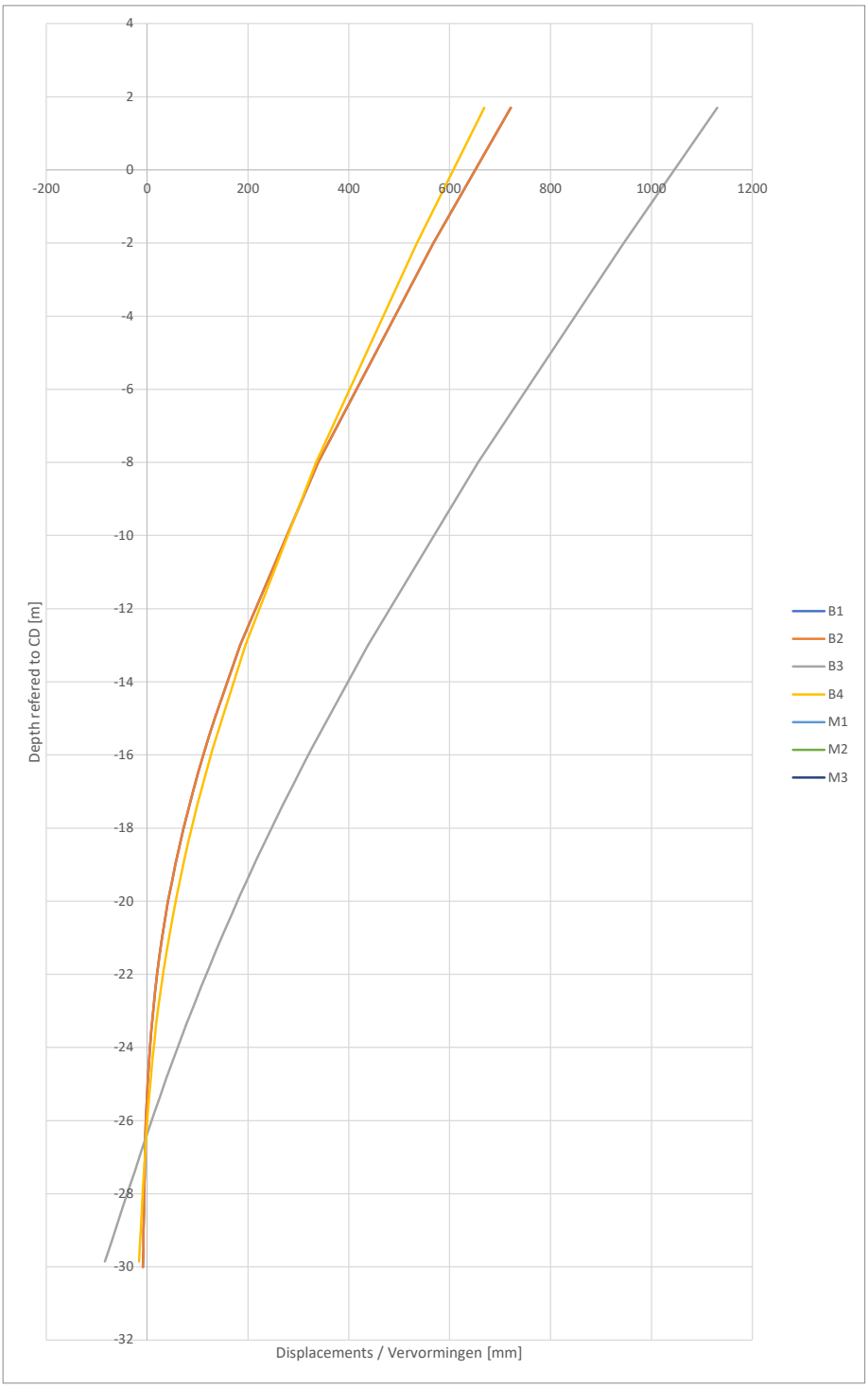

Shear force

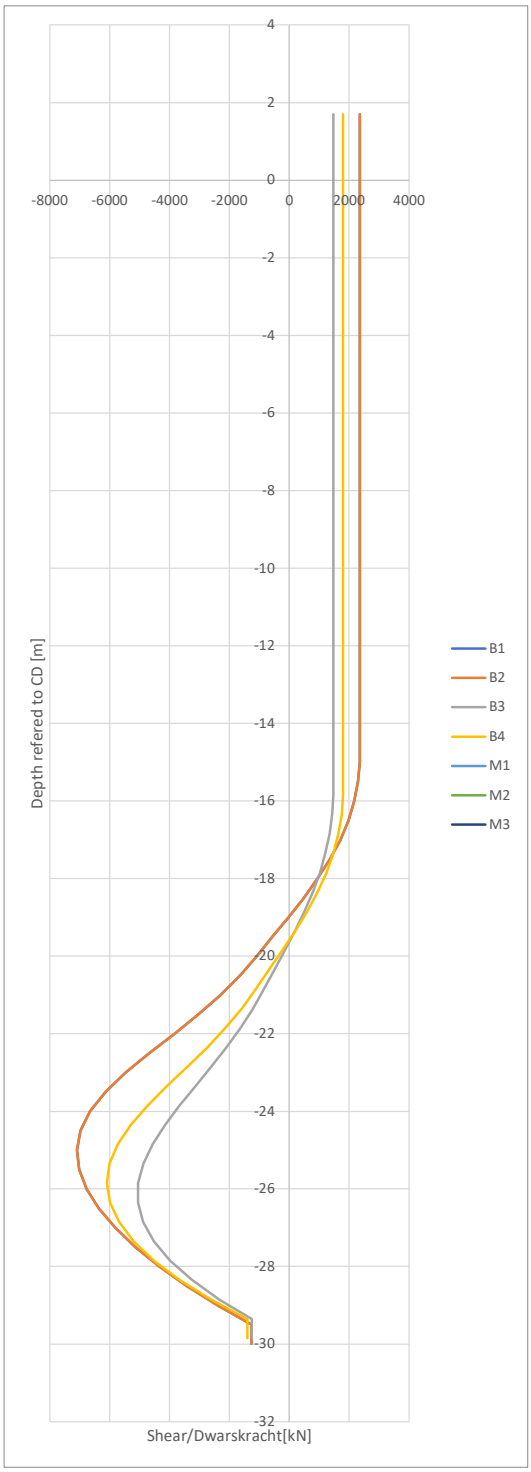

Horizontal soil pressure
Values to be divided by diameter of pile

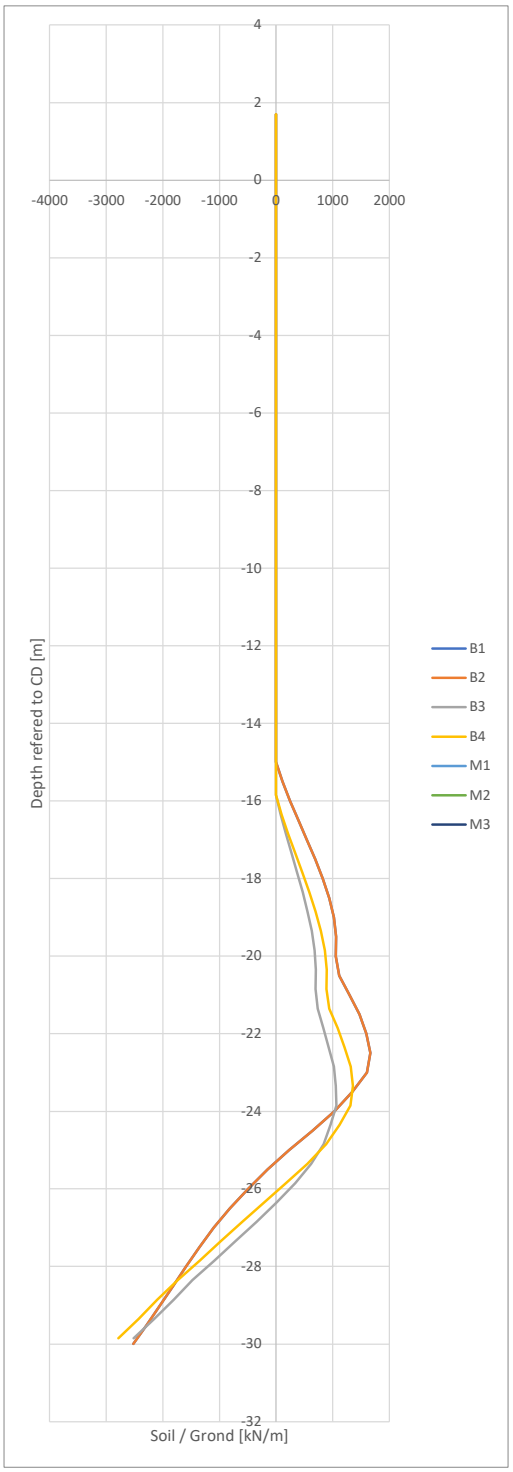

Berthing energy

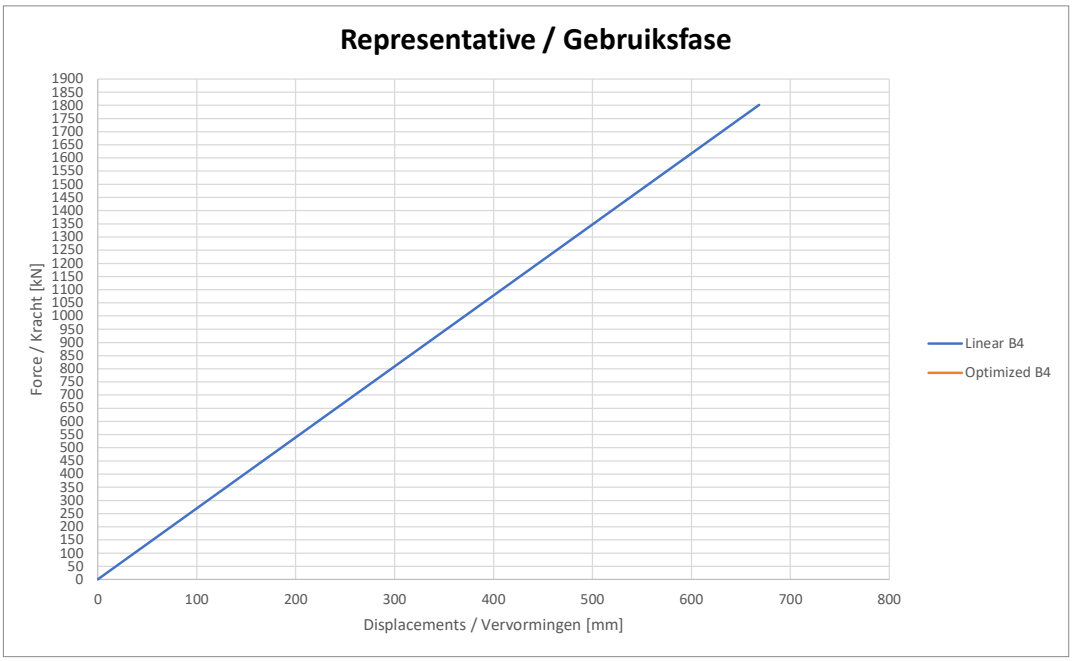

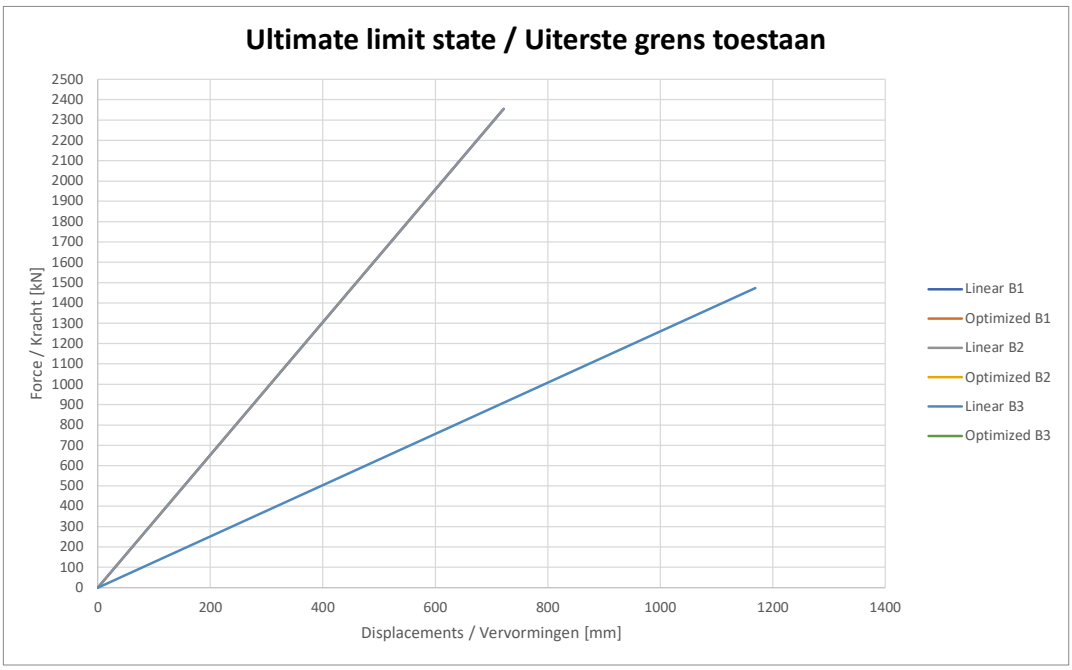

B.7. Case "Moderate"

PROJECT TITLE:			Pname test				
SUBJECT:			comments test				
PROJECT NO:	Pnumber test	FILE REF:		REV:	0.1		
PREPARED BY:		DATE:	12/12/2023	CHECKED BY:		DATE:	CPT Code: CPTcodetest

Input:

Top of pile at:	6	m NAP
Toe of pile at:	-33	m NAP
Amount of sections:	5	
MDL	-15	m NAP
Type of pile:	Berthing	

Berthing

Berthing energy:	1336	kNm, SLS
Bottom level, DD high:	-15,0	m NAP
Bottom level, DD low:	-15,9	m NAP
Force level, high:	1,7	m NAP
Force level, low:	1,7	m NAP

Slope

Consider slope:	No	
Slope inclination 1:	2,5	vert : horiz

Sections of pile

	Level of top of section [m NAP]	Diameter [mm]	Thickness [mm]	Steel grade [-]	Length of section [m]
1	6,0	2400	26	X70	8,0
2	-2,0	2400	32	X70	6,0
3	-8,0	2400	48	X70	6,0
4	-14,0	2400	55	X70	12,0
5	-26,0	2400	44	X70	7,0

Division into zones based on Figure 6-6 CROW 1005

Zone	Top [m NAP]	Bottom [m NAP]
1	6,00	-12,60
2a	-12,60	-17,40
2b	-17,40	-22,20
3	-22,20	-33,00

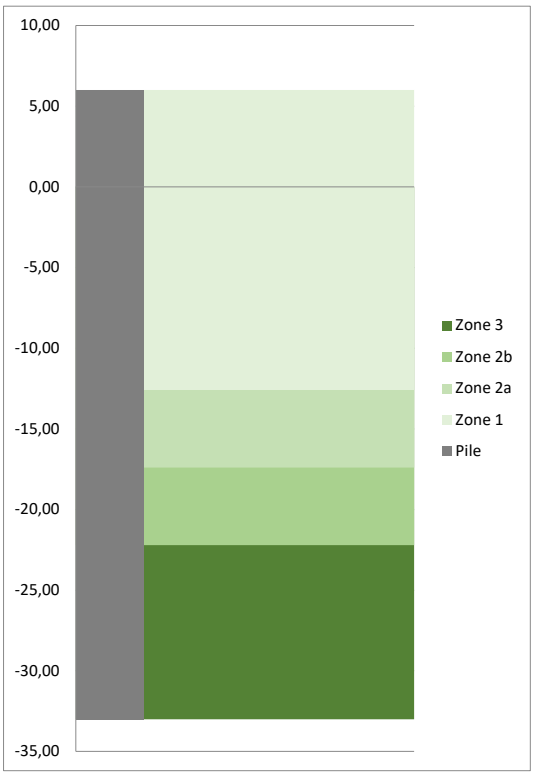

Output:

Berthing

	Berthing energy:	1937	kNm, ULS
B1	Berthing energy:	1956	kNm
	Berthing force:	5086,5	kN
	Disp - berthing force:	769,2	mm
	Displacement:	945,6	mm, top
		-13,9	mm, pile toe
B2	Berthing energy:	1956	kNm
	Berthing force:	5086,5	kN
	Disp - berthing force:	769,2	mm
	Displacement:	945,6	mm, top
		-13,9	mm, pile toe
B3	Berthing energy:	1939	kNm
	Berthing force:	2985,0	kN
	Disp - berthing force:	1299,5	mm
	Displacement:	1430,8	mm, top
		-108	mm, pile toe
B4	Berthing energy:	1362	kNm
	Berthing force:	3826,3	kN
	Disp - berthing force:	711,9	mm
	Displacement:	863,7	mm, top
		-23,9	mm, pile toe

*Note: Top and toe displacements are based on the design force: 1.05 * Berthing force (only for Sea-going vessels).*

Results for berthing per zone

Case	Ø	t	Level	Ved	Med	Zone	Class	UC	
								elastic	buckling
	[mm]	[mm]	[m NAP]	[kN]	[kNm]	[-]	[-]	[-]	[-]
1	2400	26	-2	5087	18820	z1	Class 4	0,39	0,42
2	2400	32	-8	5087	49339	z1	Class 4	0,75	0,87
3	2400	48	-12,6	5087	72737	z1	Class 4	0,78	0,85
4	2400	48	-14	5087	79858	z2a	Class 4	0,86	0,94
5	2400	55	-17,4	3999	96491	z2a	Class 3	0,90	0,81
6	2400	55	-20,5	32	104212	z2b MaxM	Class 3	0,98	0,88
7	2400	55	-22,2	2864	102521	z2b	Class 3	0,96	0,86
8	2400	55	-22,2	2864	102521	z3	Class 3	0,96	0,86
9	2400	44	-26	12422	76372	z3	Class 4	0,93	0,77

	Top level [m NAP]	Diameter [mm]	Thickness [mm]	Steel grade [-]	Length of section [m]	Weight [mtons]
1	6	2400	26	X70	8,0	12,2
2	-2	2400	32	X70	6,0	11,2
3	-8	2400	48	X70	6,0	16,7
4	-14	2400	55	X70	12,0	38,2
5	-26	2400	44	X70	7,0	17,9
						96,2

Embedding check

According to CROW 1005 a check should be done for the embedding of the pile. B4 is compared with a pile that is 5 times the diameter longer, the difference of top displacement should be less than 2 %

B4			A 5 times the diameter longer pile					
Displacement:	863,7	mm, top	Displacement:	791,7	mm, top	9,1 %	>	2,0 %

Does not comply

Embedding check (soil pressure)

B1	B2	B3	B4
FALSE	FALSE	FALSE	FALSE
50,97%	50,97%	69,39%	66,41%

For more details, check sheet 'Results berth'

Graphics

Moments

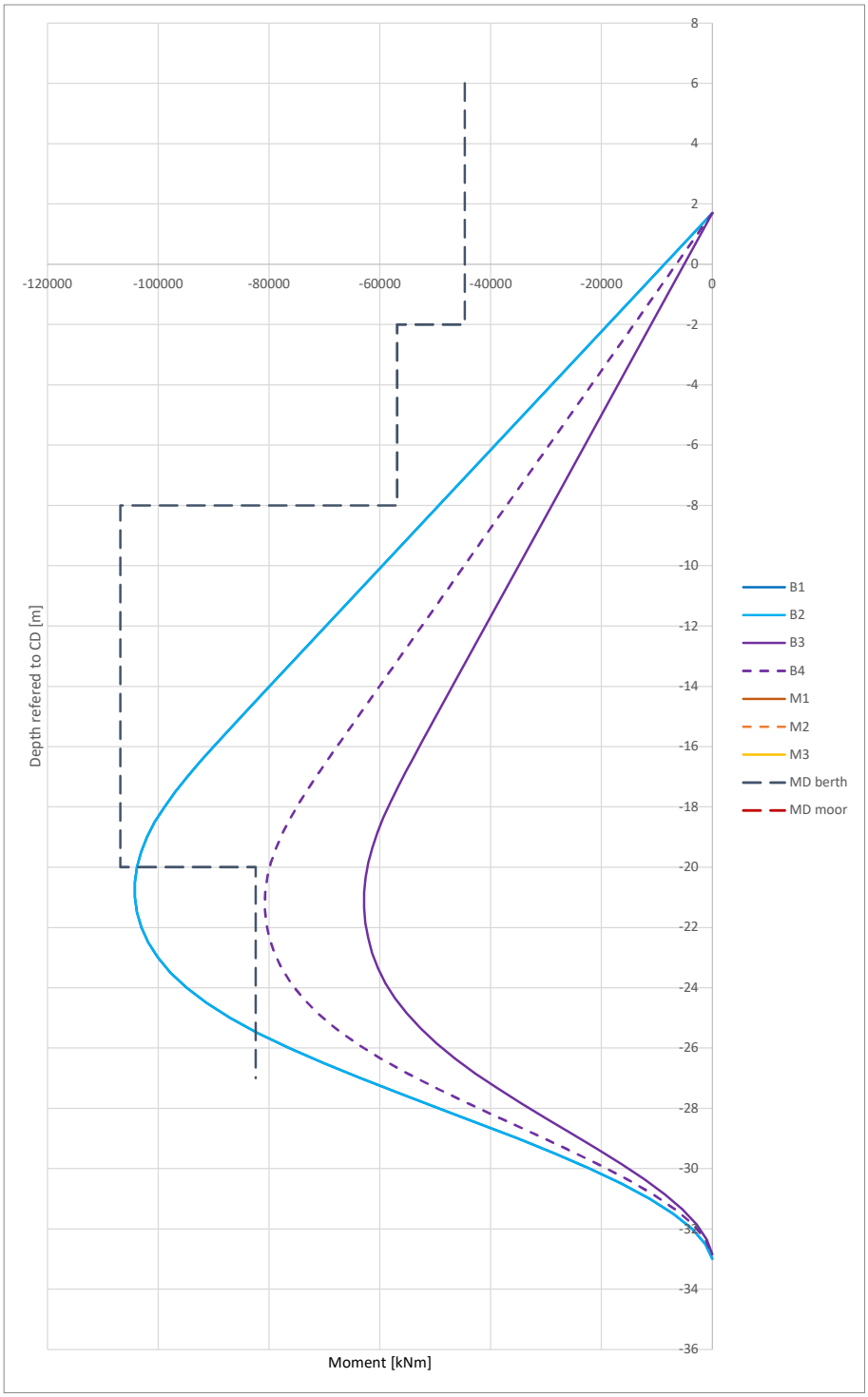

Displacements

Indicated displacements at top is at the level of acting force

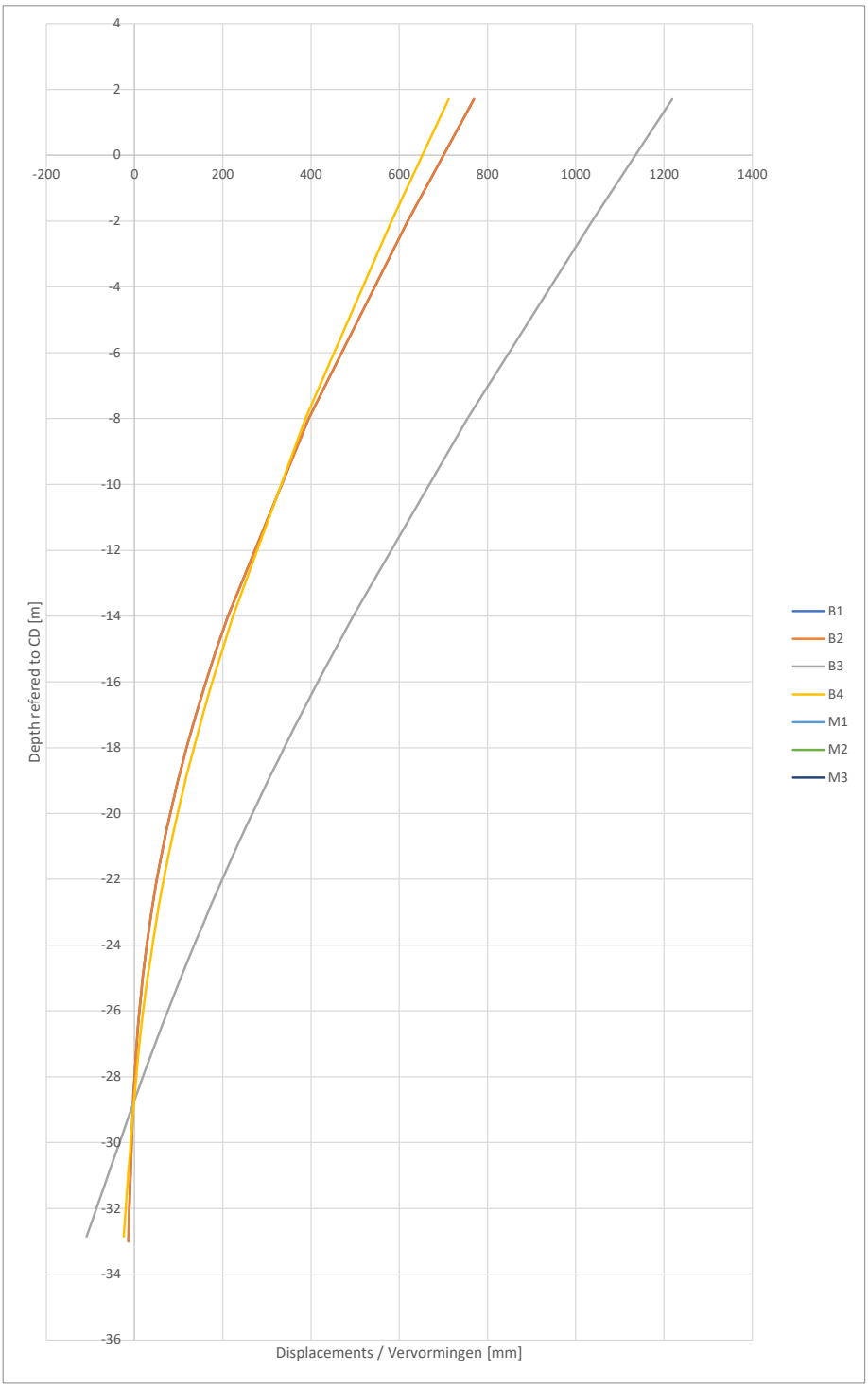

Shear force

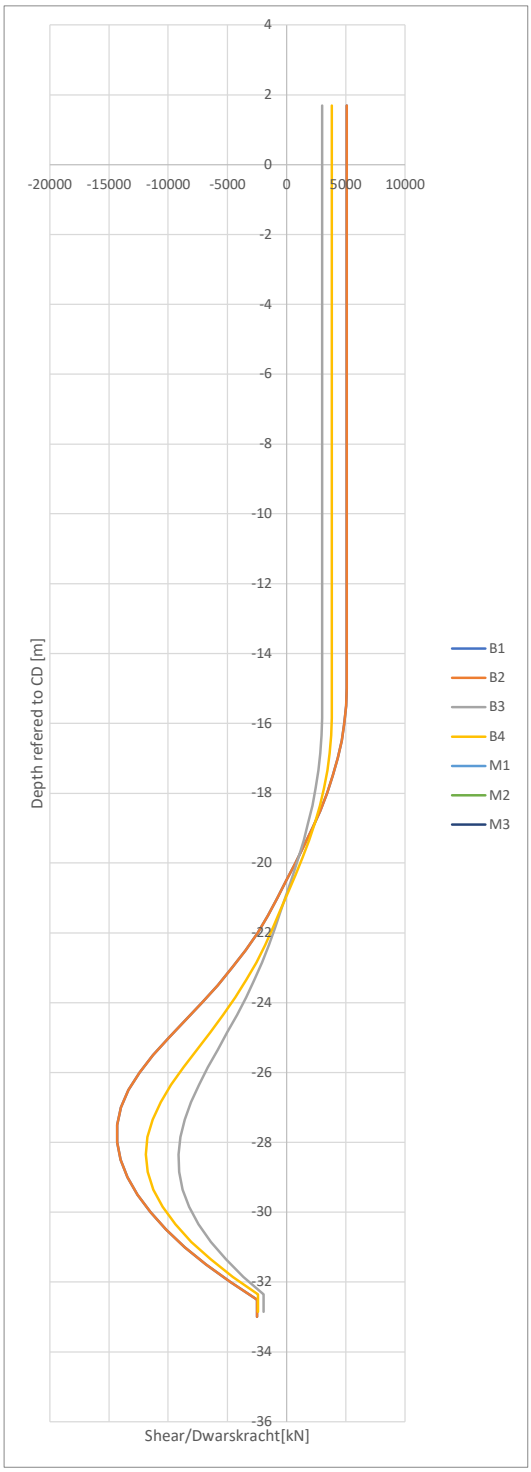

Horizontal soil pressure

Values to be divided by diameter of pile

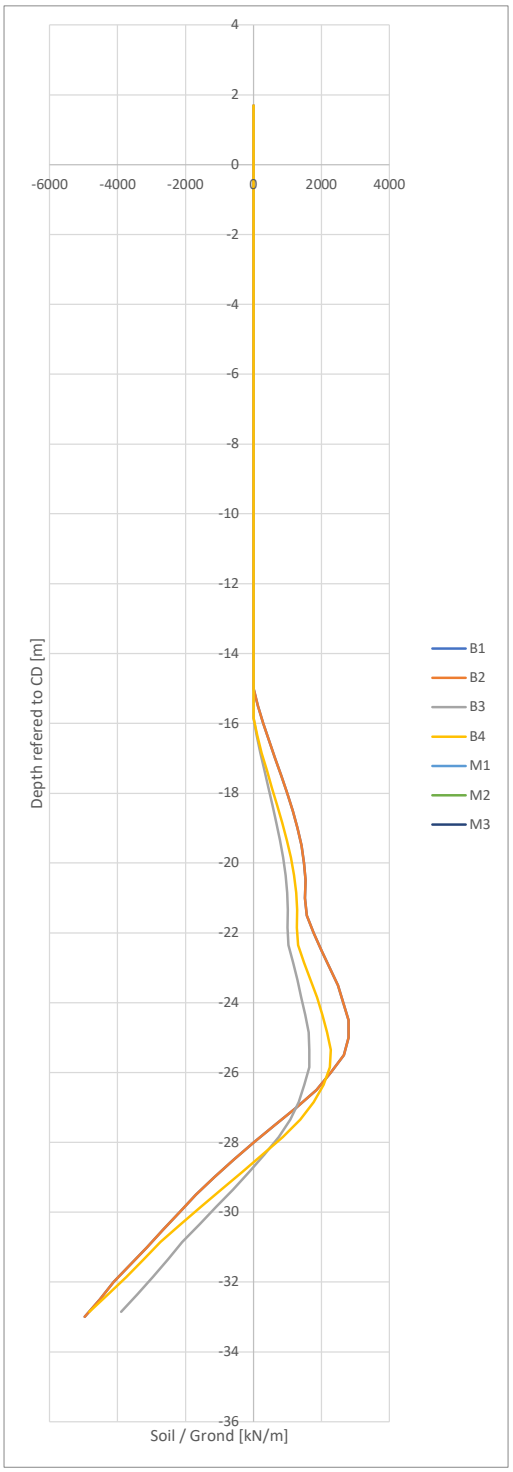

Berthing energy

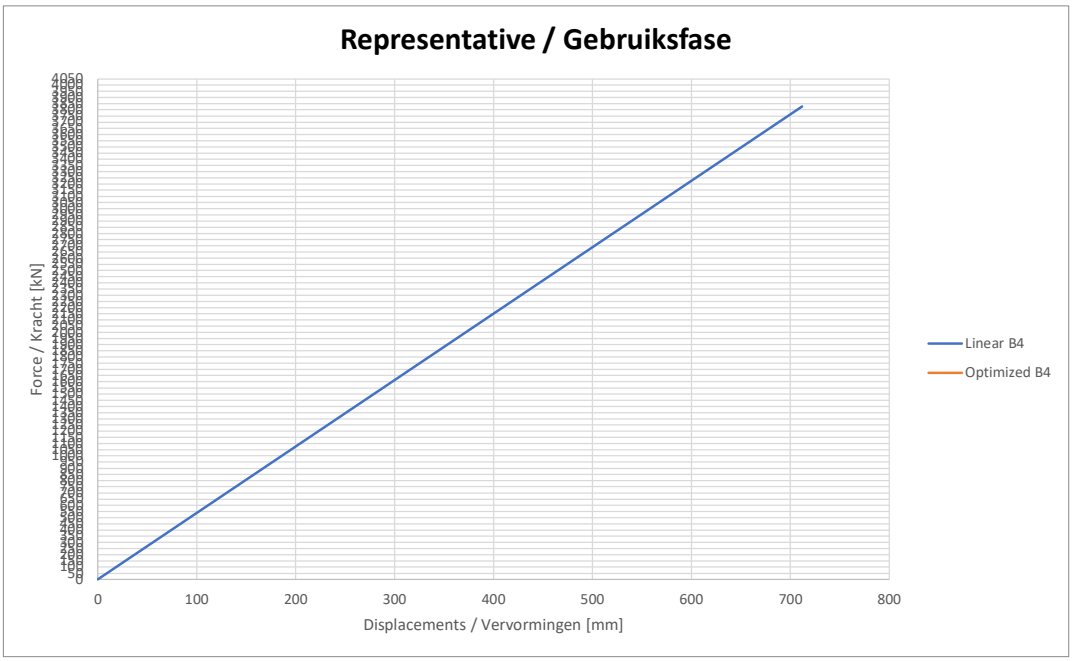

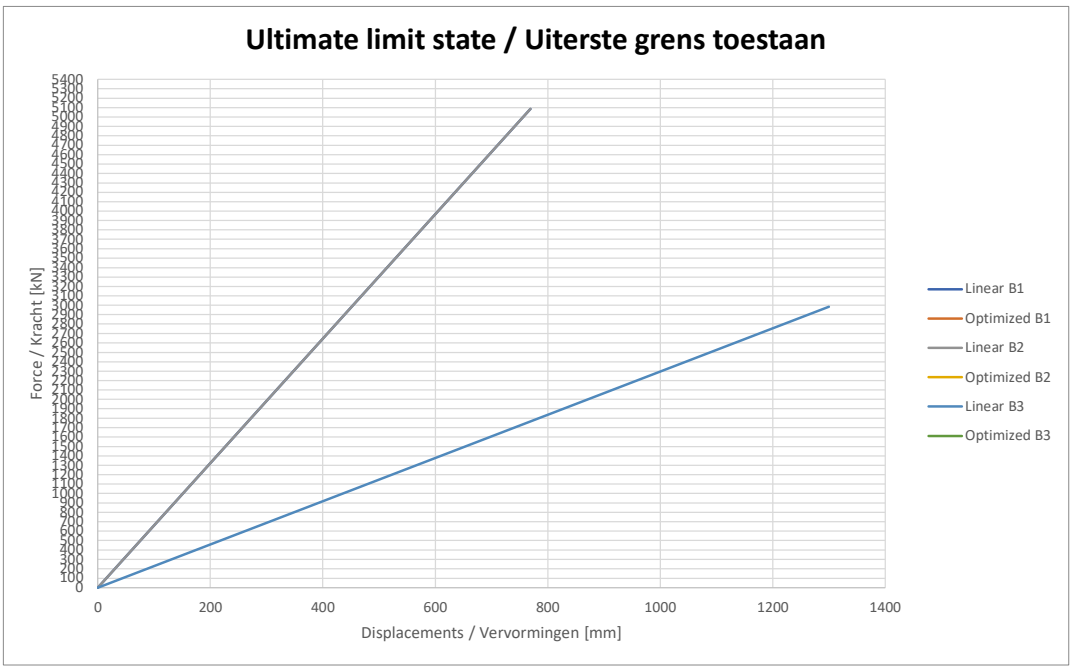

B.8. Case "Unfavourable"

PROJECT TITLE:			Pname test				
SUBJECT:			comments test				
PROJECT NO:	Pnumber test	FILE REF:		REV:	0.1		
PREPARED BY:		DATE:	12/12/2023	CHECKED BY:		DATE:	CPT Code: CPTcodetest

Input:

Top of pile at:	6	m NAP
Toe of pile at:	-41	m NAP
Amount of sections:	5	
MDL	-15	m NAP
Type of pile:	Berthing	

Berthing

Berthing energy:	2375	kNm, SLS
Bottom level, DD high:	-15,0	m NAP
Bottom level, DD low:	-15,9	m NAP
Force level, high:	1,7	m NAP
Force level, low:	1,7	m NAP

Slope

Consider slope:	No	
Slope inclination 1:	2,5	vert : horiz

Sections of pile

	Level of top of section [m NAP]	Diameter [mm]	Thickness [mm]	Steel grade [-]	Length of section [m]
1	6,0	3500	40	X70	8,0
2	-2,0	3500	50	X70	7,0
3	-9,0	3500	60	X70	7,0
4	-16,0	3500	70	X70	12,0
5	-28,0	3500	60	X70	13,0

Division into zones based on Figure 6-6 CROW 1005

Zone	Top [m NAP]	Bottom [m NAP]
1	6,00	-11,50
2a	-11,50	-18,50
2b	-18,50	-25,50
3	-25,50	-41,00

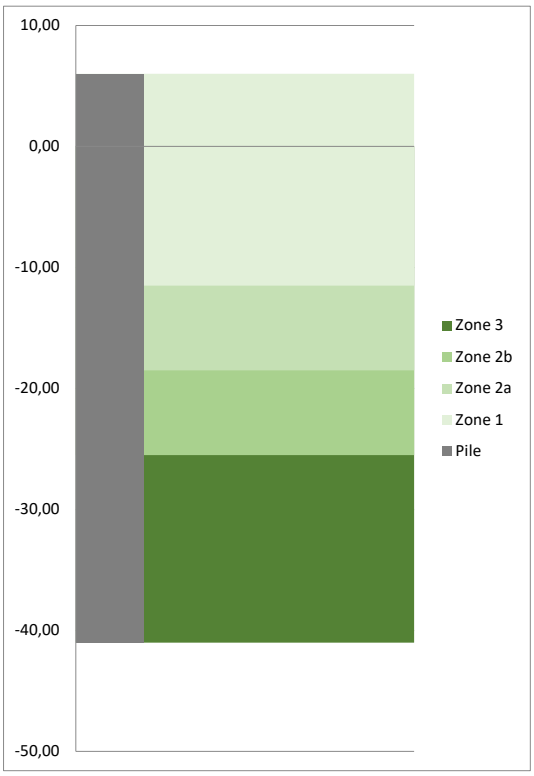

Output:

Berthing

	Berthing energy:	4038	kNm, ULS
B1	Berthing energy:	3998	kNm
	Berthing force:	12853,5	kN
	Disp - berthing force:	622,2	mm
	Displacement:	750,6	mm, top
		-6,2	mm, pile toe
B2	Berthing energy:	3998	kNm
	Berthing force:	12853,5	kN
	Disp - berthing force:	622,2	mm
	Displacement:	750,6	mm, top
		-6,2	mm, pile toe
B3	Berthing energy:	4092	kNm
	Berthing force:	8863,5	kN
	Disp - berthing force:	923,3	mm
	Displacement:	1071,8	mm, top
		-84,7	mm, pile toe
B4	Berthing energy:	2406	kNm
	Berthing force:	9521,3	kN
	Disp - berthing force:	505,4	mm
	Displacement:	606,4	mm, top
		-10	mm, pile toe

*Note: Top and toe displacements are based on the design force: 1.05 * Berthing force (only for Sea-going vessels).*

Results for berthing per zone

Case	Ø	t	Level	Ved	Med	Zone	Class	UC	
								elastic	buckling
	[mm]	[mm]	[m NAP]	[kN]	[kNm]	[-]	[-]	[-]	[-]
1	3500	40	-2	12853	47558	z1	Class 4	0,34	0,32
2	3500	50	-9	12853	137532	z1	Class 4	0,67	0,75
3	3500	60	-11,5	12853	169666	z1	Class 4	0,69	0,76
4	3500	60	-16	12560	227460	z2a	Class 4	0,91	0,85
5	3500	70	-18,5	9697	256646	z2a	Class 4	0,89	0,82
6	3500	70	-22,5	959	278734	z2b MaxM	Class 4	0,96	0,98
7	3500	70	-25,5	11105	263592	z2b	Class 4	0,91	0,96
8	3500	70	-25,5	11105	263592	z3	Class 4	0,91	0,78
9	3500	60	-28	20337	226149	z3	Class 4	0,93	0,80

Errors encountered in calculation: soil pressure might be too high. Consider increasing pile thickness or length. Please check sheet "Unity ckecks", column "m_a" and the corresponding "checks_cases" sheet.

	Top level [m NAP]	Diameter [mm]	Thickness [mm]	Steel grade [-]	Length of section [m]	Weight [mtons]
1	6	3500	40	X70	8,0	27,3
2	-2	3500	50	X70	7,0	29,8
3	-9	3500	60	X70	7,0	35,6
4	-16	3500	70	X70	12,0	71,1
5	-28	3500	60	X70	13,0	66,2
						229,9

Embedding check

According to CROW 1005 a check should be done for the embedding of the pile. B4 is compared with a pile that is 5 times the diameter longer, the difference of top displacement should be less than 2 %

B4			A 5 times the diameter longer pile					
Displacement:	606,4	mm, top	Displacement:	597,2	mm, top	1,5 %	≤	2,0 %

Complies

Embedding check (soil pressure)

B1	TRUE	B2	TRUE	B3	TRUE	B4	TRUE
	17,30%		17,30%		43,79%		23,22%

For more details, check sheet 'Results berth'

Graphics

Moments

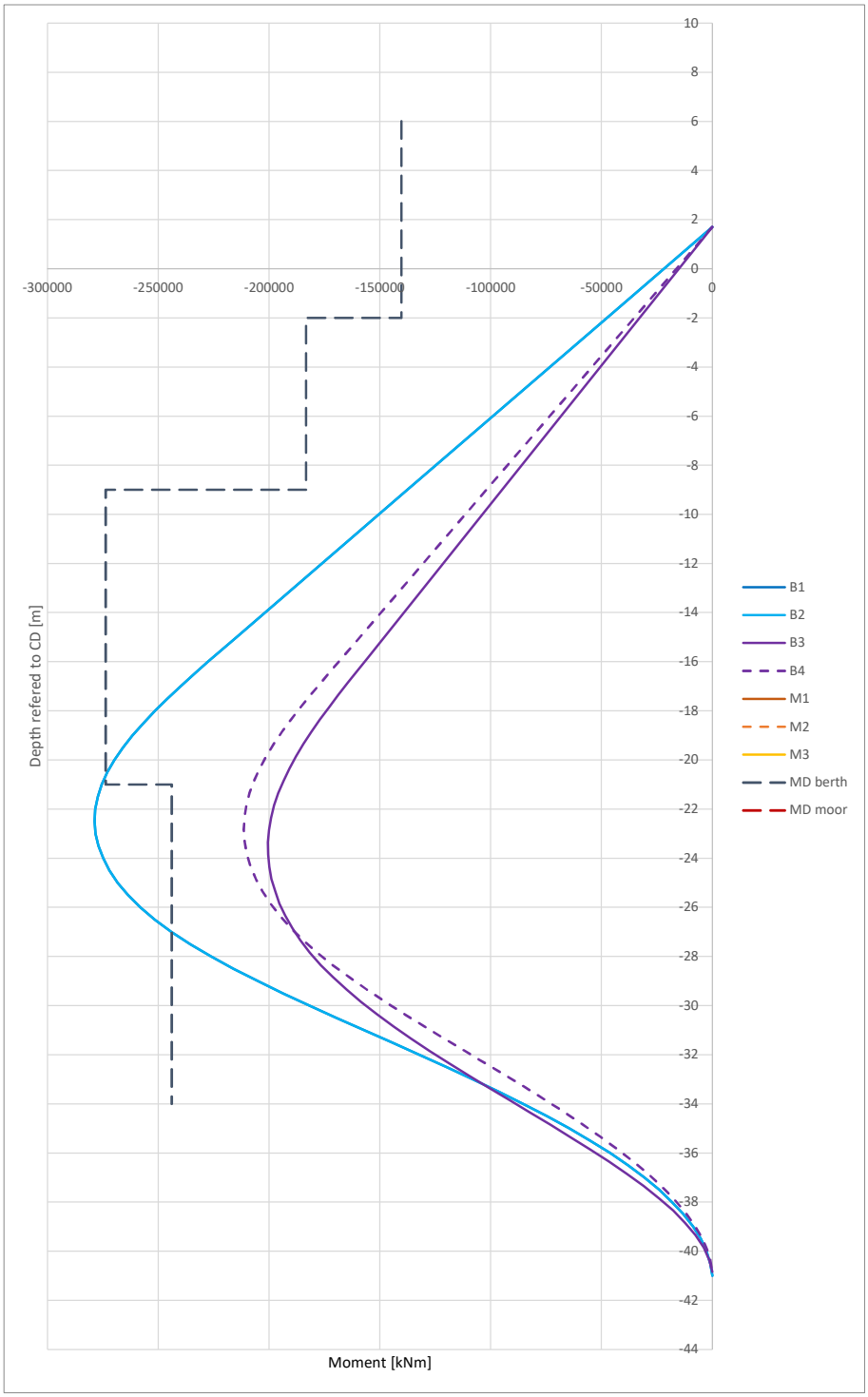

Displacements

Indicated displacements at top is at the level of acting force

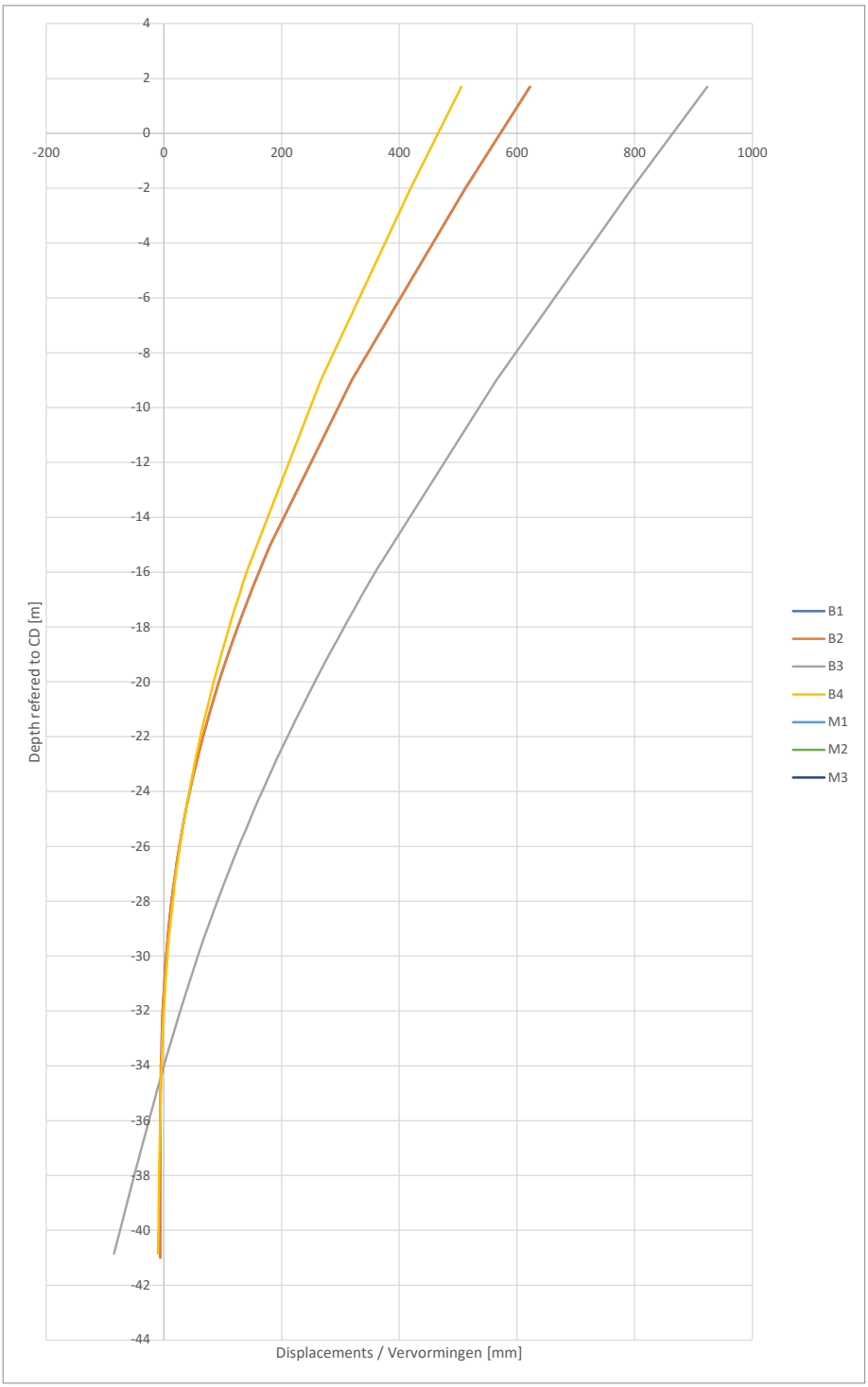

Shear force

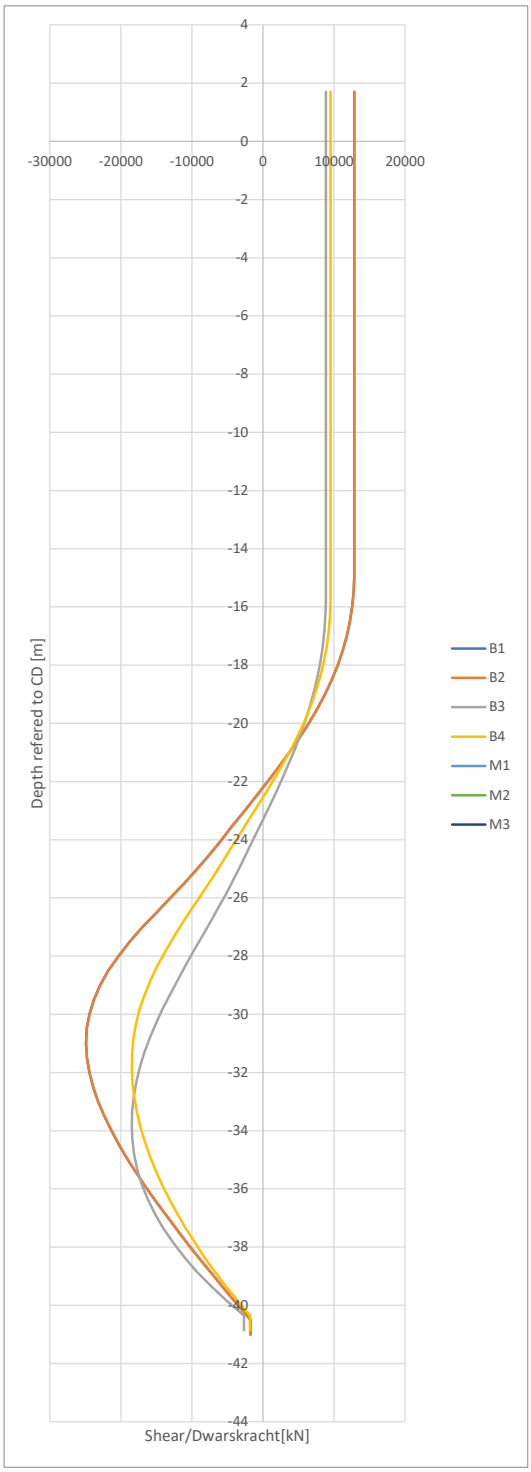

Horizontal soil pressure

Values to be divided by diameter of pile

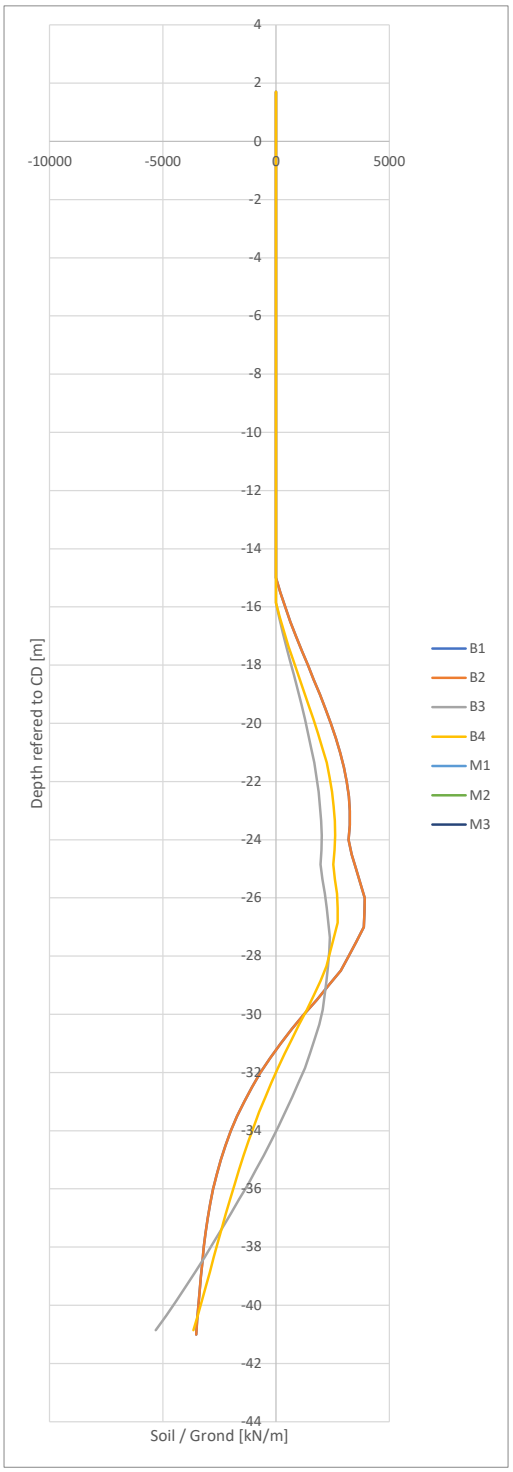

Berthing energy

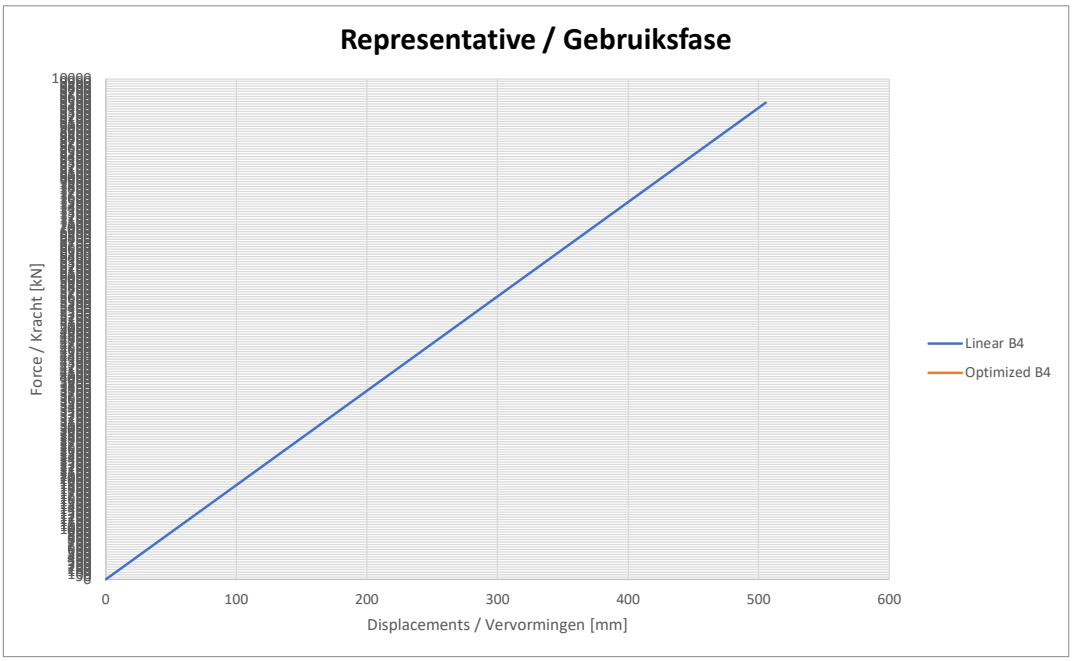

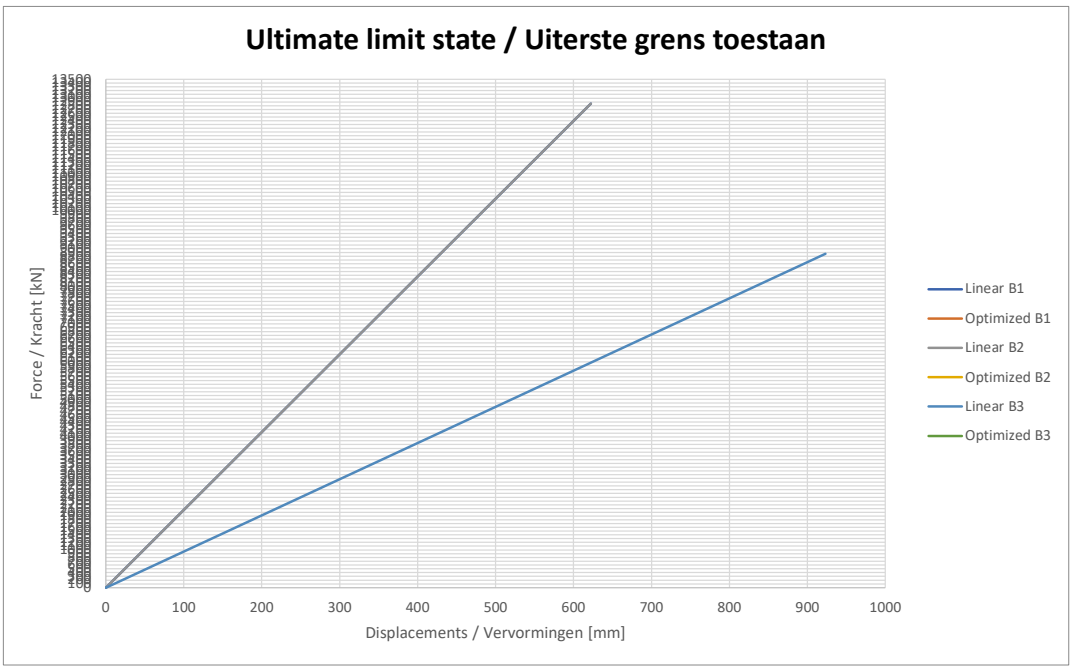

C

Derivations of partial factors

In this appendix, the partial factors are derived, and the resulting partial factors here are summarised in Chapter 5. This appendix gives the results of the intermediate steps.

Table C.1: Partial factors case clay $\beta = 3.49$

Variables	Influence coefficients	Influence factors	Design	Characteristic	Partial Factors
E	-0.727	0.529	3128	2093	1.495
$t_{4,\text{ maximum moment}}$	0.279	0.078	63.797	65	1.019
t_1	-0.261	0.068	26.394	26	1.015
f_y	0.212	0.045	501.9336	483	0.962
$\varphi_{\text{layer 2}}$	-0.193	0.037	32.91	32.5	1.016
$c_{\text{u, layer 1}}$	0.131	0.017	33.671	25	0.742
$\gamma_{\text{sat, layer 2}}$	0.0691	0.005	18.778	19	1.012
t_3	-0.0518	0.003	55.278	55	1.005
t_5	0.034	0.001	54.817	55	1.003
$\gamma_{\text{sat, layer 1}}$	-0.0279	0.001	14.066	14	1.005
t_2	-0.00193	0.000	37.003	37	1.000
θ_m	-0.462	0.213	1	1	1.000
θ_b	-0.0583	0.003	1	1	1.000

Table C.2: Partial factors case mix $\beta = 3.23$

Variables	Influence coefficients	Influence factors	Design	Characteristic	Partial Factors
E	-0.7	0.490	3006.4	2093	1.436
f_y	0.206	0.042	502.5615	483	0.961
t_2	0.184	0.034	35.71	36	1.008
$c_{\text{u, layer 2}}$	-0.149	0.022	39.213	50	0.784
$t_{\text{4, maximum moment}}$	0.13	0.017	58.789	59	1.004
t_1	-0.121	0.015	27.191	27	1.007
$\varphi_{\text{layer 3}}$	-0.0972	0.009	34.095	35	0.967
$\varphi_{\text{layer 1}}$	-0.0937	0.009	34.578	35	0.984
$\gamma_{\text{sat, layer 4}}$	0.0873	0.008	16.752	17	1.015
$c_{\text{u, layer 4}}$	0.0698	0.005	72.913	50	0.686
t_5	-0.0554	0.003	54.092	54	1.002
$c_{\text{u, layer 6}}$	-0.0463	0.002	151.8	150	1.012
$\varphi_{\text{layer 5}}$	-0.039	0.002	34.095	35	0.967
t_3	-0.0382	0.001	54.062	54	1.001
$\gamma_{\text{sat, layer 5}}$	0.0318	0.001	19.894	20	1.005
$\varphi_{\text{layer 7}}$	-0.0301	0.001	34.016	35	0.964
$\gamma_{\text{sat, layer 7}}$	0.0241	0.001	20.051	20	0.997
$\gamma_{\text{sat, layer 6}}$	0.0189	0.000	18.94	19	1.003
$\gamma_{\text{sat, layer 2}}$	0.00852	0.000	19.993	20	1.000
$\gamma_{\text{sat, layer 1}}$	0.00852	0.000	19.919	20	1.004
$\gamma_{\text{sat, layer 3}}$	0.00207	0.000	19.993	20	1.000
θ_m	-0.576	0.332	1.0397	1	1.040
θ_b	-0.0837	0.007	1.0055	1	1.006

Table C.3: Partial factors case sand $\beta = 3.2$

Variables	Influence coefficients	Influence factors	Design	Characteristic	Partial Factors
$\varphi_{\text{layer 1}}$	0.591	0.349	30.985	35	1.166
E	-0.502	0.252	2874.3	2093	1.373
$\gamma_{\text{sat, layer 1}}$	0.463	0.214	19.966	22	1.102
f_y	0.247	0.061	497.973	483	0.970
t_5	-0.187	0.035	63.087	62	1.018
t_3	0.182	0.033	64.937	66	1.016
$t_{\text{4, maximum moment}}$	0.148	0.022	73.112	74	1.012
t_1	0.0519	0.003	33.897	34	1.003
t_2	0.0249	0.001	49.95	50	1.001
θ_m	-0.164	0.027	0.97185	1	0.972
θ_b	-0.0614	0.004	1.0123	1	1.012

Table C.4: Partial factors case sand alternative $\beta = 3.27$

Variables	Influence coefficients	Influence factors	Design	Characteristic	Partial Factors
E	-0.713	0.508	3023.5	2093	1.445
f_y	0.293	0.086	498.7941	483	0.968
$\varphi_{\text{layer 1}}$	-0.261	0.068	39.821	40	0.994
t_2	-0.257	0.066	37.372	37	1.010
t_1	-0.148	0.022	34.231	34	1.007
$t_{\text{4, maximum moment}}$	0.143	0.020	64.293	65	1.011
t_3	0.105	0.011	57.469	57	0.992
t_5	-0.0837	0.007	55.432	55	1.008
$\gamma_{\text{sat, layer 1}}$	-0.0278	0.001	22.098	22	1.004
θ_m	-0.286	0.082	0.9856	1	0.986
θ_b	0.36	0.130	0.9422	1	1.061

Table C.5: Partial factors case clay Port of Roterdam $\beta = 4.38$

Variables	Influence coefficients	Influence factors	Design	Characteristic	Partial Factors
E	-0.775	0.601	3743.9	2093	1.789
$\varphi_{\text{layer 2}}$	0.45	0.203	25.809	33.75	1.382
$c_{\text{u, layer 1}}$	0.24	0.058	19.341	37.5	1.939
$\gamma_{\text{sat, layer 1}}$	0.22	0.048	13.353	14	1.048
$\gamma_{\text{sat, layer 2}}$	0.194	0.038	18.005	19	1.055
f_y	0.101	0.010	508.599	483	0.950
θ_m	-0.128	0.016	0.96238	1	0.962
θ_b	0.16	0.026	0.96197	1	1.040

Table C.6: Partial factors case clay no model uncertainty $\beta = 3.48$

Variables	Influence coefficients	Influence factors	Design	Characteristic	Partial Factors
E	-0.78	0.608	3383.4	2093	1.617
f_y	0.352	0.124	490.3899	483	0.985
$t_{\text{4, maximum moment}}$	0.281	0.079	64.596	65	1.006
$c_{\text{u, layer 1}}$	0.279	0.078	29.966	25	0.834
$\gamma_{\text{sat, layer 1}}$	0.249	0.062	13.355	14	1.048
$\gamma_{\text{sat, layer 2}}$	-0.164	0.027	19.547	19	1.029
t_3	-0.106	0.011	55.612	55	1.011
$\varphi_{\text{layer 2}}$	-0.0898	0.008	32.095	32.5	0.984
t_5	0.04	0.002	54.764	55	1.004
t_2	0.03	0.001	36.944	37	1.002
t_1	-0.0156	0.000	26.029	26	1.001

Table C.7: Partial factors case sand alternative no model uncertainty $\beta = 3.3$

Variables	Influence coefficients	Influence factors	Design	Characteristic	Partial Factors
E	-0.835	0.697	3152.5	2093	1.506
$\varphi_{\text{layer 1}}$	-0.362	0.131	40.517	40	1.018
t_1	-0.184	0.034	34.265	34	1.008
t_2	-0.183	0.033	37.264	37	1.007
f_y	0.182	0.033	506.184	483	0.954
$t_{\text{4, maximum moment}}$	0.158	0.025	64.267	65	1.011
t_3	0.14	0.020	57.348	57	0.994
t_5	0.124	0.015	54.417	55	1.011
$\gamma_{\text{sat, layer 1}}$	-0.109	0.012	22.361	22	1.016

Table C.8: Partial factors case monitored $\beta = 3.54$

Variables	Influence coefficients	Influence factors	Design	Characteristic	Partial Factors
E	-0.808	0.653	877.13	524	1.672
f_y	0.299	0.089	495.075	483	0.976
$\varphi_{\text{layer 1}}$	-0.265	0.070	36.43	35	1.054
$t_{\text{4, maximum moment}}$	-0.101	0.010	32.189	32	1.006
t_2	-0.0786	0.006	22.149	22	1.007
t_1	-0.0497	0.002	20.095	20	1.005
t_3	0.0393	0.002	27.925	28	1.003
$\gamma_{\text{sat, layer 1}}$	-0.0319	0.001	20.122	20	1.006
t_5	0.0241	0.001	27.954	28	1.002
θ_m	-0.383	0.147	1.0145	1	1.015
θ_b	0.138	0.019	0.97366	1	1.027

Table C.9: Partial factors case favourable $\beta = 3.54$

Variables	Influence coefficients	Influence factors	Design	Characteristic	Partial Factors
E	-0.772	0.596	983.08	615	1.598
$\varphi_{\text{layer 1}}$	-0.28	0.078	36.109	35	1.042
f_y	0.223	0.050	503.0928	483	0.960
$\gamma_{\text{sat, layer 1}}$	-0.156	0.024	20.498	20	1.025
t_1	-0.0572	0.003	20.091	20	1.005
t_3	0.0507	0.003	31.919	32	1.003
t_5	-0.0492	0.002	31.078	31	1.003
$t_{\text{4, maximum moment}}$	0.0426	0.002	34.932	35	1.002
t_2	0.0388	0.002	24.062	24	0.997
θ_m	-0.489	0.239	1.0196	1	1.020
θ_b	0.00827	0.000	0.9987	1	1.001

Table C.10: Partial factors case moderate $\beta = 3.30$

Variables	Influence coefficients	Influence factors	Design	Characteristic	Partial Factors
E	-0.777	0.604	1429	827	1.728
f_y	0.276	0.076	498.6492	483	0.969
$\varphi_{\text{layer 1}}$	-0.274	0.075	36.239	35	1.047
$\gamma_{\text{sat, layer 1}}$	-0.175	0.031	20.603	20	1.030
t_1	-0.124	0.015	26.208	26	1.008
t_3	0.119	0.014	37.8	38	1.005
t_5	-0.0749	0.006	38.128	38	1.003
t_2	-0.0658	0.004	32.113	32	1.004
$t_{\text{4, maximum moment}}$	0.0486	0.002	40.735	41	1.007
θ_m	-0.411	0.169	1.0119	1	1.012
θ_b	0.0533	0.003	0.99	1	1.010

Table C.11: Partial factors case unfavourable $\beta = 3.19$

Variables	Influence coefficients	Influence factors	Design	Characteristic	Partial Factors
E	-0.752	0.566	3846	2842	1.353
$\varphi_{\text{layer 1}}$	-0.416	0.173	37.279	35	1.087
f_y	0.157	0.025	507.0051	483	0.953
t_3	0.157	0.025	59.229	60	1.013
t_2	-0.15	0.023	53.233	53	1.004
$\gamma_{\text{sat, layer 1}}$	-0.129	0.017	20.413	20	1.021
t_1	-0.102	0.010	40.161	40	1.004
$t_{\text{4, maximum moment}}$	0.0938	0.009	63.527	64	1.007
t_5	-0.00413	0.000	60.021	60	1.000
θ_m	-0.39	0.152	1.0032	1	1.003
θ_b	0.0544	0.003	0.99127	1	1.009

D

Reponse Surface coding

In this appendix, the Python code for building the response surface is shown and more elaboration on the choices of parameters is presented.

- The chosen kernel was the Matern 1/2 kernel. This kernel provided better accuracy than the default kernel or the Matern 3/2 or 5/2 kernel. The training points are not as oscillating in the other dimensions, therefore a stiffer oscillatory as the Matern 1/2 fits the best.
- The default optimizer was selected as this gives the best optimization of the hyperparameters of the kernel
- The data is standardized by subtracting the mean and dividing by the variance. Standardizing the data leads to a better fit of the training points when compared to the MinMax scaler.
- Normalizing the y-values leads to better fits empirically
- The chosen parameters led to the lowest Mean Squared error of 1.1E-18.

In order to visualise the response surface, it was constructed for just two input values, namely the berthing energy and the model uncertainty. Their effect on the maximum moment is shown in Figure D.1.

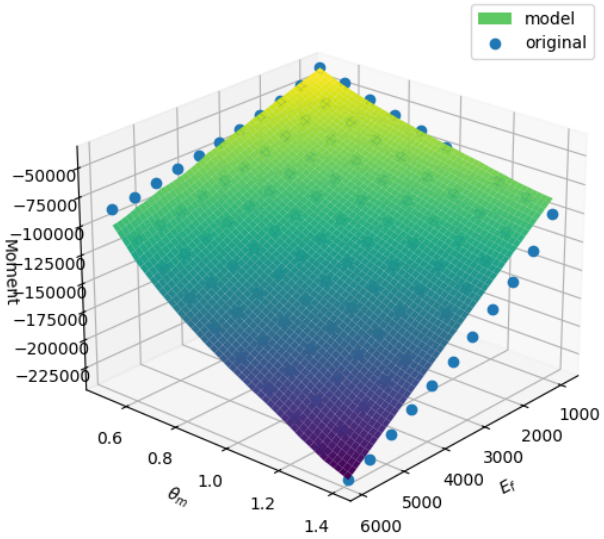

Figure D.1: Visualisation of response surface for two input

```
import numpy as np
from sklearn.gaussian_process import GaussianProcessRegressor
from sklearn.gaussian_process.kernels import DotProduct, RBF, Matern
from sklearn.preprocessing import StandardScaler
from sklearn.metrics import mean_squared_error
from matplotlib import pyplot as plt
from mpl_toolkits.mplot3d import Axes3D

import pandas as pd
from joblib import dump

#Loading training data
df = pd.read_csv(r'Path_to_data.csv', encoding='utf-16', delimiter=';', header=0,
skiprows=[])

df =df.dropna()


#Isolating the inpurt variables
X = df[['e_f', 'theta_m', 'theta_b', 'xi','angle_low0']].to_numpy()

# Create the Gaussian process regressor
model = GaussianProcessRegressor(kernel=Matern(nu=0.5),
optimizer='fmin_l_bfgs_b', normalize_y=True)

#Standardizing data
scaler = StandardScaler(with_mean=True)
X_std = scaler.fit_transform(X)
obs = np.array(df['uc_strength'])

# Train the model on the data
model.fit(X_std, obs)

#Save scaler and model for use
dump(scaler, 'scaler')
dump(model, 'model_Calandkanaal')

print(mean_squared_error(obs, model.predict(X_std)))
```